

UNIVERSIDADE FEDERAL DO RIO GRANDE DO SUL
FACULDADE DE FARMÁCIA
PROGRAMA DE PÓS-GRADUAÇÃO EM CIÊNCIAS FARMACÊUTICAS

**Desenvolvimento e avaliação da atividade neuroprotetora de nanoemulsões
revestidas por quitosana contendo ácido rosmarínico administradas pela via
nasal**

FLÁVIA NATHIELY SILVEIRA FACHEL

PORTO ALEGRE, 2018

UNIVERSIDADE FEDERAL DO RIO GRANDE DO SUL
FACULDADE DE FARMÁCIA
PROGRAMA DE PÓS-GRADUAÇÃO EM CIÊNCIAS FARMACÊUTICAS

**Desenvolvimento e avaliação da atividade neuroprotetora de nanoemulsões
revestidas por quitosana contendo ácido rosmarínico administradas pela via
nasal**

Tese apresentada por **Flávia Nathiely
Silveira Fachel** para obtenção do
TÍTULO DE DOUTORA em Ciências
Farmacêuticas.

Orientador: Prof. Dr. Helder Ferreira Teixeira

Coorientadora: Profa. Dra. Elizandra Braganhol

PORTO ALEGRE, 2018

Tese apresentada ao Programa de Pós-Graduação em Ciências Farmacêuticas, em nível de Doutorado da Faculdade de Farmácia da Universidade Federal do Rio Grande do Sul e aprovada em 3 de dezembro de 2018, pela Banca Examinadora constituída por:

Prof. Dr. Eduardo Rigon Zimmer

Universidade Federal do Rio Grande do Sul

Prof. Dra. Elenara Maria Teixeira Lemos Senna

Universidade Federal de Santa Catarina

Prof. Dr. Martin Steppe

Universidade Federal do Rio Grande do Sul

Fachel, Flávia Nathiely Silveira
Desenvolvimento e avaliação da atividade
neuroprotetora de nanoemulsões revestidas por
quitosana contendo ácido rosmarínico administradas
pela via nasal / Flávia Nathiely Silveira Fachel. --
2018.

265 f.

Orientador: Helder Ferreira Teixeira.

Coorientadora: Elizandra Braganhol.

Tese (Doutorado) -- Universidade Federal do Rio
Grande do Sul, Faculdade de Farmácia, Programa de Pós-
Graduação em Ciências Farmacêuticas, Porto Alegre,
BRRS, 2018.

1. Doenças neurodegenerativas. 2. Ácido rosmarínico.
3. Via nasal. 4. Nanoemulsões revestidas por
quitosana. 5. Terapia neuroprotetora. I. Teixeira,
Helder Ferreira, orient. II. Braganhol, Elizandra,
coorient. III. Título.

Agradecimentos a CAPES e ao CNPq que financiaram a minha bolsa de estudos, ao PPGCF da UFRGS, ao Laboratório de Desenvolvimento Galênico da Faculdade de Farmácia da UFRGS e ao Laboratório de Pesquisa em Biologia Celular da UFCSPA que possibilitaram a realização dos experimentos para a elaboração da presente tese.

*“Life is like riding a bicycle, to have balance
you need to keep moving”*

(Albert Einstein)

AGRADECIMENTOS

Ao Prof. Dr. Helder Ferreira Teixeira pela oportunidade de ingressar no doutorado, mesmo advinda de outra instituição e outra área de pesquisa, e pela confiança depositada em mim para alçarmos juntos novos desafios neste trabalho. Sua orientação, incentivo, disponibilidade, paciência e carinho foram imprescindíveis ao longo destes anos. És um exímio orientador e profissional, um exemplo a ser seguido.

À Profa. Dra. Elizandra Braganhol pela oportunidade, confiança, disponibilidade de colaboração e orientação. Suas palavras de incentivo e sua visão otimista, acreditando na minha capacidade de encarar novos desafios foram essenciais nesta trajetória, especialmente, nesta reta final. És uma excelente orientadora e profissional, com um amor e alegria de viver que contagiam a todos a sua volta.

Às professoras Letícia Scherer Koester, Valquíria Linck Bassani, Amelia Teresinha Henriques e Alethea Gatto Barschak pela disponibilidade e colaboração com este trabalho.

Aos colegas, professores e amigos do Laboratório de Desenvolvimento Galênico, essa grande família que me acolheu de uma forma incrível e que sempre esteve presente em toda esta trajetória, pela amizade, companheirismo e incentivo. Em especial, a Bruna que esteve comigo desde o início dessa trajetória pela troca de conhecimento, incentivo, carinho e amizade; a Marina que foi minha grande incentivadora e exemplo de pessoa e profissional pela paciência, carinho e amizade; a Paula que foi minha primeira coorientada de trabalho de conclusão de curso pela confiança, carinho, amizade e parceria; a Rose, uma grande profissional, que esteve presente nessa reta final pela parceria e amizade. E, aos meus grandes amigos Tainá e Kleyton que estiveram comigo desde o início do doutorado e continuam comigo, pelo carinho, apoio e por todos os momentos compartilhados.

Aos colegas do Laboratório de Pesquisa em Biologia Celular da UFCSPA pelos ensinamentos e amizade. Em especial, a Morgana que se tornou uma grande amiga, e que não mediu esforços para estar sempre disponível para me ensinar e auxiliar, mesmo com uma árdua rotina de experimentos, estágios e faculdade. A Flávia, Gabriela L., Gabriela R., Lorryne e Nicolly pelo apoio, parceria e amizade.

A Juliana que foi fundamental nessa etapa final de grandes desafios pela amizade e colaboração com o trabalho, e a Luana, uma grande amiga, a qual tive o prazer de compartilhar essa dupla rotina de UFRGS e UFCSPA com muita alegria, amizade e companheirismo.

À UFRGS, PPGCF, CAPES e CNPq pela concessão de bolsa e ao apoio financeiro concedidos. Em especial, aos funcionários, colegas e amigos do PPGCF que também foram essenciais nesta caminhada.

Aos mestres e amigos queridos Marlise Araújo dos Santos, Júlio César Marques de Lima, Airton Silveira Monza e Thais Russomano que estiveram presentes na minha trajetória de graduação e mestrado.

Aos meus amigos, que cultivei ao longo da vida, pela amizade, amor e compreensão. Em especial, a Giovana que me acompanha desde a graduação e que mesmo morando longe consegue estar muito presente em minha vida, sendo uma grande incentivadora e amiga; e as minhas grandes amigas Carla, Gabriela e Rafaela que são muito presentes em minha vida pelo incentivo, amor, paciência e amizade.

Ao meu amado Felipe que esteve presente em todos os momentos, desde as nossas idas no Mercado Público às 5:30 até a comemoração do primeiro artigo publicado, pelo apoio incondicional, amizade, compreensão nos momentos difíceis e imenso amor dedicado a mim. És parte fundamental desta conquista! À minha segunda família, que me acolheu com muito amor e que esteve sempre presente nesta trajetória, pelo incentivo, carinho e compreensão. A Marilanda e a vó Marilda por serem além de tudo minhas grandes amigas, sempre possuindo uma palavra de incentivo a ir em frente.

À minha família, minha irmã, meu irmão, meus cunhados, meus sobrinhos, meus tios e a Rosa pelo imenso amor, compreensão e incentivo a mim dedicados ao longo da minha vida. Vocês são meu porto seguro e essenciais nessa conquista! Aos meus avós *in memoriam* que foram meus grandes exemplos de amor incondicional e família pelo que ainda representam em nossas vidas. Em especial, a essa grande mulher, minha mãe, que é fonte do amor mais puro/ verdadeiro, que foi e sempre será minha maior incentivadora e companheira de todas as horas, e que é meu espelho de pessoa e profissional, e a quem tenho dedicado todas minhas vitórias. Essa vitória é nossa, mãe!

APRESENTAÇÃO

A presente tese foi redigida na forma de capítulos, com encarte de publicações, de acordo com as normas vigentes no Regimento do Programa de Pós-Graduação em Ciências Farmacêuticas da Universidade Federal do Rio Grande do Sul. Sendo assim, este exemplar encontra-se dividido, conforme descrito a seguir, em:

- Introdução;
- Objetivo geral e objetivos específicos;
- Capítulo 1 – Artigo científico de revisão: *An overview of the neuroprotective potential of rosmarinic acid and its association with nanotechnology-based delivery systems: a novel approach to treating neurodegenerative disorders*;
- Capítulo 2 – Artigo científico: *A novel, simplified and stability-indicating high-throughput ultra-fast liquid chromatography method for the determination of rosmarinic acid in nanoemulsions, porcine skin and nasal mucosa*;
- Capítulo 3 – Artigo científico: *Box-Behnken design optimization of mucoadhesive chitosan-coated nanoemulsions for rosmarinic acid nasal delivery – In vitro studies*;
- Capítulo 4 – Artigo científico: *Glioprotective effect of chitosan-coated rosmarinic acid nanoemulsions against lipopolysaccharide-induced inflammation and oxidative stress in rat astrocyte primary culture*;
- Capítulo 5 – Artigo científico: *Neuroprotective effect of chitosan-coated rosmarinic acid nanoemulsions nasal administration in Wistar rats against lipopolysaccharide-induced memory deficit*;
- Discussão geral;
- Conclusões.

RESUMO

As doenças neurodegenerativas (DN) são caracterizadas pela perda lenta e progressiva neuronal, com limitadas estratégias terapêuticas capazes de evitar sua progressão. O ácido rosmarínico (AR) é um composto encontrado em várias espécies vegetais com potencial neuroprotetor bem descrito na literatura. No entanto, devido a sua baixa biodisponibilidade oral e no sistema nervoso central, novas abordagens tem sido investigadas para contornar as limitações do AR. A presente tese objetivou desenvolver nanoemulsões (NE) revestidas por quitosana contendo AR para administração nasal visando uma terapia neuroprotetora. Inicialmente, um método rápido, simples e indicativo de estabilidade por cromatografia líquida de ultra-eficiência para determinação do AR em NE e mucosa nasal suína foi validado seguindo as guias oficiais. O método demonstrou ser específico, linear (0,5 – 10,0 $\mu\text{g}\cdot\text{mL}^{-1}$), preciso, exato e robusto para a determinação do AR em diferentes matrizes biológicas. Após, NE compostas por triglicerídeos de cadeia média, lecitina de gema de ovo e revestidas com quitosana, foram otimizadas por meio de um desenho experimental do tipo Box-Behnken. O modelo experimental mostrou-se adequado e a condição ótima foi estabelecida minimizando as respostas de tamanho de gotícula ($259,07 \pm 5,93$ nm) e índice de polidispersão ($0,274 \pm 0,01$) e maximizando os resultados de potencial zeta ($45,73 \pm 1,76$ mV) e o teor de AR ($92,66 \pm 1,43$ %). As propriedades físico-químicas e o potencial mucoadesivo das NE otimizadas foram caracterizados. O perfil de liberação/permeação do AR mostrou-se prolongado a partir das NE, com um aumento de retenção na mucosa nasal suína. Estudos *in vitro* de viabilidade e de marcação de necrose celular em fibroblastos (MRC-5) foram realizados, não sendo observada toxicidade em concentrações inferiores a 25 μM após 48 h de tratamento. Na sequência, a atividade glioprotetora das NE em modelo de inflamação e estresse oxidativo induzido por lipopolissacarídeo (LPS) em cultura primária de astrócitos foi investigada. Foi observado que o pré-tratamento com as NE é capaz de proteger o dano induzido pelo LPS, através da redução da disfunção mitocondrial, aumento do status antioxidante e da prevenção da ativação capacidade migratória dos astrócitos e do acúmulo de astrócitos reativos. Por fim, estudos *in vivo* em modelo de perda de memória induzido por LPS em ratos Wistar foram realizados, sendo evidenciada uma proteção contra o déficit de memória induzido por LPS, além de aumentar a disponibilidade cerebral do AR, confirmada pela quantificação de AR nos cérebros dos ratos ($0,173 \pm 0,038$ μg). Em conclusão, esse estudo demonstra as potencialidades das NE contendo AR administradas por via nasal como potencial estratégia na terapia neuroprotetora para tratamento de ND.

Palavras-chave: Doenças neurodegenerativas; Ácido rosmarínico; Via nasal; Nanoemulsões revestidas por quitosana; Terapia neuroprotetora.

ABSTRACT

Neurodegenerative disorders (ND) are characterized by progressive and slow neuronal loss, with limited therapeutic strategies that prevents its progression. Rosmarinic acid (RA) is a natural phenolic compound commonly found in various medicinal plants, with a well-documented neuroprotective effect. Nevertheless, due to its poor oral and central nervous system bioavailability, new approaches have been investigated to circumvent the RA limitations. The present thesis aimed to develop RA chitosan-coated nanoemulsions (NE) for nasal delivery aiming a neuroprotective therapy. Initially, a fast, simple and stability-indicating ultra-fast liquid chromatography method for the RA determination in NE and nasal mucosa was developed and successfully validated according to the official guidelines. The method showed to be specific, linear ($0.5 - 10.0 \mu\text{g}\cdot\text{mL}^{-1}$), precise, accurate and robust for RA determination in different biological matrices. After, NE composed by medium chain triglycerides and egg-lecithin, coated by chitosan were optimized using a Box-Behnken design. The experimental model was adequate, and the optimal condition was established with the minimum droplet size ($259.07 \pm 5.93 \text{ nm}$) and polydispersity index (0.274 ± 0.01), and the maximal ζ -potential ($45.73 \pm 1.76 \text{ mV}$) and content of RA ($92.66 \pm 1.43 \%$). The physicochemical properties and the mucoadhesive potential of the optimized NE were characterized. The RA release / permeation profile was extended from NE, with increased retention in the porcine nasal mucosa. *In vitro* studies of cell viability and necrosis in fibroblasts (MRC-5) were performed. No cytotoxicity was observed at concentrations below $25 \mu\text{M}$ after 48 h of treatment. Afterwards, the glioprotective activity of NE in lipopolysaccharide-induced (LPS) inflammation and oxidative stress model in rat astrocyte primary culture was investigated. It was observed that pre-treatment with NE can protect LPS-induced damage by reducing mitochondrial dysfunction, increasing antioxidant status and preventing migratory activation of astrocytes and accumulation of reactive astrocytes. Finally, *in vivo* studies on the LPS-induced memory impairment model in Wistar rats were performed, demonstrating a neuroprotective effect against LPS-induced memory deficit, as well as increasing the cerebral RA availability, confirmed by the quantification of RA in the brains of mice ($0.173 \pm 0.038 \mu\text{g}$). In conclusion, this study demonstrates the potentialities of RA NE administered by nasal route as a potential strategy in neuroprotective therapy for ND treatment.

Keywords: Neurodegenerative diseases; Rosmarinic acid; Nasal delivery; Chitosan-coated nanoemulsions; Neuroprotective therapy.

LISTA DE FIGURAS

CAPÍTULO 1

Figura 1	Chemical structure of rosmarinic acid (RA).....	54
Figura 2	Nanotechnology-based delivery systems for natural products.....	71
Figura 3	Schematic diagram demonstrating the mechanisms of drug absorption through the nose.....	74

CAPÍTULO 2

Figura 1	(A) Chromatographic profiles obtained in rosmarinic acid (RA) standard at $10 \mu\text{g}\cdot\text{mL}^{-1}$ and blank samples (specificity in the different matrices), (B) purity curve, and (C) UV spectrum of RA obtained by UFLC at 330 nm. Where, PNM: porcine nasal mucosa, PES: porcine ear skin, RF: receptor fluid (pH 5.8), NEB: blank nanoemulsion, Diluent: mobile phase.....	108
Figura 2	(A) Chromatogram, (B) zoom chromatogram, and (C) UV spectrum after alkaline hydrolysis of standard solutions of rosmarinic acid at $10 \mu\text{g}\cdot\text{mL}^{-1}$ obtained by UFLC at 330 nm.....	110
Figura 3	(A) Chromatogram, (B) zoom chromatogram, and (C) UV spectrum after dry heat at $80 \text{ }^\circ\text{C}$ of standard solutions of rosmarinic acid at $10 \mu\text{g}\cdot\text{mL}^{-1}$ obtained by UFLC at 330 nm.....	111
Figura 4	Plackett-Burman experimental design in different matrices (NEB: blank nanoemulsion, PES: porcine ear skin, PNM: porcine nasal mucosa, RF: receptor fluid). Where, bar charts representing the t-calculated for acid rosmarinic assay during robustness assessment, and their t-critical represented by the vertical line. The investigated factors were 1: column oven temperature, 2: flow rate, 3: TFA concentration, and 4: organic composition.....	115

CAPÍTULO 3

Figura 1	Response surface plots (three-dimensional) showing the effect of the oil phase concentration (X1; % w/v), lecithin to oil phase ratio (X2; w:w), and chitosan final concentration (X3, % w/v) on the size (Y1, nm), PDI (Y2), ζ -potential (Y3, mV), and rosmarinic acid content (Y4, %) in the chitosan-coated nanoemulsions.....	147
Figura 2	TEM images of RA NE (A) and RA CNE (B).....	149

Figura 3	(A) <i>In vitro</i> release profile through synthetic cellulose membrane of RA NE, RA CNE and RA RF in potassium phosphate buffer pH 5.8 at 32 ± 0.5 °C. (B) Permeation profile through porcine nasal mucosa of RA NE, RA CNE, and RA RF after 8 h of kinetic study in potassium phosphate buffer pH 5.8 at 32 ± 0.5 °C as receptor fluid. (C) Retention profile of RA NE, RA CNE, and RA RF into porcine nasal mucosa after 8 h of permeation assay. (D) Hematoxylin and eosin (H&E) staining histological (upper) and fluorescence (down) images of nasal mucosa control or treated with RA NE and RA CNE after 1 or 8 h of permeation/retention studies. Magnification 100x. (E) Fluorescent intensity detected for RA NE and RA CNE treatments after 1 or 8 h of nasal mucosa permeation/retention studies in relation to the percentage of fluorescence emitted by the control mucosa.....	151
-----------------	---	-----

Figura 4	Cell viability assessment by MTT reduction assay in fibroblasts (MRC-5) after 24 (A) and 48 (B) h of incubation with C, RA, RA NE, and RA CNE. Appropriate controls containing DMEM and 0.01% DMSO were performed.....	155
-----------------	--	-----

Figura Suplementar 1	Phase contrast and fluorescence microphotographs (insert) with PI incorporation in fibroblast cells (MRC-5) after 24 (A) and 48 (B) h of treatment with RA. Appropriate controls containing DMEM and 0.01% DMSO were performed.....	165
-----------------------------	---	-----

Figura Suplementar 2	Phase contrast and fluorescence microphotographs (insert) with PI incorporation in fibroblast cells (MRC-5) after 24 (A) and 48 (B) h of treatment with RA NE. Appropriate controls containing the corresponding concentrations of B NE were performed.....	166
-----------------------------	---	-----

Figura Suplementar 3	Phase contrast and fluorescence microphotographs (insert) with PI incorporation in fibroblast cells (MRC-5) after 24 (A) and 48 (B) h of treatment with RA CNE. Appropriate controls containing the corresponding concentrations of B CNE were performed.....	167
-----------------------------	---	-----

CAPÍTULO 4

Figura 1	Scheme of two different protocols employed in this study: protective (upper) and therapeutic (down).....	184
-----------------	--	-----

Figura 2	Analysis of primary astrocyte culture viability and proliferation following RA-free or RA loaded-nanoemulsion treatment. Astrocytes were exposed to RA, RA NE, B NE, RA CNE and B CNE at indicated concentrations and cell viability was assessed by MTT assay after 48 h (A) and 72 h (B); cell proliferation was determined by SRB assay after 72 h (C) of treatment. Cells exposed to DMSO (0.01%), B NE or B CNE were applied as controls. Values represent mean \pm SD for triplicate. Data were analyzed by ANOVA followed by Tukey's <i>post hoc</i> test.....	190
Figura 3	Analysis of primary astrocyte cell death by necrosis following RA-free or loaded-nanoemulsion treatment. Astrocytes were exposed to RA, RA NE, B NE, RA CNE and B CNE at indicated concentrations and PI incorporation was evaluated following 72 h of treatment. Representative phase contrast and fluorescence microphotographs (insert) with PI incorporation in astrocyte cells. Appropriate controls containing DMEM/10% FBS, DMSO (0.01%), B NE and B CNE were performed.....	191
Figura 4	Determination of protective and therapeutic potential of RA-free or loaded-nanoemulsion in LPS-induced astrocyte damage model. Astrocytes were exposed to RA, RA NE and RA CNE at indicated concentrations before (protective protocol; left panels) or after LPS treatment ($1 \mu\text{g}\cdot\text{mL}^{-1}$; therapeutic protocol, right panels). Following 48 h of treatment, cell viability and proliferation were assessed by MTT (A, B) and SRB (C, D), respectively. Cells exposed to DMSO (0.01%), B NE or B CNE were applied as controls. Value represent mean \pm SD for triplicate. Data were analyzed by one-way analysis of variance followed by Tukey's <i>post hoc</i> test. * $p < 0.05$, ** $p < 0.01$, and *** $p < 0.001$, different from control group; # $p < 0.05$, ## $p < 0.01$, and ### $p < 0.001$, different from LPS group.....	193
Figura 5	Determination of RA-free or loaded-nanoemulsion potential to prevent LPS-induced astrocyte death. Astrocytes were exposed to RA, RA NE, B NE, RA CNE and B CNE at indicated concentrations 3 h before LPS treatment for 48 h ($1 \mu\text{g}\cdot\text{mL}^{-1}$; protective protocol). Representative phase contrast and fluorescence microphotographs (insert) with PI incorporation in control and treated astrocytes. Cells exposed to DMSO (0.01%), B NE or B CNE were applied as controls.....	195
Figura 6	Effect of RA-free or loaded-nanoemulsion on ROS levels in astrocyte primary cultures exposed to LPS. Fluorescence microphotographs of ROS production in astrocyte cells exposed to LPS and RA, RA NE and RA CNE at indicated concentrations after 48 h in protective protocol. Cells exposed to DMSO (0.01%), B NE or B CNE were applied as controls.....	198

Figura 7	Cell migration of astrocyte cells exposed to LPS and RA, RA NE and RA CNE 6.25 (A), 12.50 (B), 25.0 (C) and 50.0 μ M (D) after 6, 18, 24 and 48 h of scratch-wound assay applying protective protocol. Cells exposed to DMEM/0.5% FBS, B NE or B CNE were applied as controls. Values represent mean \pm SD for triplicate. Data were analyzed by one-way analysis of variance followed by Tukey's post hoc test. # p < 0.05, ## p < 0.01, and ### p < 0.001, different from LPS group.	199
-----------------	---	-----

Figura 8	Immunofluorescence analysis of GFAP expression in astrocyte cells exposed to LPS and RA, RA NE and RA CNE (6.25 – 50.0 μ M) after 48 h applying protective protocol. Merged images: DAPI/DNA (blue) and GFAP (red) (magnification 200x) Cells exposed to DMSO (0.01%), B NE or B CNE were applied as controls.....	200
-----------------	--	-----

CAPÍTULO 5

Figura 1	Scheme of treatment with RA CNE, RA, B CNE and saline, and the protocol LPS-induced damage in Wistar rats.....	227
-----------------	--	-----

Figura 2	Effects of pre-treatment with saline (control and LPS), RA CNE, RA and B CNE on the total crossing (A) and rearing (B) open field test results. Data were analyzed by one-way analysis of variance followed by Tukey's post hoc test.....	233
-----------------	---	-----

Figura 3	Effects of pre-treatment with saline (control and LPS), RA CNE, RA and B CNE on recognition index after LPS-induced damage. Data were analyzed by one-way analysis of variance followed by Tukey's post hoc test. * p < 0.05, ** p < 0.01, and *** p < 0.001, different from control group; # p < 0.05, ## p < 0.01, and ### p < 0.001, different from LPS group.....	234
-----------------	---	-----

DISCUSSÃO

Figura 1	Figura ilustrativa da cavidade nasal e região olfatória (Fonte: TIMMONS, M. J.; TALLITSCH, R. B. Anatomia humana. 6.ed. Porto Alegre: Artmed, 2009)	246
-----------------	---	-----

LISTA DE TABELAS

CAPÍTULO 1

Tabela 1	<i>In vitro</i> , <i>ex vivo</i> , and <i>in vivo</i> studies of rosmarinic acid (RA) anti-inflammatory potential found in the literature.....	58
Tabela 2	Main <i>in vitro</i> and <i>in vivo</i> studies of rosmarinic acid (RA) antioxidant potential found in the literature.....	63
Tabela 3	<i>In vitro</i> and <i>in vivo</i> studies of rosmarinic acid (RA) neuroprotection found in the literature.....	69

CAPÍTULO 2

Tabela 1	Tested systems for optimization of chromatographic conditions....	107
Tabela 2	System suitability testing of RA standard.....	108
Tabela 3	Linearity of RA standard and matrices.....	112
Tabela 4	Summary of the output of the ANOVA for the evaluation of linearity.....	112
Tabela 5	Repeatability, intermediate precision, accuracy and stability evaluation of RA standard and matrices.....	114
Tabela 6	RA extraction recovery from porcine ear skin and nasal mucosa matrices.....	116
Tabela 7	UFLC method application for determination of RA in a real sample.....	117

CAPÍTULO 3

Tabela 1	Investigated factors and factor levels of Box-Behnken experimental design.....	138
Tabela 2	Box-Behnken Design arrangement and experimental values for each response for rosmarinic acid chitosan-coated nanoemulsions.....	144

Tabela 3	Associated probability values (<i>p</i> -values), error lack of fit and regression for each response.....	145
Tabela 4	Predicted and experimental values obtained from the response optimization of Box–Behnken design.....	146
Tabela 5	Physicochemical characterization and mucoadhesive capacity of nanoemulsions.....	148
Tabela 6	Morphological alterations and necrosis cell death qualitative evaluation in fibroblast cells (MRC-5) exposed to RA formulations.	157

CAPÍTULO 4

Tabela 1	Physicochemical characteristics of nanoemulsions.....	189
Tabela 2	Effect of RA-free or loaded-nanoemulsion in morphological alterations and PI incorporation in astrocyte primary cultures exposed to LPS using protective protocol.....	194
Tabela 3	Effect of RA-free or loaded-nanoemulsion on iNOS, ROS, SH and TBARS levels in astrocyte primary cultures exposed to LPS using protective protocol.....	197

CAPÍTULO 5

Tabela 1	Linearity and summary of the output of the ANOVA of RA standard, rat plasma and brain matrices.....	230
Tabela 2	Intraday and inter-day precision, accuracy and stability evaluation of RA standard, rat plasma and brain matrices.....	231
Tabela 3	RA quantification in rat brain and plasma after RA CNE and free RA protocol of nasal administration.....	232

LISTA DE ABREVIATURAS

ALT	Do inglês: Alanine aminotransferase
ANOVA	Do inglês: <i>Analysis of variance</i>
AR	Ácido rosmarínico
AST	Do inglês: Aspartate aminotransferase
B CNE	Do inglês: <i>Blank chitosan-coated nanoemulsion</i>
B NE	Do inglês: <i>Blank nanoemulsion</i>
BBB	Do inglês: <i>Blood brain barrier</i>
BBD	Do inglês: <i>Box-Behnken design</i>
BHE	Barreira hematoencefálica
CAPES	Coordenação de Aperfeiçoamento de Pessoal de Nível Superior
CAT	Do inglês: <i>Catalase</i>
ChEs	Do inglês: <i>Cholinesterases</i>
CLAE	Cromatografia líquida de alta-eficiência
CLUE	Cromatografia líquida de ultra-eficiência
CNE	Do inglês: <i>Chitosan-coated nanoemulsions</i>
CNPq	Conselho Nacional de Desenvolvimento Científico e Tecnológico
CNS	Do inglês: <i>Central nervous system</i>
COMT	Do inglês: <i>Catechol-O-methyl transferase</i>
COX2	Do inglês: <i>Cyclooxygenase-2</i>
DA	Doença de Alzheimer
DAPI	Do inglês: <i>4',6-diamidino-2-phenylindole</i>
DCFH-DA	Do inglês: <i>Dichlorodihydrofluorescein diacetate</i>
DCFH-DA	Do inglês: <i>2',7'-dichlorofluorescein diacetate</i>
DMEM	Do inglês: <i>Dulbecco's modified Eagle's medium</i>
DMSO	Do inglês: <i>Dimethyl sulfoxide</i>
DN	Doenças neurodegenerativas
DP	Doença de Parkinson
DPPH	Do inglês: <i>2,2-diphenyl-1-picrylhydrazyl</i>
DTNB	Do inglês: <i>5,5'-dithiobis-2- nitrobenzoic acid</i>
ELA	Esclerose lateral amiotrófica
EMA	Do inglês: <i>European Medicines Agency</i>
EPCR	Do inglês: <i>Endothelial protein C receptor</i>
ERK	Do inglês: <i>Extracellular ligand-regulated kinase</i>
EROs	Espécies reativas de oxigênio
FACS	Do inglês: <i>Fluorescence-activated cell sorting</i>
FAPERGS	Fundação de Amparo à Pesquisa no Estado do Rio Grande do Sul
FBS	Do inglês: <i>Fetal bovine serum</i>
FDA	Do inglês: <i>Food and Drug Administration</i>
FRAP	Do inglês: <i>Ferric reducing ability of plasma</i>
GFAP	Do inglês: <i>Glial fibrillary acidic protein</i>
GPx	Do inglês: <i>Glutathione peroxidase</i>

GSH	Do inglês: <i>Thiol-containing glutathione</i>
HCIO	Do inglês: <i>Hypochlorous acid sequestration</i>
HPLC	Do inglês: <i>High-pressure liquid chromatography</i>
ICH	Do inglês: <i>International Conference on Harmonization</i>
IL-10	Do inglês: <i>Interleukin 10</i>
IL-1β	Do inglês: <i>Interleukin 1-beta</i>
IL-6	Do inglês: <i>Interleukin 6</i>
iNOS	Do inglês: <i>Induced nitric oxide synthase</i>
iNOS	Do inglês: <i>Induced nitric oxide synthase</i>
LDL	Do inglês: <i>Low density lipoprotein</i>
LLOQ	Do inglês: <i>Lower limit of quantification</i>
LOD	Do inglês: <i>Limit of detection</i>
LOQ	Do inglês: <i>Limit of quantification</i>
LPS	Lipopolissacarídeo ou do inglês: <i>Lipopolysaccharide</i>
MAO-A	Do inglês: <i>Monoamine oxidase A</i>
MAO-A	Do inglês: <i>Monoamine oxidase B</i>
MCP-1	Do inglês: <i>Monocyte chemoattractant protein-1</i>
MCT	Do inglês: <i>Medium chain triglycerides</i>
ME	Do inglês: <i>Matrix effect</i>
MIP-1α	Do inglês: <i>Macrophage inflammatory protein-1-alpha</i>
MMP2	Do inglês: <i>Metalloproteinase-2</i>
MMP9	Do inglês: <i>Metalloproteinase-9</i>
MTT	Do inglês: <i>3-(4,5-dimethylthiazol-2-yl)-2,5-diphenyltetrazolium-bromide</i>
N	Do inglês: <i>Theoretical plates</i>
NBD PE	Do inglês: <i>N-(7-Nitrobenz-2-Oxa-1,3-Diazol-4-yl)-1,2-Dihexadecanoyl-sn-Glycero-phosphoethanolamine Triethylammonium Salt</i>
ND	Do inglês: <i>Neurodegenerative disorders</i>
NE	Nanoemulsões ou do inglês: <i>nanoemulsions</i>
NE_B	Do inglês: <i>Blank nanoemulsions</i>
NE_{RA}	Do inglês: <i>RA loaded-nanoemulsions</i>
NF-κB	Do inglês: <i>Factor nuclear kappa B</i>
NO	Do inglês: <i>Nitric oxide</i>
Nrf-2	Do inglês: <i>Erythroid nuclear factor expression</i>
oxLDL	Do inglês: <i>Oxidized low-density lipoprotein</i>
PDA	Do inglês: <i>Photodiode array</i>
PDI	Do inglês: <i>Polydispersity index</i>
PES	Do inglês: <i>Porcine ear skin</i>
PGE2	Do inglês: <i>Prostaglandin E-2</i>
PI	Do inglês: <i>Propidium iodide</i>
PMA	Do inglês: <i>Phorbol-12-myristate 13-acetate</i>
PNM	Do inglês: <i>Porcine nasal mucosa</i>
RA	Do inglês: <i>Rosmarinic acid</i>
RA CNE	Do inglês: <i>Rosmarinic acid chitosan-coated nanoemulsion</i>

RA NE	Do inglês: <i>Rosmarinic acid-loaded nanoemulsion</i>
RA RF	Do inglês: <i>Control solution with propylene glycol</i>
RF	Do inglês: <i>Receptor fluid</i>
ROS	Do inglês: <i>Reactive oxygen species</i>
RSD	Do inglês: <i>Relative standard deviation</i>
RSM	Do inglês: <i>Response surface methodology</i>
RT	Do inglês: <i>Retention time</i>
SH	Do inglês: <i>Total thiol content</i>
SLN	Do inglês: <i>Solid lipid nanoparticles</i>
SNC	Sistema nervoso central
SOD	Do inglês: <i>Superoxide dismutase</i>
SRB	Do inglês: Sulforhodamine B
SS	Do inglês: <i>RA standard solution</i>
T	Do inglês: <i>Tailing factor</i>
TACE	Do inglês: <i>TNF-α converting enzyme</i>
TBARS	Do inglês: <i>Thiobarbituric acid reactive substances</i>
TEAC	Do inglês: <i>Trolox equivalent antioxidant capacity</i>
TEM	Do inglês: <i>Transmission electron microscopy</i>
TFA	Do inglês: <i>Trifluoroacetic acid</i>
TNFα	Do inglês: <i>Tumor necrosis factor alpha</i>
UFCSPA	Universidade Federal de Ciências da Saúde de Porto Alegre
UFLC	Do inglês: <i>Ultra-fast liquid chromatography</i>
UFRGS	Universidade Federal do Rio Grande do Sul
UHPLC	Do inglês: <i>Ultra-high-performance liquid chromatography</i>
UPLC	Do inglês: <i>Ultra-performance liquid chromatography</i>

SUMÁRIO

INTRODUÇÃO	33
<i>Referências</i>	38
OBJETIVOS.....	41
<i>Objetivo geral</i>	43
<i>Objetivos específicos</i>	43
CAPÍTULO 1	45
<i>Introdução</i>	47
<i>Artigo científico de revisão:</i>	49
<i>An overview of the neuroprotective potential of rosmarinic acid and its association with nanotechnology-based delivery systems: a novel approach to treating neurodegenerative disorders</i>	49
<i>Abstract</i>	52
<i>1 Introduction</i>	53
<i>2 Rosmarinic acid (RA)</i>	54
<i>2.1 RA anti-inflammatory activity</i>	55
<i>2.2 RA antioxidant activity</i>	61
<i>2.3 RA neuroprotective potential</i>	66
<i>3 RA- loaded nanotechnology-based delivery systems</i>	71
<i>4 Conclusions</i>	76
<i>Conflicts of interest</i>	76
<i>Acknowledgments</i>	76
<i>References</i>	78
CAPÍTULO 2	91
<i>Introdução</i>	93
<i>Artigo científico:</i>	95
<i>A novel, simplified and stability-indicating high-throughput ultra-fast liquid chromatography method for the determination of rosmarinic acid in nanoemulsions, porcine skin and nasal mucosa</i>	97
<i>Abstract</i>	98
<i>Graphical abstract</i>	99
<i>1 Introduction</i>	100

2	Material and methods	101
2.1	Materials and reagents	101
2.2	Instrumentation and UFLC conditions	101
2.3	Solutions	102
2.3.1	Preparation of standard solutions	102
2.3.2	Preparation of matrices solutions	102
2.3.2.1	Nanoemulsions	102
2.3.2.2	Porcine ear skin and nasal mucosa	102
2.3.2.3	Receptor fluid for retention/permeation studies	103
2.4	UFLC method validation	103
2.4.1	System suitability	103
2.4.2	Specificity and forced degradation	103
2.4.3	Linearity	104
2.4.4	Matrix effect	105
2.4.5	Precision and accuracy	105
2.4.6	Stability	105
2.4.7	Robustness	105
2.4.8	Extraction recovery of RA from porcine skin and nasal mucosa	106
2.5	Skin and nasal retention/permeation studies	106
3	Results and discussion	107
3.1	Development of UFLC method	107
3.2	UFLC method validation	109
3.2.1	System suitability	109
3.2.2	Specificity and forced degradation	109
3.2.3	Linearity	111
3.2.4	Matrix effect	112
3.2.5	Precision and accuracy	113
3.2.6	Stability	113
3.2.7	Robustness	114
3.2.8	Extraction recovery of RA from porcine skin and nasal mucosa	115
3.3	Skin and nasal retention/permeation studies	116

4 Conclusion.....	117
Conflicts of interest.....	118
Acknowledgements.....	118
References.....	119
CAPÍTULO 3.....	125
Introdução.....	127
Artigo científico:.....	129
Box-Behnken design optimization of mucoadhesive chitosan-coated nanoemulsions for rosmarinic acid nasal delivery – In vitro studies.....	131
Abstract.....	132
Graphical abstract.....	133
1 Introduction	134
2 Materials and methods	136
2.1 Materials.....	136
2.1.1 Chitosan.....	136
2.2 Ultra-fast liquid chromatography analysis.....	137
2.3 Preparation of nanoemulsions.....	137
2.4 Preparation of chitosan-coated nanoemulsions.....	137
2.5 Box-Behnken design.....	137
2.6 Determination of optimum conditions.....	138
2.7 Physicochemical characterization of nanoemulsions.....	139
2.7.1 Rosmarinic acid content.....	139
2.7.2 Association efficiency.....	139
2.7.3 Droplet size, polydispersity index and ζ -potential.....	139
2.7.4 Nanoemulsions morphology.....	139
2.7.5 Viscosity and pH measurements.....	140
2.8 Mucoadhesive properties	140
2.9 In vitro RA release study.....	140
2.10 RA nasal mucosa permeation/retention study.....	141
2.11 Histological and fluorescence microscopy studies	141
2.12 Biological assays.....	142
2.12.1 Fibroblast cell culture and treatment	142

2.12.2	<i>Cell viability (MTT) assay</i>	143
2.12.3	<i>Propidium iodide (PI) assay</i>	143
2.13	Statistical analysis	143
3	Results and discussion	143
3.1	Box-Behnken experimental design	143
3.2	Physicochemical characterization and mucoadhesive properties of nanoemulsions	147
3.3	In vitro release studies	150
3.4	Nasal mucosa permeation/retention studies	152
3.5	Histological and fluorescence microscopy studies	152
3.6	Biological assays	153
4	Conclusion	158
	Conflicts of interest	158
	Acknowledgements	158
	References	159
	CAPÍTULO 4	169
	Introdução	171
	Artigo científico:	173
	<i>Glioprotective effect of chitosan-coated rosmarinic acid nanoemulsions against lipopolysaccharide-induced inflammation and oxidative stress in rat astrocyte primary culture</i>	173
	Graphical abstract	177
1	Introduction	178
2	Materials and methods	180
2.1	Materials	180
2.2	Preparation of RA-loaded nanoemulsions	180
2.3	Physicochemical characterization of RA-loaded nanoemulsions	181
2.4	Animals	181
2.5	Rat primary astrocyte culture	181
2.6	Treatment of astrocyte cultures	182
2.6.1	Protective and therapeutic protocols	182
2.7	Cell viability, proliferation and death by necrosis	185

2.7.1	MTT assay.....	185
2.7.2	SRB assay.....	185
2.7.3	PI incorporation assay.....	185
2.8	Oxidative stress parameters.....	186
2.8.1	NO determination	186
2.8.2	ROS assay	186
2.8.3	SH assay.....	186
2.8.4	TBARS assay.....	187
2.8.5	Protein determination	187
2.9	Cell migration.....	187
2.10	GFAP immunofluorescence analysis.....	188
2.11	Statistical analysis.....	188
3	Results.....	188
3.1	Physicochemical characterization of RA-loaded nanoemulsions.....	188
3.2	Safety profile of RA-loaded nanoemulsions and free RA in astrocyte cells.....	189
3.3	RA-loaded nanoemulsions and free RA glioprotective effect on LPS-induced inflammation and oxidative stress in astrocyte cells	192
3.4	RA-loaded nanoemulsions and free RA anti-inflammatory and antioxidant effects on LPS-induced inflammation and oxidative stress in astrocyte cells.....	196
3.5	RA-loaded nanoemulsions and free RA modulates astrocyte cells migration on LPS-induced inflammation and oxidative stress.....	198
3.6	RA-loaded nanoemulsions and free RA effects in GFAP expression on LPS-induced inflammation and oxidative stress of astrocyte cells	200
4	Discussion	201
5	Conclusion.....	204
	Conflicts of interest.....	204
	Acknowledgements.....	204
	References.....	205
	CAPÍTULO 5	211
	Introdução.....	213
	Artigo científico:.....	215

Neuroprotective effect of chitosan-coated rosmarinic acid nanoemulsions nasal administration in Wistar rats against lipopolysaccharide-induced memory deficit.....	215
Graphical abstract	219
1 Introduction.....	220
2 Materials and methods.....	221
2.1 Materials	221
2.2 Chitosan-coated nanoemulsion.....	222
2.3 Physicochemical characterization of chitosan-coated nanoemulsion.....	222
2.4 Instrumentation and chromatographic conditions	222
2.5 Standard and matrices solutions preparation.....	223
2.5.1 RA standard.....	223
2.5.2 Rat plasma matrix.....	223
2.5.3 Rat brain matrix	223
2.6 Method validation.....	223
2.6.1 System suitability.....	224
2.6.2 Specificity.....	224
2.6.3 Linearity, matrix effect and stability.....	224
2.6.4 Precision and accuracy.....	224
2.6.5 Extraction recovery	225
2.7 Animals	225
2.8 Experimental protocols	226
2.8.1 Brain and plasma distribution.....	226
2.8.2 Treatment	226
2.9 Behavioural tests	227
2.9.1 Open field test.....	227
2.9.2 Object recognition test.....	227
2.9.3 Statistical analysis	228
3 Results and Discussion	228
3.1 Physicochemical characterization of chitosan-coated nanoemulsions	228

3.2	<i>Determination of RA in brain</i>	229
3.3	<i>Neuroprotective effects of RA CNE nasal administration lipopolysaccharide-induced memory deficit</i>	232
4	<i>Conclusion</i>	234
	<i>Conflicts of interest</i>	234
	<i>Acknowledgements</i>	234
	<i>References</i>	236
	DISCUSSÃO GERAL	241
	CONCLUSÕES	261

INTRODUÇÃO

Devido ao aumento da expectativa de vida populacional, os distúrbios cerebrais são de significativo interesse global, social e econômico, afetando cerca de 1,5 bilhão de pessoas em todo o mundo (SHINDE; JINDAL; DEVARAJAN, 2011). As doenças neurodegenerativas (DN), tais como a esclerose múltipla, a doença de Alzheimer e a doença de Parkinson, representam um problema de saúde pública. Tais doenças representam um grande desafio a ser enfrentado pelos pesquisadores, por possuírem, até o momento, limitadas estratégias terapêuticas capazes de evitar a perda progressiva neuronal presente nas DN (BHULLAR; RUPASINGHE, 2013; SOOD; JAIN; GOWTHAMARAJAN, 2014). Nessas doenças, alterações no sistema imune/inflamatório, a disfunção mitocondrial, e a formação de radicais livres contribuem de forma significativa para os processos de morte neuronal e, conseqüente, progressão da doença (BARNHAM; MASTERS; BUSH, 2004; BHAT et al., 2015; FISCHER; MAIER, 2015; SOLANKI; PARIHAR; PARIHAR, 2016).

Neste contexto, os efeitos protetores de moléculas com atividades anti-inflamatória e antioxidante em modelos animais de neuroinflamação e/ou estresse oxidativo têm sido claramente demonstrados, indicando que a terapia neuroprotetora pode ser uma abordagem terapêutica atraente a longo prazo para as DN (KELSEY; WILKINS; LINSEMAN, 2010; KOPPULA et al., 2012; SOLANKI; PARIHAR; PARIHAR, 2016). Recentemente, a atenção tem sido voltada para produtos naturais com potencial neuroprotetor, com destaque para os compostos fenólicos (SOLANKI; PARIHAR; PARIHAR, 2016).

O ácido rosmarínico (AR) é um composto polifenólico (éster de ácido cafeico e ácido 3,4-di-hidroxifeniláctico) encontrado em diversas espécies vegetais, especialmente as pertencentes às famílias Boraginaceae e Lamiaceae. Essa molécula apresenta várias atividades biológicas bem documentadas, incluindo as ações anti-inflamatória, antioxidante e neuroprotetora (COSTA et al., 2013; DU et al., 2010; FALLARINI et al., 2009; GHAFFARI et al., 2014; HUANG et al., 2009; LEE et al., 2008). No entanto, devido à baixa solubilidade em água, alta instabilidade, baixa permeabilidade em membranas biológicas, incluindo a barreira hematoencefálica (BHE), e, conseqüentemente, baixa biodisponibilidade oral e no sistema nervoso central (SNC) do AR, o seu uso permanece limitado (DA SILVA et al., 2014; KUO; RAJESH, 2017; LI et al., 2018; MEDRONHO; VALENTE; COSTA, 2014; YANG et al., 2015).

Nos últimos anos, novas abordagens tecnológicas e alternativas vias de administração para o AR têm sido investigadas para contornar essas limitações (DA SILVA et al., 2014; KUO; RAJESH, 2017; LI et al., 2018; MEDRONHO; VALENTE; COSTA, 2014; YANG et al., 2015). A via nasal para entrega de fármacos diretamente ao SNC, tem se destacado como uma alternativa a outras vias de administração, principalmente pela ausência da limitação imposta pela BHE. As limitações da administração por essa via decorrem da necessidade do composto de interesse atravessar a mucosa nasal e ao limitado tempo para absorção de fármacos ocasionado pelo movimento ciliar e pela secreção de fluidos (COSTANTINO et al., 2007; GRASSIN-DELYLE et al., 2012; MUJAWAR et al., 2014; NAKAZAWA; OHSAWA, 1998; PAUN; BAGADA; RAVAL, 2010). Assim, para melhorar a absorção intranasal, algumas estratégias vêm sendo estudadas, dentre elas, o emprego de sistemas nanoestruturados associados a polímeros mucoadesivos (CASSETTARI; ILLUM, 2014; ESKANDARI et al., 2011; KUMAR et al., 2008; SHINDE; JINDAL; DEVARAJAN, 2011).

Dentre os sistemas nanoestruturados, a associação de compostos de reduzida hidrossolubilidade em nanoemulsões tem sido considerado com o propósito de aumentar sua solubilidade e permeabilidade em membranas biológicas (ANTON; VANDAMME, 2009; BRUXEL et al., 2012; DOH et al., 2013). Dentre os polímeros utilizados com propriedades mucoadesivas destaca-se a quitosana. Esse polímero é um polissacarídeo catiônico derivado da quitina, e sua propriedade mucoadesiva está relacionada com a interação eletrostática do polímero com os grupos siálicos da mucina presente nas mucosas, resultando em um aumento do tempo de residência no local de ação ou absorção, intensificando o contato do fármaco com a barreira epitelial das mucosas (CASSETTARI; ILLUM, 2014; PREGO et al., 2005, 2006).

Apesar da existência de dados na literatura relacionados à utilização de AR em DN, nenhum estudo envolvendo a utilização da via nasal e de sistemas nanoparticulados associados a polímeros mucoadesivos para aumento de sua permeabilidade e absorção no SNC visando uma terapia neuroprotetora é relatado na literatura.

Neste contexto, a presente tese de doutorado teve por objetivo principal desenvolver nanoemulsões revestidas por polímero mucoadesivo contendo AR para administração pela via nasal, visando a obtenção de uma terapia neuroprotetora. A tese está apresentada em cinco capítulos, como segue:

- O primeiro capítulo apresenta um artigo científico de revisão abordando o potencial neuroprotetor do AR e sua associação com sistemas nanotecnológicos – uma abordagem promissora para as doenças neurodegenerativas;
- O segundo capítulo apresenta um artigo científico sobre o desenvolvimento e a validação de um método analítico e bioanalítico por cromatografia líquida de ultra eficiência (CLUE) para determinação do AR em nanoemulsões, pele e mucosa nasal suína;
- O terceiro capítulo apresenta um artigo científico sobre o desenvolvimento e a otimização de nanoemulsões revestidas por quitosana contendo AR, assim como, a caracterização físico-química, perfil mucoadesivo, perfil de liberação, permeação/retenção em mucosa nasal suína, e citotoxicidade *in vitro* em fibroblastos (MRC-5) das formulações otimizadas;
- O quarto capítulo apresenta um artigo científico sobre o efeito glioprotetor das nanoemulsões revestidas por quitosana contendo AR em modelo de inflamação/estresse oxidativo induzido por lipopolissacarídeo (LPS) em cultura primária de astrócitos;
- O quinto capítulo apresenta um artigo científico sobre a atividade neuroprotetora das nanoemulsões revestidas por quitosana contendo AR em modelo *in vivo* de déficit de memória induzido por induzida por LPS.

Referências

- ANTON, N.; VANDAMME, T. F. The universality of low-energy nano-emulsification. **International Journal of Pharmaceutics**, v. 377, n. 1–2, p. 142–147, 2009.
- BARNHAM, K. J.; MASTERS, C. L.; BUSH, A. I. Neurodegenerative diseases and oxidative stress. **Nature Reviews**, v. 3, p. 205–214, 2004.
- BHAT, A. H. et al. Oxidative stress, mitochondrial dysfunction and neurodegenerative diseases; a mechanistic insight. **Biomedicine & pharmacotherapy**, v. 74, p. 101–110, 2015.
- BHULLAR, K. S.; RUPASINGHE, H. P. V. Polyphenols: Multipotent therapeutic agents in neurodegenerative diseases. **Oxidative Medicine and Cellular Longevity**, v. 2013, p. 1–18, 2013.
- BRUXEL, F. et al. Nanoemulsões como sistemas de liberação parenteral de fármacos. **Química Nova**, v. 35, n. 9, p. 1827–1840, 2012.
- CASETTARI, L.; ILLUM, L. Chitosan in nasal delivery systems for therapeutic drugs. **Journal of controlled release**, v. 190, p. 189–200, 2014.
- COSTA, P. et al. Protective effects of *Lavandula viridis* L'Hér extracts and rosmarinic acid against H₂O₂-induced oxidative damage in A172 human astrocyte cell line. **Industrial Crops and Products**, v. 50, p. 361–365, 2013.
- COSTANTINO, H. R. et al. Intranasal delivery: Physicochemical and therapeutic aspects. **International Journal of Pharmaceutics**, v. 337, n. 1–2, p. 1–24, 2007.
- DA SILVA, S. B. et al. Natural extracts into chitosan nanocarriers for rosmarinic acid drug delivery. **Pharmaceutical Biology**, v. 53, n. 5, p. 642–652, 2014.
- DOH, H. J. et al. A novel lipid nanoemulsion system for improved permeation of granisetron. **Colloids and Surfaces B: Biointerfaces**, v. 101, p. 475–480, 2013.
- DU, T. et al. Rosmarinic acid antagonized 1-methyl-4-phenylpyridinium (MPP⁺)-induced neurotoxicity in MES23.5 dopaminergic cells. **International Journal of Toxicology**, v. 29, n. 6, p. 625–633, 2010.
- ESKANDARI, S. et al. Brain delivery of valproic acid via intranasal administration of nanostructured lipid carriers: *in vivo* pharmacodynamic studies using rat electroshock model. **International Journal of Nanomedicine**, v. 6, p. 363–371, 2011.
- FALLARINI, S. et al. Clovamide and rosmarinic acid induce neuroprotective effects in *in vitro* models of neuronal death. **British Journal of Pharmacology**, v. 157, n. 6, p. 1072–1084, 2009.
- FISCHER, R.; MAIER, O. Interrelation of oxidative stress and inflammation in neurodegenerative disease: Role of TNF. **Oxidative Medicine and Cellular Longevity**, v. 2015, p. 1–18, 2015.
- GHAFFARI, H. et al. Rosmarinic acid mediated neuroprotective effects against H₂O₂-induced neuronal cell damage in N2A Cells. **Life Sciences**, v. 113, n. 1–2, p. 7–13, 2014.
- GRASSIN-DELYLE, S. et al. Intranasal drug delivery: An efficient and non-invasive

route for systemic administration - Focus on opioids. **Pharmacology and Therapeutics**, v. 134, n. 3, p. 366–379, 2012.

HUANG, R. et al. Neuroprotection in a 6-hydroxydopamine-lesioned Parkinson model using lactoferrin-modified nanoparticles. **Journal of Gene Medicine**, 2009.

KELSEY, N. A.; WILKINS, H. M.; LINSEMAN, D. A. Nutraceutical antioxidants as novel neuroprotective agents. **Molecules**, v. 15, n. 11, p. 7792–7814, 2010.

KOPPULA, S. et al. Recent advances on the neuroprotective potential of antioxidants in experimental models of Parkinson's disease. **International Journal of Molecular Sciences**, v. 13, n. 8, p. 10608–10629, 2012.

KUMAR, M. et al. Intranasal nanoemulsion based brain targeting drug delivery system of risperidone. **International Journal of Pharmaceutics**, v. 358, n. 1–2, p. 285–291, 2008.

KUO, Y. C.; RAJESH, R. Targeted delivery of rosmarinic acid across the blood–brain barrier for neuronal rescue using polyacrylamide-chitosan-poly(lactide-co-glycolide) nanoparticles with surface cross-reacting material 197 and apolipoprotein E. **International Journal of Pharmaceutics**, v. 528, n. 1–2, p. 228–241, 2017.

LEE, H. J. et al. Rosmarinic acid protects human dopaminergic neuronal cells against hydrogen peroxide-induced apoptosis. **Toxicology**, v. 250, n. 2–3, p. 109–115, 2008.

LI, S. et al. Simultaneous determination and tissue distribution studies of four phenolic acids in rat tissue by UFLC–MS/MS after intravenous administration of salvianolic acid for injection. **Biomedical Chromatography**, v. 32, n. 3, p. 1–9, 2018.

MEDRONHO, B.; VALENTE, A. J. M.; COSTA, P. Inclusion complexes of rosmarinic acid and cyclodextrins: stoichiometry, association constants, and antioxidant potential. **Colloid and Polymer Science**, v. 292, p. 885–894, 2014.

MUJAWAR, N. et al. Nasal drug delivery: problem solution and its application. **Journal of Current Pharma Research**, v. 4, n. 3, p. 1231–1245, 2014.

NAKAZAWA, T.; OHSAWA, K. Metabolism of rosmarinic acid in rats. **Journal of Natural Products**, 1998.

PAUN, J. S.; BAGADA, A A; RAVAL, M. K. Nasal drug delivery – As an effective tool for brain targeting - A review. **International Journal of Pharmaceutical and Applied Sciences**, v. 1, n. 2, p. 43–55, 2010.

PREGO, C. et al. Transmucosal macromolecular drug delivery. **Journal of Controlled Release**, v. 101, n. 1–3 SPEC. ISS., p. 151–162, 2005.

PREGO, C. et al. Efficacy and mechanism of action of chitosan nanocapsules for oral peptide delivery. **Pharmaceutical Research**, v. 23, n. 3, p. 549–556, 2006.

SHINDE, R. L.; JINDAL, A. B.; DEVARAJAN, P. V. Microemulsions and nanoemulsions for targeted drug delivery to the brain. **Current Nanoscience**, v. 7, n. 1, p. 119–133, 2011.

SOLANKI, I.; PARIHAR, P.; PARIHAR, M. S. Neurodegenerative diseases: From available treatments to prospective herbal therapy. **Neurochemistry International**, v. 95, p. 100–108, 2016.

SOOD, S.; JAIN, K.; GOWTHAMARAJAN, K. Intranasal therapeutic strategies for management of Alzheimer's disease. **Journal of Drug Targeting**, v. 22, n. 4, p. 279–94, 2014.

YANG, J. et al. Enhanced oral bioavailability and prophylactic effects on oxidative stress and hepatic damage of an oil solution containing a rosmarinic acid – phospholipid complex. **Journal of Functional Foods**, v. 19, p. 63–73, 2015.

OBJETIVOS

Objetivo geral

A presente tese teve por objetivo geral desenvolver nanoemulsões revestidas por polímero mucoadesivo contendo ácido rosmarínico para administração nasal visando uma terapia neuroprotetora.

Objetivos específicos

- Desenvolver e validar um método analítico e bioanalítico por cromatografia líquida de ultra eficiência (CLUE) para avaliação do AR em nanoemulsões e em diferentes matrizes biológicas;
- Desenvolver, otimizar e caracterizar as propriedades físico-químicas de nanoemulsões contendo ácido rosmarínico revestidas por quitosana com vistas a administração nasal;
- Avaliar *in vitro* a força mucoadesiva e o perfil de permeação/retenção do ácido rosmarínico em mucosa nasal suína a partir das nanoemulsões otimizadas;
- Investigar o perfil de citotoxicidade *in vitro* do AR e das nanoemulsões otimizadas em fibroblastos de pulmão humano (MRC-5) através de estudos de análise de viabilidade e morte celular;
- Avaliar e elucidar a atividade glioprotetora *in vitro* (cultura primária de astrócitos) do AR na sua forma livre e das nanoemulsões otimizadas em modelo de inflamação/estresse oxidativo induzido por lipopolissacarídeo (LPS);
- Avaliar e elucidar a atividade neuroprotetora *in vivo* (ratos Wistar) do AR na sua forma livre e das nanoemulsões otimizadas em modelo de déficit de memória induzido por LPS.

Introdução

O primeiro capítulo desta tese compreende um artigo científico de revisão sobre o potencial neuroprotetor do ácido rosmarínico (AR) e sua associação com sistemas nanotecnológicos – uma abordagem promissora para as doenças neurodegenerativas (DN). As DN, tais como a doença de Alzheimer, a doença de Parkinson e a esclerose lateral amiotrófica, são caracterizadas pela disfunção lenta e progressiva neuronal ocasionada pela perda de neurônios no sistema nervoso central (SNC). Devido a patogênese das DN envolver múltiplos fatores, ainda hoje, as estratégias terapêuticas são limitadas, por muitas vezes, não conseguem atingir vários sítios de ação, nem mesmo evitar a progressão da doença. Recentemente, os efeitos neuroprotetores de moléculas naturais com atividades anti-inflamatória e, principalmente, antioxidante têm sido claramente demonstrados e surgem como uma abordagem terapêutica promissora para as DN. Dentre os compostos de origem natural, o AR tem atraído a atenção nos últimos tempos, pelo considerável número de estudos que comprovam suas atividades anti-inflamatória, antioxidante e neuroprotetora. No entanto, devido à sua instabilidade, baixa solubilidade em água, baixa permeabilidade em membranas biológicas, incluindo a barreira hematoencefálica, e, baixa biodisponibilidade oral e no SNC do AR, novas abordagens tecnológicas para a veiculação e administração desse composto têm sido descritas na literatura. Neste contexto, esse capítulo teve por objetivo apresentar uma visão geral do potencial neuroprotetor do AR e discutir o uso da nanotecnologia como uma abordagem promissora para as DN.

Artigo científico de revisão:

An overview of the neuroprotective potential of rosmarinic acid and its association with nanotechnology-based delivery systems: a novel approach to treating neurodegenerative disorders

Publicado no *Neurochemistry International* (2019)

An overview of the neuroprotective potential of rosmarinic acid and its association with nanotechnology-based delivery systems: a novel approach to treating neurodegenerative disorders

Flávia Nathiely Silveira Fachel^a, Roselena Silvestri Schuh^a; Kleyton Santos Veras^a; Valquíria Linck Bassani^a, Letícia Scherer Koester^a, Amelia Teresinha Henriques^a, Elizandra Braganhol^b, Helder Ferreira Teixeira^{a,*}

^a Programa de Pós-Graduação em Ciências Farmacêuticas, Faculdade de Farmácia, Universidade Federal do Rio Grande do Sul, Porto Alegre, RS, Brazil.

^b Programa de Pós-Graduação em Biociências, Universidade Federal de Ciências da Saúde de Porto Alegre, Porto Alegre, RS, Brazil.

*Corresponding author

Helder Ferreira Teixeira

Av. Ipiranga, 2752/ 606

91650-000, Porto Alegre, RS, Brazil

Tel.: +55 51 3308 5231; fax: +55 51 3308 2165

E-mail address: helder.teixeira@ufrgs.br (Helder Ferreira Teixeira).

Abstract

Neurodegenerative disorders (ND) are characterized by slow and progressive neuronal dysfunction induced by the degeneration of neuronal cells in the central nervous system (CNS). Recently, the neuroprotective effects of natural compounds with anti-inflammatory and antioxidant activities has been clearly demonstrated. This appears to be an attractive therapeutic approach for ND, particularly regarding the use of polyphenols. In this review, we present an overview of the neuroprotective potential of rosmarinic acid (RA) and discuss the use of nanotechnology as a novel approach to treating ND. RA presents a variety of biological important activities, i.e. the modulation of pro-inflammatory cytokine expression, prevention of neurodegeneration and damage reduction. However, its poor bioavailability represents a limitation in terms of pharmacodynamics. In this sense, nanotechnology-based carriers could allow for the administration of higher but still safe amounts of RA, aiming for CNS delivery. Nasal administration could be a pleasant route for delivery to the CNS, as this represents a direct route to the CNS. With these advantages, RA-loaded nanotechnology-based therapy through the nasal route could be promising approach for the treatment of ND.

Keywords: Rosmarinic acid; Neuroprotective potential; Neurodegenerative disorders; Nanotechnology-based carriers; Brain delivery.

1 Introduction

Neurodegenerative disorders (ND) such as amyotrophic lateral sclerosis, Alzheimer's, Huntington's, and Parkinson's diseases are characterized by slow and progressive neuronal dysfunction induced by the degeneration of neuronal cells in the central nervous system (CNS). The main clinical manifestations of neuronal damage are memory and cognitive impairment, locomotor difficulty, and emotional and/or behavioral problems (Barnham et al., 2004; Liu et al., 2017; Pérez-Hernández et al., 2016; Solanki et al., 2016).

The pathogenesis of ND is considered complex and multifactorial, involving a combination of genetic and non-genetic factors; the latter is associated with most ND cases. Among the non-genetic factors, alterations in the immune-inflammatory system and oxidative stress have been highlighted to play key roles in ND development and/or progression (Andersen, 2004; Bhat et al., 2015; Ramassamy, 2006; Wang et al., 2006).

Inflammation is a protective response to cell injury or infection, intended to remove or inactivate potentially damaging agents and prevent their destructive effects. However, when the inflammatory process persists uncontrollably (chronic inflammation), it can lead to the destruction of normal tissue. This condition is especially relevant in ND due to the prolonged progression of these diseases, in which chronic neuronal damage and protein aggregates are associated with constant activation of the microglial immune-inflammatory system (Cunningham et al., 2009; Fischer and Maier, 2015; Lull and Block, 2010; Wang et al., 2006; Wyss-coray and Mucke, 2002).

Oxidative stress is the result of imbalanced oxygen metabolism and consequent high intracellular non-physiological quantities of reactive oxygen species (ROS). It is highly associated with neuronal damage in several disorders, including ND (Andersen, 2004; Barnham et al., 2004; Bhat et al., 2015; Casetta et al., 2005; Liu et al., 2017; Uttara et al., 2009).

In addition to the complex etiology of ND pathogenesis, therapeutic strategies are limited by the difficulty in reaching the desired site of action, and thus fail to prevent disease progression. Currently, few available treatments prevent temporary ND progression and improve patient symptoms. In this context, the role of neuroprotective therapies has garnered considerable interest, with the aim of improving the

management of these diseases (Bhullar and Rupasinghe, 2013; Pérez-Hernández et al., 2016; Solanki et al., 2016; Sood et al., 2014).

Recently, the neuroprotective effects of natural compounds that show anti-inflammatory and antioxidant activities has been clearly demonstrated; this appears to be an attractive therapeutic approach for ND. Among the natural products, polyphenols have attracted considerable attention as many studies have demonstrated the neuroprotective effect of a diet rich in phenolic compounds (Albarracin et al., 2012; Casetta et al., 2005; Kelsey et al., 2010; Koppula et al., 2012; Losada-Barreiro and Bravo-Díaz, 2017; Ramassamy, 2006; Solanki et al., 2016). In this review, we provide an overview of the *in vitro* and *in vivo* evidence supporting the neuroprotective potential of rosmarinic acid (RA), considering that this compound is a widely studied polyphenol (Amoah et al., 2016; Habtemariam, 2018). We also discuss the potential of nanotechnology-based delivery systems as a promising approach for ND treatment.

2 Rosmarinic acid (RA)

RA is a polyphenolic compound, an ester of caffeic acid and 3,4-dihydroxyphenyllactic acid (Figure 1) (Petersen and Simmonds, 2003). It was first isolated from rosemary (*Rosmarinus officinalis* L.) and described by Scarpati and Oriente (1958). The presence of RA has been reported in more than 30 families and 50 species of medicinal plants, particularly the Boraginaceae family and Nepetoideae sub-family of the Lamiaceae family and the species *Mentha* spp., *Melissa officinalis*, *Perilla frutescens*, *Salvia officinalis*, and *Thymus vulgaris* (Kim et al., 2015; Petersen, 2013; Petersen et al., 2009).

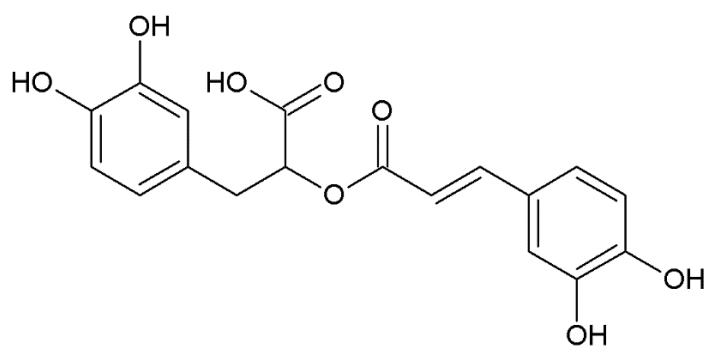


Figure 1. Chemical structure of rosmarinic acid (RA).

Various biological and pharmacological properties have been reported for RA in the literature. Among them, we can highlight some biological activities such as antidepressant (Takeda et al., 2002), anti-inflammatory (Rahbardar et al., 2017; Rocha et al., 2015), antimelanogenic (Ding et al., 2010), antioxidant (Fadel et al., 2011; Tepe et al., 2007), antitumor (Osakabe et al., 2004b), antiviral (Swarup et al., 2007), antiangiogenic (Huang and Zheng, 2006), photoprotective (Psotova et al., 2006; Sánchez-campillo et al., 2009), and neuroprotective (Khamse et al., 2015; Lee et al., 2016).

Taking into account the wide distribution of RA, its easy isolation from the plant kingdom, and its well-documented biological properties, RA has arisen as a natural molecule of interest, particularly in the current context of research into new neuroprotective therapies (Bulgakov et al., 2012; Khojasteh et al., 2014).

2.1 RA anti-inflammatory activity

The potential of natural molecules to reduce or suppress an inflammatory response has received increased attention in recent years, considering the association between inflammatory processes and multiple diseases, including ND (Cunningham et al., 2009; Perry, 2004; Wyss-coray and Mucke, 2002). There have been many studies performed *in vitro*, *ex vivo*, and *in vivo* demonstrating the anti-inflammatory activity of RA. The most important are summarized in Table 1 to better describe the roles of RA in inflammatory processes.

The first *in vitro* and *ex vivo* study was performed by Naito et al. (2003), and showed RA anti-inflammatory activity in an atherosclerosis inflammatory response induced by oxidized low-density lipoprotein (oxLDL). The authors demonstrated the inhibitory effect of RA on monocyte-endothelial interactions and on low density lipoprotein (LDL) oxidation associated with the potent free radical scavenging effect of RA. Additionally, an anti-atherosclerotic *ex vivo* effect of RA in apolipoprotein E-deficient mice was demonstrated and associated with an inhibitory effect of RA on plasma lipid peroxide production (Naito et al., 2003).

The anti-inflammatory activity of RA was also demonstrated *in vivo* in mice through topical application in skin papilloma (Osakabe et al., 2004b) and oral administration in hepatocellular carcinoma (Cao et al., 2016). In these studies, an anti-carcinogenic

effect of RA was observed, and tumor suppression was related to the regulation of proinflammatory cytokine secretion, particularly tumor necrosis factor alpha (TNF α), interleukins 1-beta (IL-1 β) and 6 (IL-6), as well as the inhibition of cellular adhesion and angiogenesis, which were associated with its antioxidant activity. Osakabe et al. provided further evidence of the anti-inflammatory activity and effectiveness of RA for seasonal allergic rhinoconjunctivitis in a randomized, double blind, age-matched, and placebo-controlled clinical trial (Osakabe et al., 2004a).

The suppression of inflammation induced by lipopolysaccharide (LPS) *in vitro* in human gingival fibroblasts and in bone marrow-derived dendritic cells, as well as *in vivo* in mice has also also reported for RA (Chu et al., 2012; Kim et al., 2008; Osakabe et al., 2002; Zdařilová et al., 2009). The findings of these studies demonstrated and confirmed the ability of RA to modulate proinflammatory cytokines (TNF α , IL-1 β and IL-6), inflammatory chemokines (monocyte chemoattractant protein-1 (MCP-1) and macrophage inflammatory protein-1-alpha (MIP-1 α)), and antioxidant mechanisms. In addition, studies performed by Chu et al. (2012) and Kim et al. (2008) demonstrated the suppression of intracellular ERK (extracellular ligand-regulated kinase) signaling by RA, also observed *in vitro* by Scheckel et al. (2008) and later by Liang et al. (2016) in an *in vivo* model of asthma.

Lembo et al. (2014) demonstrated the ability of RA to prevent damage induced by ultraviolet-B (UVB) radiation in a human keratinocyte cell line (HaCaT cells). They also confirmed the reduction of pro-inflammatory mediators (TNF α , IL-6, IL-8, MCP-1) and enhancement in protective interleukin 10 (IL-10). In the meanwhile, Ku et al. (2013) showed that RA also downregulates endothelial protein C receptor (EPCR) *in vitro* (in human endothelial cells) and *in vivo* (in a model of septicemia induced by cecal ligation and puncture). This study showed that RA treatment inhibits phorbol-12-myristate 13-acetate (PMA), TNF α , and induced EPCR release by the suppression of TNF- α converting enzyme (TACE) expression.

Rocha et al. (2015) used the carrageenan-induced paw edema model of local inflammation, hepatic ischemia-reperfusion, and thermal injury model of systemic inflammation in rats to evaluate the anti-inflammatory activity of RA administered orally or intravenously. The authors reported a reduction of about 60% in paw edema in RA-treated animals compared to control. The results were attributed to the anti-

inflammatory activity of RA associated with a reduction in pro-inflammatory cytokines (TNF α , IL-1 β , and IL-6). In a hepatic ischemia-reperfusion model, RA significantly decreased transaminase (AST and ALT) and LDH serum concentrations. In a thermal injury model, RA reduced multiorgan dysfunction markers by modulating matrix metalloproteinase-9 (MMP9) and factor nuclear kappa B (NF- κ B), also observed *in vitro* by Lee et al. (2008) and Kim et al. (2008).

Recently, Rahbardar et al. (2017) used a neuropathic pain murine model to evaluate the intraperitoneal administration of RA in the neuro-inflammatory environment. In this study, the authors observed the ability of RA to modulate neuro-inflammation through the reduction of all inflammatory and oxidative markers studied (including induced nitric oxide synthase (iNOS), cyclooxygenase-2 (COX2), IL-1 β , prostaglandin E-2 (PGE2), and matrix metalloproteinase 2 (MMP2) in treated animals. Additionally, the authors suggested RA as a potential candidate in treating different inflammatory neurological disorders.

Table 1. *In vitro*, *ex vivo*, and *in vivo* studies of rosmarinic acid (RA) anti-inflammatory potential found in the literature.

Treatment	Model	Main result	Mechanism	References
[RA] 1 – 50 μ M	<i>In vitro</i> atherosclerosis inflammatory response induced by oxLDL	Anti-inflammatory activity associate to inhibitory effect on adhesion molecule expression induced by oxLDL	Inhibitory effect on monocyte-endothelial interaction RA and LDL oxidation, associated to free radical scavenging activity	(Naito et al., 2003)
[RA] 1.52 mg/ kg/ d (oral treatment for 6 w, 1 administration/ day)	<i>Ex vivo</i> model of atherosclerosis in apolipoprotein E-deficient mice (4-w)	RA reduced aortic atherosclerotic lesion areas in mice	RA inhibitory effect on plasma lipid peroxide levels	(Naito et al., 2003)
[RA] 1 – 40 μ M (treatment for 14 h)	<i>In vitro</i> model of TNF- α -induced upregulation of CCL11 and CCR3 in human dermal fibroblasts	RA attenuated TNF- α -induced expression of CCL11 and CCR3	Suppressor effect on IKK- β activity in NF- κ B activation signalling	(Lee et al., 2006)
[RA] 0.1 – 200 μ M (treatment for 24 h or pre-treatment 1-2 h prior induction with LPS)	<i>In vitro</i> model of LPS-Induced production of MCP-1 and MIP-1 α via the MAPK pathway in bone-marrow derived dendritic cells	RA inhibited LPS-induced up-regulation in bone-marrow derived dendritic cells	RA significantly reduced the expressions of MCP-1 and MIP-1 α inhibited LPS-induced activation of MAPK and the nuclear translocation of NF- κ B	(Kim et al., 2008)
[RA] 5 – 20 μ Mol.L ⁻¹ (pre-treatment for 1 h and co-treatment)	<i>In vitro</i> model of COX2 expression in colon HT-29 and breast MCF-7 cancer cells and non-malignant breast epithelial MCF10A	RA prevented COX-2 activation by AP-1-inducing agents in both cancer and non-malignant mammary epithelial cells	RA reduced COX-2 expression and AP-1 activation also antagonized ERK1/2 activation	(Scheckel et al., 2008)
[RA] 1 μ g.mL ⁻¹ (treatment for 4 - 24 h)	<i>In vitro</i> model of oxidative stress and inflammation induced by LPS in human gingival fibroblasts	RA suppressed LPS-induced biological changes in gingival fibroblast	Reduction of ROS production, intracellular GSH depletion and lipid peroxidation, regulation of pro-inflammatory cytokines (TNF α , IL-1 β , IL-6), suppressed expression of iNOS	(Zdařilová et al., 2009)
[RA] 0.1 – 2 μ M	<i>In vitro</i> model of PMA-, TNF- α , and IL1b-induced EPCR shedding in human endothelial cells	RA decreased EPCR release	Inhibitory effect in PMA-, TNF α , IL induced EPCR shedding by suppression of TACE expression	(Ku et al., 2013)

Table 1 continuation. *In vitro*, *ex vivo*, and *in vivo* studies of rosmarinic acid (RA) anti-inflammatory potential found in the literature.

Treatment	Model	Main result	Mechanism	References
[RA] 2.7 μ M (treatment for 4 and 24 h)	<i>In vitro</i> model of UVB-induced cytokine/chemokine gene expression in HaCaT cells	RA prevent UVB-induced damage	Reduction in pro-inflammatory mediators (TNF α , IL-6, IL-8, MCP-1) and enhancement of the protective IL-10	(Lembo et al., 2014)
[RA] 150 mg.kg ⁻¹ (orally - treatment concurrently with LPS injection)	<i>In vivo</i> model of liver injury induced by LPS in D-GalN-sensitized (Male BALB/c mice 7-9-w)	RA liver protection through reduction of plasma aspartate aminotransferase levels	RA scavenging or reducing effect on superoxide or peroxyntirite	(Osakabe et al., 2002)
[RA] 1.35 mg.kg ⁻¹ (topical - pre-treatment for 30 min, 1 administration)	<i>In vivo</i> model of skin papilloma (Male BALB/c mice 7-9-w)	RA anti-carcinogenic effect via inhibition of the inflammatory response and scavenging of reactive oxygen radicals	Inhibitory effect on adhesion molecule, chemokine and eicosanoid synthesis, and on oxidative DNA injury	(Osakabe et al., 2004b)
[RA] 5, 10 and 20 mg.kg ⁻¹ (intraperitoneally - pre-treatment 1 h prior LPS administration)	<i>In vivo</i> model of acute lung injury induced by LPS (Male BALB/c mice 18-20 g)	RA potent anti-inflammatory effect in <i>in vivo</i> models of lung injury induced by LPS	Reduction in pro-inflammatory cytokines (TNF α , IL-1 β , IL-6) and suppression of intracellular signalling ERK	(Chu et al., 2012)
[RA] 1.4 μ g per mice (treatment 12 and 50 h after CLP)	<i>In vivo</i> model of septicemia induced by CLP (Male C57BL/6 mice weighing 18–20 g 6-7-w)	RA decreased EPCR release	Inhibitory effect in PMA-, TNF α , and induced EPCR release by suppression of TACE expression	(Ku et al., 2013)
[RA] 0, 25 and 50 mg.kg ⁻¹ (oral or intravenous - pre-treatment for 30 min)	<i>In vivo</i> model of local inflammation (carrageenan induced paw oedema) and systemic inflammation (hepatic ischaemia–reperfusion and thermal injury) (Male Wistar rats 100-380 g)	RA significantly decreased paw edema and systemic inflammation	Reduction in pro-inflammatory cytokines (TNF α , IL-1 β and IL-6), AST, ALT and LDH in serum concentration.; modulation of NF- κ B and MMP9	(Rocha et al., 2015)
[RA] 75, 150 and 300 mg.kg ⁻¹ (intra gastric treatment for 10 d, 1 administration/ day)	<i>In vivo</i> model of hepatocellular carcinoma (H22-xenografts) (Male SPF Kunming mice 18-22 g)	RA suppressed the tumour growth in H22-xenografts model with fewer toxic effects	Inhibitory effect on pro-inflammatory cytokines (TNF α , IL-1 β , IL-6), angiogenic factors, suppression of NF- κ B p65	(Cao et al., 2016)

Table 1 continuation. *In vitro*, *ex vivo*, and *in vivo* studies of rosmarinic acid (RA) anti-inflammatory potential found in the literature.

Treatment	Model	Main result	Mechanism	References
[RA] 5, 10 and 20 mg.kg ⁻¹ (intraperitoneally - pre-treatment 1 h prior ovalbumin administration for 4 d)	<i>In vivo</i> model of allergic asthma induced by ovalbumin (Female BALB/c mice weighing 18-20 g)	RA decreased the number of inflammatory cells and mucus hypersecretion in the airway	Suppressor effect on ERK and activation of NF-kB p38	(Liang et al., 2016)
[RA] 40 mg.kg ⁻¹ (intraperitoneal treatment concurrently with surgery, once a day for 14 d)	<i>In vivo</i> model of neuropathic pain (Male Wistar rats 230-280 g)	RA modulated neuro-inflammation	Reduction in iNOS, COX2, IL-1 β , PGE2, and MMP2	(Rahbardar et al., 2017)

[RA]: rosmarinic acid concentration; oxLDL: oxidized low-density lipoprotein; LDL: low density lipoprotein; TNF α : tumour necrosis factor alpha; CCR3: complement component 3; CCL11: motif chemokine ligand 11; MCP-1: monocyte chemoattractant protein-1; MIP-1 α : macrophage inflammatory protein-1 α ; MAPK: mitogen activated protein kinases; COX2: cyclooxygenase 2; HT-29: human colon adenocarcinoma cell line; MCF-7: human breast adenocarcinoma cell line; MCF10: human breast epithelial cell line; PMA: phorbol-12-myristate-13-acetate; IL: interleukin; EPCR: endothelial cell protein C receptor; HaCaT: immortalized nontumorigenic human epidermal cell line; LPS: lipopolysaccharides; D-GalN: D-galactosamine; CLP: cecal ligation puncture; H22: interferon-gama; AP-1: activator protein-1; ERK: extracellular-regulated kinase; GSH: glutathione; iNOS: inducible nitric oxide synthase; ROS: reactive oxygen species; TACE: transarterial chemoembolization; AST: aspartate aminotransferase; ALT: alanine aminotransferase; NF-kB: nuclear factor kappa B; MMP9: metalloproteinase 9; LDH: lactate dehydrogenase; PGE: prostaglandin E; IKK β : I κ B kinase.

2.2 RA antioxidant activity

The potential of natural molecules to inhibit the formation or eliminate free radicals has received increased interest in recent years, based on the relation that has been established between oxidative stress and many disorders, including the ND (Albarracin et al., 2012; Brewer, 2011; Yanishlieva et al., 2006). The free radical scavenger potential of RA is well-reported and has been described by several authors. The most important studies are summarized in Table 2 to better discuss the role of RA in oxidative stress (Lecomte et al., 2010; Pérez-Tortosa et al., 2012; Tepe et al., 2007; Zhu et al., 2014).

Compared to other phenolic acids and their derivatives, studies have shown that RA exhibits excellent antioxidant activity (RA > chlorogenic acid > caffeic acid > ferulic acid > coumaric acid), demonstrated by the β -carotene/linoleic acid co-oxidation, deoxyribose, DPPH (2,2-diphenyl-1-picrylhydrazyl), FRAP (ferric reducing ability of plasma), DNA damage, TEAC (Trolox equivalent antioxidant capacity), and HClO (hypochlorous acid sequestration) assays (Sevgi et al., 2015; Soobrattee et al., 2005).

In general, antioxidant compounds work by eliminating free radicals by donating their own electrons to neutralize the adverse effects of ROS. For many years, polyphenols have been thought to act by protecting molecules from oxidative damage by eliminating free radicals. However, increasing evidence shows that this is a simplified view of its mechanism of action (Losada-Barreiro and Bravo-Díaz, 2017).

Regarding RA, it is known that the presence of two catechol groups in its structure (Figure 1) is strongly associated with its antioxidant potential. Studies have shown that the antioxidant activity in the moiety related to 3,4-dihydroxyphenylactic acid is similar to the moiety of caffeic acid, suggesting that protons from one of the catechol groups may be removed to form intramolecular hydrogen bonds to stabilize the resulting radicals, although 3,4-dihydroxyphenylactic shows a great facility for donating protons (Cao et al., 2005; Fujimoto and Masuda, 2012). Conversely, other authors have reported that the moiety of caffeic acid is the first to undergo oxidation (Gil et al., 2013).

In vitro and *in vivo* studies have demonstrated different pathways of RA antioxidant activity, including increased antioxidant enzyme expression (catalase (CAT), glutathione peroxidase (GPx) and reductase, superoxide dismutase (SOD), nitric oxide synthase), reduced DNA damage, decreased amounts of oxygen and nitrogen reactive

species, and lower levels of lipoperoxidation markers (Bacanli et al., 2016; Fernando et al., 2016; Mushtaq et al., 2015, 2014; Psotova et al., 2006); the latter is being widely studied and is associated with the spontaneous insertion of RA into lipid layers (Fadel et al., 2011).

Another mechanism of action associated with RA antioxidant activity is related to the regulation of erythroid nuclear factor expression (Nrf-2), which may result in an increase in antioxidant status. Nrf-2 is responsible for regulating the basal and post-induction expression of several antioxidant enzymes, such as CAT, GPx, and SOD (Domitrović et al., 2013; Fernando et al., 2016; Shang et al., 2017)

Table 2. Main *in vitro* and *in vivo* studies of rosmarinic acid (RA) antioxidant potential found in the literature.

Treatment	Model	Main result	Mechanism	References
[RA] 0.9 –18 mg.L ⁻¹ (pre-treatment for 4 h)	<i>In vitro</i> model of UVA-induced changes in HaCaT cells	RA UVA photoprotective effect	Suppression of UVA-induced ROS production and CCR3 activation, decrease in lipid peroxidation and glutathione, and increase in ATP	(Psoťova et al., 2006)
[RA] 2.9 µg.mg ⁻¹	<i>In vitro</i> DPPH free radical-scavenging and β-carotene/linoleic acid systems	RA antioxidant activity	Free radical-scavenging capacity and inhibition of linoleic acid oxidation	(Tepe et al., 2007)
[RA] 0.25 – 100 µM	<i>In situ</i> model of lipoperoxidation in liposomes of 1,2-dilinoleoyl-sn-glycero-3-phosphocholine (DLPC)	RA spontaneously penetrates membranes to inhibit lipid peroxidation	Spontaneously insertion in lipid membranes, with a higher affinity for unsaturated lipids	(Fadel et al., 2011)
[RA] 0.25 mM	<i>In vitro</i> lipid oxidation system	RA antioxidant effect against lipid oxidation	Antioxidation reaction occurs at the catechol position of its 2-oxyphenylpropanyl moiety during the first stage of lipid oxidation	(Fujimoto and Masuda, 2012)
[RA] 3 – 13.5 mM	<i>In vitro</i> model pro-oxidant (generation of H ₂ O ₂ and free radicals by the action of peroxidase) and antioxidant (consumption of H ₂ O ₂ and free radicals) activity	RA pro-oxidant and antioxidant activity	Production of H ₂ O ₂ during its auto-oxidation and generation of free radicals (horseradish peroxidase substrate). Ability to eliminate H ₂ O ₂ and sequester free radicals	(Muñoz-Muñoz et al., 2013)
[RA] 0.1 - 0.5 mg.m ⁻¹	<i>In vitro</i> model of antioxidant (β-carotene bleaching, DPPH free radical scavenging, reducing power and chelating effect) and DNA damage protection	RA showed maximum antioxidant potential and protective effects on pBR322 plasmid DNA against the mutagenic and toxic effects of UV and H ₂ O ₂	Free-radical scavenging activity and DNA damage protection. Authors suggestion: Intercalation into DNA alter the DNA structural integrity, interrupt the production of oxidizing species	(Sevgi et al., 2015)

Table 2 continuation. Main *in vitro* and *in vivo* studies of rosmarinic acid (RA) antioxidant potential found in the literature.

Treatment	Model	Main result	Mechanism	References
[RA] 0.625, 1.25, 2.5, or 5 mM (pre-treatment 1 h prior to UVB exposure)	<i>In vitro</i> model of UVA-induced damage in HaCaT cells	RA cytoprotective activity against UVB radiation associated with ROS elimination	Increase expression and activity of SOD, CAT, heme oxygenase-1, and Nrf2	(Fernando et al., 2016)
[RA] 0 – 3 mM (treatment)	<i>In vitro</i> model of oxidative challenge elicited by t-BHP in human hepatoma HepG2 cells	RA cytoprotective activity against t-BHP cell damage	Radical-scavenging activity of RA	(Adomakobonsu et al., 2017)
[RA] 50 - 600 μ M (treatment for 4 d)	<i>In vivo</i> model of RA exposure to <i>Caenorhabditis elegans</i>	RA extended <i>C. elegans</i> lifespan	Hormesis, antioxidative / pro-oxidative properties, modulation of genetic players all contribute to <i>C. elegans</i> life extension	(Pietsch et al., 2011)
[RA] 10 mg.kg ⁻¹ (oral treatment for 21 d, 2 w after diabetes induction)	<i>In vivo</i> model of lipid peroxidation in streptozotocin - induced diabetic rats (Male Wistar rats 200-250 g)	RA prevents lipid peroxidation	Increase in AChE activity, modulation of cholinergic neurotransmission and prevention of damage oxidative stress in brain	(Mushtaq et al., 2014)
[RA] 10 mg.kg ⁻¹ (oral treatment for 21 d, 2 w after diabetes induction)	<i>In vivo</i> model of lipid peroxidation in streptozotocin - induced diabetic rats (Male Wistar rats 200-250 g)	RA effectively reduced the oxidative stress induced by streptozotocin	Normalized δ -ALA-D and other oxidative stress parameters in liver and kidney	(Mushtaq et al., 2015)
[RA] 10/20 mg.kg ⁻¹ (oral pre-treatment once a day during 7 d)	<i>In vivo</i> model of hepatotoxicity induced by carbon tetrachloride (Male and female Kunming mice 18–22 g)	RA hepatic protective effect	Reduction in the serum levels of AST and ALT. Increase antioxidative properties (SOD, CAT, GSH-Px, and TBARS)	(Yang et al., 2015)
[RA] 50, 100 and 200 mg.kg ⁻¹ (oral treatment once a day for 30 d)	<i>In vivo</i> model of aging mice (Male Kunming mice 47.56 \pm 3.61 g (20 m))	RA prevents progression of oxidative stress-related aging processes	Radical-scavenging activity, alteration of antioxidant enzymes (SOD, CAT, and GSH-Px) and inhibition of lipid peroxidation	(Zhang et al., 2015)

Table 2 continuation. Main *in vitro* and *in vivo* studies of rosmarinic acid (RA) antioxidant potential found in the literature.

Treatment	Model	Main result	Mechanism	References
[RA] 100 mg.kg ⁻¹ (intraperitoneal)	<i>In vivo</i> model of oxidative DNA damage induced by sepsis (Male Wistar rats 200-300 g)	RA attenuates sepsis-induced oxidative damage	Decreased MDA and TNF- α levels, increased GSH, SOD, and GSH-Px activities in rat liver and kidneys	(Bacanli et al., 2016)

[RA]: rosmarinic acid concentration; Nrf-2: nuclear factor erythroid 2; δ -ALA-D: Delta-aminolevulinic acid dehydratase; SOD: superoxide dismutase; CAT: catalase; TBARS: thiobarbituric acid reactive substances; MDA: malondialdehyde AChE: acetylcholine; t-BHP: t-butyl hydroperoxide; DPPH: 2,2-diphenyl-1-picrylhydrazyl; TNF α : tumour necrosis factor α ; CCR3: complement component 3; HaCaT: immortalized nontumorigenic human epidermal cell line; GSH: glutathione; ROS: reactive oxygen species; AST: aspartate aminotransferase; ALT: alanine aminotransferase; H₂O₂: hydrogen peroxide.

2.3 RA neuroprotective potential

As stated in the previous sections, the anti-inflammatory and antioxidant activities of RA have been well-established in several experimental models. The search for evidence for the neuroprotective effect of RA has been the focus of several *in vitro* and *in vivo* studies, presented in Table 3.

Table 3 shows that most of the studies correlate neuroprotective activity with the antioxidant activity of RA. *In vitro* studies involving a neurotoxicity model induced by hydrogen peroxide on dopaminergic neuronal cells (SH-SY5Y), glioblastoma cells (A172 and C6), or rat neuroblastoma cells (N2A), demonstrated the protective potential of RA against neuronal/glial damage induced by oxidative stress. As its main protection mechanism, RA induced an intracellular decrease in ROS production and/or accumulation, lipid peroxidation, and apoptotic process (Costa et al., 2013; Ghaffari et al., 2014; Lee et al., 2016, 2008). The protective effect of RA was also demonstrated *in vitro* in a neurotoxicity model induced by 6-hydroxydopamine in dopaminergic cells (MES23.5) and was correlated with a reduction in mitochondrial function and ROS production (Ren et al., 2009).

Other *in vitro* models involving oxidative stress, excitotoxicity, ischemic injury, and ciguatoxin toxicity have also been reported for RA and reinforce its protective effect on neuronal cells, mainly related to its antioxidant activity (Braidy et al., 2014; Fallarini et al., 2009). A recent study performed by Andrade et al. (2016) involving *in vitro* models of antioxidant activity (cholinesterases (ChEs), monoamine oxidases (MAO-A and MAO-B) and catechol-O-methyl transferase (COMT)) as well as *in silico* approaches showed the multifunctional profile of RA with regard to targets related to neurodegeneration. The results suggest that RA may be explored as a model for the development of new antioxidant molecules possessing additional MAO and COMT inhibitory effects to be further investigated for ND treatment (Andrade et al., 2016).

In line with the *in vitro* studies mentioned above, *in vivo* studies involving models of Parkinson's disease, epilepsy, and Alzheimer's disease have also been performed and have confirmed the neuroprotective effect of RA (Coelho et al., 2015; Khamse et al., 2015; Wang et al., 2012).

Wang et al. (2012) confirmed the results obtained by Ren et al. (2009) in a hydroxydopamine-induced Parkinson's disease model. In this study, the neuroprotective effect of RA against nigrostriatal neurodegeneration was demonstrated after RA intragastric administration for 21 days, with a reduction in iron levels in the substantia *nigra pars* and regulation of Bcl-2/Bax gene (apoptosis regulator) expression as a mechanism of action.

Regarding studies involving epilepsy, the neuroprotection of neuronal cells was also observed after RA intraperitoneal administration and intragastric administration for 7 days. The results of RA neuroprotective effect in these studies were mainly associated with the reduction of free radicals, DNA damage, and lipoperoxidation (Coelho et al., 2015; Khamse et al., 2015).

A recently developed study by Gok et al. (2018) evaluated the neuroprotective effect of RA intracerebroventricular injection over a period of 14 days in an *in vivo* model of Alzheimer's disease induced by bilateral injection of A β 42 peptide. The data showed and reinforced the neuroprotective effect of RA due to effects on the antioxidant-oxidant imbalance and cholinergic impairment, thus increasing cholinergic tonus, attenuating lipid peroxidation, and potentiating antioxidant defense (Gok et al., 2018).

Regarding the anti-inflammatory action of RA, an *in vivo* study demonstrated the neuroprotective effect of intraperitoneal administration of RA for 5 days on memory loss in a model of ischemia, correlated to a reduction in astrogliosis and improved expression of neurotrophic factors (Fonteles et al., 2016). Another *in vivo* study involving bone marrow lesions evaluated the neuroprotective effect of RA (intragastric administration for 7 days) in a model induced by laminectomy (Shang et al., 2017). The results demonstrated the neuroprotective effect of RA, possibly due to the regulation of pro-inflammatory cytokines (IL-6, IL-1b, TNF- α , and MCP-1) and associated with a reduction in ROS and modulated Nrf-2 expression.

As described above, most *in vivo* studies involving RA neuroprotection have been performed using intragastric administration. However, there have been several pharmacokinetic studies involving administered orally RA in the literature, demonstrating its poor oral bioavailability (Baba et al., 2004; Konishi et al., 2005; Nakazawa and Ohsawa, 1998; Shang et al., 2017; Wang et al., 2017; Yang et al., 2017).

Among the factors described and related to poor RA bioavailability are its poor solubility in water and inefficient membrane permeability (Casanova et al., 2016; Medronho et al., 2014). RA, as an ionizable strong acid (pKa 2.9), has a pH-dependent distribution coefficient, which can affect its solubility in bodily fluids or its permeability (Danaf et al., 2016; Hu and Li, 2011; Yang et al., 2015). Furthermore, *in vitro* studies in Caco-2 cells have demonstrated the poor permeability of RA (Konishi and Kobayashi, 2005; Yang et al., 2015). Despite conflicting results, the stability of RA has also been reported as an important factor related to its poor bioavailability, mainly following oral administration, when passage through the gastrointestinal tract occurs (Bel-Rhlid et al., 2009; da Silva et al., 2014; Gayoso et al., 2016).

Considering its poor water solubility, inefficient permeability through biological barriers, high instability, and consequently low bioavailability, new technological approaches for the administration of RA have been studied. Some strategies involve RA association/incorporation in cyclodextrins (Aksamija et al., 2016; Çelik et al., 2011; Medronho et al., 2014), phospholipid complexes (Yang et al., 2015), solid lipid nanoparticles (Bhatt et al., 2014; Campos et al., 2014, 2015, Madureira et al., 2016b, 2016a, 2015), and chitosan micro/nanoparticles (Casanova et al., 2016; da Silva et al., 2016, 2014), most of them aiming to improve oral absorption, bioavailability, and therapeutic efficacy. Among the recently demonstrated approaches designed to circumvent these problems, the use of nanotechnology-based delivery systems has emerged as a promising strategy (Cho and Borgens, 2012).

Table 3. *In vitro* and *in vivo* studies of rosmarinic acid (RA) neuroprotection found in the literature.

Treatment	Model	Main result	Neuroprotection mechanism	References
[RA] 14 – 56 μM (pre-treatment for 30 min)	<i>In vitro</i> model of H_2O_2 -induced neurotoxicity in SH-SY5Y (human dopaminergic neuronal cell line)	RA protective effect against neurotoxicity induced by oxidative stress	Regulation of apoptotic process and molecule hemeoxygenase 1	(Lee et al., 2008)
[RA] 1 – 100 $\mu\text{M.L}^{-1}$ (pre-treatment for 7 or 14 d)	<i>In vitro</i> model of oxidative stress, excitotoxicity and ischaemia–reperfusion injury in SH-SY5Y and SK-N-BE (human neuroblastoma)	RA protective effect in all <i>in vitro</i> models of neuronal death tested	Prevention of oxidative stress, intracellular Ca^{2+} overload, and expression of the c-fos gene	(Fallarini et al., 2009)
[RA] 0.01 – 0.1 mM.L^{-1} (pre-treatment for 24 h)	<i>In vitro</i> model of 6-hydroxydopamine-induced neurotoxicity in MES23.5 (dopaminergic cell line)	RA protective effect against neurotoxicity induced by 6-hydroxydopamine	Reduction of mitochondrial dysfunction and ROS production	(Ren et al., 2009)
[RA] 1 nM.L^{-1} (pre-treatment for 30 min)	<i>In vitro</i> model of neurotoxin MPP ⁺ induced neurotoxicity in MES23.5 (dopaminergic cell line)	RA protective effect against neurotoxicity induced by neurotoxin MPP ⁺	Improvement of mitochondrial dysfunction and reduction of apoptotic process	(Du et al., 2010)
[RA] 83.3 $\mu\text{M.L}^{-1}$ (treatment with H_2O_2 and RA for 24 h)	<i>In vitro</i> model of H_2O_2 -induced neurotoxicity in A172 (human astrocytes)	RA protective effect against neurotoxicity induced by oxidative stress	Reduction of accumulation of intracellular ROS	(Costa et al., 2013)
[RA] 2.8 – 280 $\mu\text{M.L}^{-1}$ (pre-treatment for 1 h)	<i>In vitro</i> model of neurotoxicity in human primary neuronal cells induced by ciguatoxin	RA potential reduction in neurotoxicity induced by ciguatoxin	Reduction of neuronal excitability	(Braidy et al., 2014)
[RA] 1 – 100 μM (pre-treatment for 12 h)	<i>In vitro</i> model of H_2O_2 -induced neurotoxicity in N2A (mouse neuroblastoma)	RA neuroprotective effect against neurotoxicity induced by oxidative stress	Reduction of lactate dehydrogenase disruption, mitochondrial dysfunction and intracellular ROS	(Ghaffari et al., 2014)
[RA] 0.5 – 5 mM (pre-treatment for 60 min)	<i>In vitro</i> models of antioxidant activity (ChEs, MAOs, COMT inhibition) and <i>in silico</i> approaches	RA showed <i>in vitro</i> multifunctional profile in targets related to neurodegeneration	Reduction in the levels of oxygen and nitrogen free radicals, and inhibition of lipid peroxidation, MAOs and COMT	(Andrade et al., 2016)
[RA] 0.5 – 10 $\mu\text{g.mL}^{-1}$ (treatment with H_2O_2 for 24 h, after treatment with RA for 24 h)	<i>In vitro</i> model of H_2O_2 -induced neurotoxicity in C6 glial cells	RA effect against neurotoxicity induced by oxidative stress	Reduction cell damage and lipid peroxidation, regulation of mRNA and expression of iNOS and COX-2	(Lee et al., 2016)

Table 3 continuation. *In vitro* and *in vivo* studies of rosmarinic acid (RA) neuroprotection found in the literature.

Treatment	Model	Main result	Neuroprotection mechanism	References
[RA] 20 mg.kg ⁻¹ (intragastric - treatment for 21 d, 1 adm/ day after Parkinson induction)	<i>In vivo</i> model of Parkinson's disease induced by 6-hydroxydopamine (Female Wistar rats 200–220 g)	RA neuroprotective effect against degeneration of nigrostriatal dopaminergic system	Reduction of nigral levels of iron and regulation of the expression of Bcl-2 / Bax gene.	(Wang et al., 2012)
[RA] 1, 2 or 4 mg.kg ⁻¹ (intraperitoneal - pre-treatment for 30 min, 1 adm)	<i>In vivo</i> model of epilepsy induced by pentylenetetrazole (Male CF1 mice 30–40 g)	RA neuroprotective effect against oxidative and DNA damage	Reduction of free radicals and DNA damage	(Coelho et al., 2015)
[RA] 10 mg.kg ⁻¹ (intragastric - pre-treatment for 7 d, 1 adm/ day)	<i>In vivo</i> model of temporal lobe epilepsy induced by kainic acid (Male Wistar rats 250–300 g)	RA neuroprotective effect preventing hippocampal neuronal loss	Reduction of free radicals and lipoperoxidation	(Khamse et al., 2015)
[RA] 0,1, 1 ou 20 mg.kg ⁻¹ (intraperitoneal - pre-treatment for 5 days, 1 adm/ day)	<i>In vivo</i> model of memory deficits induced by permanent middle cerebral artery occlusion (Male Swiss mice 25–30 g)	RA neuroprotective effect against memory deficits induced by cerebral ischemia	Reduction of astrogliosis and improvement of neurotrophic factors	(Fonteles et al., 2016)
[RA] 20 mg.kg ⁻¹ (intragastric - treatment for 7 d, 1 adm/ day after spinal cord injury induction)	<i>In vivo</i> model of spinal cord injury induced by Laminectomy (Male Wistar rats 250–275 g)	RA reverts effect of neurons apoptosis	Regulation of pro-inflammatory cytokines (IL-6, IL-1b, TNF-α, and MCP-1), reduction of ROS and modulation of expression of Nrf-2	(Shang et al., 2017)
[RA] 50 mg.kg ⁻¹ (treatment for 14 d, 1 adm/ day after intracerebroventricular injection)	<i>In vivo</i> model of Alzheimer's disease induced by bilateral injection of Aβ42 peptide (Male Wistar rats 250–300 g)	RA neuroprotective effect on antioxidant-oxidant imbalance and cholinergic damage	Increment cholinergic tone and suppression of oxidative stress via attenuating lipid peroxidation and potentiating antioxidant defence	(Gok et al., 2018)

[RA]: rosmarinic acid concentration; Nrf-2: nuclear factor erythroid 2; δ-ALA-D: Delta-aminolevulinic acid dehydratase; SOD: superoxide dismutase; CAT: catalase; TBARS: thiobarbituric acid reactive substances; MDA: malondialdehyde AChE: acetylcholine; t-BHP: t-butyl hydroperoxide; DPPH: 2,2-diphenyl-1-picrylhydrazyl; TNFα: tumour necrosis factor α; CCR3: complement component 3; HaCaT: immortalized nontumorigenic human epidermal cell line; GSH: glutathione; ROS: reactive oxygen species; AST: aspartate aminotransferase; ALT: alanine aminotransferase; H₂O₂: hydrogen peroxide; MPP⁺: 1-methyl-4-phenylpyridinium ion; ChE: cholinesterase, MAO: monoamine oxidase; COMT: catechol-O-methyl transferase; iNOS: inducible nitric oxide synthase; COX-2: cyclooxygenase-2; IL: interleukin; TNFα: tumour necrosis factor alpha; MCP-1: monocyte chemoattractant protein-1

3 RA- loaded nanotechnology-based delivery systems

Natural products have shown potential as therapeutic agents against various ND, although their performance may be less impressive partly due to their low bioavailability. In this sense, the use of nanotechnology-based delivery systems for natural products could overcome these limitations and increase therapeutic responses (Watkins et al., 2015). There are many studies demonstrating the benefits of encapsulation, such as increase in bioavailability (Bonifacio et al., 2014; Siddiqui and Sanna, 2016), targeting to specific tissues (Watkins et al., 2015), and controlled release (Kumari et al., 2012). Other benefits include the protection of volatile essential oils (Ansari et al., 2012), as well as reduction of cytotoxicity (Musthaba et al., 2009). The most commonly used nanostructures for drug delivery are polymer nanoparticles, solid lipid nanoparticles, nanostructured lipid carriers, liposomes, and nanoemulsions (Figure 2).

According to the literature, RA nanoencapsulation may improve solubility, stability, permeability across biological membranes, and bioavailability, crucial for RA therapeutic potential in ND. Overall, the possibility of targeting opens a prerogative for targets such as hard-to-reach tissues, like the brain.

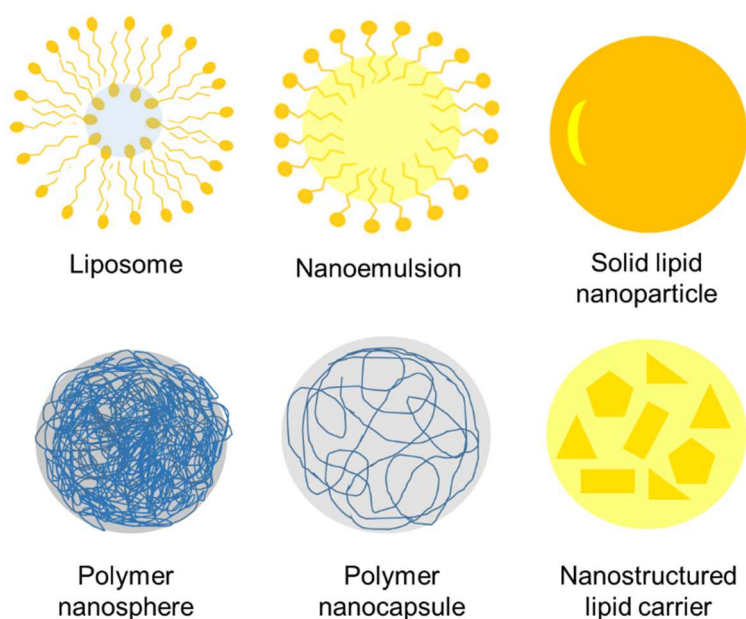


Figure 2. Nanotechnology-based delivery systems for natural products.

The first studies involving the use of nanotechnology aiming to increase the oral bioavailability of RA were developed by Campos et al. (2014) and Madureira et al., (2015) involving solid lipid nanoparticles (SLN). Campos et al. (2014) optimized RA-loaded SLN (0.15 mg/mL) using experimental design. A high association efficiency of RA (close to 99.8%) was noted for optimized formulations composed of 0.5% Witepsol® and 1-2% Tween® 80. Similar results were also observed when nanoparticles were composed of carnauba wax (Madureira et al., 2015). The optimum conditions that led to the most stable SLN was 1-1.5% carnauba wax and 2% Tween® 80. Comparing the physicochemical characteristics of RA SLN developed in both studies, the use of Witepsol® led to lower particle size diameters, despite having similar values of polydispersity index, zeta potential, and RA association efficiency. Following up these studies, Madureira et al. (2016a, 2016b) evaluated RA-loaded SLN in gastrointestinal conditions and observed that both SLN maintained RA antioxidant activity and presented a controlled release profile, with greater release under intestinal conditions; moreover, these authors demonstrated its safety through *in vitro* and *in vivo* studies (Madureira et al., 2016a, 2016b). In another study, the incorporation of a RA-rich plant extracts (*Salvia officinalis* or *Satureja montana*) in SLN composed of Witepsol® or carnauba wax was performed. RA incorporation (80%) in SLN ranging from 300 nm to 400 nm was reported for both extracts. In this study, the SLN from plant extracts were also tested under gastrointestinal conditions; the controlled release of RA was demonstrated for both formulations, although greater stability was observed for the Witepsol®-based SLN (Campos et al., 2015).

The incorporation of RA into nanotechnology-based delivery systems may bypass the inconvenience of the poor oral bioavailability of this phenolic acid. However, another barrier to the performance of rosmarinic acid is related to its poor availability in the CNS, which is significantly reduced in view of its limited ability to cross the blood-brain barrier (BBB), also described for other polyphenols (Kuo and Rajesh, 2017; Li et al., 2018; Szwajgier et al., 2017). The BBB is located at the level of the cerebral microvasculature and is critical for the maintenance of CNS homeostasis. Although it restricts the entry of potentially neurotoxic substances into the brain, it also represents an important obstacle for the delivery of therapeutic agents directly to the CNS, essential for neuroprotective therapies (Lochhead and Thorne, 2012; Mistry et al., 2009). Studies have demonstrated and confirmed that only a small amount of RA can

enter in intact form into the brain. However, its neuroprotective effect might be associated with its metabolites, which may more easily cross the BBB and also have therapeutic potential in ND (Li et al., 2018). Other studies suggest that phenolic acids can accumulate at nanomolar or micromolar concentrations, and even at this low concentration may be pharmacologically relevant (Szwajgier et al., 2017). Nevertheless, to overcome this limitation and increase RA bioavailability and activity in CNS, alternative approaches have been reported in the literature.

Kuo and Rajesh (2017) developed RA polyacrylamide-chitosan-poly(lactide-co-glycolide) nanoparticles (close to 140 nm) conjugated with cross-reacting material 197 and apolipoprotein E, and demonstrated BBB crossing aiming at Alzheimer's disease treatment. This approach rises as an alternative to RA delivery to the CNS.

On the other hand, nasal administration has emerged in recent years as a route of interest for the administration of compounds for delivery to the CNS, i.e. through the olfactory bulb, thereby circumventing the BBB (Costantino et al., 2007; Grassin-Delyle et al., 2012; Mackay-Sim and St John, 2011; Mujawar et al., 2014; Nakazawa and Ohsawa, 1998; Paun et al., 2010). In Figure 3, a schematic diagram demonstrates the possible mechanisms of drug absorption through the nose. The main advantages of this route are the rapid onset of the therapeutic effect due to the large surface area of the nasal mucosa, the absence of first-pass metabolism and non-invasiveness, and more pleasant experience for the patient (Costantino et al., 2007; Grassin-Delyle et al., 2012; Mujawar et al., 2014; Nakazawa and Ohsawa, 1998; Paun et al., 2010).

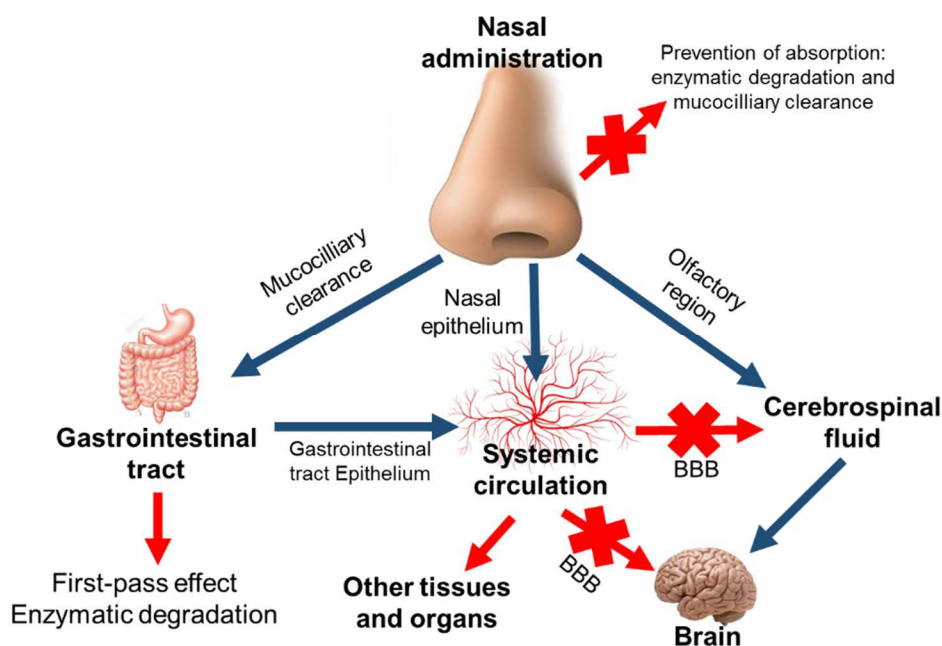


Figure 3. Schematic diagram demonstrating the mechanisms of drug absorption through the nose.

The first study involving the use of nanotechnology and the nasal route for RA delivery in ND was performed by Bhatt et al. (2014). In this study, RA-loaded SLN were developed aiming at the treatment of Huntington's disease. SLN composed of glyceryl monostearate stabilized by a mixture of surfactants (soy lecithin, Tween® 80 and hydrogenated soy phosphatidylcholine) were prepared by means of a hot homogenization technique. The procedure lead to monodisperse SLN (polydispersity index <math><0.29</math>) exhibiting a particle size close to 150 nm and an RA association efficiency higher than 60%. *In vivo* studies performed in a murine Huntington's disease model demonstrated the ability of RA-loaded SLN to attenuate motor and locomotor deficits as well as striatal oxidative stress. Pharmacokinetic studies comparing the nasal and intravenous routes for SLN administration were also performed by the same research group and demonstrated a higher effective brain concentration when RA was administered through the nasal route (Bhatt et al., 2014).

However, the main limitation for nasal absorption of active compounds is mucociliary clearance. The presence of cilia, i.e. small projections on the surface of epithelial cells, promotes the movement of mucus to the nasopharynx, followed by the rapid removal and replacement of mucus (Grassin-Delyle et al., 2012; Ugwoke et al., 2005).

Considering these limitations, some strategies have been assessed to improve the nasal absorption of drugs, such as the use of nanotechnology-based systems associated with mucoadhesive polymers to enhance drug penetration and increase residence time in the nasal mucosa (Casettari and Illum, 2014; Csaba et al., 2009; Eskandari et al., 2011; Kumar et al., 2008; Ong et al., 2014; Shinde et al., 2011; Ugwoke et al., 2005).

Our research group has been extensively studying lipid nanotechnology-based delivery systems, especially nanoemulsions, and has described the incorporation of active substances and water-insoluble plant extracts into these systems, aiming to increase their solubility and permeability through biological membranes (Argenta et al., 2014; Balestrin et al., 2016; Bruxel et al., 2012; Kelmann et al., 2008; Martini et al., 2007). However, due to the low viscosity of nanoemulsions, the association with mucoadhesive systems has been proposed to increase the direct absorption of natural compounds in the CNS following nasal delivery. Chitosan has been explored due to its interesting biological and physicochemical properties. It is a cationic polysaccharide derived from chitin with mucoadhesive properties related to the electrostatic interaction between the polymer and the sialic groups of mucin (Casettari and Illum, 2014; Fachel et al., 2018; Prego et al., 2006, 2005).

In this context, we recently developed and optimized chitosan-coated nanoemulsions (CNE) for RA nasal delivery, intended to be used as a potential neuroprotective therapy (Fachel et al., 2018). CNE containing RA ($1 \text{ mg}\cdot\text{mL}^{-1}$) with a mean size of $258.01 \pm 3.82 \text{ nm}$, a polydispersity index of 0.272 ± 0.01 , zeta potential of 44.98 ± 1.75 , and an association efficiency over 89% was achieved with medium chain triglycerides and egg lecithin (lipid phase) and obtained through an oil-in-water spontaneous emulsification procedure and further coating with chitosan. In addition, RA CNE presented *in vitro* mucoadhesive potential, extended drug release, and long-lasting permeation with greater retention at the porcine nasal mucosa, associated with a good safety profile determined using the MRC-5 cell line (normal human lung fibroblasts). These findings show that this system may be a suitable carrier for RA nasal delivery for neuroprotective therapies.

4 Conclusions

RA presents a variety of biological important activities, especially anti-inflammatory, through the prevention of oxidative neuronal damage or the modulation of pro-inflammatory cytokines and other signaling molecules. As many ND are related to the excessive production of ROS, inflammatory processes, and neurodegenerative damage, RA plays a role in the prevention of neurodegeneration or even in damage reduction. However, the poor oral bioavailability of RA represents a limitation in terms of pharmacodynamic outcomes after administration. In this sense, the formulation of RA encapsulated or complexed with nanotechnology-based delivery systems could enhance its solubility, protect it from degradation, allow it access to difficult-to reach tissues, and consequently improve its bioavailability. These formulations could be polymer or lipid-based, as long as the development is optimized to load a high but safe amount of RA. Although this formulation could circumvent some important limitations, nasal delivery could also be a pleasant route for CNS delivery, as it provides direct access to the CNS. Besides the advantages, there is a lack of studies demonstrating these combined approaches, which could produce such interesting results. In conclusion, considering the neuroprotective potential of RA discussed here, the use of nanotechnology-based therapy associated with the nasal route could represent a novel approach to ND treatment.

Conflicts of interest

The authors declare no conflict of interest.

Acknowledgments

Authors would like to thank Conselho Nacional de Desenvolvimento científico e Tecnológico (CNPq - processos 459619/2014-4; 310846/2014-5; 422298/2016-6), Fundação de Amparo à Pesquisa do Estado do Rio Grande do Sul (FAPERGS - processos 16/2551-0000265-7; 16/2551-0000473-0; 17/2551-0001273-9), and Coordenação de Aperfeiçoamento de Pessoal de Nível Superior - Brasil (CAPES - Finance Code 001) for the financial grants. F.N.S.F. and K.S.V. would like to thank CAPES and CNPq (GD#142202/2018-5) for the doctoral grant, and R.S.S. would like

to thank CNPq for the postdoctoral fellow (PDJ#151021/2018-0). V.L.B., L.S.K., A.T.H., E.B., and H.F.T. are recipients of CNPq research fellowship.

References

- Adomako-bonsu, A.G., Chan, S.L.F., Pratten, M., Fry, J.R., 2017. Toxicology *in vitro* antioxidant activity of rosmarinic acid and its principal metabolites in chemical and cellular systems : Importance of physico-chemical characteristics. *Toxicol. Vitr.* 40, 248–255. doi:10.1016/j.tiv.2017.01.016
- Aksamija, A., Polidori, A., Plasson, R., Dangles, O., Tomao, V., 2016. The inclusion complex of rosmarinic acid into beta-cyclodextrin : A thermodynamic and structural analysis by NMR and capillary electrophoresis. *Food Chem.* 208, 258–263. doi:10.1016/j.foodchem.2016.04.008
- Albarracin, S.L., Stab, B., Casas, Z., Sutachan, J.J., Samudio, I., Gonzalez, J., Gonzalo, L., Capani, F., Morales, L., Barreto, G.E., 2012. Effects of natural antioxidants in neurodegenerative disease. *Nutr. Neurosci.* 15, 1–9. doi:10.1179/1476830511Y.0000000028
- Amoah, S.K.S., Sandjo, L.P., Kratz, J.M., Biavatti, M.W., 2016. Rosmarinic acid - Pharmaceutical and clinical aspects. *Planta Med.* 82, 388–406. doi:10.1055/s-0035-1568274
- Andersen, J.K., 2004. Oxidative stress in neurodegeneration : cause or consequence ? *Nat. Rev.* 18–25. doi:10.1038/nrn1434
- Andrade, J.M. de, Passos, C. dos S., Rubio, M.A.K., Mendonça, J.N., Lopes, N.P., Henriques, A.T., 2016. Combining *in vitro* and *in silico* approaches to evaluate the multifunctional profile of rosmarinic acid from *Blechnum brasiliense* on targets related to neurodegeneration. *Chem. Biol. Interact.* 254, 135–145. doi:10.1016/j.cbi.2016.06.005
- Ansari, S.H., Islam, F., Sameem, M., 2012. Influence of nanotechnology on herbal drugs: A Review. *J. Adv. Pharm. Technol. Res.* 3, 142–146. doi:10.4103/2231-4040.101006
- Argenta, D.F., de Mattos, C.B., Misturini, F.D., Koester, L.S., Bassani, V.L., Simões, C.M.O., Teixeira, H.F., 2014. Factorial design applied to the optimization of lipid composition of topical antiherpetic nanoemulsions containing isoflavone genistein. *Int. J. Nanomedicine* 9, 4737–4747. doi:10.2147/IJN.S67732
- Baba, S., Osakabe, N., Natsume, M., Terao, J., 2004. Orally administered rosmarinic acid is present as the conjugated and/or methylated forms in plasma, and is degraded and metabolized to conjugated forms of caffeic acid, ferulic acid and m-coumaric acid. *Life Sci.* 75, 165–178. doi:10.1016/j.lfs.2003.11.028
- Bacanli, M., Aydin, S., Taner, G., Göktas, H.G., Sahin, T., Basaran, A.A., Basaran, N., 2016. Does rosmarinic acid treatment have protective role against sepsis-induced oxidative damage in Wistar Albino rats? *Hum. Exp. Toxicol.* 35. doi:10.1177/0960327115607971
- Balestrin, L.A., Bidone, J., Bortolin, R.C., Moresco, K., Moreira, J.C., Teixeira, H.F., 2016. Protective effect of a hydrogel containing *Achyrocline satureioides* extract-

loaded nanoemulsion against UV-induced skin damage. *J. Photochem. Photobiol. B Biol.* 163, 269–276. doi:10.1016/j.jphotobiol.2016.08.039

Barnham, K.J., Masters, C.L., Bush, A.I., 2004. Neurodegenerative diseases and oxidative stress. *Nat. Rev.* 3, 205–214. doi:10.1038/nrd1330

Bel-Rholid, R., Crespy, V., Pagé-Zoerkler, N., Nagy, K., Raab, T., Hansen, C.E., 2009. Hydrolysis of rosmarinic acid from rosemary extract with esterases and *Lactobacillus johnsonii* *in vitro* and in a gastrointestinal model. *J. Agric. Food Chem.* 57, 7700–7705. doi:10.1021/jf9014262

Bhat, A.H., Dar, K.B., Anees, S., Zargar, M.A., Masood, A., Sofi, M.A., Ganie, S.A., 2015. Oxidative stress, mitochondrial dysfunction and neurodegenerative diseases; a mechanistic insight. *Biomed. Pharmacother.* 74, 101–110. doi:10.1016/j.biopha.2015.07.025

Bhatt, R., Singh, D., Prakash, A., Mishra, N., 2014. Development, characterization and nasal delivery of rosmarinic acid-loaded solid lipid nanoparticles for the effective management of Huntington's disease. *Drug Deliv.* 1–9. doi:10.3109/10717544.2014.880860

Bhullar, K.S., Rupasinghe, H.P.V., 2013. Polyphenols: Multipotent therapeutic agents in neurodegenerative diseases. *Oxid. Med. Cell. Longev.* 2013, 1–18. doi:10.1155/2013/891748

Bonifacio, B.V., Silva, P.B. da, Ramos, M.A.D.S., Negri, K.M.S., Bauab, T.M., Chorilli, M., 2014. Nanotechnology-based drug delivery systems and herbal medicines: a review. *Int. J. Nanomedicine* 9, 1–15. doi:10.2147/IJN.S52634

Braidy, N., Matin, A., Rossi, F., Chinain, M., Laurent, D., Guillemin, G.J., 2014. Neuroprotective effects of rosmarinic acid on ciguatoxin in primary human neurons. *Neurotox. Res.* 226–234. doi:10.1007/s12640-013-9429-9

Brewer, M.S., 2011. Natural antioxidants: Sources, compounds, mechanisms of action, and potential applications. *Compr. Rev. Food Sci. Food Saf.* doi:10.1111/j.1541-4337.2011.00156.x

Bruxel, F., Laux, M., Wild, L.B., Fraga, M., Koester, L.S., 2012. Nanoemulsões como sistemas de liberação parenteral de fármacos. *Quim. Nova* 35, 1827–1840.

Bulgakov, V.P., Inyushkina, Y. V, Fedoreyev, S.A., 2012. Rosmarinic acid and its derivatives: biotechnology and applications. *Crit. Rev. Biotechnol.* 32, 203–217. doi:10.3109/07388551.2011.596804

Campos, D.A., Madureira, A.R., Gomes, A.M., Sarmiento, B., Pintado, M.M., 2014. Optimization of the production of solid Witepsol nanoparticles loaded with rosmarinic acid. *Colloids Surfaces B Biointerfaces* 115, 109–117. doi:10.1016/j.colsurfb.2013.10.035

Campos, D.A., Raquel, A., Sarmiento, B., Maria, A., Manuela, M., 2015. Stability of bioactive solid lipid nanoparticles loaded with herbal extracts when exposed to

simulated gastrointestinal tract conditions. *Food Res. Int.* 78, 131–140. doi:10.1016/j.foodres.2015.10.025

Cao, H., Cheng, W.-X., Li, C., Pan, X.-L., Xie, X.-G., Li, T.-H., 2005. DFT study on the antioxidant activity of rosmarinic acid. *J. Mol. Struct. THEOCHEM.* doi:10.1016/j.theochem.2005.01.029

Cao, W., Hu, C., Wu, L., Xu, L., Jiang, W., 2016. Rosmarinic acid inhibits inflammation and angiogenesis of hepatocellular carcinoma by suppression of NF- κ B signaling in H22 tumor-bearing mice. *J. Pharmacol. Sci.* 132. doi:10.1016/j.jphs.2016.09.003

Casanova, F., Estevinho, B.N., Santos, L., 2016. Preliminary studies of rosmarinic acid microencapsulation with chitosan and modified chitosan for topical delivery. *Powder Technol.* 297, 44–49. doi:10.1016/j.powtec.2016.04.014

Casetta, I., Govoni, V., Granieri, E., 2005. Oxidative stress, antioxidants and neurodegenerative diseases. *Curr. Pharm. Des.* 11, 2033–52. doi:10.2174/1381612054065729

Casettari, L., Illum, L., 2014. Chitosan in nasal delivery systems for therapeutic drugs. *J. Control. Release* 190, 189–200. doi:10.1016/j.jconrel.2014.05.003

Çelik, S.E., Özyürek, M., Tufan, A.N., Güçlü, K., Apak, R., 2011. Spectroscopic study and antioxidant properties of the inclusion complexes of rosmarinic acid with natural and derivative cyclodextrins. *Spectrochim. Acta Part A Mol. Biomol. Spectrosc.* 78, 1615–1624. doi:10.1016/j.saa.2011.02.017

Cho, Y., Borgens, R. Ben, 2012. Polymer and nano-technology applications for repair and reconstruction of the central nervous system. *Exp. Neurol.* 233, 126–144. doi:10.1016/j.expneurol.2011.09.028

Chu, X., Ci, X., He, J., Jiang, L., Wei, M., Cao, Q., Guan, M., Xie, X., Deng, X., He, J., 2012. Effects of a natural prolyl oligopeptidase inhibitor, rosmarinic acid, on lipopolysaccharide-induced acute lung injury in mice. *molecules* 17, 3586–3598. doi:10.3390/molecules17033586

Coelho, V.R., Vieira, C.G., de Souza, L.P., Moysés, F., Basso, C., Papke, D.K.M., Pires, T.R., Siqueira, I.R., Picada, J.N., Pereira, P., 2015. Antiepileptogenic, antioxidant and genotoxic evaluation of rosmarinic acid and its metabolite caffeic acid in mice. *Life Sci.* 122, 65–71. doi:10.1016/j.lfs.2014.11.009

Costa, P., Sarmiento, B., Gonçalves, S., Romano, A., 2013. Protective effects of *Lavandula viridis* L'Hér extracts and rosmarinic acid against H₂O₂-induced oxidative damage in A172 human astrocyte cell line. *Ind. Crops Prod.* 50, 361–365. doi:10.1016/j.indcrop.2013.07.054

Costantino, H.R., Illum, L., Brandt, G., Johnson, P.H., Quay, S.C., 2007. Intranasal delivery: Physicochemical and therapeutic aspects. *Int. J. Pharm.* 337, 1–24. doi:10.1016/j.ijpharm.2007.03.025

Csaba, N., Garcia-Fuentes, M., Alonso, M.J., 2009. Nanoparticles for nasal

vaccination. *Adv. Drug Deliv. Rev.* 61, 140–157. doi:10.1016/j.addr.2008.09.005

Cunningham, C., Campion, S., Lunnon, K., Murray, C.L., Woods, J.F.C., Deacon, R.M.J., Rawlins, J.N.P., Perry, V.H., 2009. Systemic inflammation induces acute behavioral and neurodegenerative disease. *Biol. Psychiatry* 65, 304–312. doi:10.1016/j.biopsych.2008.07.024

da Silva, S.B., Amorim, M., Fonte, P., Madureira, R., Ferreira, D., Pintado, M., Sarmiento, B., 2014. Natural extracts into chitosan nanocarriers for rosmarinic acid drug delivery. *Pharm. Biol.* 53, 642–652. doi:10.3109/13880209.2014.935949

da Silva, S.B., Ferreira, D., Pintado, M., Sarmiento, B., 2016. Chitosan-based nanoparticles for rosmarinic acid ocular delivery — *In vitro* tests. *Int. J. Biol. Macromol.* 84, 112–120. doi:10.1016/j.ijbiomac.2015.11.070

Danaf, N. Al, Melhem, R.A., Assaf, K.I., Nau, W.M., Digambara, P., 2016. Photophysical properties of neutral and dissociated forms of rosmarinic acid. *J. Lumin.* 175, 50–56. doi:10.1016/j.jlumin.2016.02.011

Ding, H., Chou, T., Liang, C., 2010. Antioxidant and antimelanogenic properties of rosmarinic acid methyl ester from *Origanum vulgare*. *Food Chem.* 123, 254–262. doi:10.1016/j.foodchem.2010.04.025

Domitrović, R., Škoda, M., Vasiljev Marchesi, V., Cvijanović, O., Pernjak Pugel, E., Štefan, M.B., 2013. Rosmarinic acid ameliorates acute liver damage and fibrogenesis in carbon tetrachloride-intoxicated mice. *Food Chem. Toxicol.* 51, 370–378. doi:10.1016/j.fct.2012.10.021

Du, T., Li, L., Song, N., Xie, J., Jiang, H., 2010. Rosmarinic acid antagonized 1-methyl-4-phenylpyridinium (MPP⁺)-induced neurotoxicity in MES23.5 dopaminergic cells. *Int. J. Toxicol.* 29, 625–633. doi:10.1177/1091581810383705

Eskandari, S., Varshosaz, J., Minaiyan, M., Tabbakhian, M., 2011. Brain delivery of valproic acid via intranasal administration of nanostructured lipid carriers: *in vivo* pharmacodynamic studies using rat electroshock model. *Int. J. Nanomedicine* 6, 363–371. doi:10.2147/IJN.S15881

Fachel, F.N.S., Medeiros-Neves, B., Dal Prá, M., Schuh, R.S., Veras, K.S., Bassani, V.L., Koester, L.S., Henriques, A.T., Braganhol, E., Teixeira, H.F., 2018. Box-Behnken design optimization of mucoadhesive chitosan-coated nanoemulsions for rosmarinic acid nasal delivery—*In vitro* studies. *Carbohydr. Polym.* 199, 572–582. doi:10.1016/j.carbpol.2018.07.054

Fadel, O., El Kirat, K., Morandat, S., 2011. The natural antioxidant rosmarinic acid spontaneously penetrates membranes to inhibit lipid peroxidation *in situ*. *Biochim. Biophys. Acta* 1808, 2973–2980. doi:10.1016/j.bbamem.2011.08.011

Fallarini, S., Miglio, G., Paoletti, T., Minassi, a., Amoruso, a., Bardelli, C., Brunelleschi, S., Lombardi, G., 2009. Clovamide and rosmarinic acid induce neuroprotective effects in *in vitro* models of neuronal death. *Br. J. Pharmacol.* 157, 1072–1084. doi:10.1111/j.1476-5381.2009.00213.x

Fernando, P.M.D.J., Piao, M.J., Kang, K.A., Ryu, Y.S., Hewage, S.R.K.M., Chae, S.W., Hyun, J.W., 2016. Rosmarinic acid attenuates cell damage against UVB radiation-induced oxidative stress via enhancing antioxidant effects in human HaCaT cells. *Biomol. Ther.* 24, 75–84. doi:10.4062/biomolther.2015.069

Fischer, R., Maier, O., 2015. Interrelation of oxidative stress and inflammation in neurodegenerative disease : Role of TNF. *Oxid. Med. Cell. Longev.* 2015, 1–18.

Fonteles, A.A., de Souza, C.M., De souza, J.C.N., Menezes, A.P.F., Carmo, M.R. dos S., Fernandes, F.D.P., de Araújo, P.R., de Andrade, G.M., 2016. Rosmarinic acid prevents against memory deficits in ischemic mice. *Behav. Brain Res.* 297, 91–103.

Fujimoto, A., Masuda, T., 2012. Antioxidation mechanism of rosmarinic acid , identification of an unstable quinone derivative by the addition of odourless thiol. *Food Chem.* 132, 901–906. doi:10.1016/j.foodchem.2011.11.062

Gayoso, L., Claerbout, A.S., Calvo, M.I., Cavero, R.Y., Astiasarán, I., Ansorena, D., 2016. Bioaccessibility of rutin, caffeic acid and rosmarinic acid: Influence of the *in vitro* gastrointestinal digestion models. *J. Funct. Foods* 26, 428–438. doi:10.1016/j.jff.2016.08.003

Ghaffari, H., Venkataramana, M., Ghassam, B.J., Chandra Nayaka, S., Nataraju, a, Geetha, N.P., Prakash, H.S., 2014. Rosmarinic acid mediated neuroprotective effects against H₂O₂-induced neuronal cell damage in N2A Cells. *Life Sci.* 113, 7–13. doi:10.1016/j.lfs.2014.07.010

Gil, E.D.S., Enache, T.A., Oliveira-brett, A.M., 2013. Redox behaviour of verbascoside and rosmarinic acid. *Comb. Chem. High Throughput Screen.* 1, 92–97.

Gok, D.K., Hidisoglu, E., Ocak, G.A., Er, H., Acun, A.D., Yargıoğlu, P., 2018. Protective role of rosmarinic acid on amyloid beta 42-induced echoic memory decline: Implication of oxidative stress and cholinergic impairment. *Neurochem. Int.* 118, 1–13. doi:10.1016/j.neuint.2018.04.008

Goldsmith, M., Abramovitz, L., Peer, D., 2014. Precision nanomedicine in neurodegenerative diseases. *ACS Nano* 8, 1958–1965. doi:10.1021/nn501292z

Grassin-Delyle, S., Buenestado, A., Naline, E., Faisy, C., Blouquit-Laye, S., Couderc, L.J., Le Guen, M., Fischler, M., Devillier, P., 2012. Intranasal drug delivery: An efficient and non-invasive route for systemic administration - Focus on opioids. *Pharmacol. Ther.* 134, 366–379. doi:10.1016/j.pharmthera.2012.03.003

Habtemariam, S., 2018. Molecular pharmacology of rosmarinic and salvianolic acids: Potential seeds for Alzheimer's and vascular dementia drugs. *Int. J. Mol. Sci.* 19. doi:10.3390/ijms19020458

Hu, M., Li, X., 2011. *Bioavailability: basic principles, advanced concepts and applications*, 1st ed. New Jersey: John Wiley & Sons.

Huang, S., Zheng, R., 2006. Rosmarinic acid inhibits angiogenesis and its mechanism of action *in vitro*. *Cancer Lett.* 239, 271–280. doi:10.1016/j.canlet.2005.08.025

- Kelmann, R.G., Kuminek, G., Teixeira, H.F., Koester, L.S., 2008. Preliminary study on the development of nanoemulsions for carbamazepine intravenous delivery: an investigation of drug polymorphic transition. *Drug Dev. Ind. Pharm.* 34, 53–58. doi:10.1080/03639040701506387
- Kelsey, N. a., Wilkins, H.M., Linseman, D. a., 2010. Nutraceutical antioxidants as novel neuroprotective agents. *Molecules* 15, 7792–7814. doi:10.3390/molecules15117792
- Khamse, S., Sadr, S.S., Roghani, M., Hasanzadeh, G., Mohammadian, M., 2015. Rosmarinic acid exerts a neuroprotective effect in the kainate rat model of temporal lobe epilepsy: Underlying mechanisms. *Pharm. Biol.* 53, 1818–25. doi:10.3109/13880209.2015.1010738
- Khojasteh, A., Mirjalili, M.H., Hidalgo, D., Corchete, P., Palazon, J., 2014. New trends in biotechnological production of rosmarinic acid. *Biotechnol. Lett.* 2393–2406. doi:10.1007/s10529-014-1640-0
- Kim, G.-D., Park, Y.S., Jin, Y.-H., Park, C.-S., 2015. Production and applications of rosmarinic acid and structurally related compounds. *Appl. Microbiol. Biotechnol.* 99, 2083–2092. doi:10.1007/s00253-015-6395-6
- Kim, H.K., Lee, J.J., Lee, J.S., Park, Y.-M., Yoon, T.R., 2008. Rosmarinic acid down-regulates the LPS-induced production of monocyte chemoattractant protein-1 (MCP-1) and macrophage inflammatory protein-1alpha (MIP-1alpha) via the MAPK pathway in bone-marrow derived dendritic cells. *Mol. Cells* 26, 583–589.
- Konishi, Y., Hitomi, Y., Yoshida, M., Yoshioka, E., 2005. Pharmacokinetic study of caffeic and rosmarinic acids in rats after oral administration. *J. Agric. Food Chem.* 53, 4740–4746. doi:10.1021/jf0478307
- Konishi, Y., Kobayashi, S., 2005. Transepithelial transport of rosmarinic acid in intestinal Caco-2 cell monolayers. *Biosci. Biotechnol. Biochem.* doi:10.1271/bbb.69.583
- Koppula, S., Kumar, H., More, S.V., Kim, B.W., Kim, I.S., Choi, D.K., 2012. Recent advances on the neuroprotective potential of antioxidants in experimental models of Parkinson's disease. *Int. J. Mol. Sci.* 13, 10608–10629. doi:10.3390/ijms130810608
- Ku, S.-K., Yang, E.-J., Song, K.-S., Bae, J.-S., 2013. Rosmarinic acid down-regulates endothelial protein C receptor shedding *in vitro* and *in vivo*. *Food Chem. Toxicol.* 59, 311–315. doi:10.1016/j.fct.2013.06.003
- Kumar, M., Misra, A., Babbar, a. K., Mishra, a. K., Mishra, P., Pathak, K., 2008. Intranasal nanoemulsion based brain targeting drug delivery system of risperidone. *Int. J. Pharm.* 358, 285–291. doi:10.1016/j.ijpharm.2008.03.029
- Kumari, A., Kumar, V., Yadav, S.K., 2012. Nanotechnology: A tool to enhance therapeutic values of natural plant products. *Trends Med. Res.* 7, 34–42.
- Kuo, Y.C., Rajesh, R., 2017. Targeted delivery of rosmarinic acid across the blood–brain barrier for neuronal rescue using polyacrylamide-chitosan-poly(lactide-co-

glycolide) nanoparticles with surface cross-reacting material 197 and apolipoprotein E. *Int. J. Pharm.* 528, 228–241. doi:10.1016/j.ijpharm.2017.05.039

Lecomte, J., Giraldo, L.J.L., Laguerre, M., Baréa, B., Villeneuve, P., 2010. Synthesis, characterization and free radical scavenging properties of rosmarinic acid fatty esters. *J. Am. Oil Chem. Soc.* 87, 615–620. doi:10.1007/s11746-010-1543-8

Lee, A.Y., Wu, T.T., Hwang, B.R., Lee, J., Lee, M., Lee, S., Cho, E.J., 2016. The neuroprotective effect of the methanolic extract of *Perilla frutescens* var . japonica and rosmarinic acid against H₂O₂ -induced oxidative stress in C6 glial cells. *Biomol. Ther.* 24, 338–345. doi:10.4062/biomolther.2015.135

Lee, H.J., Cho, H.-S., Park, E., Kim, S., Lee, S.-Y., Kim, C.-S., Kim, D.K., Kim, S.-J., Chun, H.S., 2008. Rosmarinic acid protects human dopaminergic neuronal cells against hydrogen peroxide-induced apoptosis. *Toxicology* 250, 109–115. doi:10.1016/j.tox.2008.06.010

Lee, J., Jung, E., Kim, Y., Lee, J., Park, J., Hong, S., Hyun, C.-G., Park, D., Kim, Y.S., 2006. Rosmarinic acid as a downstream inhibitor of IKK-beta in TNF-alpha-induced upregulation of CCL11 and CCR3. *Br. J. Pharmacol.* 148, 366–75. doi:10.1038/sj.bjp.0706728

Lembo, S., Balato, A., Caprio, R. Di, Cirillo, T., Giannini, V., Gasparri, F., Monfrecola, G., 2014. The Modulatory effect of ellagic acid and rosmarinic acid on ultraviolet-B-induced cytokine / chemokine gene expression in skin keratinocyte (HaCaT) cells. *Biomed Res. Int.* 346793, 1–8. doi:10.1155/2014/346793

Li, S., Xie, X., Li, D., Yu, Z., Tong, L., Zhao, Y., 2018. Simultaneous determination and tissue distribution studies of four phenolic acids in rat tissue by UFLC–MS/MS after intravenous administration of salvianolic acid for injection. *Biomed. Chromatogr.* 32, 1–9. doi:10.1002/bmc.4128

Liang, Z., Xu, Y., Wen, X., Nie, H., Hu, T., Yang, X., 2016. Rosmarinic acid attenuates airway inflammation and hyperresponsiveness in a murine model of asthma. *Molecules* 11. doi:10.3390/molecules21060769

Liu, Z., Zhou, T., Ziegler, A.C., Dimitrion, P., Zuo, L., 2017. Oxidative stress in neurodegenerative diseases: From molecular mechanisms to clinical applications. *Oxid. Med. Cell. Longev.* 2017, 1–11. doi:10.1155/2017/2525967

Lochhead, J.J., Thorne, R.G., 2012. Intranasal delivery of biologics to the central nervous system. *Adv. Drug Deliv. Rev.* 64, 614–628. doi:10.1016/j.addr.2011.11.002

Losada-Barreiro, S., Bravo-Díaz, C., 2017. Free radicals and polyphenols: The redox chemistry of neurodegenerative diseases. *Eur. J. Med. Chem.* 133, 379–402. doi:10.1016/j.ejmech.2017.03.061

Lull, M.E., Block, M.L., 2010. Microglial activation and chronic neurodegeneration. *Neurotherapeutics* 7, 354–365. doi:10.1016/j.nurt.2010.05.014

Mackay-Sim, A., St John, J.A., 2011. Olfactory ensheathing cells from the nose:

Clinical application in human spinal cord injuries. *Exp. Neurol.* 229, 174–180. doi:10.1016/j.expneurol.2010.08.025

Madureira, A.R., Campos, D.A., Fernandes, J.C., Marques, C., Gullón, B., Rodríguez-alcalá, L.M., Calhau, C., Maria, A., Manuela, M., Reis, F., 2016a. Safety profile of solid lipid nanoparticles loaded with rosmarinic acid for oral use: *in vitro* and animal approaches. *Int. J. Nanomedicine* 11, 3621–3640. doi:10.2147/IJN.S104623

Madureira, A.R., Campos, D.A., Fonte, P., Nunes, S., Reis, F., Gomes, A.M., Sarmiento, B., Pintado, M.M., 2015. Characterization of solid lipid nanoparticles produced with carnauba wax for rosmarinic acid oral delivery. *RSC Adv.* 5, 22665–22673. doi:10.1039/C4RA15802D

Madureira, A.R., Campos, D.A., Oliveira, A., Sarmiento, B., Pintado, M.M., Gomes, A.M., 2016b. Insights into the protective role of solid lipid nanoparticles on rosmarinic acid bioactivity during exposure to simulated gastrointestinal conditions. *Colloids Surfaces B Biointerfaces* 139, 277–284. doi:10.1016/j.colsurfb.2015.11.039

Martini, É., Carvalho, E., Teixeira, H., Leão, F., De Oliveira, M.C., 2007. Adsorção de oligonucleotídeos em nanoemulsões obtidas por emulsificação espontânea. *Quim. Nova* 30, 930–934. doi:10.1590/S0100-40422007000400032

Medronho, B., Valente, A.J.M., Costa, P., 2014. Inclusion complexes of rosmarinic acid and cyclodextrins: stoichiometry, association constants, and antioxidant potential. *Colloid Polym. Sci.* 292, 885–894. doi:10.1007/s00396-013-3124-5

Mistry, A., Stolnik, S., Illum, L., 2009. Nanoparticles for direct nose-to-brain delivery of drugs. *Int. J. Pharm.* 379, 146–157. doi:10.1016/j.ijpharm.2009.06.019

Mujawar, N., Ghatage, S., Navale, S., Sankpal, B., Patil, S., 2014. Nasal Drug Delivery: Problem Solution and Its Application. *J. Curr. Pharma Res.* 4, 1231–1245.

Muñoz-Muños, J., Garcia-Molina, F., Ros, E., Tudela, J., García-Casanovas, F., Rodríguez-Lopez, J., 2013. Prooxidant and antioxidant activities of rosmarinic. *J. Food Biochem.* 37, 396–408. doi:10.1111/j.1745-4514.2011.00639.x

Mushtaq, N., Schmatz, R., Ahmed, M., Pereira, L.B., Costa, P., Reichert, K.P., Dalenogare, D., Pelinson, L.P., Bellumori, M., Morsch, V.M., Schetinger, M.R., 2015. Protective effect of rosmarinic acid against oxidative stress biomarkers in liver and kidney of streptozotocin-induced diabetic rats. *J. Physiol. Biochem.* 71, 743–751. doi:10.1007/s13105-015-0438-4

Mushtaq, N., Schmatz, R., Pereira, L.B., Ahmad, M., Stefanello, N., Vieira, J.M., Abdalla, F., Rodrigues, M. V, Baldissarelli, J., Pelinson, L.P., Dalenogare, D.P., Reichert, K.P., Dutra, E.M., Mulinacci, N., Innocenti, M., Bellumori, M., Morsch, V.M., Schetinger, M.R., 2014. Rosmarinic acid prevents lipid peroxidation and increase in acetylcholinesterase activity in brain of streptozotocin-induced diabetic rats. *Cell Biochem. Funct.* 287–293. doi:10.1002/cbf.3014

Musthaba, S.M., Baboota, S., Ahmed, S., Ahuja, A., Ali, J., 2009. Status of novel drug delivery technology for phytotherapeutics. *Expert Opin. Drug Deliv.* 6, 625–637. doi:10.1517/17425240902980154

Naito, Y., Oka, S., Yoshikawa, T., 2003. Inflammatory response in the pathogenesis of atherosclerosis and its prevention by rosmarinic acid, a functional ingredient of rosemary. *Food Factors Heal. Promot. Dis. Prev.* 208–212. doi:10.1021/bk-2003-0851.ch018

Nakazawa, T., Ohsawa, K., 1998. Metabolism of rosmarinic acid in rats. *J. Nat. Prod.* doi:10.1021/np980072s

Ong, W., Shalini, S., Costantino, L., 2014. Nose-to-brain drug delivery by nanoparticles in the treatment of neurological disorders. *Curr. Med. Chem.* 21, 4247–4256.

Osakabe, N., Takano, H., Sanbongi, C., Yasuda, A., Yanagisawa, R., Inoue, K., Yoshikawa, T., 2004a. Anti-inflammatory and anti-allergic effect of rosmarinic acid (RA); inhibition of seasonal allergic rhinoconjunctivitis (SAR) and its mechanism. *Biofactors* 21, 127–131. doi:10.1093/carcin/bgh034

Osakabe, N., Yasuda, A., Natsume, M., Sanbongi, C., Kato, Y., Osawa, T., Yoshikawa, T., 2002. Rosmarinic acid, a major polyphenolic component of *Perilla frutescens*, reduces lipopolysaccharide (LPS)-induced liver injury in D-galactosamine (D-GalN)-sensitized mice. *Free Radic. Biol. Med.* 33, 798–806. doi:10.1016/S0891-5849(02)00970-X

Osakabe, N., Yasuda, A., Natsume, M., Yoshikawa, T., 2004b. Rosmarinic acid inhibits epidermal inflammatory responses: Anticarcinogenic effect of *Perilla frutescens* extract in the murine two-stage skin model. *Carcinogenesis* 25, 549–557. doi:10.1093/carcin/bgh034

Paun, J.S., Bagada, a a, Raval, M.K., 2010. Nasal drug delivery – As an effective tool for brain targeting - A review. *Int. J. Pharm. Appl. Sci.* 1, 43–55.

Pérez-Hernández, J., Zaldívar-Machorro, V.J., Villanueva-Porras, D., Vega-Ávila, E., Chavarría, A., 2016. A potential alternative against neurodegenerative diseases. *Oxid. Med. Cell. Longev.* 1–19. doi:10.1155/2016/8378613

Pérez-Tortosa, V., López-Orenes, A., Martínez-Pérez, A., Ferrer, M.A., Calderón, A.A., 2012. Antioxidant activity and rosmarinic acid changes in salicylic acid-treated *Thymus membranaceus* shoots. *Food Chem.* 130, 362–369. doi:10.1016/j.foodchem.2011.07.051

Perry, V.H., 2004. The influence of systemic inflammation on inflammation in the brain : implications for chronic neurodegenerative disease. *Brain, Behav. Immun.* 18, 407–413. doi:10.1016/j.bbi.2004.01.004

Petersen, M., 2013. Rosmarinic acid : new aspects. *Phytochem. Rev.* 12, 207–227. doi:10.1007/s11101-013-9282-8

Petersen, M., Abdullah, Y., Benner, J., Eberle, D., Gehlen, K., Hücherig, S., Janiak, V.,

Kim, K.H., Sander, M., Weitzel, C., Wolters, S., 2009. Evolution of rosmarinic acid biosynthesis. *Phytochemistry*. doi:10.1016/j.phytochem.2009.05.010

Petersen, M., Simmonds, M.S.J., 2003. Rosmarinic acid. *Phytochemistry* 62, 121–125. doi:10.1016/S0031-9422(02)00513-7

Pietsch, K., Saul, N., Chakrabarti, S., Stu, S.R., Menzel, R., Steinberg, C.E.W., 2011. Hormetins , antioxidants and prooxidants : defining quercetin- , caffeic acid- and rosmarinic acid-mediated life extension in *C . elegans*. *Biogerontology* 12, 329–347. doi:10.1007/s10522-011-9334-7

Prego, C., Fabre, M., Torres, D., Alonso, M.J., 2006. Efficacy and mechanism of action of chitosan nanocapsules for oral peptide delivery. *Pharm. Res.* 23, 549–556. doi:10.1007/s11095-006-9570-8

Prego, C., García, M., Torres, D., Alonso, M.J., 2005. Transmucosal macromolecular drug delivery. *J. Control. Release* 101, 151–162. doi:10.1016/j.jconrel.2004.07.030

Pspotova, J., Svobodova, A., Kolarova, H., Walterova, D., 2006. Photoprotective properties of *Prunella vulgaris* and rosmarinic acid on human keratinocytes. *J. Photochem. Photobiol. B Biol.* 84, 167–174. doi:10.1016/j.jphotobiol.2006.02.012

Rahbardar, M.G., Amin, B., Mehri, S., Mirnajafi-Zadeh, S.J., Hosseinzadeh, H., 2017. Anti-inflammatory effects of ethanolic extract of *Rosmarinus officinalis* L . and rosmarinic acid in a rat model of neuropathic pain. *Biomed. Pharmacother.* 86, 441–449.

Ramassamy, C., 2006. Emerging role of polyphenolic compounds in the treatment of neurodegenerative diseases: A review of their intracellular targets. *Eur. J. Pharmacol.* 545, 51–64. doi:10.1016/j.ejphar.2006.06.025

Ren, P., Jiang, H., Li, R., Wang, J., Song, N., Xu, H.M., Xie, J.X., 2009. Rosmarinic acid inhibits 6-OHDA-induced neurotoxicity by anti-oxidation in MES23.5 cells. *J. Mol. Neurosci.* 39, 220–225. doi:10.1007/s12031-009-9182-y

Rocha, J., Eduardo-figueira, M., Barateiro, A., Fernandes, A., Brites, D., Bronze, R., Duarte, C.M.M., 2015. Anti-inflammatory effect of rosmarinic acid and an extract of *Rosmarinus officinalis* in rat models of local and systemic inflammation. *Basic Clin. Pharmacol. Toxicol.* 116, 398–413. doi:10.1111/bcpt.12335

Sánchez-campillo, M., Gabaldon, J.A., Castillo, J., Benavente-garcía, O., Baño, M.J. Del, Alcaraz, M., Vicente, V., Alvarez, N., Lozano, J.A., 2009. Rosmarinic acid, a photo-protective agent against UV and other ionizing radiations. *Food Chem. Toxicol.* 47, 386–392. doi:10.1016/j.fct.2008.11.026

Scarpati, M.L., Oriente, G., 1958. Isolamento e costituzione dell'acido rosmarinico (dal *rosmarinus off.*). *Ric Sci* 28, 2329–2333.

Scheckel, K. a, Degner, S.C., Romagnolo, D.F., 2008. Rosmarinic Acid Antagonizes activator protein-1 – dependent activation of cyclooxygenase-2 expression in human cancer. *J. Nutr.* 2098–2107. doi:10.3945/jn.108.090431.)

Schuh, R., Baldo, G., Teixeira, H., 2016. Nanotechnology applied to treatment of mucopolysaccharidoses. *Expert Opin. Drug Deliv.* 13, 1709–1718. doi:10.1080/17425247.2016.1202235

Sevgi, K., Tepe, B., Sarikurkcu, C., 2015. Antioxidant and DNA damage protection potentials of selected phenolic acids. *Food Chem. Toxicol.* 77, 12–21.

Shang, A.-J., Yang, Y., Wang, H.-Y., Tao, B.-Z., Wang, J., Wang, Z.-F., Zhou, D.-B., 2017. Spinal cord injury effectively ameliorated by neuroprotective effects of rosmarinic acid. *Nutr. Neurosci.* 20, 172–179. doi:10.1080/1028415X.2015.1103460

Shinde, R.L., Jindal, A.B., Devarajan, P. V., 2011. Microemulsions and nanoemulsions for targeted drug delivery to the brain. *Curr. Nanosci.* 7, 119–133. doi:10.2174/157341311794480282

Siddiqui, I.A., Sanna, V., 2016. Impact of nanotechnology on the delivery of natural products for cancer prevention and therapy. *Mol. Nutr. Food Res.* 60, 1330–1341. doi:10.1002/mnfr.201600035

Solanki, I., Parihar, P., Parihar, M.S., 2016. Neurodegenerative diseases: From available treatments to prospective herbal therapy. *Neurochem. Int.* 95, 100–108. doi:10.1016/j.neuint.2015.11.001

Soobrattee, M. a., Neergheen, V.S., Luximon-Ramma, A., Aruoma, O.I., Bahorun, T., 2005. Phenolics as potential antioxidant therapeutic agents: Mechanism and actions. *Mutat. Res. - Fundam. Mol. Mech. Mutagen.* 579, 200–213. doi:10.1016/j.mrfmmm.2005.03.023

Sood, S., Jain, K., Gowthamarajan, K., 2014. Intranasal therapeutic strategies for management of Alzheimer's disease. *J. Drug Target.* 22, 279–94. doi:10.3109/1061186X.2013.876644

Swarup, V., Ghosh, J., Ghosh, S., Saxena, A., Basu, A., 2007. Antiviral and Anti-Inflammatory effects of rosmarinic acid in an experimental murine model of Japanese encephalitis. *Antimicrob. Agents Chemother.* 51, 3367–3370. doi:10.1128/AAC.00041-07

Szwajgier, D., Borowiec, K., Pustelniak, K., 2017. The neuroprotective effects of phenolic acids: Molecular mechanism of action. *Nutrients* 9, 1–21. doi:10.3390/nu9050477

Takeda, H., Tsuji, M., Inazu, M., Egashira, T., Matsumiya, T., 2002. Rosmarinic acid and caffeic acid produce antidepressive-like effect in the forced swimming test in mice. *Eur. J. Pharmacol.* 449, 261–267. doi:S0014-2999(02)02037-X

Tepe, B., Eminagaoglu, O., Akpulat, H.A., Aydin, E., 2007. Antioxidant potentials and rosmarinic acid levels of the methanolic extracts of *Salvia verticillata* (L.) subsp. *verticillata* and *S. verticillata* (L.) subsp. *amasiaca* (Freyn & Bornm.) Bornm. *Food Chem.* 100, 985–989. doi:10.1016/j.foodchem.2005.10.062

Ugwoke, M.I., Agu, R.U., Verbeke, N., Kinget, R., 2005. Nasal mucoadhesive drug

delivery: Background, applications, trends and future perspectives. *Adv. Drug Deliv. Rev.* 57, 1640–1665. doi:10.1016/j.addr.2005.07.009

Uttara, B., Singh, A. V, Zamboni, P., Mahajan, R.T., 2009. Oxidative stress and neurodegenerative diseases: a review of upstream and downstream antioxidant therapeutic options. *Curr. Neuropharmacol.* 7, 65–74. doi:10.2174/157015909787602823

Wang, J., Li, G., Rui, T., Kang, A., Li, G., Fu, T., Li, J., Cai, B., 2017. Pharmacokinetics of rosmarinic acid in rats by LC- MS / MS: absolute bioavailability and dose proportionality. *RSC Adv.* 7, 9057–9063. doi:10.1039/C6RA28237G

Wang, J., Wen, L.-L., Huang, Y., Chen, Y., Ku, M., 2006. Dual effects of antioxidants in neurodegeneration: Direct neuroprotection against oxidative stress and indirect protection via suppression of glia-mediated inflammation. *Curr. Pharm. Des.* 12, 3521–3533.

Wang, J., Xu, H., Jiang, H., Du, X., Sun, P., Xie, J., 2012. Neurorescue effect of rosmarinic acid on 6-hydroxydopamine-lesioned nigral dopamine neurons in rat model of Parkinson's disease. *J. Mol. Neurosci.* 47, 113–119. doi:10.1007/s12031-011-9693-1

Watkins, R., Wu, L., Zhang, C., Davis, R.M., Xu, B., 2015. Natural product-based nanomedicine: recent advances and issues. *Int. J. Nanomedicine* 10, 6055–6074. doi:10.2147/IJN.S92162

Wyss-coray, T., Mucke, L., 2002. Inflammation in Neurodegenerative Disease — A Double-Edged Sword. *Neuron* 35, 419–432.

Yang, J., Zhang, L., Li, J., Chen, L., Zheng, Q., Chen, T., Chen, Z., Fu, T., Di, L., 2015. Enhanced oral bioavailability and prophylactic effects on oxidative stress and hepatic damage of an oil solution containing a rosmarinic acid – phospholipid complex. *J. Funct. Foods* 19, 63–73. doi:10.1016/j.jff.2015.09.013

Yang, J.H., Mao, K.J., Huang, P., Ye, Y.J., Guo, H.S., Cai, B.C., 2017. Effect of piperine on the bioavailability and pharmacokinetics of rosmarinic acid in rat plasma using UPLC-MS/MS. *Xenobiotica* 0, 1–8. doi:10.1080/00498254.2017.1292564

Yanishlieva, N. V, Marinova, E., Pokorny, J., 2006. Natural antioxidants from herbs and spices. *Eur. J. Lipid Sci. Technol.* 108, 776–793. doi:10.1002/ejlt.200600127

Zdařilová, A., Svobodová, A., Šimánek, V., Ulrichová, J., 2009. *Prunella vulgaris* extract and rosmarinic acid suppress lipopolysaccharide-induced alteration in human gingival fibroblasts. *Toxicol. Vitr.* 23, 386–392. doi:10.1016/j.tiv.2008.12.021

Zhang, Y., Chen, X., Yang, L., Zu, Y., Lu, Q., 2015. Effects of rosmarinic acid on liver and kidney antioxidant enzymes, lipid peroxidation and tissue ultrastructure in aging mice. *Food Funct.* 6, 927–931. doi:10.1039/C4FO01051E

Zhu, F., Asada, T., Sato, A., Koi, Y., Nishiwaki, H., Tamura, H., 2014. Rosmarinic acid extract for antioxidant, antiallergic, and α - glucosidase inhibitory activities, isolated by

supramolecular technique and solvent extraction from *Perilla* leaves. J. Agric. Food Chem. 62, 885–892. doi:10.1021/jf404318j

Introdução

O segundo capítulo desta tese apresenta um artigo científico sobre o desenvolvimento e a validação de um método analítico e bioanalítico por cromatografia líquida de ultra eficiência (CLUE) para determinação do ácido rosmarínico (AR). Atualmente, há um crescente interesse no desenvolvimento de novas formulações tópicas contendo AR, especialmente, devido à sua atividade antioxidante bem documentada. Para tanto, o desenvolvimento e validação de métodos específicos, precisos e rápidos para identificação e quantificação desse composto reveste-se de especial importância. Apesar de existirem métodos descritos na literatura para determinação do AR, em sua maioria tratam-se de métodos por cromatografia líquida de alta eficiência (CLAE) para extratos vegetais, com eluição no modo gradiente e um longo período de análise. Para contornar essas desvantagens, o uso de técnicas de cromatografia líquida de alto rendimento, como CLUE, tem sido proposta. Na literatura, poucos artigos relatam o uso destas técnicas para a quantificação do AR, sendo esta a primeira vez em que a utilização da técnica por CLUE é reportada para determinação do AR em sistemas nanoestruturados lipídicos e em amostras biológicas. Neste contexto, o presente capítulo teve por objetivo desenvolver e validar um método sensível, simples, rápido e indicativo de estabilidade por CLUE para a quantificação de AR em nanoemulsões, assim como, em mucosa nasal suína visando aplicação em estudos de permeação/retenção.

Artigo científico:

A novel, simplified and stability-indicating high-throughput ultra-fast liquid chromatography method for the determination of rosmarinic acid in nanoemulsions, porcine skin and nasal mucosa

Publicado no *Journal of Chromatography B*, 2018

A novel, simplified and stability-indicating high-throughput ultra-fast liquid chromatography method for the determination of rosmarinic acid in nanoemulsions, porcine skin and nasal mucosa

Flávia N.S. Fachel, Marina C. Nemitz, Bruna Medeiros-Neves, Kleyton S. Veras, Valquíria L. Bassani, Letícia S. Koester, Amelia T. Henriques, and Helder F. Teixeira*

Programa de Pós-Graduação em Ciências Farmacêuticas, Faculdade de Farmácia, Universidade Federal do Rio Grande do Sul, Av. Ipiranga 2752, CEP 90610-000, Porto Alegre, RS, Brazil.

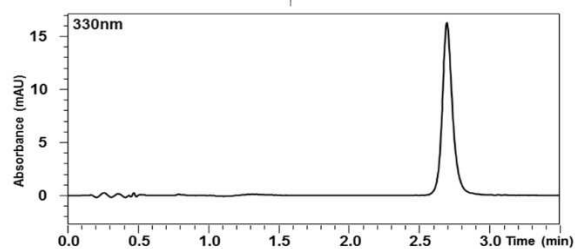
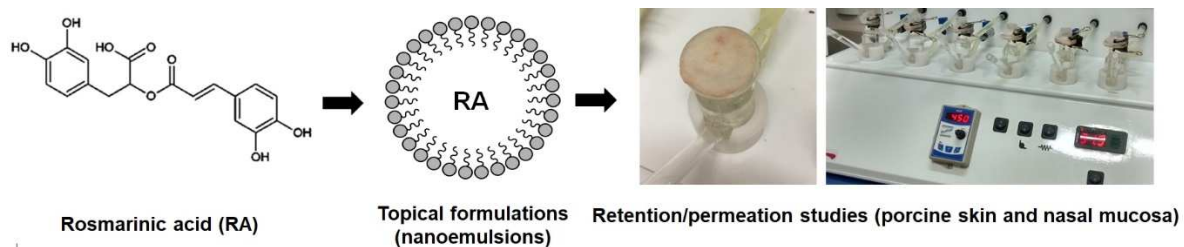
*Corresponding author. Tel.: (+55) 51 3308 5231; fax: (+55) 51 3308 2165. E-mail address: helder.teixeira@ufrgs.br (Helder Ferreira Teixeira).

Abstract

Currently, there is an increasing interest on the development of topical formulations containing rosmarinic acid (RA) due to its well-documented antioxidant activity. This study aimed to develop and validate a stability-indicating ultra-fast liquid chromatography (UFLC) method for the determination of RA in nanoemulsions, porcine skin and nasal mucosa intended to be applied in permeation/retention studies and for development of topical nanoemulsions. Chromatographic separation was carried out using a C18 column packed with 2.6 μm particle size in isocratic conditions using as mobile phase water:acetonitrile (83:17, v/v), acidified with 0.1% trifluoroacetic acid (v/v), with a total time of analysis of 3.5 min and detection at 330 nm. RA analysis was specific in the presence of both non-biological (blank nanoemulsion and receptor fluid) and biological matrices (porcine ear skin and porcine nasal mucosa). No interference of degradation products of RA was verified after different stress conditions such as acidic, alkaline, oxidative, light exposure (UV-A and UV-C) and thermal demonstrating the method stability-indicating property. The analytical (0.1–10.0 $\mu\text{g}\cdot\text{mL}^{-1}$) and bioanalytical (0.5–10.0 $\mu\text{g}\cdot\text{mL}^{-1}$) linearity was proved by analysis of the standard curves of RA and no matrix effect was observed. The method was sensitive, precise and accurate, and showed recovery higher than 85%. The method was considered robust as evaluated by a Plackett-Burman experimental design. In the validated conditions, the RA was determined in the nanoemulsions obtained by spontaneous emulsification procedure ($1.007 \pm 0.040 \text{ mg}\cdot\text{mL}^{-1}$), porcine ear skin ($1.13 \pm 0.19 \mu\text{g}\cdot\text{cm}^{-2}$) and nasal mucosa ($22.46 \pm 3.99 \mu\text{g}\cdot\text{cm}^{-2}$) after retention/permeation studies. Thus, a highly sensitive, simple, fast and stability-indicating method was developed for RA analysis during the development of topical nanoemulsions and bioanalytical assays in complex matrices.

Key-words: Rosmarinic acid; Stability-indicating UFLC method; Skin; Nasal mucosa; Topical nanoemulsions; Retention/permeation studies.

Graphical abstract



Determination of rosmarinic acid by an UFLC stability-indicating method

1 Introduction

Rosmarinic acid (RA) is a polyphenolic compound, an ester of caffeic acid and 3,4-dihydroxyphenyllactic acid, commonly found in species from the Boraginaceae and Lamiaceae family [1,2]. It was first isolated from *Rosmarinus officinalis* L. and has various biological activities reported, including antiviral, antimicrobial, anti-tumoral, anti-inflammatory and antioxidant properties. Among these activities, a well-documented literature reports the ability of RA in protecting skin and brain against the damage caused by reactive species of oxygen [1–5]. Recently, the incorporation of RA into polymeric- and lipid-nanotechnology-based delivery systems has been proposed aiming to improve the RA stability and its permeability through biological membranes [6–10].

The development and validation of analytical methods for the accurate identification and quantification of bioactive compounds in analytical and/or bioanalytical samples with absence of interference of degradation products is a key consideration in the pharmaceutical development field [11,12]. Analytical assay of RA was mainly focused on its determination in plant extracts by high-pressure liquid chromatography (HPLC) [13–25], mainly due to advantages in terms of sensitivity, specificity and accuracy of this technique, although most of them operates in gradient mode and require a quite long period of time of analysis (normally upper than 14 min). The use of high-throughput liquid chromatography technologies has been proposed to circumvent these drawbacks, reducing the time of analysis, and consequently decreasing the environmental impact by reducing solvent consumption [26,27]. Only few approaches employing these technologies are available for RA assay in *Symphytum officinale* L. [28], Shengxiong glucose injections [29] and *Perilla frutescens* (L.) Britt. [30]. Bioanalytical assay of RA was also found in some studies mainly focused in beagle, pig, and rat plasma [15,29,31]. However, none stability-indicating method was found for RA.

Our research group has been recently interested in the development of topical nanoemulsions as delivery systems for RA. Nanoemulsions have been considered as a potential lipid-nanotechnology-based delivery system for topical administration and improvement of permeability and stability of poorly-soluble molecules. Such systems are nanodispersion of oily droplets in an external aqueous phase, stabilized by an

appropriate surfactant system [32–35]. Thus, in this study we have described for the first time the development and validation of a fast and an isocratic stability-indicating UFLC analytical and bioanalytical method for RA assay in pharmaceutical nanoemulsions, as well as in porcine ear skin and nasal mucosa intended to be used in further retention/permeation studies for topical formulations development.

2 Material and methods

2.1 Materials and reagents

The reference standard of RA with a purity over than 98% was purchased from Carbosynth Ltd. (Berkshire, UK). Liquid Chromatography grade methanol, acetonitrile and trifluoroacetic acid were obtained from Tedia (Rio de Janeiro, Brazil). Ultra-pure water used in UFLC was produced using a Milli-Q apparatus (Millipore, Billerica, USA). Medium chain triglycerides (MCT) and egg-lecithin (Lipoid E-80[®]) were purchased from Lipoid GmbH (Ludwigshafen, Germany). Potassium phosphate monobasic and dibasic were obtained from Nuclear (CAQ, São Paulo, Brazil). Porcine ears and porcine nasal mucosa were supplied from a local slaughterhouse (Ouro do Sul – Cooperativa dos Suinocultores do Caí Superior Ltda., Harmonia, Brazil).

2.2 Instrumentation and UFLC conditions

The RA analyses were performed using a Shimadzu Prominence series UFLC system equipped with a temperature controlled automatic injector, a photodiode array (PDA) detector and an LC solutions software for data processing (Kyoto, Japan). Chromatographic separation was carried out in a Kinetex C18 column (100 x 2.1 mm i.d.; particle size, 2.6 μm ; Phenomenex, USA) guarded by a pre-column filter in-line Ultra (Phenomenex, USA) at 55 $^{\circ}\text{C}$. The mobile phase was composed of water and acetonitrile (83:17, v/v) with pH approximately 2.5, acidified with 0.1% trifluoroacetic acid (v/v), filtered through a 0.22 μm porous nylon membrane and degassed under vacuum, set at isocratic mode up to 3.5 min. The samples were kept at 4 $^{\circ}\text{C}$ in the auto-sampler, and a volume of 3 μL was injected. Eluent system was pumped at a flow rate of 0.55 $\text{mL}\cdot\text{min}^{-1}$ and detection wavelength was set to 330 nm.

2.3 Solutions

2.3.1 Preparation of standard solutions

A RA stock solution ($1 \text{ mg}\cdot\text{mL}^{-1}$) was obtained by weighting accurately 10 mg of rosmarinic acid into a 10 mL calibrated volumetric flask, dissolved in methanol. Standard solutions were obtained from the dilutions of an adequate aliquot of stock in water/acetonitrile mixture (80:20; v:v). The stock and diluted standard solutions were kept in darkness at $4 \pm 2 \text{ }^\circ\text{C}$.

2.3.2 Preparation of matrices solutions

2.3.2.1 Nanoemulsions

RA loaded-nanoemulsions (NE_{RA}) were prepared by spontaneous emulsification procedure as previously described by our research group [35]. The final formulations were composed by RA 0.1% (w/v), medium chain triglycerides 8.0% (w/v), egg lecithin 2.0% (w/v), and water up to 100%. The oil components were dissolved in ethanol, and after were poured into the water phase under magnetic stirring. Subsequently, a process of evaporation at $40 \text{ }^\circ\text{C}$ under reduced pressure removed the organic solvent and concentrated RA up to $1 \text{ mg}\cdot\text{mL}^{-1}$. RA amount in nanoemulsions were determined diluting appropriate aliquots of nanoemulsion in a water/acetonitrile mixture (80:20; v:v), filtered by $0.22 \text{ }\mu\text{m}$ nylon syringes filter. Blank nanoemulsions (NE_{B}) were prepared in similar conditions in the absence of RA.

2.3.2.2 Porcine ear skin and nasal mucosa

The porcine ear skin (PES) was excised from the outer region of the porcine ear and stored at $-20 \text{ }^\circ\text{C}$ until use, for up to a maximum of one month. To the extraction procedure, the PES (surface area $1.80 \pm 0.02 \text{ cm}^2$, thickness $1.0 \pm 0.1 \text{ mm}$) was reduced to tiny pieces and placed in different test tubes, 2 mL of methanol were added on the tubes and the samples were maintained in an ultrasound bath for 45 min.

The porcine nasal mucosa (PNM) was carefully removed from the nasal turbinates obtained by an incision along the nasal septum of the porcine heads, as previously described by Barbi et al. (2014) [36]. The PNM was stored at $-20 \text{ }^\circ\text{C}$ until use, for up to a maximum of one month. For extraction procedure, the PNM (surface area $1.80 \pm$

0.02 cm²) was reduced to tiny pieces and placed in different test tubes, 4 mL of methanol were added on the tubes and the samples were maintained in an ultrasound bath for 120 min. Appropriate aliquots of PES and PNM solutions were filtered by 0.22 µm nylon syringes filter, and then analyzed.

2.3.2.3 Receptor fluid for retention/permeation studies

Potassium phosphate buffer pH 7.4 and 5.8 were chosen to be the receptor fluid (RF) for the retention skin and nasal permeation studies, respectively. Appropriate aliquots of RF were filtered by 0.22 µm nylon syringes filter, and then analyzed.

2.4 UFLC method validation

The UFLC developed method was fully validated in terms of specificity/selectivity, linearity, matrix effect, precision, accuracy, extraction recovery, and stability, according to the official guidelines, that is: ICH specifications [37] for the validation of analytical procedure in non-biological matrices (nanoemulsion and receptor fluid), and the EMA and FDA recommendations [38,39] for the validation of bioanalytical procedure in biological matrices (porcine skin and nasal mucosa tissue). Analysis of variance (ANOVA) and Student's t test were used to analyze the results using a significance level of $\alpha = 0.05$.

2.4.1 System suitability

System suitability tests were performed to verify the adequacy of the chromatographic system for the analysis. The parameters of peak area, retention time, theoretical plates and tailing factor of RA were measured and evaluated [40].

2.4.2 Specificity and forced degradation

The specificity was determined by comparing chromatograms obtained for pure standard RA solution, matrices spiked with RA at the concentration of 10 µg·mL⁻¹ and solutions containing only the matrices (blank samples). In order to verify the presence or absence of interferences from matrices, the peak corresponding to RA was analyzed and identified in each spiked matrix by UV spectra between 250 and 370 nm, peak purity and retention time.

Forced degradation protocols were also performed. The stock RA standard solutions were submitted to acid and alkaline hydrolysis, oxidative stress, photolytic and temperature degradation. Briefly, acid hydrolysis was investigated by adding Hydrochloric acid (HCl) to the standard solutions to achieve the final concentration of 1.0 M. Alkaline hydrolysis was investigated by adding Sodium hydroxide (NaOH) to the standard solutions to achieve the final concentration of 0.0015 M. After different periods of exposure, both solutions were neutralized with base and acid, respectively. To assess oxidative stress condition hydrogen peroxide (H₂O₂) 30% was added in the standard solutions. In order to prevent temperature and photolytic degradation in these conditions, all solutions were kept in room temperature (25 °C) and protected from light. The effect of light exposure was performed in an UV-A (center of emission 360 nm, bandwidth 40 nm) and an UV-C (center of emission 254 nm) chambers with controlled temperature (25 °C). The standard solution was transferred into 1 cm² disposable cuvettes fixed to the chambers in a horizontal position, and exposed to radiation. To assess temperature degradation, standard solutions were exposed to dry heat at 70 °C. After removal from degradation conditions in pre-established times (not exceeding 30 h), the samples were prepared for analysis by diluting to 10 µg·mL⁻¹ with the mobile phase, and analyzed determining the peak purity of RA using a PDA detector. All solutions were filtered through a 0.22 µm nylon syringes filter.

2.4.3 Linearity

Three standard curves were obtained by plotting the measured peak area versus the concentration of RA standard in non-biological matrices (0.1, 2.0, 4.0, 6.0, 8.0, and 10.0 µg·mL⁻¹) and in biological matrices (0.5, 2.0, 4.0, 6.0, 8.0, and 10.0 µg·mL⁻¹), by six replicates per concentration in three consecutive days. The method linearity was evaluated by regression analysis using the least square method, and the curves were described in the form of $y = ax + b$. The limit of detection and the limit of quantitation (LOD and LOQ, respectively) were determined from the slope and the standard deviation of the response of the calibration curves. The lower LOQ (LLOQ) for the analyte RA was considered the lowest concentration which could be quantitatively determined with precision and accuracy ≤20%.

2.4.4 Matrix effect

The matrix effect was assessed by the comparison of slopes of each standard curve obtained in biological and non-biological matrices during the linearity assay (Section 2.4.3) and the slope of pure RA standard curve.

2.4.5 Precision and accuracy

The precision was determined as both repeatability and intermediate precision, and expressed as the relative standard deviations (% RSD) for each level of RA. The intra-day precision (repeatability) was obtained by analysing RA at four levels in the presence of non-biological (0.1, 2.0, 6.0, 10.0 $\mu\text{g}\cdot\text{mL}^{-1}$) and biological (0.5, 2.0, 6.0, 10.0 $\mu\text{g}\cdot\text{mL}^{-1}$) matrices, with six determinations per concentration within a day. The inter-day precision (intermediate precision) was evaluated by assaying RA samples of the same concentration levels on three different days.

The accuracy was determined by means of assays carried out by adding known amounts of the RA standard at four different levels (0.1 or 0.5, 2.0, 6.0, 10.0 $\mu\text{g}\cdot\text{mL}^{-1}$) to the post extraction matrices. Samples were analyzed in six replicates at each level. The accuracy was evaluated as the standardized correlation between the experimental value and the theoretical value, as follows: formula $\text{RE \%} = (\text{mean experimental concentration} \times 100 / \text{mean theoretical concentration})$.

2.4.6 Stability

RA-spiked non-biological and biological matrices were processed and stored in the UFLC vials at ambient temperature (25^o C), intending to overestimate the time consumed during routine analysis. The stability was determined by performing the analysis of peak area and observing any change in the chromatographic pattern of the stored samples compared with a freshly prepared sample.

2.4.7 Robustness

The Plackett-Burman design was used to investigate the robustness in each matrix. The selected factors were: column oven temperature (54; 56 °C), flow rate (0.54; 0.56 $\text{mL}\cdot\text{min}^{-1}$), TFA concentration (0.08; 0.12%), and organic composition (16.5; 17.5%). The four factors were analyzed in low levels (-1) and high levels (+1), and were tested

with eight experiments designed in accordance with Heyden et al. (2001) [41]. The responses were evaluated in terms of percentages of RA in the matrices obtained in relation to the standard solution through statistical interpretation (t-test). The method was considered robust when t_{calc} was lower than t_{critical} of the experiment.

2.4.8 Extraction recovery of RA from porcine skin and nasal mucosa

The recovery of RA was evaluated from porcine skin or nasal mucosa spiked with RA at four levels (0.5, 2.0, 6.0, 10.0 $\mu\text{g}\cdot\text{mL}^{-1}$) and submitted to a subsequent extraction procedure. For this, biological matrices and the known amounts of RA were added in separate test tubes. Then, methanol was also added, and the samples were maintained in an ultrasound bath for 45 min for porcine skin or 120 min for nasal mucosa, filtered through a 0.22 μm nylon syringes filter and quantified by UFLC. The recovery was expressed as percentages, determined comparing the theoretical final concentration based on the value added in each tube and the experimental result obtained after extraction procedure.

2.5 Skin and nasal retention/permeation studies

Franz type diffusion cells, which presented a diffusion surface area of approximately 1.80 cm^2 and a receptor volume of 12.0 mL, were used to evaluate the RA retention/permeation studies. The excised circular PES and PNM were prepared as described in Section 2.3.2.2 and previously immersed in potassium phosphate buffer pH 7.4 and 5.8 solution, respectively, during 30 min. PES and PNM membranes were mounted between the donor and receptor compartments (Section 2.3.2.3). The bathing solution was stirred at 450 rpm and kept under a controlled temperature of 32 ± 1.0 °C in skin retention studies and of 34 ± 1.0 °C in nasal mucosa permeation studies. In the donor compartment about 500 μL of NE_{RA} (0.1% w/v or 1 $\text{mg}\cdot\text{mL}^{-1}$), prepared as described in Section 2.3.2.1, were placed maintaining the sink conditions. After 8 h, an aliquot of RF was collected, and the skin or nasal mucosa was cleaned using a cotton swab, removed from the cell and extracted as described in Section 2.3.2.2. Appropriate aliquots of all samples were filtered by 0.22 μm nylon syringes filter, and then analyzed by the UFLC method.

3 Results and discussion

3.1 Development of UFLC method

RA has been analyzed using different methodologies of detection and quantification [13–25]. Most of them are time-consuming chromatographic separation methods and mainly focused on the RA assay in plant extracts. In this study, UFLC was selected based on its ability to promote ultra-high-speed analysis and high precision, therefore increasing analysis cost-efficiency [26]. A C₁₈ column packed with 2.6 µm particle size was chosen considering the evaluation of the performance obtained for analysis of isolated RA. Acetonitrile and 0.1% (v/v) trifluoroacetic acid were chosen because their chromatographic performance and ability to ensure the ionization suppression of RA during the analysis. The optimization of chromatographic conditions was assessed testing different isocratic elution systems (Table 1) adapted from a previous gradient HPLC method using the same mobile phase [17]. High temperature and high flow rates (Method J) were needed to allow the system to maintain an adequate pressure and to obtain a faster time of analysis (RA retention time: 2.65 min; total run time: 3.50 min). The wavelength at 330 nm was selected once it was the maximum UV absorption for RA under these conditions. The RA chromatogram obtained by the developed method is shown in Fig. 1 and the most important chromatography parameters are presented in Table 2.

Table 1

Tested systems for optimization of chromatographic conditions.

Isocratic elution systems	Organic phase (% v/v)	Flow rate (mL.min ⁻¹)	Temperature (°C)
Method A	25	0.35	35
Method B	25	0.40	40
Method C	23	0.40	40
Method D	23	0.45	45
Method E	21	0.45	45
Method F	21	0.50	45
Method G	19	0.45	50
Method H	19	0.50	55
Method I	17	0.50	55
Method J	17	0.55	55

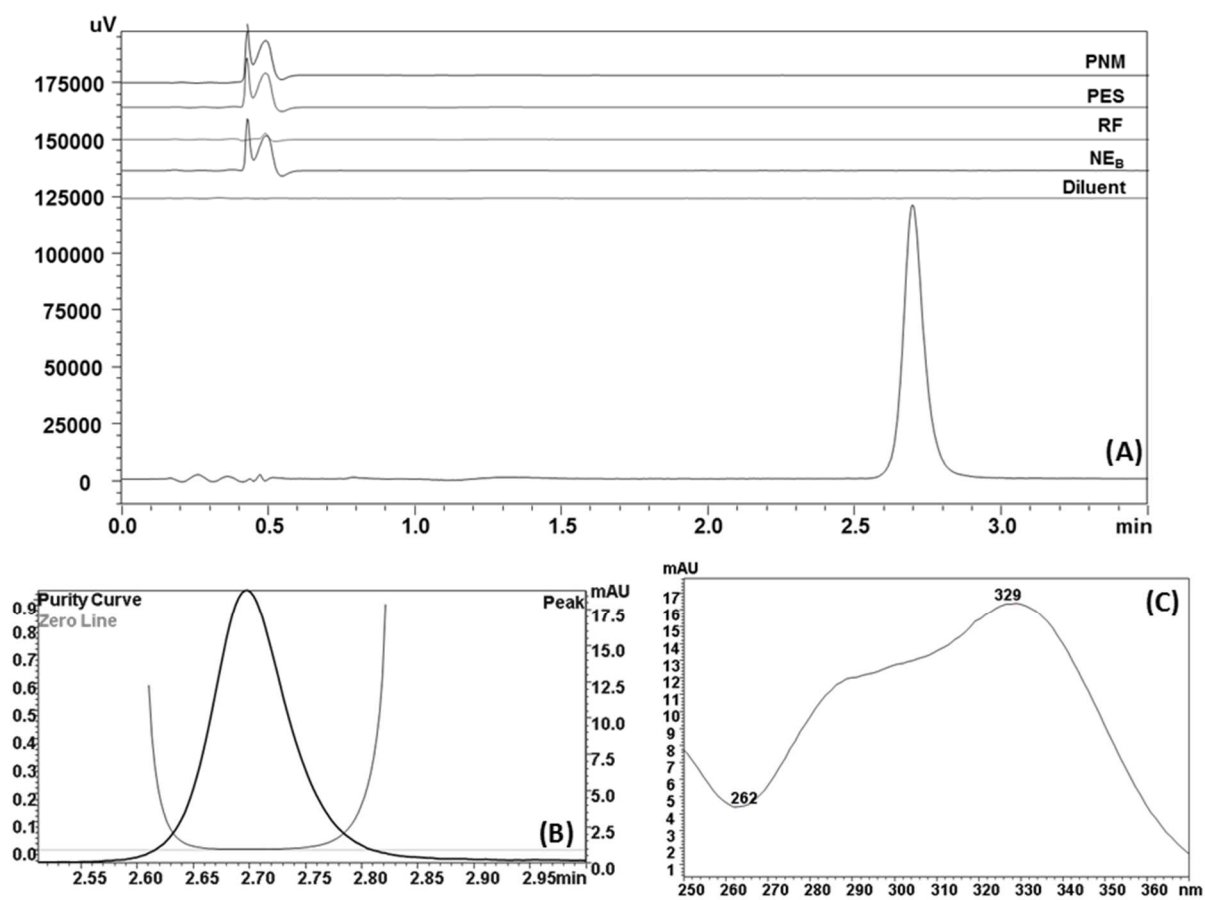
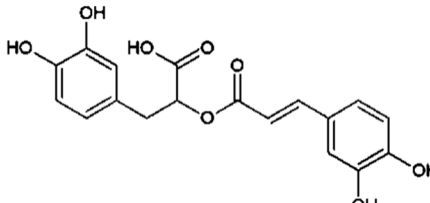


Fig. 1

(A) Chromatographic profiles obtained in rosmarinic acid (RA) standard at $10 \mu\text{g}\cdot\text{mL}^{-1}$ and blank samples (specificity in the different matrices), (B) purity curve, and (C) UV spectrum of RA obtained by UFLC at 330 nm. Where, PNM: porcine nasal mucosa, PES: porcine ear skin, RF: receptor fluid (pH 5.8), NE_B: blank nanoemulsion, Diluent: mobile phase.

Table 2

System suitability testing of RA standard.

Compound	Chemical Structure	RT	N	T
RA		2.65	6503.35	1.222

RT: retention time (min); T: tailing factor; N: theoretical plates; RA: rosmarinic acid.

The method herein developed is the first that improves an isocratic system for pure RA analysis and for the development of RA-loaded nanoemulsions with shorter runtimes in comparison with previous literature [13–25,30]. Concerning RA determination in biological matrices only few studies stated the development and validation of bioanalytical methods, although, none of them studied RA application in porcine skin and nasal mucosa retention/permeation assays [15,29,31,42].

3.2 UFLC method validation

3.2.1 System suitability

The standard RA routine analysis was achieved under the conditions of UFLC developed method. The parameters values and their relative standard deviation (RSD, %) for RA analysis (Table 2) was: 2.65 (0.163) min, 6503.35 (0.500), and 1.22 (0.253) for retention time, theoretical plates and tailing factor, respectively. In summary, the results for each parameter demonstrated that the system is suitable for RA analysis, according to Shabir, 2003.

3.2.2 Specificity and forced degradation

The peak purity data from RA evaluation in spiked-matrices demonstrated that the method was specific for the RA assay even in the presence of complex matrices. Moreover, no co-eluting substances from matrices were detected at the same retention time of RA (Fig. 1). Thus, these results show that the method is specific for RA determination in nanoemulsions, as well as in receptor fluid, porcine skin and nasal mucosa during permeation/retention studies.

The method ability for accurately estimate RA with absence of interference of degradation products is very important during the development of products, especially for stability or bioanalytical studies. In this sense, the stability-indicating properties of UFLC method were also evaluated. RA standard solutions were exposed to acid, alkaline, oxidative, photolytic and thermal stress conditions and further analysed. When submitted to oxidative stress and UV-A light at 25 °C during 24 h no significant changes in RA amounts were observed. In contrast, when the RA standard solutions were exposed to acid (4 h), alkaline (15 min), UV-C light (24 h) and high temperature (30 h) conditions, RA degraded $17.2 \pm 1.1\%$, $19.8 \pm 2.7\%$, $15.0 \pm 2.9\%$ and $18.3 \pm 3.0\%$, respectively. On the opposite, previous literature has showed that the RA did not

degrade appreciably over light and temperature exposure [43] that could be related with the stress experimental conditions used in this study. It is also important to highlight that all RA peaks after stress conditions presented appropriate purity, demonstrating that the degradation products are not co-eluting with them.

Nevertheless, it could only be observed in the chromatograms the degradation products of alkaline and dry heat conditions. As can be seen in Fig. 2 and 3, the peaks corresponding to these degradation products are efficiently separated from the RA peak (resolution > 3.0). The maximum UV absorptions of degradation products visualized in chromatograms were 266/328 for alkaline degradation product and 270/323 for thermal degradation product. According to these results the developed method can be considered adequate for studies concerning RA even in the presence of degradation products.

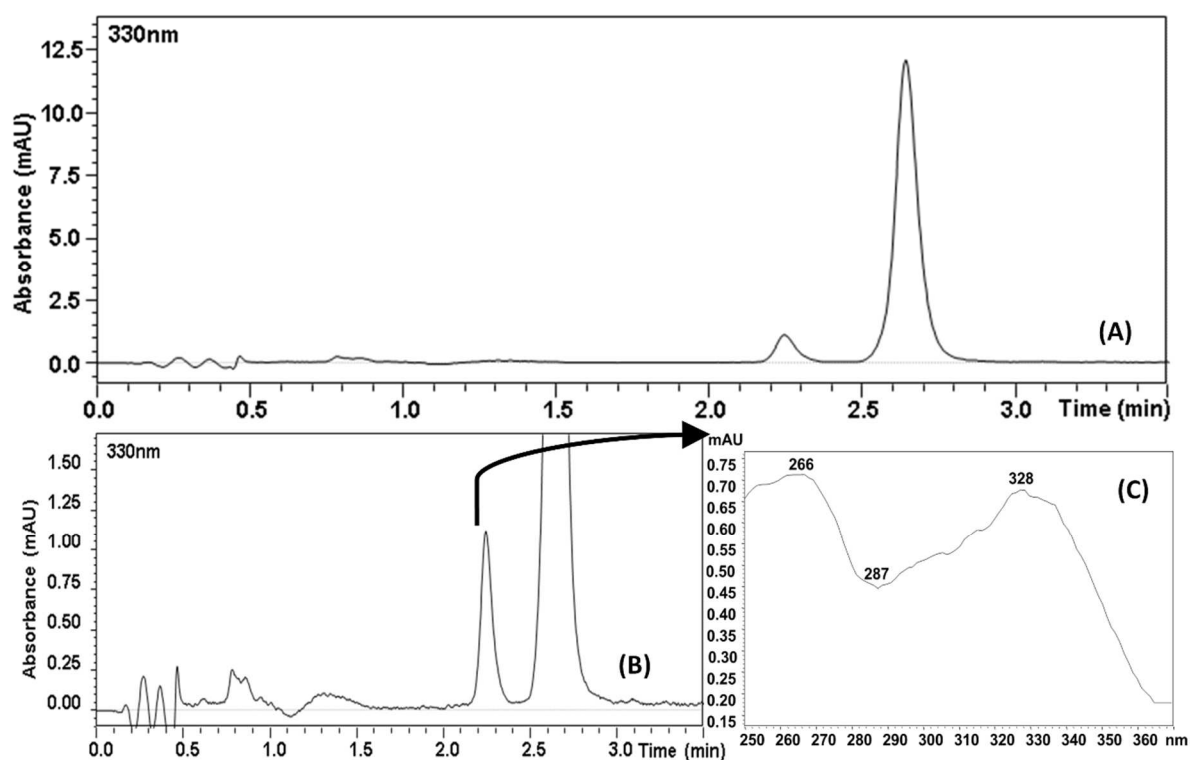


Fig. 2

(A) Chromatogram, (B) zoom chromatogram, and (C) UV spectrum after alkaline hydrolysis of standard solutions of rosmarinic acid at $10 \mu\text{g}\cdot\text{mL}^{-1}$ obtained by UFLC at 330 nm.

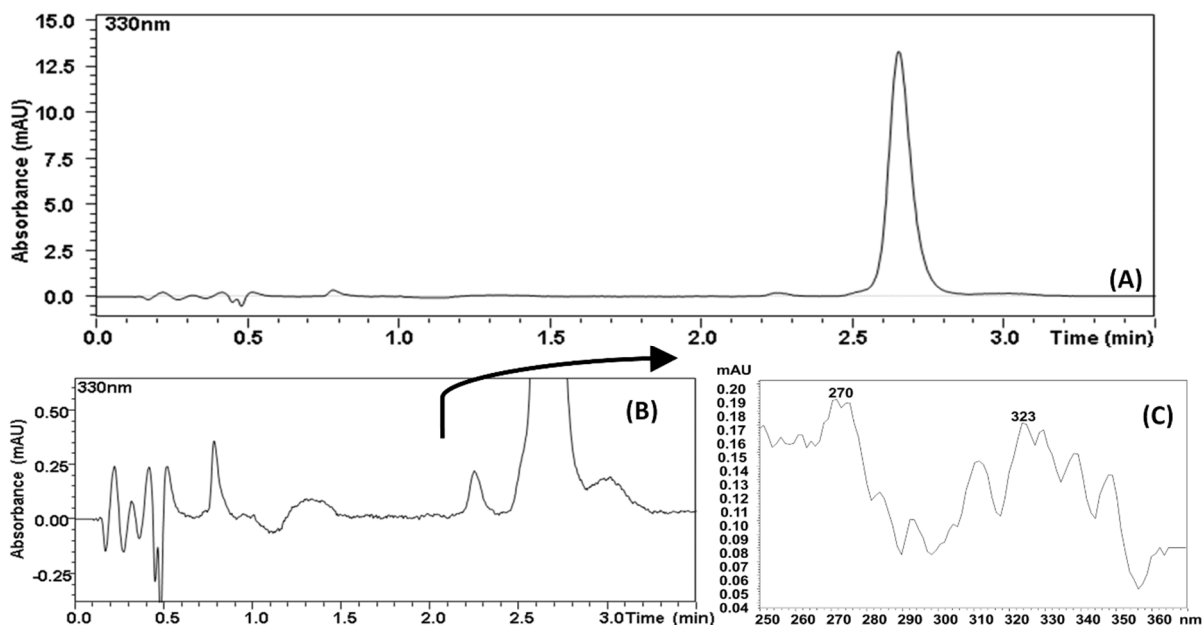


Fig. 3

(A) Chromatogram, (B) zoom chromatogram, and (C) UV spectrum after dry heat at 70 °C of standard solutions of rosmarinic acid at $10 \mu\text{g}\cdot\text{mL}^{-1}$ obtained by UFLC at 330 nm.

3.2.3 Linearity

RA standard curves analyses were performed by linearity evaluation. Examination of the correlation coefficients demonstrated that the method was linear for RA in all matrices in the tested range as shown in Table 3. The LOD and LOQ calculated results are also presented in Table 3. The LLOQ was fixed at 0.1 and $0.5 \mu\text{g}\cdot\text{mL}^{-1}$ for non-biological and biological matrices, respectively, as it was the lowest concentration of RA that could be quantified with acceptable precision and accuracy.

The statistical evaluation of regression significance and confidence interval on the intercepts, observed in Table 4, demonstrates the linear regression and the absence of linearity deviation.

Table 3

Linearity of RA standard and matrices.

Matrix	Range $\mu\text{g}\cdot\text{mL}^{-1}$	Regression Equation	R	LOQ LOD		ME %
				$\mu\text{g}\cdot\text{mL}^{-1}$		
SS	0.1 – 10.0	$y = 8288.5x - 156.48$	0.9996	0.24	0.08	-
NE _B	0.1 – 10.0	$y = 8465.8x - 175.19$	0.9999	0.13	0.04	2.09
RF	0.1 – 10.0	$y = 8385.9x - 149.31$	0.9997	0.21	0.07	1.16
PES	0.5 – 10.0	$y = 8598.8x + 85.422$	0.9981	0.52	0.17	3.61
PNM	0.5 – 10.0	$y = 7860.3x - 847.03$	0.9979	0.55	0.18	-5.45

SS: RA standard solution; NE_B: blank nanoemulsion; RF: receptor fluid (pH 5.8); PES: porcine ear skin; PNM: porcine nasal mucosa; R = correlation coefficient; LOQ = limit of quantification; LOD = limit of detection; ME = matrix effect.

Table 4

Summary of the output of the ANOVA for the evaluation of linearity.

	Regression	Intercept		
	Significance F	p-value	Lower 95%	Upper 95%
SS	2.94E-82 ^a	0.441 ^b	-560.58	247.61
NEB	3.42E-96 ^a	0.120 ^b	-471.85	121.46
RF	1.05E-85 ^a	0.397 ^b	-500.28	201.65
PES	4.93E-65 ^a	0.850 ^b	-815.21	986.06
PNM	6.70E-64 ^a	0.055 ^b	-2000.66	306.61

SS: RA standard solution; NE_B: blank nanoemulsion; RF: receptor fluid (pH 5.8); PES: porcine ear skin; PNM: porcine nasal mucosa.

^a 95% confidence level = significant linear regression.

^b 95% confidence level = no significant linearity deviation.

3.2.4 Matrix effect

During an analytical and bioanalytical validation the evaluation of the matrix effect is crucial to guarantee the correct quantification of reference compound whatever of the presence of the matrix [44,45]. The matrix effects were calculated by comparing the slopes obtained from rosmarinic acid standard curves with the biological and non-biological matrices spiked curves. When analyzed according to Niessen et al. (2006) [46] the matrix effects is considered low for range response between $-20 < \text{ME}\% < 20$,

medium for range response between $-50 < \text{ME}\% < -20$ or $20 > \text{ME}\% > 50$, and high for range response $\text{ME}\% < -50$ or $\text{ME}\% > 50$. The results obtained for matrix effects (Table 3) of rosmarinic acid were lower than 5.45% in module and indicates a low matrix effect exhibited by rosmarinic acid.

3.2.5 Precision and accuracy

The repeatability, intermediate precision and accuracy data for the RA assay in different matrices are presented in Table 5. The spiked-matrices were evaluated by analyzing the RA at concentrations of $0.1 \mu\text{g}\cdot\text{mL}^{-1}$ or $0.5 \mu\text{g}\cdot\text{mL}^{-1}$ (LLOQ), $2.0 \mu\text{g}\cdot\text{mL}^{-1}$ (lowest concentration), $6.0 \mu\text{g}\cdot\text{mL}^{-1}$ (medium concentration), and $10.0 \mu\text{g}\cdot\text{mL}^{-1}$ (highest concentration) for each sample. The intra-day precision results demonstrated a relative standard deviation (RSD, %) lower than 3.92% for analytical assays (SS, NE_B and RF) and lower than 12.07% for bioanalytical assays (PES and PNM). The inter-day precision RSD results were lower than 3.02% for analytical assays and lower than 10.03 for bioanalytical assays. The accuracy data for RA in all matrices were within 91.09 to 108.10% range. According to official guidelines [37–39] the developed method can be considered precise and accurate.

3.2.6 Stability

The stability data demonstrated that the RA concentration in SS, NE_B, RF and PES matrices remained constant after 24 h of storage at room temperature. The amounts of RA in these matrices were within 90.05% and 103.74% range after this period of time as showed in Table 5. On the other hand, the range of RA reduced to values between 53.10% and 76.57% in PNM matrix after the same period of time, showing an instability for storage samples in PNM matrix and demonstrating that the samples must be analyzed freshly prepared.

Table 5

Repeatability, intermediate precision, accuracy and stability evaluation of RA standard and matrices.

	Level ($\mu\text{g/mL}$)	Precision (RSD)				Accuracy (%)	SE (%)
		First day ^a	Second day ^a	Third day ^a	Inter-day ^b		
SS	0.1	1.57	2.42	1.61	1.93	98.67	98.26
	2.0	1.82	1.07	0.49	1.18	99.60	96.56
	6.0	0.86	0.88	0.65	1.03	99.94	98.74
	10.0	0.73	1.07	0.28	1.71	99.80	99.95
NE _B	0.1	2.98	3.92	3.12	3.02	102.5	103.74
	2.0	2.03	0.73	1.49	1.55	97.77	97.98
	6.0	1.55	0.68	0.68	1.03	100.33	100.11
	10.0	0.22	0.37	0.17	0.27	99.60	102.97
RF	0.1	1.27	1.41	3.10	3.01	98.34	95.20
	2.0	3.49	1.96	1.87	2.66	100.33	96.15
	6.0	0.80	0.64	1.00	1.83	99.58	97.65
	10.0	1.75	0.95	1.17	1.21	99.76	97.14
PES	0.5	3.21	1.20	2.31	4.39	91.09	90.05
	2.0	1.69	2.67	0.58	5.37	101.52	94.45
	6.0	0.41	2.93	2.01	4.23	100.72	94.82
	10.0	2.71	1.35	0.75	3.32	100.80	97.77
PNM	0.5	12.07	9.55	8.74	10.03	108.10	53.10
	2.0	3.49	4.33	0.56	7.28	100.04	63.86
	6.0	2.42	1.37	1.38	3.23	98.28	71.34
	10.0	2.15	2.36	1.30	3.02	101.24	76.57

SS: RA standard solution; NE_B: blank nanoemulsion; RF: receptor fluid (pH 5.8); PES: porcine ear skin; PNM: porcine nasal mucosa; SE: stability evaluation in matrices (24 h).

^a six replicates per day.

^b n = 3 days; RSD = relative standard deviation (%).

3.2.7 Robustness

The responses obtained after applying the Plackett-Burman design were percentage of RA obtained in each matrix in relation to the standard solution. The investigated

factors include column oven temperature (54; 56 °C), flow rate (0.54; 0.56 mL.min⁻¹), TFA concentration (0.08; 0.12%), and organic composition (16.5; 17.5%). The statistical interpretation of the data demonstrated no significant factors for all matrices with t-values lower than the t-critical values ($\alpha = 0.05$) as shown in Fig. 4. In summary, the robustness of a model refers to its ability to remain unchanged by deliberate and small variations in the conditions of analysis [41]. In this context, the results of RA assay with the variations made in the experimental conditions demonstrated no significant changes, indicating the proposed method's robustness.

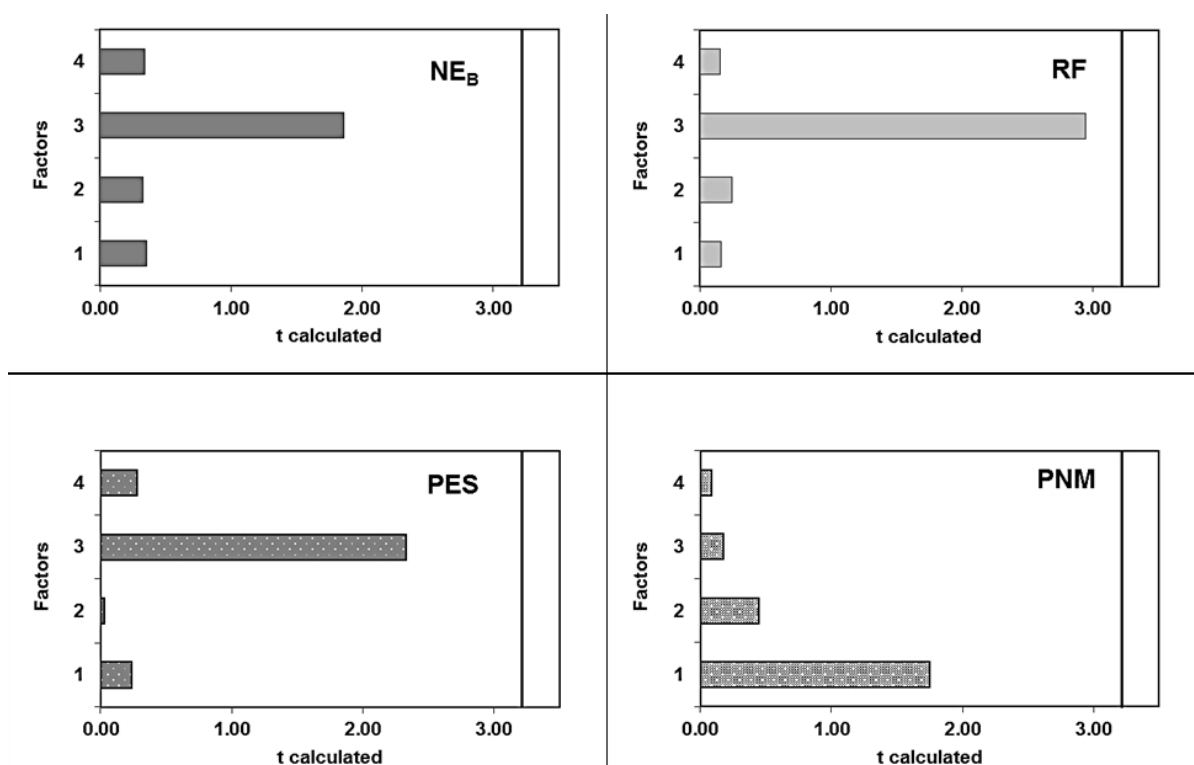


Fig. 4

Plackett-Burman experimental design in different matrices (NE_B: blank nanoemulsion, PES: porcine ear skin, PNM: porcine nasal mucosa, RF: receptor fluid). Where, bar charts representing the t-calculated for acid rosmarinic assay during robustness assessment, and their t-critical represented by the vertical line. The investigated factors were 1: column oven temperature, 2: flow rate, 3: TFA concentration, and 4: organic composition.

3.2.8 Extraction recovery of RA from porcine skin and nasal mucosa

The procedure for extraction recovery of RA from porcine skin and nasal mucosa was established after preliminary studies involving different parameters such as variation of time in an ultrasound bath, different types (water, acetonitrile and methanol) and

amount of solvents used until reaching a recovery threshold. The recovery results were within FDA recommendations for bioanalytical procedures validation [38] and were obtained through quantification of previously spiked-matrices with RA and after extraction procedure. The results are shown in Table 6. The recovery data demonstrated that the addition of 2 mL of methanol with extraction during 45 min in an ultrasound bath and 4 mL of methanol with extraction during 120 min in an ultrasound bath was for RA satisfactory recovery (higher than 85%) from porcine ear skin and porcine nasal mucosa, without any matrix components interference and with an adequate precision (RSD lower than 10.6%).

Table 6

RA extraction recovery from porcine ear skin and nasal mucosa matrices.

Matrix	Level ($\mu\text{g}\cdot\text{mL}^{-1}$)	Recovery (%) (RSD)
PES	0.5	85.21 (1.2)
	2.0	88.63 (9.0)
	6.0	85.34 (10.6)
	10.0	86.69 (4.0)
PNM	0.5	86.97 (8.1)
	2.0	85.90 (8.2)
	6.0	88.32 (5.9)
	10.0	88.67 (9.5)

PES: porcine ear skin; PNM: porcine nasal mucosa; RSD = relative standard deviation (%).

3.3 Skin and nasal retention/permeation studies

The validated method was applied to estimate the amount of RA in a RA-loaded nanoemulsion, as well as in receptor fluid, porcine skin and nasal mucosa layers after permeation/retention assays (Table 7). The results show RSD values lower than 17.80%, which indicates adequate precision of the method for these applications. Furthermore, the quantification of RA incorporated into a monodispersed nanoemulsion showed an amount of $1.007 \pm 0.040 \text{ mg}\cdot\text{mL}^{-1}$, resulting in an adequate repeatability.

Table 7

UFLC method application for determination of RA in a real sample

Method application	Mean ^a (RSD)
<i>Sample</i>	
NE _{RA} (mg·mL ⁻¹)	1.007 (3.95)
<i>Skin retention</i>	
PES (μg·cm ⁻²)	1.13 (17.12)
RF (μg·mL ⁻¹)	< LLOQ
<i>Nasal mucosa permeation</i>	
PNM (μg·cm ⁻²)	22.46 (17.80)
RF (μg·mL ⁻¹)	89.75 (16.14)

NE_{RA}: RA loaded-nanoemulsion; PES: porcine ear skin; PNM: porcine nasal mucosa; RF: receptor fluid; LLOQ: lower limit of quantification; RSD = relative standard deviation (%).

^a Mean of six replicates.

Concerning skin retention studies, the developed method was able to assay RA in porcine ear skin tissue with satisfactory precision. No RA was detected in the receptor fluid even after 8 h of experiment. Porcine ear skin membrane was chosen to investigate the retention study once the authors reported its validity as an *in vitro* model for human skin according to Sekkat et al. (2002) [47]. This is an important finding due to the scarce literature concerning the RA skin determination during permeation/retention studies [42].

In addition, the method was able to quantify RA after 8 h of nasal permeation assay in receptor fluid and porcine nasal mucosa tissue with satisfactory precision. The porcine nasal mucosa membrane is a useful model due to its similarity with the composition of the nasal human mucosa according described by Wadell et al. (2003) [48]. Finally, it is important to emphasize that this is the first description of the RA permeation through nasal mucosa in the literature.

4 Conclusion

In the present study, a simple, efficient, fast and stability-indicating UFLC method was successfully developed and validated for determination of RA in nanoemulsions, porcine ear skin, porcine nasal mucosa, receptor fluid (potassium phosphate buffer)

aiming the application in development of new topical nanoemulsions and retention/permeation studies. The results demonstrated a highly sensitive and selective method, without any interference from the matrices and degradation products, able to quantify rosmarinic acid with precision, accuracy, robustness and low matrix effect in different complex matrices (non-biological and biological).

Conflicts of interest

The authors declare no conflict of interest.

Acknowledgements

The authors are gratefully acknowledged to the Coordenação de Aperfeiçoamento de Pessoal de Nível Superior (CAPES), to the Conselho Nacional de Desenvolvimento científico e Tecnológico (CNPq), and to the Fundação de Amparo à Pesquisa no Estado do Rio Grande do Sul (FAPERGS) for the scholarships and the financial support.

References

- [1] M. Petersen, M.S.J. Simmonds, Rosmarinic acid, *Phytochemistry*. 62 (2003) 121–125. doi:10.1016/S0031-9422(02)00513-7.
- [2] G.-D. Kim, Y.S. Park, Y.-H. Jin, C.-S. Park, Production and applications of rosmarinic acid and structurally related compounds, *Appl. Microbiol. Biotechnol.* 99 (2015) 2083–2092. doi:10.1007/s00253-015-6395-6.
- [3] S. Baba, N. Osakabe, M. Natsume, J. Terao, Orally administered rosmarinic acid is present as the conjugated and/or methylated forms in plasma, and is degraded and metabolized to conjugated forms of caffeic acid, ferulic acid and m-coumaric acid, *Life Sci.* 75 (2004). doi:10.1016/j.lfs.2003.11.028.
- [4] R. Bhatt, N. Mishra, P.K. Bansal, Phytochemical, pharmacological and pharmacokinetics effects of rosmarinic acid, *J. Pharm. Sci. Innov.* 2 (2013) 28–34. doi:10.7897/2277-4572.02215.
- [5] S.M. Yoo, J.R. Kang, Antioxidation Effects of rosmarinic acid on human skin melanoma cells treated with hydrogen peroxide, *J. Korean Soc. Appl. Biol. Chem.* 52 (2009) 247–251. doi:10.3839/jksabc.2009.044.
- [6] R. Bhatt, D. Singh, A. Prakash, N. Mishra, Development, characterization and nasal delivery of rosmarinic acid-loaded solid lipid nanoparticles for the effective management of Huntington's disease., *Drug Deliv.* (2014) 1–9. doi:10.3109/10717544.2014.880860.
- [7] A.R. Madureira, D.A. Campos, P. Fonte, S. Nunes, F. Reis, A.M. Gomes, B. Sarmiento, M.M. Pintado, Characterization of solid lipid nanoparticles produced with carnauba wax for rosmarinic acid oral delivery, *RSC Adv.* 5 (2015) 22665–22673. doi:10.1039/C4RA15802D.
- [8] B. Medronho, A.J.M. Valente, P. Costa, Inclusion complexes of rosmarinic acid and cyclodextrins: stoichiometry, association constants, and antioxidant potential, *Colloid Polym. Sci.* (2014) 885–894. doi:10.1007/s00396-013-3124-5.
- [9] J. Yang, L. Zhang, J. Li, L. Chen, Q. Zheng, T. Chen, Z. Chen, T. Fu, L. Di, Enhanced oral bioavailability and prophylactic effects on oxidative stress and hepatic damage of an oil solution containing a rosmarinic acid – phospholipid complex, *J. Funct. Foods.* 19 (2015) 63–73. doi:10.1016/j.jff.2015.09.013.
- [10] S.B. da Silva, D. Ferreira, M. Pintado, B. Sarmiento, Chitosan-based nanoparticles for rosmarinic acid ocular delivery — *In vitro* tests, *Int. J. Biol. Macromol.* 84 (2016) 112–120. doi:10.1016/j.ijbiomac.2015.11.070.
- [11] S.B. da Silva, A. Oliveira, D. Ferreira, B. Sarmiento, M. Pintado, Development and validation method for simultaneous quantification of phenolic compounds in natural extracts and nanosystems., *Phytochem. Anal.* 24 (2013) 638–44. doi:10.1002/pca.2446.
- [12] F.A.E. Yazbi, E.M. Hassan, E.F. Khamis, M.A.A. Ragab, M.A. Hamdy, Stability indicating HPLC-DAD method for analysis of Ketorolac binary and ternary mixtures in eye drops: Quantitative analysis in rabbit aqueous humor, *J. Chromatogr. B.* 1068–1069 (2017) 218–225.

doi:10.1016/J.JCHROMB.2017.10.024.

- [13] H. Wang, G.J. Provan, K. Helliwell, Determination of rosmarinic acid and caffeic acid in aromatic herbs by HPLC, *Food Chem.* 87 (2004) 307–311. doi:10.1016/j.foodchem.2003.12.029.
- [14] V. Canelas, C.T. da Costa, Quantitative HPLC analysis of rosmarinic acid in extracts of *Melissa officinalis* and spectrophotometric measurement of their antioxidant activities, *J. Chem. Educ.* 84 (2007) 1502–1504. doi:10.1021/ed084p1502.
- [15] D. Jirovský, P. Kosina, M. Myslíňová, J. Stýskala, J. Ulrichová, V. Šimánek, HPLC analysis of rosmarinic acid in feed enriched with aerial parts of *Prunella vulgaris* and its metabolites in pig plasma using dual-channel coulometric detection, *J. Agric. Food Chem.* 55 (2007) 7631–7637. doi:10.1021/jf070883e.
- [16] S. Achamlale, B. Rezzonico, M. Grignon-Dubois, Rosmarinic acid from beach waste: Isolation and HPLC quantification in *Zostera detritus* from Arcachon lagoon, *Food Chem.* 113 (2009) 878–883. doi:10.1016/j.foodchem.2008.07.040.
- [17] Agência Nacional de Vigilância Sanitária, Farmacopeia Brasileira, 2010.
- [18] R.O. Couto, E.C. Conceição, L.T. Chaul, E.M.S. Oliveira, S.F. Alves, K.R. Rezende, M.T.F. Bara, J.R. Paula, Validated HPLC-PDA method for rosmarinic acid quantification in rosemary, *Lat. Am. J. Pharm.* 30 (2011) 1951–1956.
- [19] N. Öztürk, M. Tunçel, U.D. Uysal, E.M. Oncu-Kaya, O. Koyuncu, Determination of rosmarinic acid by high-performance liquid chromatography and its application to certain salvia species and rosemary, *Food Anal. Methods.* 4 (2011) 300–306. doi:10.1007/s12161-010-9164-2.
- [20] A. Gudzenko, Development and validation of a method for the determination of rosmarinic acid in *Mentha piperita* L. using solid-phase extraction and RP-HPLC with photodiode array detection, *J. Chem. Pharm. Res.* 5 (2013) 40–45.
- [21] K.B. De Oliveira, B.H. De Oliveira, A HPLC/DAD Determination of rosmarinic acid in *Salvia officinalis*: Sample preparation optimization by factorial design, *Artic. J. Braz. Chem. Soc.* 24 (2013) 85–91.
- [22] J. Liu, Y. Wan, Z. Zhao, H. Chen, Determination of the content of rosmarinic acid by HPLC and analytical comparison of volatile constituents by GC-MS in different parts of *Perilla frutescens* (L.) Britt., *Chem. Cent. J.* 7 (2013) 61. doi:10.1186/1752-153X-7-61.
- [23] M. Modarres, J. Asili, M. Lahouti, A. Gangali, M. Iranshahy, A. Sahebkar, Simultaneous determination of rosmarinic acid, salvianolic acid b and caffeic acid in *Salvia leriifolia* Benth. root, leaf and callus extracts using a high-performance liquid chromatography with diode-array detection technique, *J. Liq. Chromatogr. Relat. Technol.* 37 (2014) 1721–1730. doi:10.1080/10826076.2013.807466.
- [24] A.N. Adham, Comparative extraction methods , phytochemical constituents , fluorescence analysis and HPLC validation of rosmarinic acid content in *Mentha piperita* , *Mentha longifolia* and *Osimum basilicum*, *J. Pharmacogn. Phytochem.* 3 (2015) 130–139.
- [25] M. Caroch, L. Barros, R.C. Calhelha, A. Ćirić, M. Soković, C. Santos-Buelga,

- P. Morales, I.C.F.R. Ferreira, *Melissa officinalis* L. decoctions as functional beverages: a bioactive approach and chemical characterization, *Food Funct.* (2015). doi:10.1039/C5FO00309A.
- [26] N. Troncoso, H. Sierra, L. Carvajal, P. Delpiano, Fast high performance liquid chromatography and ultraviolet – visible quantification of principal phenolic antioxidants in fresh rosemary, *J. Chromatography A*. 1100 (2005) 20–25. doi:10.1016/j.chroma.2005.09.008.
- [27] M. Hernández-Mesa, L. Carbonell-Rozas, C. Cruces-Blanco, A.M. García-Campaña, A high-throughput UHPLC method for the analysis of 5-nitroimidazole residues in milk based on salting-out assisted liquid–liquid extraction, *J. Chromatogr. B*. 1068–1069 (2017) 125–130. doi:10.1016/J.JCHROMB.2017.10.016.
- [28] V. Savic, S. Savic, V. Nikolic, L. Nikolic, S. Najman, J. Lazarevic, A. Djordjevic, The identification and quantification of bioactive compounds from the aqueous extract of comfrey root by UHPLC-DAD-HESI-MS method and its microbial activity, *Hem. Ind.* 69 (2015) 1–8. doi:10.2298/HEMIND131202013S.
- [29] L. Zheng, Z. Gong, Y. Lu, Y. Xie, Y. Huang, Y. Liu, Y. Lan, A. Wang, Y. Wang, A UPLC-MS/MS method for simultaneous determination of danshensu, protocatechuic aldehyde, rosmarinic acid, and ligustrazine in rat plasma, and its application to pharmacokinetic studies of Shenxiong glucose injection in rats, *J. Chromatogr. B Anal. Technol. Biomed. Life Sci.* 997 (2015) 210–217. doi:10.1016/j.jchromb.2015.06.008.
- [30] F. Zhu, T. Asada, A. Sato, Y. Koi, H. Nishiwaki, H. Tamura, Rosmarinic acid extract for antioxidant, antiallergic, and α -glucosidase inhibitory activities, isolated by supramolecular technique and solvent extraction from *Perilla* leaves, *J. Agric. Food Chem.* 62 (2014). doi:10.1021/jf404318j.
- [31] X. Li, C. Yu, W. Sun, G. Liu, J. Jia, Y. Wang, Simultaneous determination of magnesium lithospermate B, rosmarinic acid, and lithospermic acid in beagle dog serum by liquid chromatography/tandem mass spectrometry, *Rapid Commun. Mass Spectrom.* 18 (2004) 2878–2882. doi:10.1002/rcm.1703.
- [32] M.C. Nemitz, R.C. Moraes, L.S. Koester, V.L. Bassani, G.L. von Poser, H.F. Teixeira, Bioactive soy isoflavones: extraction and purification procedures, potential dermal use and nanotechnology-based delivery systems, *Phytochem. Rev.* 14 (2014) 849–869. doi:10.1007/s11101-014-9382-0.
- [33] G.K. Zorzi, E.L.S. Carvalho, G.L. Von Poser, H.F. Teixeira, On the use of nanotechnology-based strategies for association of complex matrices from plant extracts, *Brazilian J. Pharmacogn.* 25 (2015) 426–436. doi:10.1016/j.bjp.2015.07.015.
- [34] D.F. Argenta, J. Bidone, F.D. Misturini, L.S. Koester, V.L. Bassani, C.M. Simbes, H.F. Teixeira, *In Vitro* evaluation of mucosa permeation/retention and antiherpes activity of genistein from cationic nanoemulsions., *J. Nanosci. Nanotechnol.* 16 (2016) 1282–90. doi:10.1166/jnn.2016.11676.
- [35] D. Fasolo, V.L. Bassani, H.F. Teixeira, Development of topical nanoemulsions containing quercetin and 3- O -methylquercetin, *Pharmazie.* 64 (2009) 726–730.

doi:10.1691/ph.2009.8357.

- [36] M.D.S. Barbi, F.C. Carvalho, C.P. Kiill, H.D.S. Barud, S.H. Santagneli, S.J.L. Ribeiro, M.P.D. Gremiao, Preparation and characterization of chitosan nanoparticles for AZT nasal delivery., *J. Nanosci. Nanotechnol.* 14 (2014). doi:10.1166/jnn.2015.9180.
- [37] International Conference on Harmonization (ICH), Validation of Analytical Procedures : Text and Methodology Q2 (R1), Tech. Requir. Regist. Pharm. Hum. Use. (2005) 1–13.
- [38] Food and Drug Administration (FDA), Guidance for Industry: Bioanalytical Method Validation, Cent. Drug Eval. Res. (2013) 1–34.
- [39] European Medicine Agency (EMA), Guideline on bioanalytical method validation, (2012) 1–2.
- [40] G.A. Shabir, Validation of high-performance liquid chromatographic methods for the pharmaceutical analysis: Understanding the differences and similarities between the requirements of the US Food and Drug Administration, and the US Pharmacopeia and the International Con, *J. Chromatogr. A.* 987 (2003) 57–66. doi:http://dx.doi.org/10.1016/S0021-9673(02)01536-4.
- [41] Y. V. Heyden, A. Nijhuis, J. Smeyers-Verbeke, B.G.M. Vandeginste, D.L. Massart, Guidance for robustness/ruggedness tests in method validation, *J. Pharm. Biomed. Anal.* 24 (2001) 723–753. doi:10.1016/S0731-7085(00)00529-X.
- [42] A. Stelmakienė, K. Ramanauskienė, V. Briedis, Release of rosmarinic acid from semisolid formulations and its penetration through human skin *ex vivo*, *Acta Pharm.* 65 (2015). doi:10.1515/acph-2015-0012.
- [43] Y. Zhang, J.P. Smuts, E. Dodbiba, R. Rangarajan, J.C. Lang, D.W. Armstrong, Degradation study of carnosic acid, carnosol, rosmarinic acid, and rosemary extract (*Rosmarinus officinalis* L.) assessed using HPLC, *J. Agric. Food Chem.* 60 (2012) 9305–9314. doi:dx.doi.org/10.1021/jf302179c.
- [44] M.C. Nemitz, F.K.J. Yatsu, J. Bidone, L.S. Koester, V.L. Bassani, C. V. Garcia, A.S.L. Mendez, G.L. Von Poser, H.F. Teixeira, A versatile, stability-indicating and high-throughput ultra-fast liquid chromatography method for the determination of isoflavone aglycones in soybeans, topical formulations, and permeation assays, *Talanta.* 134 (2015) 183–193. doi:10.1016/j.talanta.2014.10.062.
- [45] E. Watanabe, Y. Kobara, K. Baba, H. Eun, Aqueous acetonitrile extraction for pesticide residue analysis in agricultural products with HPLC-DAD, *Food Chem.* 154 (2014) 7–12. doi:10.1016/j.foodchem.2013.12.075.
- [46] W.M.A. Niessen, P. Manini, R. Andreoli, Matrix effects in quantitative pesticide analysis using liquid chromatography–mass spectrometry, *Mass Spectrom. Rev.* 25 (2006) 881–899. doi:10.1002/mas.
- [47] N. Sekkat, Y.N. Kalia, R.H. Guy, Biophysical study of porcine ear skin *in vitro* and its comparison to human skin *in vivo*, *J. Pharm. Sci.* 91 (2002) 2376–2381. doi:10.1002/jps.10220.
- [48] C. Wadell, E. Bjork, O. Camber, Permeability of porcine nasal mucosa correlated

with human nasal absorption, *Eur. J. Pharm. Sci.* 18 (2003) 47–53.
doi:10.1016/S0928-0987(02)00240-3.

Introdução

O terceiro capítulo compreende um artigo científico o qual aborda o desenvolvimento e otimização de nanoemulsões revestidas por quitosana contendo ácido rosmarínico (AR) para administração pela via nasal empregando-se um modelo experimental do tipo Box-Behnken. Recentemente, atenção tem sido voltada a compostos naturais com atividade anti-inflamatória e antioxidante, tendo em vista a relação entre a neuroinflamação, estresse oxidativo e as doenças neurodegenerativas. O AR é um composto fenólico encontrado em várias espécies de plantas medicinais e com atividades anti-inflamatória, antioxidante e neuroprotetora bem descritas na literatura. No entanto, devido a sua baixa solubilidade e permeabilidade em membranas biológicas, incluindo a barreira hematoencefálica (BHE), sua alta instabilidade e, conseqüente baixa biodisponibilidade, principalmente evidenciadas pela via oral, as abordagens tecnológicas para esse composto são bastante limitadas. Para contornar estas desvantagens, novas estratégias para sua administração e veiculação precisam ser estudadas. Podemos destacar o emprego de vias alternativas de administração, dentre elas a via nasal como forma de entrega direta de fármacos ao sistema nervoso central, associadas ao uso de sistemas nanotecnológicos lipídicos revestidos por polímeros mucoadesivos. Na literatura, não há relatos do emprego de nanoemulsões revestidas por polímero mucoadesivo para administração do AR por via nasal visando a obtenção de uma atividade neuroprotetora. Neste sentido, o presente capítulo teve como objetivo desenvolver, otimizar e caracterizar nanoemulsões contendo AR revestidas por quitosana, bem como avaliar os perfis de mucoadesão, liberação e permeação em mucosa nasal suína, além, de investigar a toxicidade in vitro, em fibroblastos (MRC-5), dessas formulações.

Artigo científico:

Box-Behnken design optimization of mucoadhesive chitosan-coated nanoemulsions
for rosmarinic acid nasal delivery – *In vitro* studies

Publicado no *Carbohydrate Polymers*, 2018

Box-Behnken design optimization of mucoadhesive chitosan-coated nanoemulsions for rosmarinic acid nasal delivery – *In vitro* studies

Flávia Nathiely Silveira Fachel^a, Bruna Medeiros-Neves^a, Morgana Dal Prá^b, Roselena Silvestri Schuh^a; Kleyton Santos Veras^a, Valquíria Linck Bassani^a, Letícia Scherer Koester^a, Amelia Teresinha Henriques^a, Elizandra Braganhol^b, Helder Ferreira Teixeira^{a,*}

^a Programa de Pós-Graduação em Ciências Farmacêuticas, Faculdade de Farmácia, Universidade Federal do Rio Grande do Sul, Porto Alegre, RS, Brazil.

^b Departamento de Ciências Básicas da Saúde, Universidade Federal de Ciências da Saúde de Porto Alegre, Porto Alegre, RS, Brazil

*Corresponding author. Tel.: (+55) 51 3308 5231; fax: (+55) 51 3308 2165.

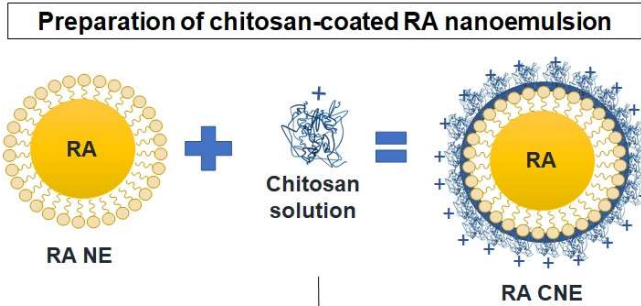
E-mail address: helder.teixeira@ufrgs.br (Helder Ferreira Teixeira).

Abstract

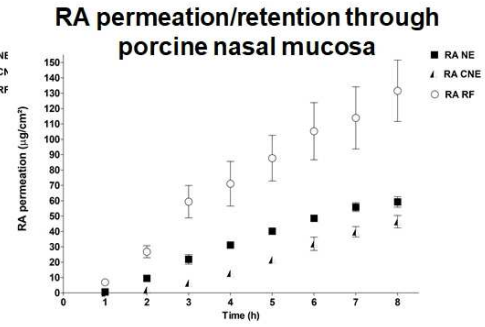
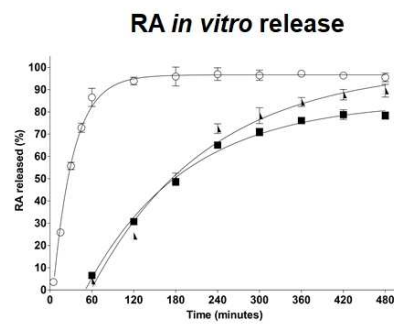
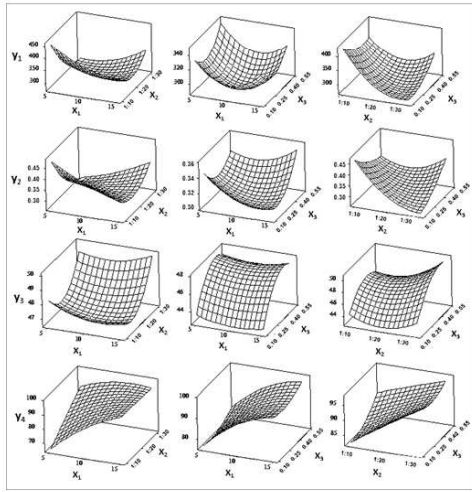
Mucoadhesive chitosan-coated nanoemulsions for rosmarinic acid (RA) nasal delivery were optimized. The optimum ratio between the formulation components that led to minimum droplet size and PDI, and maximal ζ -potential and RA content was obtained using Box-Behnken design (BBD). Optimized conditions were 8.5% oil phase (w/v), 3:10 lecithin to oil phase ratio (w/w), and 0.1% chitosan final concentration (w/v). Physicochemical characterization, mucoadhesion measurement, *in vitro* release and permeation/retention were performed. Optimized chitosan-coated RA nanoemulsions presented adequate physicochemical characteristics, higher mucoadhesive potential, prolonged drug release, and long-lasting permeation time with a higher RA penetration/retention through porcine nasal mucosa. Cell viability and death by necrosis in fibroblasts cells were also evaluated to investigate the formulations safety. Formulations did not induce cytotoxicity following 24 h (3.125–50 μ M) or 48 h (3.125–25 μ M) of treatments. Overall results demonstrated that optimized chitosan-coated nanoemulsion showed to be a suitable carrier for RA nasal delivery aiming neuroprotective therapies.

Keywords: Box-Behnken design; Chitosan-coated nanoemulsions; Rosmarinic acid; *In vitro* studies; Cytotoxicity; Nasal delivery.

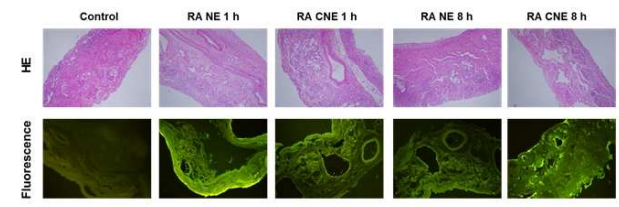
Graphical abstract



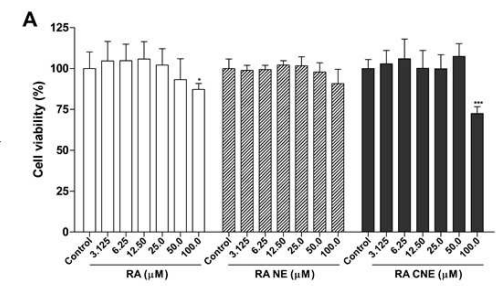
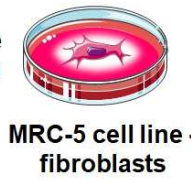
Optimization by Box-Behnken design



Histology and fluorescence images through porcine nasal mucosa



Safety profile investigation



1 Introduction

Neurodegenerative disorders (ND), such as amyotrophic lateral sclerosis, Alzheimer's and Parkinson's diseases, are characterized by progressive loss of specific groups of neuronal cells. There are numerous common features involved in ND pathogenesis, although extensive evidence suggest that neuronal damage might be induced by alterations in immune/inflammatory and redox systems. In this regard, naturally occurring compounds with anti-inflammatory and/or antioxidant activities, such as polyphenols, have been investigated aiming the development of neuroprotective therapies (Andrade et al., 2016; Barnham, Masters, & Bush, 2004; Bhullar & Rupasinghe, 2013; Solanki, Parihar, & Parihar, 2016).

Rosmarinic acid (RA), an ester of caffeic acid and 3,4-dihydroxyphenyllactic acid, is a natural phenolic compound commonly found in various medicinal plants, mainly from Boraginaceae family and sub-family Nepetoideae from Lamiaceae family (Baba, Osakabe, Natsume, & Terao, 2004; Petersen & Simmonds, 2003). RA has a number of reported biological activities, including anti-inflammatory and antioxidant (Bhatt, Mishra, & Bansal, 2013; Petersen & Simmonds, 2003; Soobrattee, Neergheen, Luximon-Ramma, Aruoma, & Bahorun, 2005). A current well-documented literature has demonstrated RA neuroprotective effects due to its abilities to modulate pro-inflammatory cytokines, mitochondrial dysfunction and oxidative stress (Andrade et al., 2016; Costa, Sarmiento, Gonçalves, & Romano, 2013; Du, Li, Song, Xie, & Jiang, 2010; Fallarini et al., 2009; Ghaffari et al., 2014; Lee et al., 2008; Ren et al., 2009). Nevertheless, besides RA poor permeability through biological barriers, high instability, and consequently low bioavailability, technological approaches to circumvent these problems are limited. Therefore, some alternatives for RA delivery, protection, and release aiming the improvement of its bioavailability have been investigated (Bhatt, Singh, Prakash, & Mishra, 2014; da Silva et al., 2014; da Silva, Ferreira, Pintado, & Sarmiento, 2016; Madureira et al., 2015; Medronho, Valente, & Costa, 2014; J. Yang et al., 2015).

Nasal delivery has been studied mainly due to various advantages associated to this route, as rapid onset of action and avoidance of gastrointestinal and hepatic first-pass effects (Grassin-Delyle et al., 2012; Lochhead & Thorne, 2012). Furthermore, it offers a non-invasive and practical alternative route of administration for bypassing blood

brain barrier (BBB) and ensuring direct central nervous system (CNS) delivery, being an interesting approach for the administration of low oral bioavailable drugs (Baltzley, Mohammad, Malkawi, & Al-Ghananeem, 2014; Sood, Jain, & Gowthamarajan, 2014). Although the BBB is essential for maintaining CNS homeostasis, it also represents a major obstacle to the direct brain delivery of therapeutics for ND treatment (Lochhead & Thorne, 2012; Mistry, Stolnik, & Illum, 2009; Saraiva et al., 2016).

The main limitations of nasal route are the limited drug permeability in nasal mucosa and the need for rapidly crossing nasal mucosa, since the mucociliary clearance limits the time for nasal absorption of drug (Grassin-Delyle et al., 2012; Lochhead & Thorne, 2012; Sood et al., 2014). Being commonly considered the combination of mucoadhesive polymers and penetration enhancers for improvement of nasal drugs absorption (Dudhani & Kosaraju, 2010; Wang, Chi, & Tang, 2008).

Lipid-nanotechnology-based delivery systems associated with positive charged polymers have been designed to increase drug permeability, stability, and residence time through nasal cavity aiming to improve therapeutic efficacy (Casettari & Illum, 2014; Kumar et al., 2008; Sood et al., 2014). In this context, chitosan-coated nanoemulsions have been considered a promising approach for nasal delivery. Nanoemulsions are nanodispersion of oily droplets in an external aqueous phase frequently considered to improve the penetration of poorly-soluble molecules through biological barriers (Fachel et al., 2018; Fasolo, Bassani, & Teixeira, 2009). Chitosan is a biocompatible, biodegradable and safe cationic polysaccharide, derived from the deacetylation of chitin, widely used due to its well-known mucoadhesive and permeation enhancing properties (Casettari & Illum, 2014; Domard, 2011; Prego, García, Torres, & Alonso, 2005).

In this study, we hypothesized that the association of RA-loaded nanoemulsions with the biopolymer chitosan would enhance RA stability, mucoadhesive properties, penetration/retention, and residence time in nasal mucosa intended to be used as a new approach in neuroprotective therapies. Considering the hypothesis mentioned above, this study was conducted to develop and optimize chitosan-coated RA nanoemulsions for nasal delivery. The main properties of the formulations were also assessed, as physicochemical characterization, mucoadhesive properties, and *in vitro* release and permeation/retention assays through porcine nasal mucosa. Finally, to

investigate the safety of the developed formulations, cell viability and death in MRC-5 fibroblast cell line were evaluated.

2 Materials and methods

2.1 Materials

RA reference standard with over 98% purity was purchased from Carbosynth Ltd. (Berkshire, GB). Acetonitrile, methanol, and trifluoroacetic acid were of liquid chromatographic grade and obtained from Tedia (Rio de Janeiro, BR). Ultra-pure water was obtained by reverse osmosis using a Milli-Q apparatus (Millipore, Billerica, US). Egg-lecithin (Lipoid E-80®) and medium chain triglycerides (MCT) were purchased from Lipoid GmbH (Ludwigshafen, DE). porcine stomach mucin (type II), Dulbecco's modified Eagle's medium (DMEM), 3,(4,5-dimethyl)-2,5diphenyl-tetrazolium bromide salt (MTT) and propidium iodide (PI) were obtained from Sigma-Aldrich Co. (St. Louis, US). Monobasic and dibasic potassium phosphate were purchased from Nuclear (CAQ, São Paulo, BR). Porcine nasal mucosa was obtained from Ouro do Sul - Cooperativa dos Suinocultores do Caí Superior Ltda. (Harmonia, BR). NBD-PE (N-(7-Nitrobenz-2-Oxa-1,3-Diazol-4-yl)-1,2-Dihexadecanoyl-sn-Glycero-phosphoethanolamine Triethylammonium Salt) fluorescent labeled phospholipid was supplied by Thermo Fisher Scientific (Waltham, US). Glacial acetic acid and dimethyl sulfoxide (DMSO) was supplied by Dinâmica Química Contemporânea Ltda. (Diadema, BR). Fetal bovine serum (FBS) and trypsin solution were obtained from Gibco (Grand Island, US).

2.1.1 Chitosan

Low molecular weight chitosan (50,000-190,000 Da, 75-85% deacetylated) was purchased from Sigma-Aldrich Co. (St. Louis, US). From commercial chitosan first was carried out a purification procedure to obtain the neutral form as described by Signini & Campana Filho (1998). Molecular weight of purified chitosan was determined through viscometry, using Mark-Houwink equation and the viscosimetric constants determined by Roberts & Domszy (1982). The degree of deacetylation of purified chitosan was also performed through ¹H NMR spectroscopy as described by Hirai, Odani, & Nakajima (1991). The chemical characterization results obtained for purified chitosan were 180,000 Da of molecular weight and 74.9% degree of deacetylation.

2.2 Ultra-fast liquid chromatography analysis

The determination of RA in formulations, and in both *in vitro* and permeation/retention studies was carried-out by a previously developed and fully validated, according to the official guidelines, ultra-fast liquid chromatography (UFLC) method (Fachel et al., 2018). The system consisted of a Shimadzu Prominence series coupled to a photodiode array (PDA) detector and an automatic injector controlled by LC-Solution software (Kyoto, JP). Chromatographic separation was carried out in a Kinetex® C18 column (100 x 2.1 mm i.d.; 2.6 µm; Phenomenex, US) at 55 °C with a flow rate of 0.55 mL.min⁻¹ and detection wavelength of 330 nm. The mobile phase was set at isocratic mode and was composed of water and acetonitrile (83:17, v/v), acidified with 0.1% trifluoroacetic acid (v/v).

2.3 Preparation of nanoemulsions

Nanoemulsions were prepared by oil-in-water spontaneous emulsification procedure (Fasolo et al., 2009). Oil components, composed of RA, MCT, and egg-lecithin, were dissolved in ethanol and poured into the water phase under magnetic stirring for 15 min. Then, nanoemulsions were submitted to a final evaporation process at 40 °C under reduced pressure for complete organic solvent removal, and subsequent water evaporation until reaching 2 mg.mL⁻¹ RA concentration.

2.4 Preparation of chitosan-coated nanoemulsions

Positively-charged nanoemulsions were prepared by coating RA nanoemulsions with chitosan (Kumar et al., 2008). Chitosan solution was prepared in glacial acetic acid 0.1% (v/v). Nanoemulsions were mixed with chitosan solution at 1:1 ratio and submitted to magnetic stirring during 15 min for appropriate surface coating of formulations.

2.5 Box-Behnken design

A response surface methodology (RSM) in form of a Box-Behnken design (BBD) was chosen to statistically optimize chitosan-coated RA nanoemulsions for three experimental factors (X_1 ; X_2 ; X_3) in three factor levels (-1; 0; +1) (Table 1) based on the main effects on droplet size (Y_1), polydispersity index or PDI (Y_2), ζ-potential (Y_3), and RA content (Y_4). Minitab® 17.0.1 software was used to perform the study and for

further statistical analyses. A total of 15 runs in random order were designed by the software with three replicates at central point in order to estimate the pure error (Table 2).

Table 1

Investigated factors and factor levels of Box-Behnken experimental design.

Factor	Level		
	Low Level (-1)	Intermediate Level (0)	High Level (+1)
X ₁ Oil Phase concentration (% w/v)	5.0	10.0	15.0
X ₂ Lecithin to oil phase ratio (w:w)	1:10	2:10	3:10
X ₃ Chitosan final concentration (% w/v)	0.10	0.30	0.50

The response surface regression procedure was used to fit the experimental results by using the following second-order polynomial equation:

$$Y = \beta_0 + \sum_{i=1}^K \beta_i X_i + \sum_{i=1}^K \beta_{ii} X_i^2 + \sum_{1 \leq i < j \leq K} \beta_{ij} X_i X_j + e$$

(Eq. 1)

Where, β_0 , β_i , β_{ii} , and β_{ij} represent the regression coefficients of, constant, linear, quadratic, and interactions terms, respectively, while X_i , X_j and X_k represent the independent variables, k represent the number of variables and Y is the predicted response (Montgomery, 2001).

Analysis of variance (ANOVA) was conducted to confirm the fitted mathematical model. The adequacy of the second-order polynomial model was expressed by significance of regression coefficients, coefficient of determination (R^2), and the lack of fit for each studied response. Three-dimensional response surface plots were used to represent the interaction and influence of variables on responses.

2.6 Determination of optimum conditions

The optimized formulation was established by analysing the response surface plots and the composite desirability function, targeting the minimum droplet size and PDI, with maximal ζ -potential and RA content attainable. The mathematical model's predictive capacity was assessed by comparison between predicted responses and new five independent experiments using the optimal conditions estimated responses

on the same day (Bezerra, Santelli, Oliveira, Villar, & Escaleira, 2008; Nemitz et al., 2017).

2.7 Physicochemical characterization of nanoemulsions

Optimized chitosan-coated RA nanoemulsions (RA CNE) were characterized regarding the determination of RA content, loading efficiency, droplet size, PDI, ζ -potential, pH, viscosity, and morphology. RA nanoemulsions (RA NE) before chitosan coating were also characterized for comparison purpose.

2.7.1 Rosmarinic acid content

The determination of RA content was assessed diluting appropriate aliquots of RA-loaded nanoemulsions before and after chitosan coating in water: acetonitrile (80:20, v/v), filtering, and analysing through a previously developed and validated ultra-fast liquid chromatography method (Fachel et al., 2018).

2.7.2 Association efficiency

Association efficiency was assessed using ultrafiltration membranes (Ultrafree®-MC 10,000 MW, Merck Millipore, Billerica, US). Aliquots of 250 μ L of RA-loaded nanoemulsions before and after chitosan coating were centrifuged at 2,500 rpm in a micro type centrifuge (MCD-2000®, M.R.C. Ltd., IL) for 25 min. The ultrafiltrate obtained was evaluated employing a previously developed and validated ultra-fast liquid chromatography method (Fachel et al., 2018).

2.7.3 Droplet size, polydispersity index and ζ -potential

The droplet size and PDI were determined by photon correlation spectroscopy at 25 °C after appropriate dilution of samples in water. The ζ -potential was determined by electrophoretic mobility at 25 °C after appropriate dilution with 1 mM NaCl solution. The measurements were performed using a Zetasizer Nano-ZS90® (Malvern Instruments, England, GB) equipment.

2.7.4 Nanoemulsions morphology

Droplet morphology of nanoemulsions was assessed by transmission electron microscopy (TEM) using a JEM-1220EXII microscope (Jeol Ltd., JP). Samples were

previously diluted in water (1:10, v/v), distributed on formvar-coated copper grids (200 mesh), and stained with uranyl acetate (2%).

2.7.5 Viscosity and pH measurements

The viscosity was determined by capillary viscometry in an Ostwald viscometer at 20 °C ± 0.1 °C using a number 2 capillary. The flow time through the capillary and density of the formulations were taken into account to perform the tests and calculate the relative viscosity (cP). The pH was directly measured in nanoemulsions using a pH-meter DM-22 (Digimed Analítica Ltda., BR).

2.8 Mucoadhesive properties

Mucoadhesion measurements from RA NE, and RA CNE were estimated by previously reported method (Barbi et al., 2014), using a texture analyser TAXTplus® (Stable Micro Systems, GB). Nasal mucosa was taken from pigs obtained from a local slaughterhouse. Heads of animals were divided by an incision along nasal septum and respiratory mucosa was carefully removed from nasal turbinates and stored at -20 °C for a maximum period of 1 month. Porcine nasal mucosa hydrated with artificial nasal mucus, described by Barbi et al. (2014), was used as mucosal model. Nasal mucosa was attached to upper movable probe (10 mm of diameter) of a mucoadhesion ring, and samples were kept in the lower platform of instrument. The measurement was performed with a triggered force of 2 mN, and no force was applied for 60 s, then the probe was raised at a constant speed of 0.5 mm/s. The maximal force (mN) required for detachment of samples from nasal mucosa model was used to compare mucoadhesive characteristics of formulations.

2.9 In vitro RA release study

In vitro RA release from RA NE, RA CNE and RA RF (rosmarinic acid control solution with receptor fluid) were evaluated on a Franz type diffusion cell, with a diffusion surface of approximately 1.80 cm², through 50 nm pore size synthetic membranes of ester cellulose (Millipore®). The receptor compartment was filled with 12 mL of potassium phosphate buffer pH 5.8. The bathing solution was stirred at 450 rpm and kept under a controlled temperature (34 ± 1 °C). In the donor compartment, 500 µL of each tested formulation were placed maintaining sink conditions. To estimate RA

content released from formulations during 8 h of time interval, samples of 1.0 mL of receptor fluid were withdrawn at 15, 30, 45, 60, 120, 180, 240, 300, 360, 420 and 480 min and the same volume of fresh fluid was added to receptor compartment in order to maintain a constant volume. Appropriate aliquots of all samples were filtered and then analyzed by UFLC method as described in Section 2.2. The area under curve from RA NE, RA CNE and RA RF were calculated and compared using GraphPad Prism 5 Software. As well, the release kinetics of RA from nanoemulsion were assessed by zero order ($Q = Q_0 + Kt$), first order ($\log Q = \log Q_0 - \frac{Kt}{2.303}$) and Higuchi ($Q = Kt^{1/2}$) mathematical equations, where K is the model release constant, Q_0 is the initial concentration of drug and Q is the amount of drug released in time t .

2.10 RA nasal mucosa permeation/retention study

RA nasal mucosa permeation/retention from RA NE, RA CNE and RA RF were evaluated on a Franz type diffusion cell, as described above, through excised mucosa membrane. Porcine nasal mucosa, obtained from a local slaughterhouse (Harmonia, BR), was prepared as described in Section 2.8 and previously immerse in potassium phosphate buffer pH 5.8 solution during 15 min. Then, nasal mucosa membrane was mounted between donor and acceptor compartments. The receptor compartment was filled with 12 mL of potassium phosphate buffer pH 5.8. The bathing solution was stirred at 450 rpm and kept under a controlled temperature (34 ± 1 °C). In the donor compartment, 500 μ L of each tested formulation were placed maintaining the sink conditions. Samples of 1.0 mL of receptor fluid were withdrawn at hourly intervals and the same volume of fresh fluid was added to receptor compartment in order to maintain a constant volume. After 8 h, mucosa was cleaned using a cotton swab, removed from cell and cut in small pieces. RA retained at membrane nasal mucosa was then extracted with methanol using an ultrasound bath during 120 min (Fachel et al., 2018). Appropriate aliquots of all samples were filtered and then analyzed by UFLC method as described in Section 2.2.

2.11 Histological and fluorescence microscopy studies

For histological studies, after 1 h and 8 h of permeation/retention assay (Section 2.10), mucosa was cleaned using a cotton swab, removed from the Franz cell, cut in small pieces and immersed in a 10% buffered formalin solution.

Following, tissue cuts were dehydrated, embedded in paraffin, and sectioned in 6 μm slices, which were mounted on clear glass slides, stained with hematoxylin and eosin (H&E) and covered with a thin glass coverslip. Images were captured using a digital camera connected to the microscope (100x magnification; Olympus BX51TF, JP).

For fluorescence experiments, a fluorescent dye, NBD-PE, was added during the preparation of nanoemulsions (Section 2.3 and 2.4) by spontaneous emulsification process. The NBD-PE labelled phospholipid (1%; w/v) was dissolved in ethanol with the other lipids and RA-loaded nanoemulsions were evaluated before and after chitosan coating. Approximately 500 μL of each fluorescent nanoemulsion was placed in the donor compartment of Franz cells, and nasal mucosa permeation/retention study was performed under the same experimental conditions described in Section 2.10. After 1 h and 8 h, mucosa was cleaned using a cotton swab, removed from cell, mounted with Tissue-Tek® O.C.T.™ (Sakura Finetechnical Co., Ltd., Tokyo, JP) onto a metal sample holder, flash frozen in liquid nitrogen and stored at $-20\text{ }^{\circ}\text{C}$. Vertical slices of 30 μm thickness were obtained with a cryostat (CM 1,850; Leica Microsystems, Wetzlar, DE), which were mounted on slides using Fluoromount-G™ (ThermoFisher, Waltham, US) and analyzed under a fluorescence microscope (100x magnification; Olympus BX51TF, JP).

2.12 Biological assays

2.12.1 Fibroblast cell culture and treatment

MRC-5 cell line (normal human lung fibroblasts) was obtained from American Type Culture Collection (ATCC). Cells were cultured in DMEM medium supplemented with 10% FBS and maintained at $37\text{ }^{\circ}\text{C}$ in a humidified 5% CO_2 atmosphere. 5×10^3 and 1×10^4 cells per well were seeded in 96 and 48-well plates for MTT (3(4,5-dimethyl)-2,5diphenyl-tetrazolium bromide) and PI (propidium iodide) incorporation assays, respectively. These plates were kept at $37\text{ }^{\circ}\text{C}$ in a humidified 5% CO_2 atmosphere for 24 h and were further treated with free RA or RA-loaded nanoemulsions (RA NE and RA CNE) at 3.125, 6.25, 12.5, 25, 50 and 100 μM concentrations. Appropriate controls containing DMSO and nanoemulsions without RA (B NE and B CNE) were performed. After 24 and 48 h of treatment, cell viability and cell death by necrosis were determined by MTT and PI methods, as described below.

2.12.2 Cell viability (MTT) assay

Cell viability was estimated using dehydrogenases-dependent 3(4,5-dimethyl)-2,5-diphenyl-tetrazolium bromide (MTT) reduction assay. This method is based on the ability of viable cells to reduce yellow tetrazolium MTT to blue formazan in the mitochondria. Following 24 or 48 h of exposition, treatment was removed and MTT solution (5 mg/mL) was added to culture media at a final concentration of 0.5 mg/mL. Cells were incubated for 60 min at 37 °C in a humidified 5% CO₂ atmosphere. Then, the medium was removed, and plates were shaken with dimethyl sulfoxide (DMSO) for 30 min. The absorbance was measured at 492 nm using a spectrophotometer SpectraMax® M2 (Molecular Devices, US) and results were expressed as percentage of control (Chassot et al., 2015; da Silveira et al., 2017).

2.12.3 Propidium iodide (PI) assay

Fluorescent image analysis of PI incorporation was used to assess cell death by necrosis. Cells were incubated with PI (7.5 µM) for 60 min at the end of treatments. An inverted microscope (Olympus IX71, JP) fitted with a standard rhodamine filter was excited at 515 e 560 nm using PI fluorescence. Images were captured using a digital camera connected to the microscope.

2.13 Statistical analysis

In all experiments, except the related to Section 2.5, results were shown as the mean ± standard deviation of at least three independent experiments. One-way analysis of variance (ANOVA) followed by Tukey's *post-hoc* was used to compare mean values with GraphPad Prism 5 Software. Differences among mean values were considered statistically significant when $p < 0.05$.

3 Results and discussion

3.1 Box-Behnken experimental design

Preliminary studies showed that different parameters may play a role on droplet size, PDI, and ζ-potential of chitosan-coated nanoemulsions, including oil phase concentration, lecithin to oil phase ratio, and chitosan final concentration (data not shown).

To evaluate all identified parameters together, a BBD, a multivariate technique based on RSM, was chosen for statistically optimize chitosan-coated RA nanoemulsions. This experimental design is applied to optimize the conditions during a development process and is assorted as a rotatable or nearly rotatable second-order design based on three-level incomplete factorial projects (Ferreira et al., 2007). Furthermore, it is an important alternative to avoid time-wasting in experiments, once it assembles several factors at different levels in a small number of runs (Kaiser et al., 2013).

A total of 15 runs were carried out to perform the optimization, based on the effects of the most impacting factors, selected in a screening study, on droplet size (Y_1), PDI (Y_2), ζ -potential (Y_3) and RA content (Y_4). The results for all experiments obtained during BBD analysis are described in Table 2. In summary, the response values for Y_1 , Y_2 , Y_3 and Y_4 ranged from 270.23 to 448.40 nm, 0.269 to 0.490, 41.97 to 48.63 mV, and 82.72 to 100.79 % of RA, respectively.

Table 2

Box-Behnken Design arrangement and experimental values for each response for rosmarinic acid chitosan-coated nanoemulsions.

Run	X ₁	X ₂	X ₃	Y ₁	Y ₂	Y ₃	Y ₄
1	-1	1	0	288.33	0.269	49.03	82.72
2	0	-1	-1	425.77	0.456	44.93	83.31
3	0	1	1	356.70	0.408	49.57	96.60
4	-1	0	-1	339.10	0.339	43.67	80.13
5	1	-1	0	352.10	0.340	47.90	100.79
6	1	1	0	365.23	0.378	50.83	98.80
7	0	-1	1	387.30	0.360	46.57	88.01
8	-1	-1	0	448.40	0.490	47.37	61.37
9	-1	0	1	343.70	0.334	48.63	87.54
10	1	0	1	325.17	0.360	47.50	95.82
11	1	0	-1	330.63	0.319	41.97	89.25
12	0	0	0	286.50	0.315	48.30	89.05
13	0	0	0	296.87	0.297	46.60	92.14
14	0	0	0	283.73	0.314	45.50	87.78
15	0	1	-1	270.23	0.272	44.80	98.65

X₁: oil phase concentration (% w/v); X₂: lecithin to oil phase ratio (w:w); X₃: final chitosan concentration (% w/v); Y₁: droplet size (nm); Y₂: PDI; Y₃: ζ -potential (mV); Y₄: rosmarinic acid content (%).

The predicted responses values were expressed by the following second-order polynomial equation using coded variables:

$$Y_1 = 979.7 - 37.38X_1 - 37.47X_2 - 573X_3 + 0.983X_1^2 + 0.4992X_2^2 + 576X_3^2 + 0.866X_1X_2 - 2.52X_1X_3 + 15.62 X_2X_3 \quad (\text{Eq. 2})$$

$$Y_2 = 1.1325 - 0.04017X_1 - 0.04499X_2 - 0.906X_3 + 0.000490X_1^2 + 0.000483X_2^2 + 0.431X_3^2 + 0.001298X_1X_2 + 0.01167X_1X_3 + 0.02896 X_2X_3 \quad (\text{Eq. 3})$$

$$Y_3 = 49.73 - 0.565X_1 - 0.689X_2 + 28.9X_3 + 0.0192X_1^2 + 0.01504X_2^2 - 45.9X_3^2 + 0.0063X_1X_2 + 0.142X_1X_3 + 0.392 X_2X_3 \quad (\text{Eq. 4})$$

$$Y_4 = 18.3 + 7.10X_1 + 2.02X_2 - 2.5X_3 - 0.144X_1^2 - 0.0014X_2^2 + 53.2X_3^2 - 0.1167X_1X_2 - 0.21X_1X_3 - 0.84 X_2X_3 \quad (\text{Eq. 5})$$

The suitability of BBD was demonstrated by the high coefficient of determination values (Table 3) obtained for all responses ($R^2=0.9844, 0.9861, 0.8759$ and 0.8455 for Y_1, Y_2, Y_3 and Y_4 , respectively). Furthermore, once no evidence of inadequacy was observed by lack-of-fit (Table 3), the mathematical models showed to be suitable for the analysis of response surface ($p > 0.05$). A large regression coefficient and a minor p -value would indicate a more significant effect on response variables for any of the terms in the models (Montgomery, 2001).

Table 3

Associated probability values (p -values), error lack of fit and regression for each response.

	R^2	Lack of Fit	p -values								
			Linear			Quadratic			Interaction		
			X_1	X_2	X_3	X_1^2	X_2^2	X_3^2	X_1X_2	X_1X_3	X_2X_3
Y_1	0.9844	0.232	0.193	0.000*	0.187	0.007*	0.000*	0.014*	0.001*	0.664	0.002*
Y_2	0.9861	0.374	0.346	0.000*	0.079	0.115	0.001*	0.044*	0.000*	0.117	0.000*
Y_3	0.8759	0.543	0.904	0.118	0.008*	0.54	0.094	0.053	0.67	0.848	0.314
Y_4	0.8455	0.071	0.011*	0.065	0.406	0.335	0.968	0.556	0.132	0.951	0.625

*Significant $p < 0.05$. R^2 : coefficient of determination; X_1 : oil phase concentration (% w/v); X_2 : lecithin to oil phase ratio (w/w); X_3 : final chitosan concentration (% w/v); Y_1 : droplet size (nm); Y_2 : PDI; Y_3 : ζ -potential (mV); Y_4 : rosmarinic acid content (%).

Associated probability values (*p*-value) was used to determine the significance of each coefficient (Montgomery, 2001). It was observed that lecithin to oil phase ratio was significant in linear (X_2), quadratic (X_2^2) and interaction (X_1X_2 and X_2X_3) terms for both droplet size (Y_1) and PDI (Y_2) determinations (Table 3). Nevertheless, for chitosan (Y_3) and oil phase (Y_4) concentrations were significant on ζ -potential (X_3) and on RA content (X_4), respectively, only in linear terms (Table 3).

Response surface plots for each response condition (Fig. 1) and composite desirability function were also analysed to optimize the formulation. The optimized conditions were 8.5% oil phase (w/v), 3:10 lecithin to oil phase ratio (w:w), and 0.1% (w/v) chitosan concentration with a 0.9353 calculated composite desirability index. Five replicates were performed under the optimal conditions as predicted by the models, to validate the predictive capacity of the mathematical model's equations developed. The comparison of average values obtained from these five experiments and the predicted values of the developed model are shown in Table 4 and demonstrated a good predictive capacity of models.

Table 4

Predicted and experimental values obtained from the response optimization of Box–Behnken design.

Responses	Predicted value	Experimental value ^a
Size (nm)	271.63	259.07 ± 5.93
PDI	0.2537	0.274 ± 0.01
ζ -potential (mV)	44.51	45.73 ± 1.76
RA Content (%)	95.34	92.66 ± 1.43

^a Mean ± SD of five determinations.

RA: rosmarinic acid; SD: standard deviation.

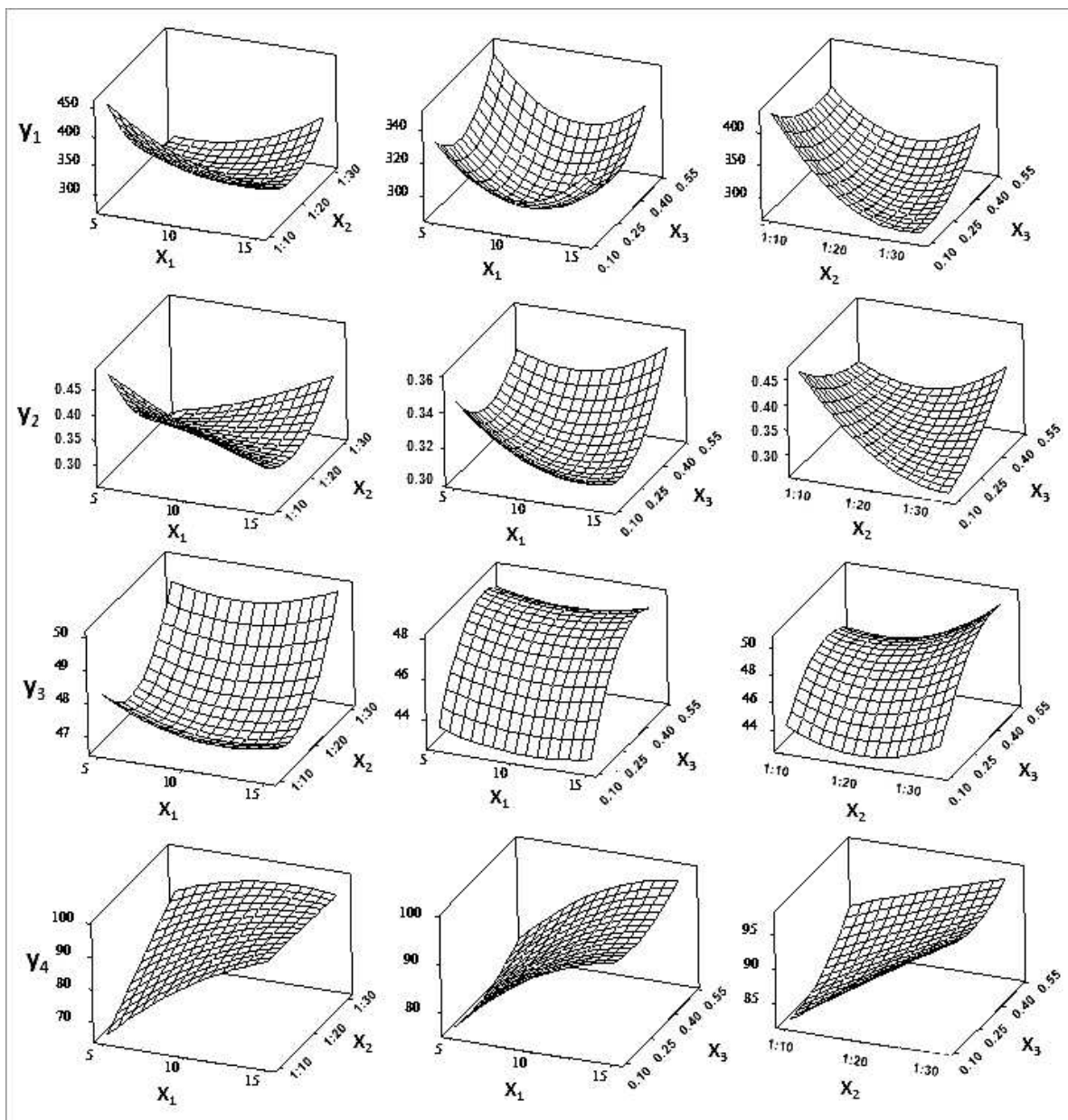


Fig. 1 Response surface plots (three-dimensional) showing the effect of the oil phase concentration (X_1 ; % w/v), lecithin to oil phase ratio (X_2 ; w:w), and chitosan final concentration (X_3 , % w/v) on the size (Y_1 , nm), PDI (Y_2), ζ -potential (Y_3 , mV), and rosmarinic acid content (Y_4 , %) in the chitosan-coated nanoemulsions.

3.2 Physicochemical characterization and mucoadhesive properties of nanoemulsions

An adequate physicochemical characterization of nanoemulsions is important to obtain well-defined nanostructures intended for therapeutic application (Bhattacharjee, 2016). The results from characterization of RA-loaded nanoemulsions before (RA NE) and

after chitosan coating (RA CNE) are summarized in Table 5. The results of RA content and association efficiency for RA NE and RA CNE were similar and higher than 92% and 89%.

Table 5
Physicochemical characterization and mucoadhesive capacity of nanoemulsions.

	RA NE	RA CNE
RA content (%)	95.12 ± 4.38	92.74 ± 1.38
Association Efficiency (%)	90.41 ± 0.20	89.04 ± 0.57
Size (nm)	236.3 ± 10.11	258.01 ± 3.82*
PDI	0.170 ± 0.02	0.272 ± 0.01*
ζ-potential (mV)	-25.07 ± 0.85	44.98 ± 1.75
pH	4.02 ± 0.09	4.18 ± 0.007
Viscosity (cP)	1.36 ± 0.009	3.80 ± 0.035*
Mucoadhesive Force (mN)	5.29 ± 0.24	7.33 ± 0.12***

Mean ± SD of three determinations.

RA: rosmarinic acid; RA NE: rosmarinic acid nanoemulsion; RA CNE: rosmarinic acid chitosan-coated nanoemulsion; SD: standard deviation.

Data were analyzed one-way analysis of variance (ANOVA) followed by Tukey's *post-hoc*.

*Significantly higher ($p < 0.05$) as compared with RA NE.

***Significantly higher ($p < 0.001$) as compared with RA NE.

RA NE and RA CNE exhibited droplet size of approximately 236 and 258 nm and PDI of 0.17 and 0.27, respectively, which is in accordance to previously reported for nanoemulsions obtained by spontaneous emulsification procedure (Argenta et al., 2016; Balestrin et al., 2016; Fasolo et al., 2009). Additionally, monodisperse RA-loaded nanoemulsions before (RA NE, PDI<0.2) and after (RA CNE, PDI<0.3) chitosan coating were achieved (Bshara, Osman, Mansour, & El-Shamy, 2014). RA CNE also promoted a significant increase in droplet size and PDI ($p < 0.05$), which could be explained by the adsorption of chitosan on surface of formulations (da Silva et al., 2014, 2016).

Droplet morphology of RA NE and RA CNE nanoemulsions is shown in Fig. 2A and 2B, respectively. TEM micrographs revealed similar nanodroplets, before and after chitosan coating, with spheroid shape, well-defined edge, and displaying a size in a 200–300 nm range with typical appearance of oil–water nanoemulsions. However, RA CNE oil droplet seems to be more irregular when compared to RA NE, which is probably associated with the presence of chitosan on surface of nanoemulsions (Prego et al., 2005).

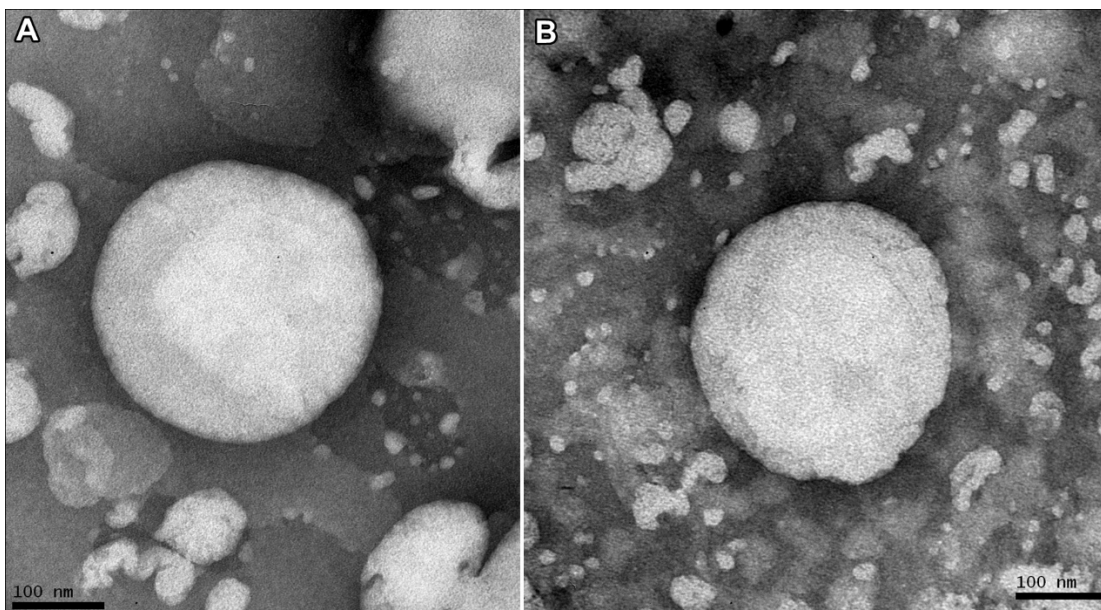


Fig. 2

TEM images of RA NE (A) and RA CNE (B).

TEM: transmission electron microscopy; RA NE: rosmarinic acid nanoemulsion; RA CNE: chitosan-coated rosmarinic acid nanoemulsion. Magnification 200K.

Table 5 also exhibits the viscosity of formulations. Regarding this parameter, results indicate a significant increase of viscosity (up to 3.8 cP) for RA CNE when compared to RA NE. These data confirmed that the addition of a polymer in nanoemulsions may be favourable to increase the residence time in nasal cavity through reduction of mucociliary clearance rate (Casettari & Illum, 2014).

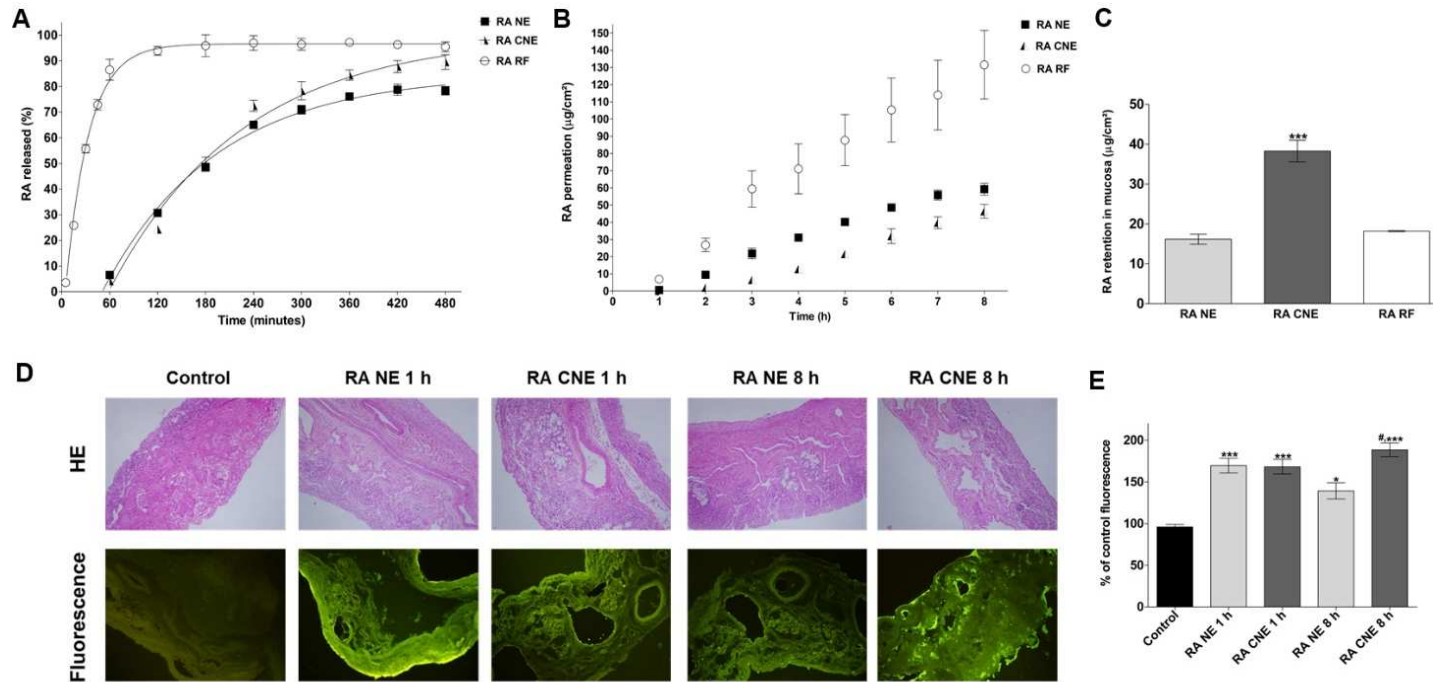
The ζ -potential and pH results (Table 5) from RA NE and RA CNE showed ζ -potential around -25 and +45 mV, and pH 4.02 and 4.18, respectively. These results showed a ζ -potential > 20 mV in module, suggesting physical stability of formulations. Furthermore, RA NE exhibited a negative value of ζ -potential at a 4.02 pH, related with the presence of negatively-charged phospholipids and free fatty acids present in egg-lecithin (Fasolo et al., 2009; S. C. Yang & Benita, 2000). Whereas, RA CNE exhibited a positive charge at a pH close to 4.0, which was attributed to the presence of the cationic polysaccharide chitosan on the surface of nanoemulsions (Prego et al., 2005). A positively-charged surface is a crucial characteristic for surface mucoadhesion, through a possible electrostatic interaction with the negatively-charged sialic groups from mucin present on mucosal surfaces (Barbi et al., 2014; Casettari & Illum, 2014).

The results from mucoadhesion measurement of RA NE and RA CNE by detachment test are also summarized in Table 5. The mucoadhesive force of RA CNE was found to be significantly higher ($p < 0.0001$) than RA NE, which demonstrates RA CNE mucoadhesive potential. Chitosan has been widely used as a mucoadhesive polymer in the development of delivery systems for nasal route, aiming to long lasting nasal uptake increasing the residence time and contact with the mucosa (Barbi et al., 2014; Prego et al., 2005).

3.3 *In vitro* release studies

In vitro RA release profile from RA NE, RA CNE and RA RF through synthetic cellulose ester membranes is shown in Fig. 3A. In summary, after 8 h of kinetics RA NE, RA CNE and RA RF releases approximately $78.4 \pm 1.67\%$, $89.5 \pm 2.86\%$ and $95.5 \pm 1.92\%$ of RA, respectively. Formulations have similar release profiles in terms of RA concentration ($p > 0.05$) at almost all-time points. RA CNE started quite slower and at the third hour of analysis it overpassed the amount of RA released when compared with RA NE. These results may be attributed to the higher viscosity of RA CNE, which may act as a barrier for initial drug release. Both nanoemulsions slowed RA release, as the area under curve obtained for RA NE and RA CNE was significantly smaller ($p < 0.05$) in comparison with RA control solution. Determination of coefficients obtained in different kinetic models for RA NE and RA CNE show that formulations follow the first order kinetic ($r^2 > 0.9358$), although it was not observed for free RA control solution ($r^2 = 0.6627$).

Prolonged released and kinetics observed for formulations *in vitro* could be explained by RA diffusion from the oil core of nanoemulsions and is a key factor in the development of nasal drug delivery systems. Sustained drug delivery is commonly reported in the literature for nanoemulsions (Kelman, Kuminek, Teixeira, & Koester, 2007). As observed for the formulations herein developed, RA-loaded solid lipid nanoparticles were also able to prolong RA release, as previously reported by Bhatt et al. (2014), resulting in approximately 75 % of RA released in 7 h of study.

**Fig. 3**

(A) *In vitro* release profile through synthetic cellulose membrane of RA NE, RA CNE and RA RF in potassium phosphate buffer pH 5.8 at 32 ± 0.5 °C. (B) Permeation profile through porcine nasal mucosa of RA NE, RA CNE, and RA RF after 8 h of kinetic study in potassium phosphate buffer pH 5.8 at 32 ± 0.5 °C as receptor fluid. (C) Retention profile of RA NE, RA CNE, and RA RF into porcine nasal mucosa after 8 h of permeation assay. (D) Hematoxylin and eosin (H&E) staining histological (upper) and fluorescence (down) images of nasal mucosa control or treated with RA NE and RA CNE after 1 or 8 h of permeation/retention studies. Magnification 100x. (E) Fluorescent intensity detected for RA NE and RA CNE treatments after 1 or 8 h of nasal mucosa permeation/retention studies in relation to the percentage of fluorescence emitted by the control mucosa. RA RF: rosmarinic acid control solution with receptor fluid; RA NE: rosmarinic acid nanoemulsion; RA CNE: chitosan-coated rosmarinic acid nanoemulsion; SD: standard deviation. (A, E) Data represent mean \pm SD of three determinations. (B, C) Data represent mean \pm SD of five determinations. Data were analyzed one-way analysis of variance (ANOVA) followed by Tukey's *post-hoc*. (C) ***Significantly higher ($p < 0.0001$) as compared with RA NE and RA RF. (D) * Significantly higher ($p < 0.05$) as compared with control; *** Significantly higher ($p < 0.0001$) as compared with control.

3.4 Nasal mucosa permeation/retention studies

Studies using animal models are commonly employed to evaluate the potential for nasal drug absorption. In this study, the porcine nasal mucosa membrane was chosen to investigate nasal permeation/retention profiles from RA formulations, once it presents morphological similarities with human mucosa, combined with the ethical consideration (Wadell & Björk, 1999; Wadell, Bjork, & Camber, 2003). To the best of our knowledge, there is no study in literature addressing RA permeation/retention through nasal mucosa using animal models, being the first time that this application is reported.

Permeation profile through porcine nasal mucosa of RA NE, RA CNE and RA RF are shown in Fig. 3B. Briefly, after 8 h of kinetics, RA NE, RA CNE and RA RF permeated approximately $60 \pm 3.38 \mu\text{g}\cdot\text{cm}^{-2}$, $46.7 \pm 4.04 \mu\text{g}\cdot\text{cm}^{-2}$ and $132 \pm 20.0 \mu\text{g}\cdot\text{cm}^{-2}$, respectively. The RA flux through the nasal mucosa was $7.5 \mu\text{g}\cdot\text{cm}^{-2}\cdot\text{h}^{-1}$, $5.8 \mu\text{g}\cdot\text{cm}^{-2}\cdot\text{h}^{-1}$ and $16.44 \mu\text{g}\cdot\text{cm}^{-2}\cdot\text{h}^{-1}$ for RA NE, RA CNE and RA RF, respectively. As can be seen, RA NE and RA CNE slowed permeation of RA across the nasal mucosa ($p < 0.05$). However, RA CNE promoted a slower kinetics of permeation, in comparison with RA NE, probably due to the potential mucoadhesive characteristics that chitosan confers to the formulation, which could result in an extended RA time of action (Prego et al., 2005).

Concerning the amount of RA retained into porcine mucosa nasal after 8 h of kinetics, RA CNE exhibited a higher RA retention ($p < 0.0001$) compared with RA NE and RA RF, as shown in Fig. 3C. These results demonstrated the highest penetrating potential from RA CNE and reinforced the presence of a strong interaction of the chitosan-coated nanoemulsion with nasal mucosa.

3.5 Histological and fluorescence microscopy studies

Histological and fluorescence microscopy evaluation was carried out to better investigate the increased RA retention from RA CNE as shown in nasal mucosa permeation/retention study. For fluorescence microscopy images the fluorescent labelled phospholipid NBD-PE was applied as fluorescence marker since it is easily dispersed in the interface of nanoemulsions. Nasal mucosa was exposed to RA NE or

RA CNE and tissues were analysed by histological and fluorescence microscopy following 1 and 8 h of permeation/retention protocols. Tissues not exposed to permeation/retention protocols were considered as control of experiment. As can be seen in Fig. 3D, histological images after treatment with both nanoemulsions even after 1 or 8 h maintained a structure similar to untreated mucosa, with three layers of epithelia (basal, middle and superficial, the last surrounded by mucus). Furthermore, fluorescence images (Fig. 3D) revealed that the fluorescence was distributed throughout the mucosa layers when NBD-PE was incorporated in the nanoemulsions. The fluorescent intensity detected for RA NE and RA CNE after 1 or 8 h of nasal mucosa permeation/retention studies are shown in Fig. 3E. Significantly higher ($p < 0.05$) amount of fluorescence were detected for both RA NE and RA CNE, even in 1 or 8 h, in comparison with the control, untreated porcine mucosa. Moreover, RA CNE exhibited a markedly higher ($p < 0.05$) fluorescent area when compared with RA NE after 8 h. These results suggest that there is higher RA CNE retention in nasal mucosa, which are in accordance with the amount of RA retained into porcine nasal mucosa from RA CNE after 8 h of permeation assay.

3.6 Biological assays

To assess the safety profile of new formulations *in vitro* studies, through MTT and PI assays, using cell cultures have been widely used and considered an effective approach (Chassot et al., 2015; da Silveira et al., 2017; Eisenbrand et al., 2002). In the present study, the toxicological/safety profile of RA-loaded nanoemulsions (RA NE and RA CNE) and free RA was evaluated *in vitro* on MRC-5 cell line (normal human lung fibroblast cells), a cell line extensively studied and characterized in cytotoxicity assays and easily maintained in culture (Barile, 1997; Mazzarino et al., 2015; Musa, Kannan, Masudi, & Rahman, 2012). Additionally, the fibroblasts are connective-tissue cells present in nasal mucosa, an important aspect for nasal delivery (Harkema, Carey, & Wagner, 2006; Lochhead & Thorne, 2012). RA concentrations ranging between 3.125 to 100 μM and treatment time (24 and 48 h) were selected based on previous literature, which reported the cytotoxicity evaluation of RA performed in different cell types (Huang & Zheng, 2006; Hur, Suh, Kim, & Won, 2007; Hur, Yun, & Won, 2004; Kolettas et al., 2006).

As shown in Fig. 4, free RA and RA nanoemulsions (RA NE and RA CNE) did not induce a significant cytotoxic activity on MRC-5 cells at 3.125 to 50 μM concentrations of RA, in relation to controls (DMSO or nanoemulsions without RA) after 24 (A) and 48 (B) h of treatments ($p > 0.05$). No cytotoxicity was observed for RA NE even at 100 μM RA concentration at 24 and 48 h, which might be associated with the absence of chitosan in this nanoemulsion. However, a significant cytotoxic activity of free RA (87.2 ± 3.6 and $66.0 \pm 23\%$) and RA CNE (72.5 ± 4.2 and $81.1 \pm 11.9\%$) at the higher RA concentration (100 μM) was observed following 24 and 48 h of treatment, respectively, when compared to control (100%) ($p < 0.05$). These data are in accordance to the previously reported by Yoshida et al., (2005) which show RA cytotoxic effect at similar concentrations.

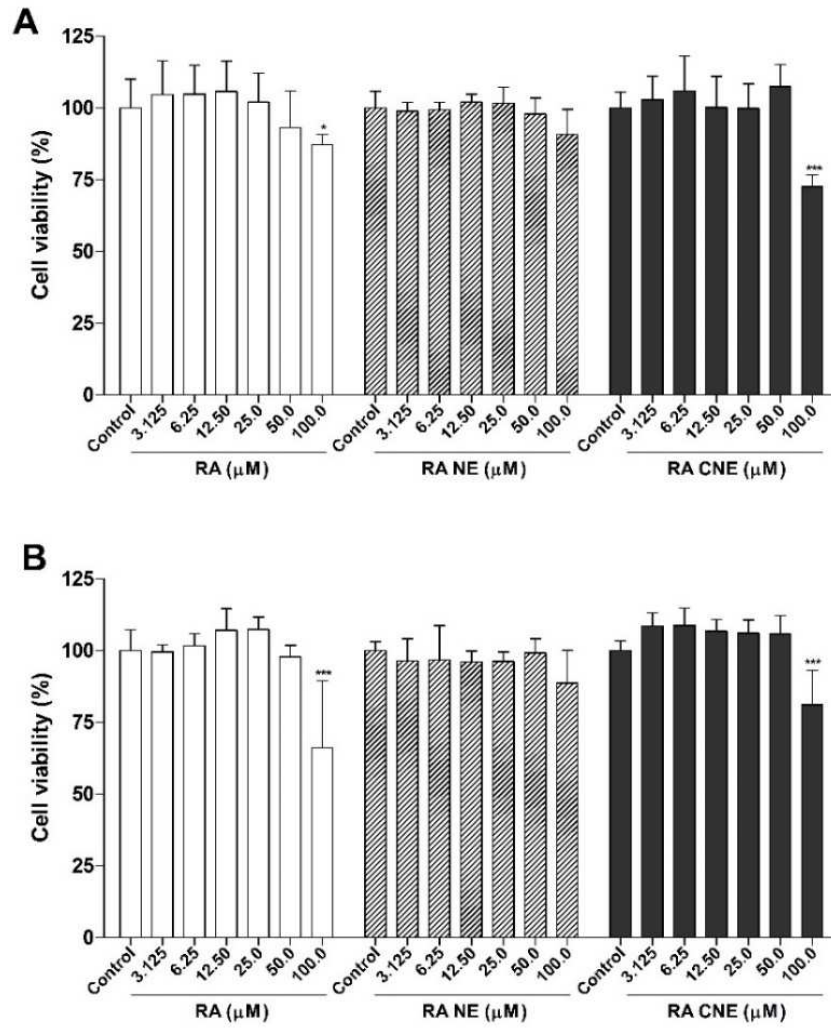


Fig. 4

Cell viability assessment by MTT reduction assay in fibroblasts (MRC-5) after 24 (A) and 48 (B) h of incubation with C, RA, RA NE, and RA CNE. Appropriate controls containing DMEM and 0.01% DMSO were performed.

RA: free rosmarinic acid; RA NE: rosmarinic acid nanoemulsion; RA CNE: chitosan-coated rosmarinic acid nanoemulsion; SD: standard deviation.

Data represent mean \pm SD for six determinations.

Data were analyzed one-way analysis of variance (ANOVA) followed by Tukey's *post-hoc*.

*Significantly lower ($p < 0.05$) as compared with RA (C, 3.125 μ M, 6.25 μ M, 25.0 μ M and 50 μ M).

***Significantly lower ($p < 0.0001$) as compared with RA and RA CNE (C, 3.125 μ M, 6.25 μ M, 25.0 μ M and 50 μ M).

To further investigate the safety of formulations, the characterization of cell death mechanism was performed for the first time for RA by PI incorporation assay, which is applied to evaluate necrosis. Qualitative evaluation of morphological alterations and PI incorporation in phase contrast and fluorescence microphotographs of MRC-5 cells are shown in Table 6 and Supplementary Fig.s 1 to 3, respectively. As could be seen in Table 6, no morphological alterations or PI incorporation were observed in fibroblasts exposed to free RA up to 50 μM after 24 or 48 h of treatment. These data are in accordance to cytotoxicity of free RA at 100 μM observed by MTT assay. On the other hand, as demonstrated in Table 6, fibroblasts exposed to RA NE and RA CNE exhibit morphological alterations at 50 and 25 μM , although PI incorporation was observed in 100 and 50 μM after 24 and 48 h of treatments, respectively. Corresponding volumes of nanoemulsions without RA were used as controls. Table 6 also show morphological alterations and PI incorporation at same or even lower corresponding concentrations of RA NE and RA CNE. These results demonstrated that the occurrence of necrosis is time-dependent and might be associated to nanotechnology-based formulations at concentrations ≤ 50 μM and demonstrated that the developed formulations could be safely used for nasal delivery up to 25 μM RA concentration.

Table 6

Morphological alterations and necrosis cell death qualitative evaluation in fibroblast cells (MRC-5) exposed to RA formulations.

Treatment time (h)		24						48					
Concentrations (μM)		3.125	6.25	12.50	25.0	50	100	3.125	6.25	12.50	25.0	50	100
RA	M	No	No	No	No	No	Yes	No	No	No	No	No	Yes
	PI	No	No	No	No	No	Yes	No	No	No	No	No	Yes
RA NE	M	No	No	No	No	Yes	Yes	No	No	No	Yes	Yes	Yes
	PI	No	No	No	No	No	Yes	No	No	No	No	Yes	Yes
B NE	M	No	No	No	Yes	Yes	Yes	No	No	Yes	Yes	Yes	Yes
	PI	No	No	No	Yes	Yes	Yes	No	No	Yes	Yes	Yes	Yes
RA CNE	M	No	No	No	No	Yes	Yes	No	No	No	Yes	Yes	Yes
	PI	No	No	No	No	No	Yes	No	No	No	No	Yes	Yes
B CNE	M	No	No	No	Yes	Yes	Yes	No	No	Yes	Yes	Yes	Yes
	PI	No	No	No	Yes	Yes	Yes	No	No	Yes	Yes	Yes	Yes

MRC-5 cells were treated with RA, RA NE and RA CNE. Following 24 or 48 h of treatment PI incorporation assay was performed. Appropriate controls containing corresponding volumes of B NE and B CNE were performed.

M: morphological alterations; PI: propidium iodide incorporation; No: absence; Yes: presence; RA: free rosmarinic acid; RA NE: rosmarinic acid nanoemulsion; RA CNE: chitosan-coated rosmarinic acid nanoemulsion; B NE: blank nanoemulsion; B CNE: blank chitosan coated-nanoemulsion.

4 Conclusion

In this study, we have demonstrated for the first time the development and optimization of chitosan-coated RA nanoemulsions for nasal delivery. We also have proved our hypothesis demonstrating RA CNE mucoadhesive potential associated with a prolonged drug release and a long-lasting permeation time with a higher RA penetration/retention through nasal mucosa, supported by fluorescence images. Different concentrations of oil phase, lecithin to oil phase ratio, and chitosan final concentration were evaluated to obtain an optimized formulation with minimum droplet size and PDI, and maximal ζ -potential and RA content. The optimum condition was obtained using a RSM in form of BBD. RA-loaded nanoemulsions, before and after chitosan coating, combined adequate physicochemical characteristics. Furthermore, the set of results showed a strong interaction between the chitosan-coated nanoemulsion and the nasal mucosa. Both types of nanoemulsions, as well as free RA, presented no cytotoxicity after 24 h (3.125 – 50 μ M) and 48 h (3.125 – 25 μ M), as indicated by cell viability (MTT) or cell death by necrosis (PI incorporation) assays in fibroblast culture. Consequently, the developed chitosan-coated nanoemulsion could be considered a suitable carrier intended to be used for RA nasal drug delivery aiming at neuroprotective therapy.

Conflicts of interest

The authors declare no conflict of interest.

Acknowledgements

The authors are grateful to the Conselho Nacional de Desenvolvimento Científico e Tecnológico (CNPq/Brazil) and to the Fundação de Amparo à Pesquisa no Estado do Rio Grande do Sul (FAPERGS/Brazil) for financial support. F.N.S.F., B.M.N., K.S.V. and R.S.S. thank Coordenação de Aperfeiçoamento de Pessoal de Nível Superior (CAPES/Brazil) and CNPq for their scholarship.

References

- Andrade, J. M. de, Passos, C. dos S., Rubio, M. A. K., Mendonça, J. N., Lopes, N. P., & Henriques, A. T. (2016). Combining *in vitro* and *in silico* approaches to evaluate the multifunctional profile of rosmarinic acid from *Blechnum brasiliense* on targets related to neurodegeneration. *Chemico-Biological Interactions*, *254*, 135–145. <https://doi.org/10.1016/j.cbi.2016.06.005>
- Argenta, D. F., Bidone, J., Misturini, F. D., Koester, L. S., Bassani, V. L., Simbes, C. M., & Teixeira, H. F. (2016). *In vitro* evaluation of mucosa permeation/retention and antiherpes activity of genistein from cationic nanoemulsions. *Journal of Nanoscience and Nanotechnology*, *16*(2), 1282–90. <https://doi.org/10.1166/jnn.2016.11676>
- Baba, S., Osakabe, N., Natsume, M., & Terao, J. (2004). Orally administered rosmarinic acid is present as the conjugated and/or methylated forms in plasma, and is degraded and metabolized to conjugated forms of caffeic acid, ferulic acid and m-coumaric acid. *Life Sciences*, *75*, 165–178. <https://doi.org/10.1016/j.lfs.2003.11.028>
- Balestrin, L. A., Bidone, J., Bortolin, R. C., Moresco, K., Moreira, J. C., & Teixeira, H. F. (2016). Protective effect of a hydrogel containing *Achyrocline satureioides* extract-loaded nanoemulsion against UV-induced skin damage. *Journal of Photochemistry and Photobiology B: Biology*, *163*, 269–276. <https://doi.org/10.1016/j.jphotobiol.2016.08.039>
- Baltzley, S., Mohammad, A., Malkawi, A. H., & Al-Ghananeem, A. M. (2014). Intranasal drug delivery of olanzapine-loaded chitosan nanoparticles. *AAPS PharmSciTech*, *15*(6), 1598–1602. <https://doi.org/10.1208/s12249-014-0189-5>
- Barbi, M. D. S., Carvalho, F. C., Kiill, C. P., Barud, H. D. S., Santagneli, S. H., Ribeiro, S. J. L., & Gremiao, M. P. D. (2014). Preparation and characterization of chitosan nanoparticles for AZT nasal delivery. *Journal of Nanoscience and Nanotechnology*, *14*, 1–10. <https://doi.org/10.1166/jnn.2015.9180>
- Barile, F. A. (1997). Continuous cell lines as a model for drug toxicity assessment. In J. V. Castell & M. J. Gómez-Lechón (Eds.), *In Vitro Methods in Pharmaceutical Research* (1st, pp. 33–54). Valencia, Spain: Academic Press. <https://doi.org/10.1016/B978-012163390-5.50004-1>
- Barnham, K. J., Masters, C. L., & Bush, A. I. (2004). Neurodegenerative diseases and oxidative stress. *Nature Reviews*, *3*, 205–214. <https://doi.org/10.1038/nrd1330>
- Bezerra, M. A., Santelli, R. E., Oliveira, E. P., Villar, L. S., & Escalera, L. a. (2008). Response surface methodology (RSM) as a tool for optimization in analytical chemistry. *Talanta*, *76*(5), 965–977. <https://doi.org/10.1016/j.talanta.2008.05.019>
- Bhatt, R., Mishra, N., & Bansal, P. K. (2013). Phytochemical, pharmacological and pharmacokinetics effects of rosmarinic acid. *Journal of Pharmaceutical and Scientific Innovation*, *2*(2), 28–34. <https://doi.org/10.7897/2277-4572.02215>
- Bhatt, R., Singh, D., Prakash, A., & Mishra, N. (2014). Development, characterization

and nasal delivery of rosmarinic acid-loaded solid lipid nanoparticles for the effective management of Huntington's disease. *Drug Delivery*, 1–9. <https://doi.org/10.3109/10717544.2014.880860>

Bhattacharjee, S. (2016). DLS and zeta potential - What they are and what they are not? *Journal of Controlled Release*, 235, 337–351. <https://doi.org/10.1016/j.jconrel.2016.06.017>

Bhullar, K. S., & Rupasinghe, H. P. V. (2013). Polyphenols: Multipotent therapeutic agents in neurodegenerative diseases. *Oxidative Medicine and Cellular Longevity*, 2013, 1–18. <https://doi.org/10.1155/2013/891748>

Bshara, H., Osman, R., Mansour, S., & El-Shamy, A. E. H. a. (2014). Chitosan and cyclodextrin in intranasal microemulsion for improved brain bupirone hydrochloride pharmacokinetics in rats. *Carbohydrate Polymers*, 99, 297–305. <https://doi.org/10.1016/j.carbpol.2013.08.027>

Casettari, L., & Illum, L. (2014). Chitosan in nasal delivery systems for therapeutic drugs. *Journal of Controlled Release*, 190, 189–200. <https://doi.org/10.1016/j.jconrel.2014.05.003>

Chassot, J. M., Ribas, D., Silveira, E. F., Grünspan, L. D., Pires, C. C., Farago, P. V., ... Cruz, L. (2015). Beclomethasone dipropionate-loaded polymeric nanocapsules: development, *in vitro* cytotoxicity, and *in vivo* evaluation of acute lung injury. *Journal of Nanoscience and Nanotechnology*, 15(1), 855–864. <https://doi.org/10.1166/jnn.2015.9178>

Costa, P., Sarmiento, B., Gonçalves, S., & Romano, A. (2013). Protective effects of *Lavandula viridis* L'Hér extracts and rosmarinic acid against H₂O₂-induced oxidative damage in A172 human astrocyte cell line. *Industrial Crops and Products*, 50, 361–365. <https://doi.org/10.1016/j.indcrop.2013.07.054>

da Silva, S. B., Amorim, M., Fonte, P., Madureira, R., Ferreira, D., Pintado, M., & Sarmiento, B. (2014). Natural extracts into chitosan nanocarriers for rosmarinic acid drug delivery. *Pharmaceutical Biology*, 53(5), 642–652. <https://doi.org/10.3109/13880209.2014.935949>

da Silva, S. B., Ferreira, D., Pintado, M., & Sarmiento, B. (2016). Chitosan-based nanoparticles for rosmarinic acid ocular delivery — *In vitro* tests. *International Journal of Biological Macromolecules*, 84, 112–120. <https://doi.org/10.1016/j.ijbiomac.2015.11.070>

da Silveira, E. F., Azambuja, J. H., Rosa, T., Carvalho, T. R. De, Kunzler, A., Daniel, S., ... Braganhol, E. (2017). Interactions selective *in vitro* antitumoral activity and inhibit cancer cell growth in a preclinical model of glioblastoma multiforme. *Chemico-Biological*, 266, 1–9. <https://doi.org/10.1016/j.cbi.2017.02.001>

Domard, A. (2011). A perspective on 30 years research on chitin and chitosan. *Carbohydrate Polymers*, 84(2), 696–703. <https://doi.org/10.1016/j.carbpol.2010.04.083>

- Du, T., Li, L., Song, N., Xie, J., & Jiang, H. (2010). Rosmarinic acid antagonized 1-methyl-4-phenylpyridinium (MPP⁺)-induced neurotoxicity in MES23.5 dopaminergic cells. *International Journal of Toxicology*, *29*(6), 625–633. <https://doi.org/10.1177/1091581810383705>
- Dudhani, A. R., & Kosaraju, S. L. (2010). Bioadhesive chitosan nanoparticles: Preparation and characterization. *Carbohydrate Polymers*, *81*(2), 243–251. <https://doi.org/10.1016/j.carbpol.2010.02.026>
- Eisenbrand, G., Pool-Zobel, B., Baker, V., Balls, M., Blaauboer, B. J., Boobis, A., ... Kleiner, J. (2002). Methods of *in vitro* toxicology. *Food and Chemical Toxicology*, *40*(2–3), 193–236. [https://doi.org/10.1016/S0278-6915\(01\)00118-1](https://doi.org/10.1016/S0278-6915(01)00118-1)
- Fachel, F. N. S., Nemitz, M. C., Medeiros-Neves, B., Veras, K. S., Bassani, V. L., Koester, L. S., ... Teixeira, H. F. (2018). A novel, simplified and stability-indicating high-throughput ultra-fast liquid chromatography method for the determination of rosmarinic acid in nanoemulsions, porcine skin and nasal mucosa. *Journal of Chromatography B*, *1083*, 233–241. <https://doi.org/10.1016/j.jchromb.2018.03.020>
- Fallarini, S., Miglio, G., Paoletti, T., Minassi, a., Amoruso, a., Bardelli, C., ... Lombardi, G. (2009). Clovamide and rosmarinic acid induce neuroprotective effects in *in vitro* models of neuronal death. *British Journal of Pharmacology*, *157*(6), 1072–1084. <https://doi.org/10.1111/j.1476-5381.2009.00213.x>
- Fasolo, D., Bassani, V. L., & Teixeira, H. F. (2009). Development of topical nanoemulsions containing quercetin and 3- O -methylquercetin. *Pharmazie*, *64*, 726–730. <https://doi.org/10.1691/ph.2009.8357>
- Ferreira, S. L. C., Bruns, R. E., Ferreira, H. S., Matos, G. D., David, J. M., Brandão, G. C., ... dos Santos, W. N. L. (2007). Box-Behnken design: An alternative for the optimization of analytical methods. *Analytica Chimica Acta*, *597*(2), 179–186. <https://doi.org/10.1016/j.aca.2007.07.011>
- Ghaffari, H., Venkataramana, M., Ghassam, B. J., Chandra Nayaka, S., Nataraju, a, Geetha, N. P., & Prakash, H. S. (2014). Rosmarinic acid mediated neuroprotective effects against H₂O₂-induced neuronal cell damage in N2A Cells. *Life Sciences*, *113*(1–2), 7–13. <https://doi.org/10.1016/j.lfs.2014.07.010>
- Grassin-Delyle, S., Buenestado, A., Naline, E., Faisy, C., Blouquit-Laye, S., Couderc, L. J., ... Devillier, P. (2012). Intranasal drug delivery: An efficient and non-invasive route for systemic administration - Focus on opioids. *Pharmacology and Therapeutics*, *134*(3), 366–379. <https://doi.org/10.1016/j.pharmthera.2012.03.003>
- Harkema, J. R., Carey, S. A., & Wagner, J. G. (2006). The Nose Revisited: A Brief Review of the comparative structure, function, and toxicologic pathology of the nasal epithelium. *Toxicologic Pathology*, *34*(3), 252–269. <https://doi.org/10.1080/01926230600713475>
- Hirai, A., Odani, H., & Nakajima, A. (1991). Determination of degree of deacetylation of chitosan by H NMR spectroscopy. *Polymer Bulletin*, *26*(1), 87–94.

<https://doi.org/10.1007/bf00299352>

Huang, S., & Zheng, R. (2006). Rosmarinic acid inhibits angiogenesis and its mechanism of action *in vitro*. *Cancer Letters*, 239(2), 271–280. <https://doi.org/10.1016/j.canlet.2005.08.025>

Hur, Y.-G., Suh, C.-H., Kim, S., & Won, J. (2007). Rosmarinic acid induces apoptosis of activated T cells from rheumatoid arthritis patients via mitochondrial pathway. *Journal of Clinical Immunology*, 27(1), 36–45. <https://doi.org/10.1007/s10875-006-9057-8>

Hur, Y.-G., Yun, Y., & Won, J. (2004). Rosmarinic acid induces p56lck-dependent apoptosis in Jurkat and peripheral T cells via mitochondrial pathway independent from Fas/Fas ligand interaction. *Journal of Immunology (Baltimore, Md. : 1950)*, 172, 79–87. <https://doi.org/10.4049/jimmunol.172.1.79>

Kaiser, S., Verza, S. G., Moraes, R. C., Pittol, V., Peñaloza, E. M. C., Pavei, C., & Ortega, G. G. (2013). Extraction optimization of polyphenols, oxindole alkaloids and quinovic acid glycosides from cat's claw bark by Box–Behnken design. *Industrial Crops and Products*, 48, 153–161. <https://doi.org/10.1016/j.indcrop.2013.04.026>

Kelmann, R. G., Kuminek, G., Teixeira, H. F., & Koester, L. S. (2007). Carbamazepine parenteral nanoemulsions prepared by spontaneous emulsification process. *International Journal of Pharmaceutics*, 342(1–2), 231–239. <https://doi.org/10.1016/j.ijpharm.2007.05.004>

Kolettas, E., Thomas, C., Leneti, E., Skoufos, I., Mbatsi, C., Sisoula, C., ... Evangelou, A. (2006). Rosmarinic acid failed to suppress hydrogen peroxide-mediated apoptosis but induced apoptosis of Jurkat cells which was suppressed by Bcl-2. *Molecular and Cellular Biochemistry*, 285(1–2), 111–120. <https://doi.org/10.1007/s11010-005-9064-8>

Kumar, M., Misra, A., Babbar, a. K., Mishra, a. K., Mishra, P., & Pathak, K. (2008). Intranasal nanoemulsion based brain targeting drug delivery system of risperidone. *International Journal of Pharmaceutics*, 358(1–2), 285–291. <https://doi.org/10.1016/j.ijpharm.2008.03.029>

Lee, H. J., Cho, H.-S., Park, E., Kim, S., Lee, S.-Y., Kim, C.-S., ... Chun, H. S. (2008). Rosmarinic acid protects human dopaminergic neuronal cells against hydrogen peroxide-induced apoptosis. *Toxicology*, 250(2–3), 109–115. <https://doi.org/10.1016/j.tox.2008.06.010>

Lochhead, J. J., & Thorne, R. G. (2012). Intranasal delivery of biologics to the central nervous system. *Advanced Drug Delivery Reviews*, 64(7), 614–628. <https://doi.org/10.1016/j.addr.2011.11.002>

Madureira, A. R., Campos, D. A., Fonte, P., Nunes, S., Reis, F., Gomes, A. M., ... Pintado, M. M. (2015). Characterization of solid lipid nanoparticles produced with carnauba wax for rosmarinic acid oral delivery. *RSC Adv.*, 5, 22665–22673. <https://doi.org/10.1039/C4RA15802D>

Mazzarino, L., Loch-Neckel, G., Bubniak, L. dos S., Ourique, F., Otsuka, I., Halila, S., ... Borsali, R. (2015). Nanoparticles made from xyloglucan-block-polycaprolactone copolymers: Safety assessment for drug delivery. *Toxicological Sciences*, *147*(1), 104–115. <https://doi.org/10.1093/toxsci/kfv114>

Medronho, B., Valente, A. J. M., & Costa, P. (2014). Inclusion complexes of rosmarinic acid and cyclodextrins: stoichiometry, association constants, and antioxidant potential. *Colloid and Polymer Science*, *292*, 885–894. <https://doi.org/10.1007/s00396-013-3124-5>

Mistry, A., Stolnik, S., & Illum, L. (2009). Nanoparticles for direct nose-to-brain delivery of drugs. *International Journal of Pharmaceutics*, *379*(1–2), 146–157. <https://doi.org/10.1016/j.ijpharm.2009.06.019>

Montgomery, D. C. (2001). *Design and Analysis of Experiments, 5th edition*. John Wiley and Sons, New York.

Musa, M., Kannan, T. P., Masudi, S. M., & Rahman, I. A. (2012). Assessment of DNA damage caused by locally produced hydroxyapatite-silica nanocomposite using Comet assay on human lung fibroblast cell line. *Molecular & Cellular Toxicology*, *8*(1), 53–60. <https://doi.org/10.1007/s13273-012-0007-7>

Nemitz, M. C., Fachel, F. N. S., Beckenkamp, A., Buffon, A., Teixeira, H. F., & Poser, G. L. von. (2017). Soybeans isoflavone aglycone-rich extracts: Optimization by different bioprocesses and production of a purified fraction with promising wound healing property. *Industrial Crops and Products*, *105*(April), 193–202. <https://doi.org/10.1016/j.indcrop.2017.04.065>

Petersen, M., & Simmonds, M. S. J. (2003). Rosmarinic acid. *Phytochemistry*, *62*(2), 121–125. [https://doi.org/10.1016/S0031-9422\(02\)00513-7](https://doi.org/10.1016/S0031-9422(02)00513-7)

Prego, C., García, M., Torres, D., & Alonso, M. J. (2005). Transmucosal macromolecular drug delivery. *Journal of Controlled Release*, *101*(1–3 SPEC. ISS.), 151–162. <https://doi.org/10.1016/j.jconrel.2004.07.030>

Ren, P., Jiang, H., Li, R., Wang, J., Song, N., Xu, H. M., & Xie, J. X. (2009). Rosmarinic acid inhibits 6-OHDA-induced neurotoxicity by anti-oxidation in MES23.5 cells. *Journal of Molecular Neuroscience*, *39*(1–2), 220–225. <https://doi.org/10.1007/s12031-009-9182-y>

Roberts, G. a. F., & Domszy, J. G. (1982). Determination of the viscometric constants for chitosan. *International Journal of Biological Macromolecules*, *4*(6), 374–377. [https://doi.org/10.1016/0141-8130\(82\)90074-5](https://doi.org/10.1016/0141-8130(82)90074-5)

Saraiva, C., Praça, C., Ferreira, R., Santos, T., Ferreira, L., & Bernardino, L. (2016). Nanoparticle-mediated brain drug delivery: Overcoming blood-brain barrier to treat neurodegenerative diseases. *Journal of Controlled Release*, *235*, 34–47. <https://doi.org/10.1016/j.jconrel.2016.05.044>

Signini, R., & Campana Filho, S. P. (1998). Purificação e caracterização de quitosana

comercial. *Polímeros*, 8(4). <https://doi.org/10.1590/S0104-14281998000400009>

Solanki, I., Parihar, P., & Parihar, M. S. (2016). Neurodegenerative diseases: From available treatments to prospective herbal therapy. *Neurochemistry International*, 95, 100–108. <https://doi.org/10.1016/j.neuint.2015.11.001>

Soobrattee, M. a., Neergheen, V. S., Luximon-Ramma, a., Aruoma, O. I., & Bahorun, T. (2005). Phenolics as potential antioxidant therapeutic agents: Mechanism and actions. *Mutation Research - Fundamental and Molecular Mechanisms of Mutagenesis*, 579(1–2), 200–213. <https://doi.org/10.1016/j.mrfmmm.2005.03.023>

Sood, S., Jain, K., & Gowthamarajan, K. (2014). Optimization of curcumin nanoemulsion for intranasal delivery using design of experiment and its toxicity assessment. *Colloids and Surfaces B: Biointerfaces*, 113, 330–337. <https://doi.org/10.1016/j.colsurfb.2013.09.030>

Wadell, C., & Björk, E. (1999). Nasal drug delivery – evaluation of an *in vitro* model using porcine nasal mucosa. *European Journal of Pharmaceutical Sciences*, 7, 197–206. [https://doi.org/10.1016/S0928-0987\(98\)00023-2](https://doi.org/10.1016/S0928-0987(98)00023-2)

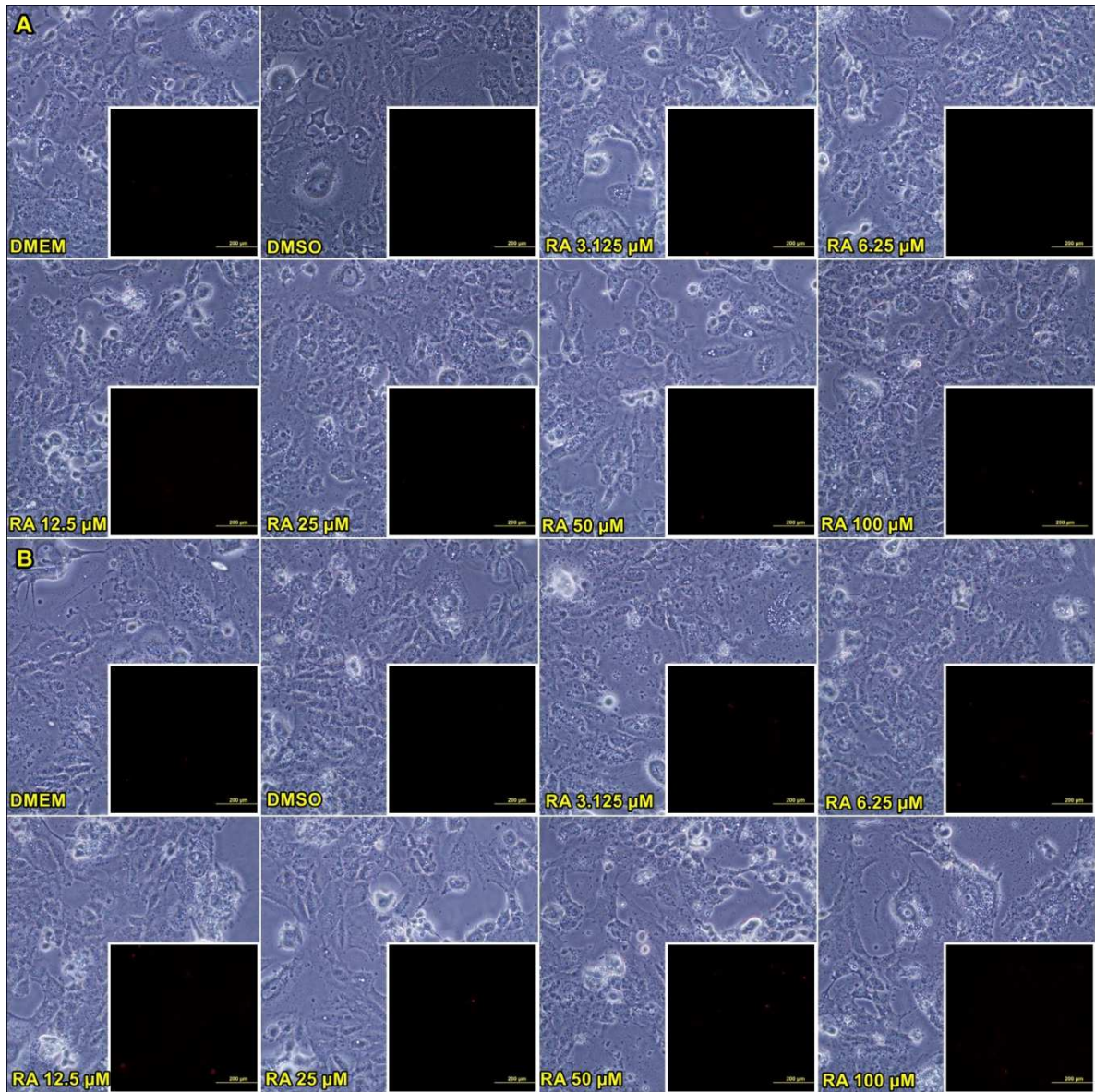
Wadell, C., Bjork, E., & Camber, O. (2003). Permeability of porcine nasal mucosa correlated with human nasal absorption. *European Journal of Pharmaceutical Sciences*, 18, 47–53. [https://doi.org/10.1016/S0928-0987\(02\)00240-3](https://doi.org/10.1016/S0928-0987(02)00240-3)

Wang, X., Chi, N., & Tang, X. (2008). Preparation of estradiol chitosan nanoparticles for improving nasal absorption and brain targeting. *European Journal of Pharmaceutics and Biopharmaceutics*. <https://doi.org/10.1016/j.ejpb.2008.07.005>

Yang, J., Zhang, L., Li, J., Chen, L., Zheng, Q., Chen, T., ... Di, L. (2015). Enhanced oral bioavailability and prophylactic effects on oxidative stress and hepatic damage of an oil solution containing a rosmarinic acid – phospholipid complex. *Journal of Functional Foods*, 19, 63–73. <https://doi.org/10.1016/j.jff.2015.09.013>

Yang, S. C., & Benita, S. (2000). Enhanced absorption and drug targeting by positively charged submicron emulsions. *Drug Development Research*, 486(50), 476–486. [https://doi.org/10.1002/1098-2299\(200007/08\)50:3/4<476::AID-DDR31>3.0.CO;2-6](https://doi.org/10.1002/1098-2299(200007/08)50:3/4<476::AID-DDR31>3.0.CO;2-6)

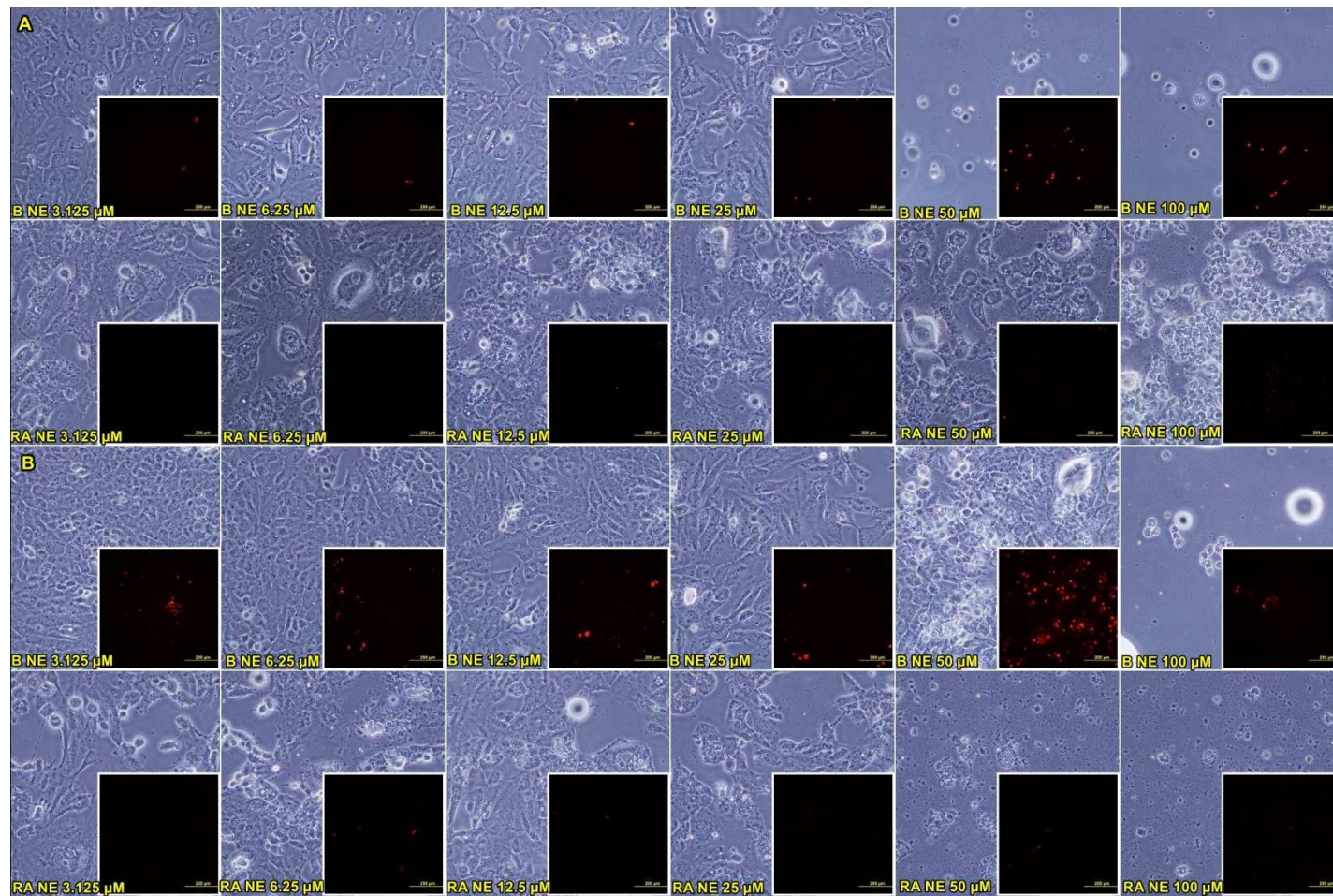
Yoshida, M., Fuchigami, M., Nagao, T., Okabe, H., Matsunaga, K., Takata, J., ... Fujioka, T. (2005). Antiproliferative constituents from Umbelliferae plants VII . Active triterpenes and rosmarinic acid from *Centella asiatica*. *Biological and Pharmaceutical Bulletin*, 28(1), 173–175. <https://doi.org/http://doi.org/10.1248/bpb.28.173>



Supplementary Fig. 1

Phase contrast and fluorescence microphotographs (insert) with PI incorporation in fibroblast cells (MRC-5) after 24 (A) and 48 (B) h of treatment with RA. Appropriate controls containing DMEM and 0.01% DMSO were performed.

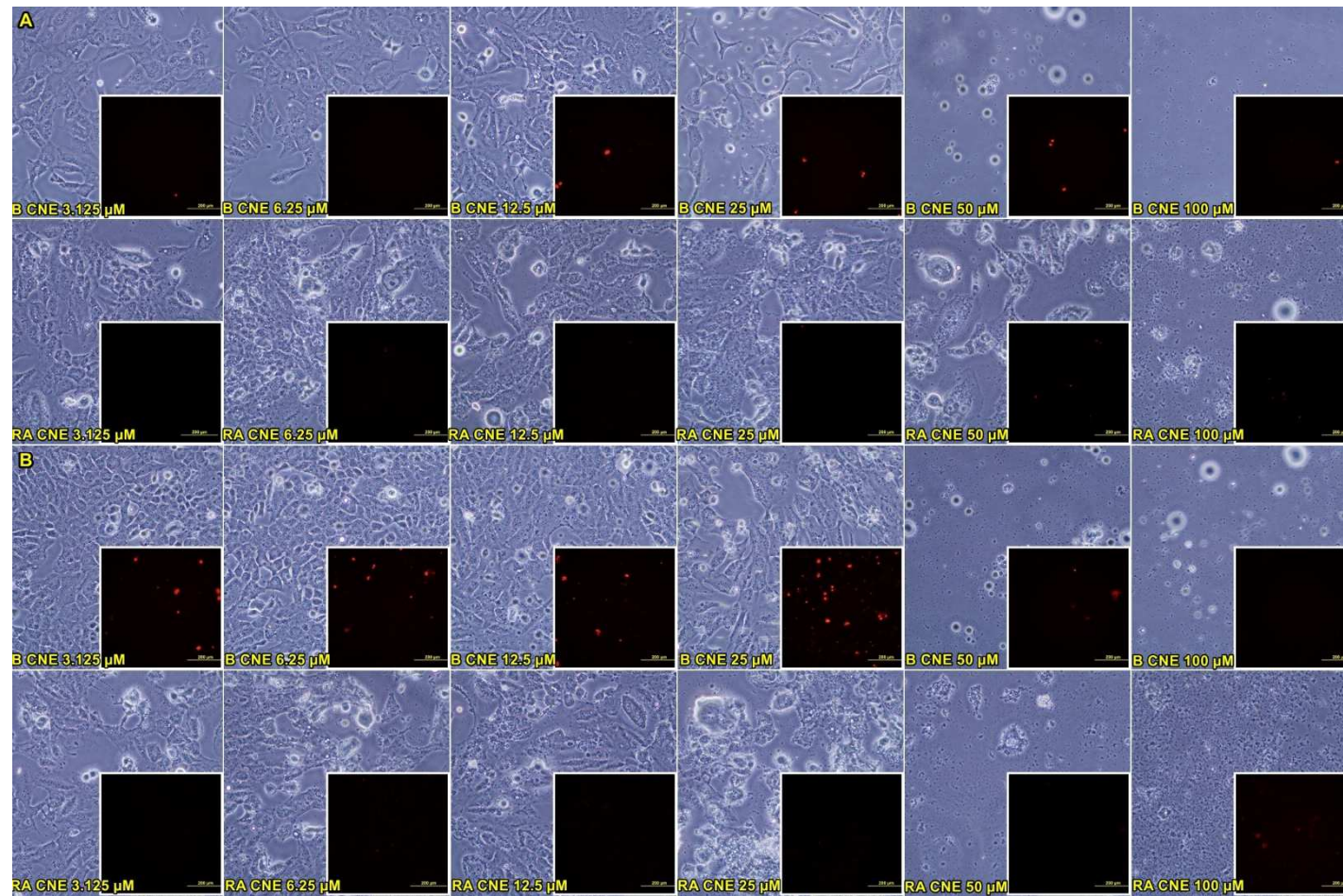
DMEM: Dulbecco's modified Eagle's medium; DMSO: Dimethyl sulfoxide; RA: free rosmarinic acid.



Supplementary Fig. 2

Phase contrast and fluorescence microphotographs (insert) with PI incorporation in fibroblast cells (MRC-5) after 24 (A) and 48 (B) h of treatment with RA NE. Appropriate controls containing the corresponding concentrations of B NE were performed.

B NE: blank nanoemulsion; RA NE: rosmarinic acid nanoemulsion.



Supplementary Fig. 3

Phase contrast and fluorescence microphotographs (insert) with PI incorporation in fibroblast cells (MRC-5) after 24 (A) and 48 (B) h of treatment with RA CNE. Appropriate controls containing the corresponding concentrations of B CNE were performed.

B CNE: blank chitosan coated-nanoemulsion; DMEM: Dulbecco's modified Eagle's medium; RA CNE: chitosan-coated rosmarinic acid nanoemulsion.

Introdução

O quarto capítulo da presente tese compreende um artigo científico que aborda o potencial glioprotetor das nanoemulsões revestidas por quitosana contendo ácido rosmarínico (AR) no ambiente de inflamação e estresse oxidativo induzido por lipopolissacarídeo (LPS) em cultura primária de astrócitos. Sabe-se que o emprego de compostos naturais moduladores dos processos inflamatórios e do estresse oxidativo, como o AR, pode ser uma abordagem terapêutica atraente para as doenças neurodegenerativas (DN), tendo em vista, que ainda hoje o desenvolvimento de terapias neuroprotetoras efetivas são de grande interesse na área farmacêutica. Para tanto, a presente tese no seu terceiro capítulo visou o desenvolvimento e otimização de novas formulações, mais efetivas, associando-se o emprego do AR e nanoemulsões mucoadesiva como uma nova abordagem tecnológica para terapias neuroprotetoras em DN. Para avaliação da atividade neuroprotetora dessas novas abordagens terapêuticas frente as DN, modelos in vitro envolvendo inflamação e/ou estresse oxidativo têm sido comumente empregados. Dentre esses modelos, o emprego de células gliais, como os astrócitos, e dano induzido por LPS tem se destacado, justamente, pela capacidade de simular o estresse oxidativo e a reação inflamatória presentes no sistema nervoso central (SNC) e comuns as DN. Neste contexto, o presente capítulo foi conduzido de forma a avaliar o potencial protetor e/ou terapêutico do AR na sua forma livre e nas nanoemulsões otimizadas em modelo de inflamação/estresse oxidativo induzido por LPS em cultura primária de astrócitos, através dos ensaios de viabilidade, proliferação e morte celular por necrose. Parâmetros oxidativos, migração celular e expressão do marcador de astrócitos reativos (GFAP) também foram avaliados.

Artigo científico:

Glioprotective effect of chitosan-coated rosmarinic acid nanoemulsions against lipopolysaccharide-induced inflammation and oxidative stress in rat astrocyte primary culture

A ser submetido no *Cellular and Molecular Neurobiology*

Introdução

O quinto capítulo compreende um artigo científico em andamento que aborda o potencial neuroprotetor da administração pela via nasal de nanoemulsões revestidas por quitosana contendo ácido rosmarínico (AR) contra o déficit de memória induzido por lipopolissacarídeo (LPS) em ratos Wistar. As doenças neurodegenerativas (DN) ainda representam um importante problema clínico devido à falta de estratégias terapêuticas que previnam com sucesso sua progressão, sendo as terapias neuroprotetoras e uso de compostos naturais uma abordagem promissora. Para tanto, a presente tese visou, em seus capítulos 3 e 4, o desenvolvimento, otimização e avaliação in vitro da atividade glioprotetora de nanoemulsões revestidas por quitosana contendo AR para administração pela via nasal como uma nova abordagem tecnológica visando terapia neuroprotetora em DN. Neste contexto, o presente capítulo foi conduzido de forma a avaliar o efeito neuroprotetor da administração nasal das nanoemulsões revestidas por quitosana contendo AR contra o déficit de memória induzido por LPS em ratos Wistar. Além disso, para investigar e garantir que o protocolo de administração nasal das nanoemulsões revestidas por quitosana contendo AR foi capaz de atingir o cérebro, primeiro validamos o método por cromatografia líquida de ultra eficiência previamente desenvolvido, capítulo 2, em matrizes de plasma e cérebro de ratos.

Artigo científico:

Neuroprotective effect of chitosan-coated rosmarinic acid nanoemulsions nasal administration in Wistar rats against lipopolysaccharide-induced memory deficit

A ser submetido no *Experimental Neurology* (Estudos em andamento)

Neuroprotective effect of chitosan-coated rosmarinic acid nanoemulsions nasal administration in Wistar rats against lipopolysaccharide-induced memory deficit

Flávia Nathiely Silveira Fachel^a, Luana Roberta Michels^a, Juliana Hofstätter Azambuja^b, Gabriela Spies Lenz^b, Valquíria Linck Bassani^a, Letícia Scherer Koester^a, Amelia Teresinha Henriques^a, Alethea Gatto Barschak^c, Elizandra Braganhol^b, Helder Ferreira Teixeira^{a,*}

^a Programa de Pós-Graduação em Ciências Farmacêuticas, Faculdade de Farmácia, Universidade Federal do Rio Grande do Sul, Porto Alegre, RS, Brazil

^b Programa de Pós-Graduação em Biociências, Universidade Federal de Ciências da Saúde de Porto Alegre, Porto Alegre, RS, Brazil

^c Programa de Pós-Graduação em Patologia, Universidade Federal de Ciências da Saúde de Porto Alegre, Porto Alegre, RS, Brazil

*Corresponding author. Tel.: (+55) 51 3308 5231; fax: (+55) 51 3308 2165.

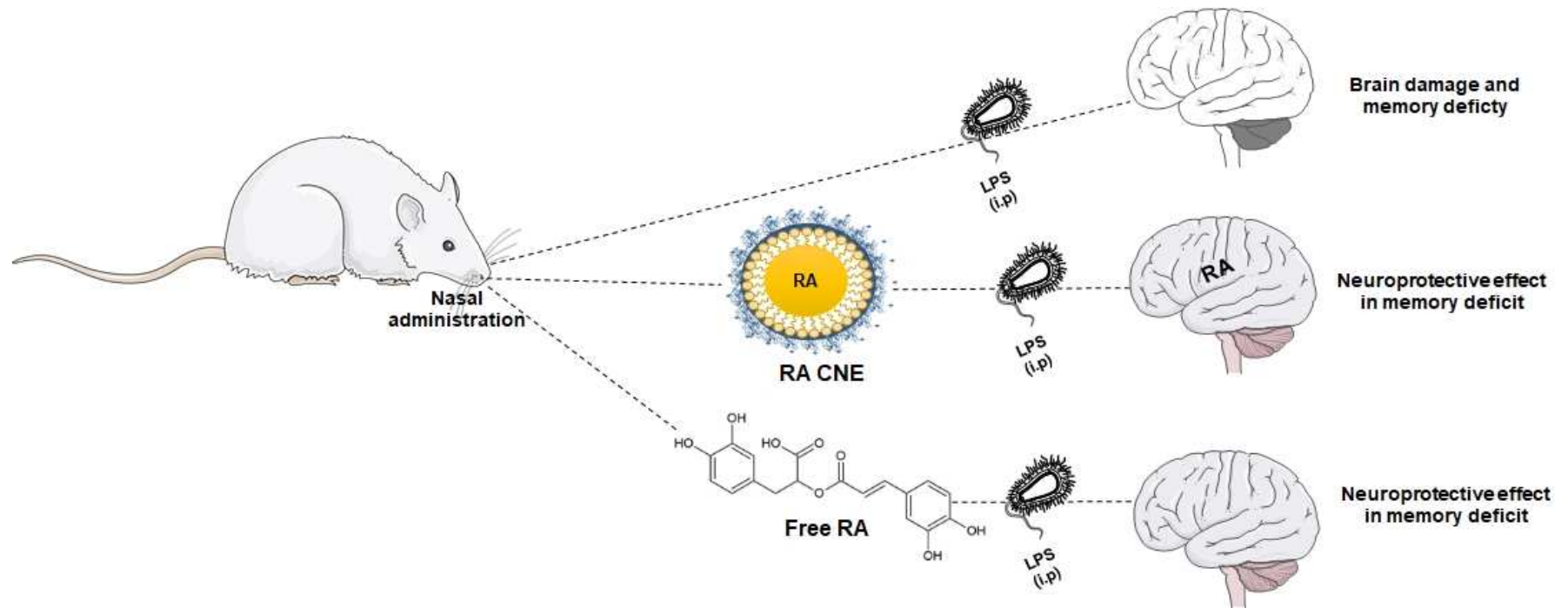
E-mail address: helder.teixeira@ufrgs.br (Helder Ferreira Teixeira).

Abstract

Neurodegenerative disorders (ND) represent an important clinical problem due to the lack of therapeutic strategies that successfully prevent its progression, being the neuroprotective therapies an emerging approach for ND. Rosmarinic acid (RA) is a phenolic compound with a well-documented neuroprotective potential. Nevertheless, RA poor oral bioavailability and low permeability in the central nervous system (CNS) represent a great challenge for its neuroprotective potential. In this context, the present study was conducted aiming at evaluating the neuroprotective effect of chitosan-coated RA nanoemulsions (RA CNE) nasal administered in Wistar rats against LPS-induced memory deficit. We demonstrated that nasal administration (n.a., 100 μ L per nostril) twice a day (7 am/ 7 pm) for six days of RA CNE (2 mg.mL⁻¹) and free RA (2 mg.mL⁻¹) were able to protect against memory deficits induced by LPS (250 μ g.mL⁻¹) administered intraperitoneally ($p < 0.001$). It was also observed that RA CNE nasal administration facilitates RA brain permeability (0.173 \pm 0.038 μ g). In conclusion, RA CNE nasal administration is a promising approach for neuroprotective therapies in ND. Further studies to comprehend the impact of the use of mucoadhesive nanotechnology-based delivery systems in CNS are still necessary.

Keywords: Rosmarinic acid; Chitosan-coated nanoemulsions; Lipopolysaccharide; Wistar rats; Neuroprotective effect.

Graphical abstract



1 Introduction

Neurodegenerative disorders (ND), such as multiple sclerosis, Alzheimer's and Parkinson's diseases, represent an important clinical problem due to its complex etiology (genetic and non-genetic factors) and the absence of therapeutic strategies that successfully prevent disease progression (Pérez-Hernández et al., 2016; Solanki et al., 2016). Among the non-genetic factors, recent studies have demonstrated that alterations in immune/inflammatory and redox systems can contribute significantly to neuronal damage and ND progression. In this sense, the neuroprotective effects of natural compounds with anti-inflammatory and antioxidant activities has assembled considerable interest of researchers (Bhat et al., 2015; Fischer and Maier, 2015).

Rosmarinic acid (RA) is a phenolic compound, an ester of caffeic acid and 3,4-dihydroxyphenyllactic acid, present in numerous species of medicinal plants (Kim et al., 2015; Petersen, 2013). This natural compound has various biological activities reported in literature, including a well-documented anti-inflammatory and antioxidant activities, and, recently, associated with its neuroprotective potential demonstrated *in vitro* (Andrade et al., 2016; Costa et al., 2013; Du et al., 2010; Fallarini et al., 2009; Ghaffari et al., 2014; Huang et al., 2009; Lee et al., 2008) and *in vivo* (Coelho et al., 2015; Fonteles et al., 2016; Khamse et al., 2015; Shang et al., 2017; Wang et al., 2012). RA neuroprotection *in vivo* studies were frequently performed using intragastric administration, and did not consider the RA poor oral bioavailability described in literature (Baba et al., 2004). To overcome these limitation some technological strategies have been investigated to improves its oral bioavailability (Madureira et al., 2016; Medronho et al., 2014). However, another barrier to the RA performance in ND is associated to its poor availability in the central nervous system (CNS), in view of its limited ability to cross the blood-brain barrier (BBB) (Kuo and Rajesh, 2017; Li et al., 2018; Szwajgier et al., 2017).

BBB characterizes an important obstacle for therapeutic agent delivery in CNS, which is critical for neuroprotective therapies (Lochhead and Thorne, 2012). An emerging approach for drug delivery directly to CNS is the use of nasal route, mainly due to its capability to bypass BBB by olfactory region (Paun et al., 2010). Bhatt et al. (2014) reported the use of nasal route for RA delivery associated with solid lipid nanoparticles

(SLN) aiming the treatment of Huntington's disease. However, the main limitation of the nasal route is the mucociliary clearance and fluid secretion that limited the time for drug absorption. Thus, to improve the nasal drug absorption, some strategies have been studied, among them, the use of penetration enhancers associated with mucoadhesive polymers (Casettari and Illum, 2014; Prego et al., 2005).

Recently, our research group developed and optimized chitosan-coated RA nanoemulsions (RA CNE) (Fachel et al., 2018a), and demonstrated the glioprotective effect against LPS-induced damage in astrocytes (Fachel et al., unpublished) intended to be used as a new potential neuroprotective therapy through nasal delivery. We also have demonstrated that the association of lipid-nanotechnology-based delivery systems with mucoadhesive biopolymers have been a promising strategy to improve RA penetration through biological barriers and its residence time in nasal cavity (Fachel et al., 2018a).

In this context, the present study was conducted aiming to evaluate the neuroprotective effect of RA CNE nasal administration in Wistar rats against LPS-induced memory deficit. The RA availability in brain was also evaluated using a validated ultra-fast liquid chromatography (UFLC) method.

2 Materials and methods

2.1 Materials

RA reference standard with over 98% purity was purchased from Carbosynth Ltd. (Berkshire, GB). Acetonitrile, methanol, and trifluoroacetic acid liquid chromatographic grade were supplied from Tedia (Rio de Janeiro, BR). Reverse osmosis using a Milli-Q apparatus (Millipore, Billerica, US) was employed to obtain ultra-pure water. Egg-lecithin (Lipoid E-80[®]) and medium chain triglycerides (MCT) were attained from Lipoid GmbH (Ludwigshafen, DE). Low molecular weight chitosan and LPS from *Escherichia coli* (055: B5) were supplied from Sigma-Aldrich Co. (St. Louis, US). Glacial acetic was obtained by Dinâmica Química Contemporânea Ltda. (Diadema, BR). Potassium phosphate monobasic and dibasic were supplied from Nuclear (São Paulo, BR).

2.2 Chitosan-coated nanoemulsion

Chitosan-coated RA nanoemulsion (RA CNE) was prepared as previously optimized and described by our research group (Fachel et al., 2018a). First, RA-loaded nanoemulsions were prepared by oil-in-water spontaneous emulsification procedure. Oil components (RA 0.4% (w/v), MCT 6% (w/v) and egg-lecithin 2.5% (w/v) were dissolved in ethanol and then poured into the water phase under magnetic stirring. Subsequently, a process of evaporation at 40°C under reduced pressure removed the organic solvent and concentrated RA until 4 mg.mL⁻¹. RA CNE was further prepared by coating the RA-loaded nanoemulsion prepared with chitosan solution (0.2%, w/v). The RA-loaded nanoemulsion were mixed with the chitosan solution at 1:1 ratio and submitted to magnetic stirring. An appropriate control without RA were also prepared and was called as blank chitosan-coated nanoemulsions (B CNE).

2.3 Physicochemical characterization of chitosan-coated nanoemulsion

RA CNE and B CNE were characterized concerning droplet size, PDI, ζ -potential, RA association efficiency and content (when applicable). To determine the droplet size and PDI photon correlation spectroscopy was employed after appropriate dilution of samples in water using a Zetasizer Nano-ZS90[®] (Malvern Instruments, England, GB) equipment. To determine ζ -potential electrophoretic mobility was used after appropriate dilution of samples in NaCl 1 mM using a Zetasizer Nano-ZS90[®] (Malvern Instruments, England, GB) equipment. RA association efficiency and content of samples were carried-out as previously described by Fachel et al. (2018a).

2.4 Instrumentation and chromatographic conditions

Ultra-fast liquid chromatography system (UFLC Shimadzu Prominence series system) equipped with an automatic injector, a photodiode array (PDA) detector and an LC solutions software (Kyoto, Japan) was employed for RA analyses. Kinetex C18 column (100 x 2.1 mm i.d.; particle size, 2.6 μ m; Phenomenex, USA) guarded by a pre-column filter in-line Ultra (Phenomenex, USA) was employed for chromatographic separation at 55°C, flow rate of 0.55 mL.min⁻¹, injection volume of 3 μ L and detection wavelength of 330 nm. An isocratic eluent composed of water and acetonitrile (83:17, v/v), acidified with 0.1% trifluoroacetic acid (v/v), was employed up to 3.5 min (Fachel et al., 2018b).

2.5 Standard and matrices solutions preparation

2.5.1 RA standard

A stock solution of RA ($1 \text{ mg}\cdot\text{mL}^{-1}$) was prepared in methanol. The stock solution was then diluted in water/acetonitrile mixture (80:20; v:v) to obtain a series of working standard solutions. The stock and standard solution were maintained in darkness at $4 \pm 2^\circ\text{C}$.

2.5.2 Rat plasma matrix

Plasma matrix from Wistar rats was prepared by protein precipitation using trichloroacetic acid 5% (w/v). Plasma homogenates were centrifugated (1,000 *g*, 10 min), the supernatants were collected, diluted in water/acetonitrile mixture (80:20; v:v) and filtered through a 0.22 μm nylon syringes filter. Protocol for animal samples was approved by the Committee of Ethics and Animal Experimentation of Federal University of Health Sciences of Porto Alegre, Brazil, under the protocol number 220/2017.

2.5.3 Rat brain matrix

Brain matrix from Wistar rats was obtained by homogenization of tissue with methanol and further sonication in ultrasonic bath for 30 min. Brain homogenates were centrifuged (1,000 *g*, 10 min), the supernatants were collected and filtered through a 0.22 μm nylon syringes filter. Protocol for animal samples was approved by the Committee of Ethics and Animal Experimentation of Federal University of Health Sciences of Porto Alegre, Brazil, under the protocol number 220/2017.

2.6 Method validation

The UFLC method previously developed and validated by our research group (Fachel et al., 2018b) was validated in terms of specificity, linearity, matrix effect, stability, precision, accuracy and extraction recovery for rat plasma and brain, according to the official guidelines (European Medicine Agency (EMA), 2012; Food and Drug Administration (FDA), 2013; International Conference on Harmonization (ICH), 1996).

2.6.1 System suitability

Before method validation, system suitability parameters (peak area, retention time, theoretical plates and tailing factor of RA) were achieved to verify the appropriateness of the chromatographic system for the proposed analysis (Shabir, 2003).

2.6.2 Specificity

The specificity was obtained by comparing chromatograms (peak purity and retention time) of pure RA standard solution with chromatograms of matrices (plasma and brain) spiked with RA at the concentration of $10 \mu\text{g}\cdot\text{mL}^{-1}$ and matrices solutions (blank samples).

2.6.3 Linearity, matrix effect and stability

The linearity was determined by regression analysis using the least square method. Three standard curves were obtained in three consecutive days by plotting the measured peak area versus the RA concentration in standard and matrices (0.1, 2.0, 4.0, 6.0, 8.0, and $10.0 \mu\text{g}\cdot\text{mL}^{-1}$), by six replicates per concentration. Analysis of variance (ANOVA) were used to analyze the results using a significance level of $\alpha=0.05$.

The matrix effect of plasma and brain was evaluated by the comparison of RA-spiked matrices standard curve slopes obtained during the linearity assay with pure RA standard curve slope.

The stability of RA standard and RA-spiked matrices was assessed by performing the analysis of peak area and detecting any alteration in the chromatographic pattern of the stored samples (room temperature = $25 \pm 1^\circ\text{C}$) for 24 h compared with a freshly prepared sample, intending to overestimate the time expended during routine analysis.

2.6.4 Precision and accuracy

The precision was evaluated as both intra-day precision (repeatability) and inter-day precision (intermediate precision) expressed as the relative standard deviations (% RSD) at four RA different levels (0.1, 2.0, 6.0, $10.0 \mu\text{g}\cdot\text{mL}^{-1}$), in six replicates at each level.

The accuracy was evaluated by adding known amounts of the RA standard at four different levels (0.1, 2.0, 6.0, 10.0 $\mu\text{g}\cdot\text{mL}^{-1}$), in six replicates at each level, and was determined as follows: $\text{AC \%} = (\text{mean experimental concentration} \times 100 / \text{mean theoretical concentration})$.

2.6.5 Extraction recovery

The RA extraction recovery was evaluated from Wistar rats plasma and brain spiked with known amounts of RA standard leading to a theoretical concentration of 0.1, 2.0, 6.0 and 10.0 $\mu\text{g}\cdot\text{mL}^{-1}$. To plasma matrices trichloroacetic acid 5% (w/v) in proportion 1:1 (v:v) was added. Then, plasma homogenates were centrifugated (1,000 g, 10 min), the supernatants were collected and diluted in water/acetonitrile mixture (80:20; v:v). Brain tissues (previously washed with saline) were homogenized with 2 mL of methanol per g of tissue in an IKA® Ultra-Turrax T8 mixer (IKA Works Inc., Wilmington, US). All matrices were filtered through a 0.22 μm nylon syringes filter and analyzed by UFLC method. The recovery was expressed as percentage, assessed by comparing the theoretical final concentration based on the spiked amount and the experimental result attained after extraction procedure.

2.7 Animals

Male Wistar rats (60 days old), weighing 350–450 g, were used in this study. The animals had *ad libitum* access to food and water and were maintained in the Central Animal House of Federal University of Health Sciences of Porto Alegre under a standard cycle of lighting conditions (12 h dark–light), controlled temperature ($22 \pm 2^\circ\text{C}$) and relative humidity (45%–55%). All animal procedures were approved by the Committee of Ethics and Animal Experimentation of Federal University of Health Sciences of Porto Alegre, Brazil, under the protocol number 220/2017. Procedures for the use and care of animals were assumed according to the Brazilian Guidelines for the Care and Use of Animals in Scientific Research Activities and the National Council of Control of Animal Experimentation.

2.8 Experimental protocols

2.8.1 Brain and plasma distribution

Three Male Wistar rats were given nasal administration (n.a., 100 μ L per nostril) of RA CNE (2 mg.mL⁻¹, total of RA/dose = 200 μ g) and free RA (2 mg.mL⁻¹ in potassium phosphate buffer pH 5.8, total of RA/dose = 200 μ g) twice a day (7 am/ 7 pm) for six days. Plasma and brain tissue were promptly removed after 1 h of last RA CNE. Each tissue sample was immediately processed as described in item 2.4.5.

2.8.2 Treatment

Twenty-five male Wistar rats were randomly selected to perform behavioral tests and they were divided into five groups: control (saline); LPS (i.p. 250 μ g.kg⁻¹); RA CNE (2 mg.mL⁻¹, total of RA/dose = 200 μ g) + LPS; free RA (2 mg.mL⁻¹ in potassium phosphate buffer pH 5.8, total of RA/dose = 200 μ g) + LPS; and B CNE (vehicle) + LPS. The animals were pre-treated by nasal administration (n.a., 100 μ L per nostril) of RA CNE, RA, B CNE and saline (control and LPS groups) twice a day (7 am/ 7 pm) for six days based on Carvalho et al. (2017) protocol, since protective protocol of LPS-induced damage in astrocytes demonstrated more promising results (Fachel et al., unpublished). In the sixth day, the animals received the last administration 1 h prior training test for object recognition. LPS was dissolved in saline (250 μ g.mL⁻¹) and intraperitoneally (i.p.) administered after training of object recognition. After 24 h the animals were euthanized immediately after object recognition test with novel object. All information described above are shown in Fig. 1 scheme.

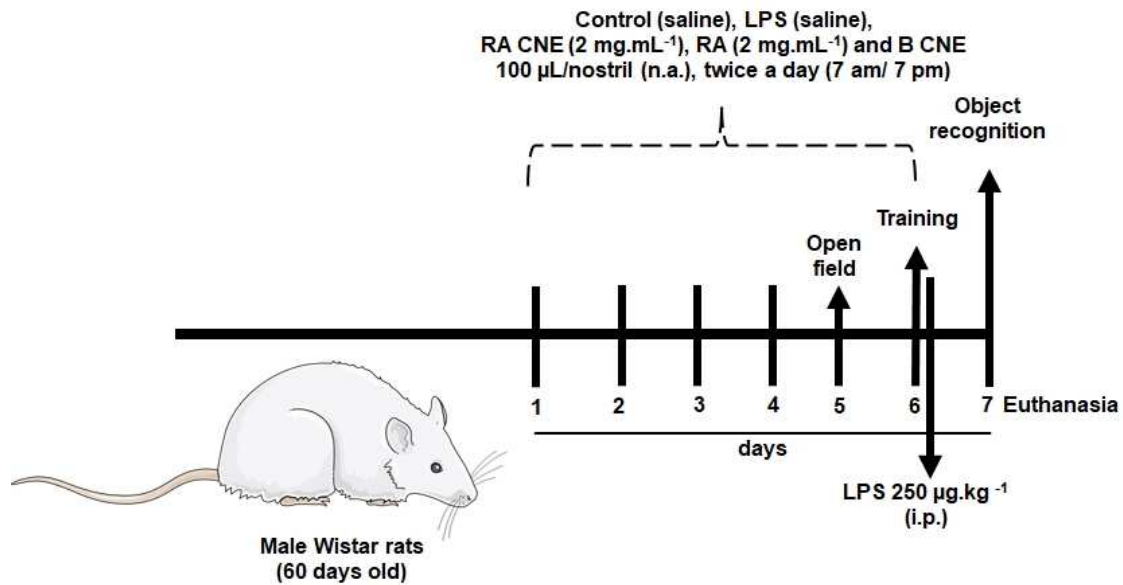


Figure 1

Scheme of treatment with RA CNE, RA, B CNE and saline, and the protocol LPS-induced damage in Wistar rats.

LPS: lipopolysaccharide; RA CNE: chitosan-coated rosmarinic acid nanoemulsion; RA: free rosmarinic acid; B CNE: blank chitosan-coated nanoemulsion.

2.9 Behavioural tests

2.9.1 Open field test

As shown in Fig. 1, after 5 days of pre-treatment of different groups, the animals experienced an open field test, which was also used as habituation to the apparatus. In this test, the male Wistar rats were individually placed in the center of an arena apparatus (90-cm diameter, 36-cm high walls) with the floor divided in 25 parts (9 central and 16 peripheral squares) (Costa et al., 2015). Animals remained within the setup for 5 min and the total crossing and rearing response were analyzed. After each individual session, the arena was cleaned with 40% ethanol.

2.9.2 Object recognition test

Object recognition test was used to evaluate the effect of LPS and RA treatments on memory evocation (Carvalho et al., 2017; Pacheco et al., 2018). As shown in Fig. 1,

one day after the open field test, the animals experienced the object recognition test. First, a training session was performed; basically, the animals were placed individually in the center of arena and they were allowed to explore freely two identical objects (object 1 and 2) for 5 min. Later, the animals received LPS (i.p. 250 $\mu\text{g}\cdot\text{mL}^{-1}$) and 24 h after LPS administration they were submitted to object recognition test session. For that, the animals were placed again in center of arena for 5 min to explore freely, with one of the previous objects (2) replaced by a new object (object 3). The objects were pairs of plastic mounting blocks and were placed in a symmetrical position inside the apparatus. The time spent exploring the familiar and novel object was recorded. Exploration only was considered when animals were sniffing or touching the objects. After each individual session, the arena and objects were cleaned with 40% ethanol. Recognition index was used to analyze the results obtained for each male Wistar rat and was calculated as follows: recognition index = $\text{TN}/(\text{TF} + \text{TN})$, where TF is the time spent exploring the familiar object 1 and TN is the time spent exploring the new object 3 (Pacheco et al., 2018).

2.9.3 Statistical analysis

Results were shown as the mean \pm standard deviation (SD) and statistical analysis were performed using one-way analysis of variance (ANOVA) followed by Tukey's post-hoc using GraphPad Prism 5 Software. When $p < 0.05$, the differences between mean values were considered statistically significant.

3 Results and Discussion

3.1 Physicochemical characterization of chitosan-coated nanoemulsions

In the present study, RA CNE and B CNE were prepared and characterized. Monodisperse nanoemulsions with a mean droplet size of approximately 310 nm and a polydispersity index lower than 0.3 was achieved from chitosan-coating procedure of nanoemulsions obtained by spontaneous emulsification. Nanoemulsions also presented ζ -potential higher than 35 mV in module, suggestive of physical stability. Furthermore, RA association efficiency and content was over 90% and 85%. Well-defined nanostructures of RA CNE, even with 0.2 % (w/v) of RA (double oil-content),

and B CNE were obtained and are in agreement with our previous report (Fachel et al., 2018a), demonstrating that experimental conditions were well controlled.

3.2 Determination of RA in brain

In the present study, we first validated the UFLC method previously developed by our research group to guarantee that it is possible to use the same developed methodology for application in more two biological matrices, rat plasma and brain, as well as the ability of free RA and RA CNE reaches the brain and plasma through nasal route are not completely understood.

Regarding the system suitability, overall results demonstrated that the UFLC method is suitable for RA analysis in rat plasma and brain (Shabir, 2003). The parameters values and their relative standard deviation (RSD, %) were: retention time of 2.63 (0.05) min, theoretical plates of 5446.82 (0.08), and tailing factor of 1.25 (0.06).

The method was specific for RA determination in rat plasma and brain matrices, as well as the RA peak purity was demonstrated in RA spiked-matrices and no co-eluting substances in the same RA retention time were detected in matrices. As presented in Table 1, the method was linear for RA determination in rat plasma and brain matrices in range of 0.1 – 10 $\mu\text{g}\cdot\text{mL}^{-1}$ according with correlation coefficients. Linear regression and the absence of linearity deviation was also demonstrated by ANOVA evaluation of regression significance and confidence interval on the intercepts. LOQ was fixed 0.1 $\mu\text{g}\cdot\text{mL}^{-1}$ as it was the lowest concentration of RA that could be quantified with acceptable precision and accuracy. The results for rat plasma and brain matrices effects (Table 1) were lower than 2.7% and indicates a low matrix effect in RA analysis (Fachel et al., 2018b; Niessen et al., 2006).

Table 1. Linearity and summary of the output of the ANOVA of RA standard, rat plasma and brain matrices.

	RA standard	Rat plasma matrix	Rat brain matrix	
Range ($\mu\text{g}\cdot\text{mL}^{-1}$)	0.1 – 10.0	0.1 – 10.0	0.1 – 10.0	
Regression equation	$y = 8592x - 183.18$	$y = 8777.8x - 238.3$	$y = 8829.7x - 40.559$	
R	0.9996	0.9994	0.9996	
Matrix effect (%)	-	2.12	2.69	
Regression	Significance F	2.239E-94 ^a	6.376E-90 ^a	1.851E-97 ^a
	<i>p</i> -value	0.32600 ^b	0.2865 ^b	0.8226 ^b
Intercept	Lower 95%	-556.1767	-693.4420	-377.8245
	Upper 95%	187.8070	208.5224	301.3503

^a95% confidence level= significant linear regression; ^b95% confidence level= no significant linearity deviation; RA: rosmarinic acid; R: correlation coefficient.

The results obtained for intra and inter-day precision, accuracy and stability in standard and rat plasma and brain matrices are shown in Table 2. The method was considered precise and accurate for RA determination in rat plasma and brain matrices according to official guidelines (European Medicine Agency (EMA), 2012; Food and Drug Administration (FDA), 2013; International Conference on Harmonization (ICH), 1996). The intra-day and inter-day precision results demonstrated a relative standard deviation (RSD, %) lower than 5%. The accuracy ranged within 104.69 to 110.99% range. The stability data also demonstrated that the RA concentration remained constant in matrices even after 24 h of storage (room temperature = $25 \pm 1^\circ\text{C}$).

RA extraction recovery from rat plasma and brain recovery are presented in Table 2 and were established after preliminary studies. The recovery was higher than 84.9% and lower than 105.1%, without interference of matrix components and with adequate precision RSD lower than 11.5% for both matrices in accordance with FDA recommendations for bioanalytical procedures validation (Food and Drug Administration (FDA), 2013).

Table 2. Intraday and inter-day precision, accuracy, stability evaluation and extraction recovery of RA standard, rat plasma and brain matrices.

	Level ($\mu\text{g/mL}$)	Precision ($\mu\text{g/mL}$ (RSD))				Accuracy (%)	SE (%)	ER (%)
		First day ^a	Second day ^a	Third day ^a	Inter-day			
RA standard	0.1	0.11 (3.99)	0.11(3.99)	0.11(3.99)	0.11(3.51)	105.53	104.69	-
	2.0	1.97 (4.11)	1.99 (1.38)	2.06 (2.68)	2.01(3.31)	97.01	95.58	-
	6.0	6.31 (1.38)	6.35 (0.21)	6.24 (0.33)	6.30 (1.06)	101.24	102.37	-
	10.0	10.24 (0.73)	10.32 (0.67)	10.19 (0.44)	10.25 (0.77)	98.76	99.41	-
Rat plasma matrix	0.1	0.12 (1.34)	0.11 (2.54)	0.11 (2.18)	0.11(4.36)	108.94	110.99	84.91
	2.0	1.97 (0.82)	2.05 (2.24)	2.00 (2.16)	2.01(2.40)	96.63	95.68	89.39
	6.0	6.23 (1.37)	6.39 (1.03)	6.31 (1.26)	6.31 (1.56)	101.34	99.94	88.18
	10.0	10.25 (0.47)	10.33 (0.45)	10.25 (0.39)	10.27 (0.53)	99.01	100.25	90.49
Rat brain matrix	0.1	0.10 (4.88)	0.09 (1.10)	0.09 (2.44)	0.09 (3.81)	91.97	90.44	93.72
	2.0	2.02 (1.80)	2.11 (2.99)	2.03 (1.55)	2.05 (2.90)	98.86	96.85	97.82
	6.0	6.23 (1.25)	6.35 (2.38)	6.22 (1.72)	6.26 (2.01)	100.38	99.91	105.07
	10.0	10.32 (0.26)	10.34 (0.88)	10.24 (0.55)	10.30 (0.68)	99.24	99.21	98.55

^asix replicates per day; RSD= relative standard deviation (%); SE: stability evaluation in 24 hours; ER: extraction recovery; RA: rosmarinic acid.

To further investigate and earlier guarantee that protocol of RA nasal administration reaches the brain, we first tested the brain and plasma distribution of RA CNE and free RA employing the UFLC method validated (Table 3). RA brain concentration after nasal administration (n.a., 100 μL per nostril) twice a day (7 am/ 7 pm) for six days from RA CNE (2 mg. mL^{-1}) was found to be $0.173 \pm 0.038 \mu\text{g}$. However, none RA was quantified in plasma from RA CNE. These data confirmed that the addition of biopolymer chitosan in nanoemulsions may be favorable to increase RA penetration/retention and residence time in nasal cavity (Fachel et al., 2018a). In opposite, none RA was found in brain (<LOQ), as well as in plasma, of free RA (2 mg. mL^{-1}) in Wistar rats, as expected, possible due to its low residence time in nasal cavity. In literature, only one study by Bhatt et al. (2014) reported that RA reaches Wistar rats brain by intranasal administration due threw Cather tube of RA-loaded SLN. Being the first time that was demonstrated that RA availability in brain through nasal administration of mucoadhesive nanoemulsions containing RA.

Table 3. RA quantification in rat brain and plasma after RA CNE and free RA protocol of nasal administration.

	Rat brain	Rat plasma
RA CNE	0.173 ± 0.038 µg	<LOQ
RA	<LOQ	<LOQ

RA CNE: chitosan-coated rosmarinic acid nanoemulsion; RA: free rosmarinic acid; LOQ: limit of quantification.

3.3 Neuroprotective effects of RA CNE nasal administration lipopolysaccharide-induced memory deficit

To further investigate the neuroprotective effect of new therapeutic approaches for ND different *in vivo* models have been employed, including the lipopolysaccharide (LPS)-induced memory impairment (Carvalho et al., 2017; Pacheco et al., 2018). LPS is a gram-negative bacteria membrane component able to induce neuroinflammatory reaction in CNS *in vitro* and *in vivo*, acting in cytokines release, reactive species production, neuronal loss, impairment of memory and others (Carvalho et al., 2017; Noworyta-Sokolowska et al., 2013).

Regarding the behavioural tests, the Fig. 2 presents the open field test employed as habituation to apparatus and also to quantify locomotor activity and identify motor disabilities and exploratory alterations in male Wistar rats before object recognition (Pacheco et al., 2018). As could be observed the pre-treatment with saline (control and LPS), RA CNE, RA and B CNE did not significant change the number of total crossings or rearing, suggesting that locomotor or exploratory capacity are normal for all groups.

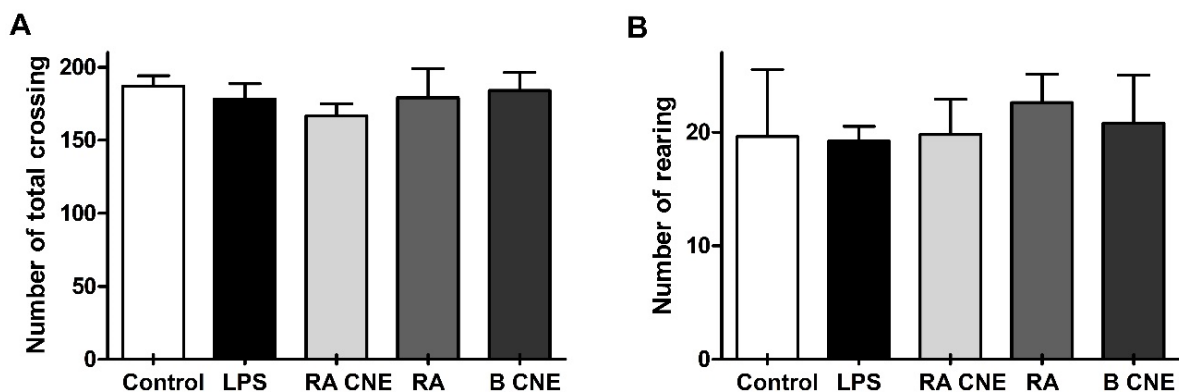


Figure 2

Effects of pre-treatment with saline (control and LPS), RA CNE, RA and B CNE on the total crossing (A) and rearing (B) open field test results. Data were analyzed by one-way analysis of variance followed by Tukey's post hoc test.

LPS: lipopolysaccharide; RA CNE: chitosan-coated rosmarinic acid nanoemulsion; RA: free rosmarinic acid; B CNE: blank chitosan-coated nanoemulsion.

Regarding the object recognition test (Fig. 3), the results demonstrated that LPS (250 $\mu\text{g.mL}^{-1}$) administered intraperitoneally induced a memory impairment, due to the reduction ($p < 0.001$) of recognition index as compared with control group, also observed in B CNE (vehicle) group. It was also observed that RA CNE and free RA were able to protect against memory deficits induced by LPS, due to the increase ($p < 0.001$) of recognition index as compared with LPS group. These findings are agreement with previous studies that also demonstrated that RA prevented the memory impairments induced by $\text{A}\beta_{25-35}$ (Alkam et al., 2007; Lee et al., 2016) and permanent middle cerebral artery occlusion (Fonteles et al., 2016) in mice through object recognition task. Nevertheless, these results are related with free RA even orally or intraperitoneally administered. The present study is the first to employ the object recognition behavioral test and the nasal administration. Additionally, considering the use of nanotechnology-based delivery systems and mucoadhesive polymers for RA nasal administration. An important feature, taking to account the RA limited ability to cross the BBB reported in literature (Kuo and Rajesh, 2017; Li et al., 2018; Szwajgier et al., 2017).

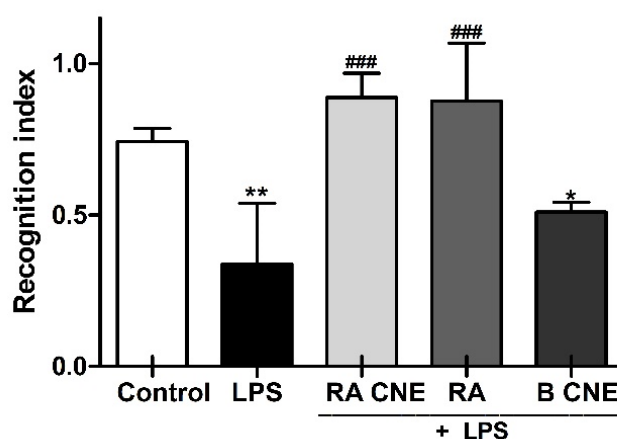


Figure 3

Effects of pre-treatment with saline (control and LPS), RA CNE, RA and B CNE on recognition index after LPS-induced damage. Data were analyzed by one-way analysis of variance followed by Tukey's post hoc test. * $p < 0.05$, ** $p < 0.01$, and *** $p < 0.001$, different from control group; # $p < 0.05$, ## $p < 0.01$, and ### $p < 0.001$, different from LPS group.

LPS: lipopolysaccharide; RA CNE: chitosan-coated rosmarinic acid nanoemulsion; RA: free rosmarinic acid; B CNE: blank chitosan-coated nanoemulsion.

4 Conclusion

In present study, the RA CNE, as well as the free RA, nasal administration exerts a neuroprotective effect against LPS-induced memory deficits. Furthermore, it was also observed that the RA-CNE nasal administration can facilitates the RA availability in brain, confirmed by the RA quantification in brain using a validated UFLC method. In this context, RA CNE nasal administration may be a promising approach for neuroprotective therapies in ND, however further studies to comprehend the impact of the use of mucoadhesive nanotechnology-based delivery systems in CNS still necessary.

Conflicts of interest

The authors declare no conflict of interest.

Acknowledgements

The authors are gratefully acknowledged to Conselho Nacional de Desenvolvimento científico e Tecnológico (CNPq - processos 459619/2014-4; 310846/2014-5;

422298/2016-6), Fundação de Amparo à Pesquisa do Estado do Rio Grande do Sul (FAPERGS - processos 16/2551-0000265-7; 16/2551-0000473-0; 17/2551-0001273-9), and Coordenação de Aperfeiçoamento de Pessoal de Nível Superior - Brasil (CAPES - Finance Code 001) for the financial grants. F.N.S.F., J.H.A. and L.R.M. would like to thank CAPES, CNPq (GD#141739/2017-7 and GD#142202/2018-5) and UFCSPA for the doctoral grant. V.L.B., L.S.K., A.T.H., E.B., and H.F.T. are recipients of CNPq research fellowship.

References

- Alkam, T., Nitta, A., Mizoguchi, H., Itoh, A., Nabeshima, T., 2007. A natural scavenger of peroxynitrites, rosmarinic acid, protects against impairment of memory induced by A β _{25–35}. *Behav. Brain Res.* 180, 139–145. doi:10.1016/j.bbr.2007.03.001
- Andrade, J.M. de, Passos, C. dos S., Rubio, M.A.K., Mendonça, J.N., Lopes, N.P., Henriques, A.T., 2016. Combining *in vitro* and *in silico* approaches to evaluate the multifunctional profile of rosmarinic acid from *Blechnum brasiliense* on targets related to neurodegeneration. *Chem. Biol. Interact.* 254, 135–145. doi:10.1016/j.cbi.2016.06.005
- Baba, S., Osakabe, N., Natsume, M., Terao, J., 2004. Orally administered rosmarinic acid is present as the conjugated and/or methylated forms in plasma, and is degraded and metabolized to conjugated forms of caffeic acid, ferulic acid and m-coumaric acid. *Life Sci.* 75, 165–178. doi:10.1016/j.lfs.2003.11.028
- Bhat, A.H., Dar, K.B., Anees, S., Zargar, M.A., Masood, A., Sofi, M.A., Ganie, S.A., 2015. Oxidative stress, mitochondrial dysfunction and neurodegenerative diseases; a mechanistic insight. *Biomed. Pharmacother.* 74, 101–110. doi:10.1016/j.biopha.2015.07.025
- Bhatt, R., Singh, D., Prakash, A., Mishra, N., 2014. Development, characterization and nasal delivery of rosmarinic acid-loaded solid lipid nanoparticles for the effective management of Huntington's disease. *Drug Deliv.* 1–9. doi:10.3109/10717544.2014.880860
- Carvalho, F.B., Gutierrez, J.M., Bueno, A., Agostinho, P., Zago, A.M., Vieira, J., Frühauf, P., Cechella, J.L., Nogueira, C.W., Oliveira, S.M., Rizzi, C., Spanevello, R.M., Duarte, M.M.F., Duarte, T., Dellagostin, O.A., Andrade, C.M., 2017. Anthocyanins control neuroinflammation and consequent memory dysfunction in mice exposed to lipopolysaccharide. *Mol. Neurobiol.* 54, 3350–3367. doi:10.1007/s12035-016-9900-8
- Casettari, L., Illum, L., 2014. Chitosan in nasal delivery systems for therapeutic drugs. *J. Control. Release* 190, 189–200. doi:10.1016/j.jconrel.2014.05.003
- Coelho, V.R., Vieira, C.G., de Souza, L.P., Moysés, F., Basso, C., Papke, D.K.M., Pires, T.R., Siqueira, I.R., Picada, J.N., Pereira, P., 2015. Antiepileptogenic, antioxidant and genotoxic evaluation of rosmarinic acid and its metabolite caffeic acid in mice. *Life Sci.* 122, 65–71. doi:10.1016/j.lfs.2014.11.009
- Costa, P., Sarmiento, B., Gonçalves, S., Romano, A., 2013. Protective effects of *Lavandula viridis* L'Hér extracts and rosmarinic acid against H₂O₂-induced oxidative damage in A172 human astrocyte cell line. *Ind. Crops Prod.* 50, 361–365. doi:10.1016/j.indcrop.2013.07.054
- Costa, P.A., Poli, J.H.Z., Sperotto, N.D.M., Moura, D.J., Saffi, J., Nin, M.S., Barros, H.M.T., 2015. Brain DNA damage and behavioral changes after repeated intermittent acute ethanol withdrawal by young rats. *Psychopharmacology (Berl.)* 232, 3623–3636. doi:10.1007/s00213-015-4015-x
- Du, T., Li, L., Song, N., Xie, J., Jiang, H., 2010. Rosmarinic acid antagonized 1-methyl-4-phenylpyridinium (MPP⁺)-induced neurotoxicity in MES23.5 dopaminergic cells. *Int.*

J. Toxicol. 29, 625–633. doi:10.1177/1091581810383705

European Medicine Agency (EMA), 2012. Guideline on bioanalytical method validation.

Fachel, F.N.S., Medeiros-Neves, B., Dal Prá, M., Schuh, R.S., Veras, K.S., Bassani, V.L., Koester, L.S., Henriques, A.T., Braganhol, E., Teixeira, H.F., 2018a. Box-Behnken design optimization of mucoadhesive chitosan-coated nanoemulsions for rosmarinic acid nasal delivery—*In vitro* studies. Carbohydr. Polym. 199, 572–582. doi:10.1016/j.carbpol.2018.07.054

Fachel, F.N.S., Nemitz, M.C., Medeiros-Neves, B., Veras, K.S., Bassani, V.L., Koester, L.S., Henriques, A.T., Teixeira, H.F., 2018b. A novel, simplified and stability-indicating high-throughput ultra-fast liquid chromatography method for the determination of rosmarinic acid in nanoemulsions, porcine skin and nasal mucosa. J. Chromatogr. B 1083, 233–241. doi:10.1016/j.jchromb.2018.03.020

Fallarini, S., Miglio, G., Paoletti, T., Minassi, a., Amoroso, a., Bardelli, C., Brunelleschi, S., Lombardi, G., 2009. Clovamide and rosmarinic acid induce neuroprotective effects in *in vitro* models of neuronal death. Br. J. Pharmacol. 157, 1072–1084. doi:10.1111/j.1476-5381.2009.00213.x

Fischer, R., Maier, O., 2015. Interrelation of Oxidative Stress and Inflammation in Neurodegenerative Disease : Role of TNF. Oxid. Med. Cell. Longev. 2015, 1–18.

Fonteles, A.A., de Souza, C.M., De souza, J.C.N., Menezes, A.P.F., Carmo, M.R. dos S., Fernandes, F.D.P., de Araújo, P.R., de Andrade, G.M., 2016. Rosmarinic acid prevents against memory deficits in ischemic mice. Behav. Brain Res. 297, 91–103.

Food and Drug Administration (FDA), 2013. Guidance for Industry: Bioanalytical Method Validation. Cent. drug Eval. Res.

Ghaffari, H., Venkataramana, M., Ghassam, B.J., Chandra Nayaka, S., Nataraju, a, Geetha, N.P., Prakash, H.S., 2014. Rosmarinic acid mediated neuroprotective effects against H₂O₂-induced neuronal cell damage in N2A Cells. Life Sci. 113, 7–13. doi:10.1016/j.lfs.2014.07.010

Huang, R., Han, L., Li, J., Ren, F., Ke, W., Jiang, C., Pei, Y., 2009. Neuroprotection in a 6-hydroxydopamine-lesioned Parkinson model using lactoferrin-modified nanoparticles. J. Gene Med. doi:10.1002/jgm.1361

International Conference on Harmonization (ICH), 1996. Guidance for industry: Q2B validation of analytical procedures: methodology, Technical requirements for registration tripartite guideline. doi:62 FR 27464

Khamse, S., Sadr, S.S., Roghani, M., Hasanzadeh, G., Mohammadian, M., 2015. Rosmarinic acid exerts a neuroprotective effect in the kainate rat model of temporal lobe epilepsy: Underlying mechanisms. Pharm. Biol. 53, 1818–25. doi:10.3109/13880209.2015.1010738

Kim, G.-D., Park, Y.S., Jin, Y.-H., Park, C.-S., 2015. Production and applications of rosmarinic acid and structurally related compounds. Appl. Microbiol. Biotechnol. 99, 2083–2092. doi:10.1007/s00253-015-6395-6

Kuo, Y.C., Rajesh, R., 2017. Targeted delivery of rosmarinic acid across the blood–brain barrier for neuronal rescue using polyacrylamide-chitosan-poly(lactide-co-

glycolide) nanoparticles with surface cross-reacting material 197 and apolipoprotein E. *Int. J. Pharm.* 528, 228–241. doi:10.1016/j.ijpharm.2017.05.039

Lee, A.Y., Hwang, B.R., Lee, M.H., Lee, S., Cho, E.J., 2016. *Perilla frutescens* var. japonica and rosmarinic acid improve amyloid- β_{25-35} induced impairment of cognition and memory function. *Nutr. Res. Pract.* 10, 274–281. doi:10.4162/nrp.2016.10.3.274

Lee, H.J., Cho, H.-S., Park, E., Kim, S., Lee, S.-Y., Kim, C.-S., Kim, D.K., Kim, S.-J., Chun, H.S., 2008. Rosmarinic acid protects human dopaminergic neuronal cells against hydrogen peroxide-induced apoptosis. *Toxicology* 250, 109–115. doi:10.1016/j.tox.2008.06.010

Li, S., Xie, X., Li, D., Yu, Z., Tong, L., Zhao, Y., 2018. Simultaneous determination and tissue distribution studies of four phenolic acids in rat tissue by UFLC–MS/MS after intravenous administration of salvianolic acid for injection. *Biomed. Chromatogr.* 32, 1–9. doi:10.1002/bmc.4128

Lochhead, J.J., Thorne, R.G., 2012. Intranasal delivery of biologics to the central nervous system. *Adv. Drug Deliv. Rev.* 64, 614–628. doi:10.1016/j.addr.2011.11.002

Madureira, A.R., Campos, D.A., Fernandes, J.C., Marques, C., Gullón, B., Rodríguez-alcalá, L.M., Calhau, C., Maria, A., Manuela, M., Reis, F., 2016. Safety profile of solid lipid nanoparticles loaded with rosmarinic acid for oral use: *in vitro* and animal approaches. *Int. J. Nanomedicine* 11, 3621–3640. doi:10.2147/IJN.S104623

Medronho, B., Valente, A.J.M., Costa, P., 2014. Inclusion complexes of rosmarinic acid and cyclodextrins: stoichiometry, association constants, and antioxidant potential. *Colloid Polym. Sci.* 292, 885–894. doi:10.1007/s00396-013-3124-5

Niessen, W.M.A., Manini, P., Andreoli, R., 2006. Matrix effects in quantitative pesticide analysis using liquid chromatography–mass spectrometry. *Mass Spectrom. Rev.* 25, 881–899. doi:10.1002/mas

Noworyta-Sokolowska, K., Górska, A., Golembiowska, K., 2013. LPS-induced oxidative stress and inflammatory reaction in the rat striatum. *Pharmacol. Reports* 65, 863–869.

Pacheco, S.M., Soares, M.S.P., Gutierrez, J.M., Gerzson, M.F.B., Carvalho, F.B., Azambuja, J.H., Schetinger, M.R.C., Stefanello, F.M., Spanevello, R.M., 2018. Anthocyanins as a potential pharmacological agent to manage memory deficit, oxidative stress and alterations in ion pump activity induced by experimental sporadic dementia of Alzheimer's type. *J. Nutr. Biochem.* 56, 193–204. doi:10.1016/j.jnutbio.2018.02.014

Paun, J.S., Bagada, a a, Raval, M.K., 2010. Nasal drug delivery – As an effective tool for brain targeting - A review. *Int. J. Pharm. Appl. Sci.* 1, 43–55.

Pérez-Hernández, J., Zaldívar-Machorro, V.J., Villanueva-Porras, D., Vega-Ávila, E., Chavarría, A., 2016. A potential alternative against neurodegenerative diseases. *Oxid. Med. Cell. Longev.* 1–19. doi:10.1155/2016/8378613

Petersen, M., 2013. Rosmarinic acid: new aspects. *Phytochem. Rev.* 12, 207–227. doi:10.1007/s11101-013-9282-8

Prego, C., García, M., Torres, D., Alonso, M.J., 2005. Transmucosal macromolecular

drug delivery. *J. Control. Release* 101, 151–162. doi:10.1016/j.jconrel.2004.07.030

Shabir, G.A., 2003. Validation of high-performance liquid chromatographic methods for the pharmaceutical analysis: Understanding the differences and similarities between the requirements of the US Food and Drug Administration, and the US Pharmacopeia and the International Con. *J. Chromatogr. A* 987, 57–66. doi:http://dx.doi.org/10.1016/S0021-9673(02)01536-4

Shang, A.-J., Yang, Y., Wang, H.-Y., Tao, B.-Z., Wang, J., Wang, Z.-F., Zhou, D.-B., 2017. Spinal cord injury effectively ameliorated by neuroprotective effects of rosmarinic acid. *Nutr. Neurosci.* 20, 172–179. doi:10.1080/1028415X.2015.1103460

Solanki, I., Parihar, P., Parihar, M.S., 2016. Neurodegenerative diseases: From available treatments to prospective herbal therapy. *Neurochem. Int.* 95, 100–108. doi:10.1016/j.neuint.2015.11.001

Szwajgier, D., Borowiec, K., Pustelniak, K., 2017. The neuroprotective effects of phenolic acids: Molecular mechanism of action. *Nutrients* 9, 1–21. doi:10.3390/nu9050477

Wang, J., Xu, H., Jiang, H., Du, X., Sun, P., Xie, J., 2012. Neurorescue effect of rosmarinic acid on 6-hydroxydopamine-lesioned nigral dopamine neurons in rat model of Parkinson's disease. *J. Mol. Neurosci.* 47, 113–119. doi:10.1007/s12031-011-9693-1

DISCUSSÃO GERAL

As doenças neurodegenerativas (DN), tais como a doença de Alzheimer (DA), a doença de Parkinson (DP) e a esclerose lateral amiotrófica (ELA), são caracterizadas pela disfunção lenta e progressiva neuronal ocasionada pela perda de neurônios no sistema nervoso central (SNC) (LIU et al., 2017; PÉREZ-HERNÁNDEZ et al., 2016).

A DA é a DN mais comum, caracterizada pela perda de neurônios principalmente no córtex e no hipocampo. É associada à formação de placas extracelulares e de agregados neurofibrilares, compostos predominantemente de agregados proteicos formados por beta-amiloide (A β) e pela proteína tau, respectivamente. A DP é caracterizada pela perda de neurônios dopaminérgicos na região da substância *nigra pars compacta*. Na DP, os neurônios afetados contêm agregados proteicos, os chamados corpos de Lewy, que consistem predominantemente de β -sinucleína (FISCHER; MAIER, 2015). Em contrapartida, a ELA é caracterizada por um distúrbio multissistêmico que envolve o ataque do sistema imunológico aos oligodendrócitos. Este fato, resulta na desmielinização e subsequente degeneração axonal dos neurônios afetados. Ataques imunes repetidos desencadeiam a formação de placas e a degeneração dos neurônios motores localizados no córtex, tronco cerebral e medula espinhal (FISCHER; MAIER, 2015). Nessas doenças, as manifestações clínicas destes danos neuronais surgem na forma de comprometimento da memória, déficit cognitivo, dificuldade locomotora e problemas emocionais e/ou comportamentais (BARNHAM; MASTERS; BUSH, 2004; LIU et al., 2017; PÉREZ-HERNÁNDEZ et al., 2016; SOLANKI; PARIHAR; PARIHAR, 2016).

A patogênese das DN é considerada complexa e multifatorial (ANDERSEN, 2004; BHAT et al., 2015; RAMASSAMY, 2006; WANG et al., 2006), encontrando-se alterações inflamatórias, as quais estão associadas a uma constante ativação do sistema imune-inflamatório na microglia devido à presença de danos neuronais crônicos e agregados proteicos (CUNNINGHAM et al., 2009; FISCHER; MAIER, 2015; LULL; BLOCK, 2010; WANG et al., 2006; WYSS-CORAY; MUCKE, 2002). Além disso, um segundo mecanismo amplamente estudado relaciona-se a disfunção mitocondrial e ao estresse oxidativo considerando-se as elevadas quantidades intracelulares não fisiológicas das espécies reativas de oxigênio (EROs) nessas

doenças (ANDERSEN, 2004; BARNHAM; MASTERS; BUSH, 2004; BHAT et al., 2015; CASSETTA; GOVONI; GRANIERI, 2005; LIU et al., 2017; UTTARA et al., 2009).

Por envolver múltiplos fatores, as estratégias terapêuticas são limitadas, muitas vezes, nem mesmo evitando a progressão da doença. Os poucos tratamentos existentes atualmente, auxiliam na melhoria sintomática dos pacientes. Neste contexto, o papel das terapias neuroprotetoras tem sido considerada como uma linha de investigação promissora para o tratamento dessas doenças (BHULLAR; RUPASINGHE, 2013; PÉREZ-HERNÁNDEZ et al., 2016; SOLANKI; PARIHAR; PARIHAR, 2016; SOOD; JAIN; GOWTHAMARAJAN, 2014). Nos últimos anos, os efeitos neuroprotetores de moléculas naturais com atividades anti-inflamatória e antioxidante têm sido claramente demonstrado e surgem como uma abordagem terapêutica interessante para as DN.

Dentre os compostos de origem natural, os compostos fenólicos têm se destacado pelo considerável número de estudos que comprovam a atividade neuroprotetora de dietas ricas em polifenóis (ALBARRACIN et al., 2012; CASSETTA; GOVONI; GRANIERI, 2005; KELSEY; WILKINS; LINSEMAN, 2010; KOPPULA et al., 2012; LOSADA-BARREIRO; BRAVO-DÍAZ, 2017; RAMASSAMY, 2006; SOLANKI; PARIHAR; PARIHAR, 2016).

O ácido rosmarínico (AR) é um composto polifenólico que apresenta-se como uma molécula natural de interesse no contexto atual de busca por novas terapias neuroprotetoras, diante das suas propriedades anti-inflamatória e antioxidantes e sua ampla distribuição e facilidade de obtenção no reino vegetal (KIM et al., 2015; PETERSEN, 2013; PETERSEN et al., 2009). No entanto, devido a sua instabilidade, alta instabilidade evidenciada principalmente no trato gastrointestinal, baixa solubilidade em água, baixa permeabilidade em membranas biológicas, incluindo a barreira hematoencefálica (BHE) e consequente baixa biodisponibilidade, evidenciada principalmente pela via oral e no SNC, torna-se necessário a busca por novas alternativas para veiculação, proteção e administração do AR para tentar superar tais limitações (CAMPOS et al., 2014; DA SILVA et al., 2014; MEDRONHO; VALENTE; COSTA, 2014; YANG et al., 2015).

Embora a via nasal esteja frequentemente associada à produção de um efeito local, como os exemplos típicos de corticoides e vasoconstritores, e sistêmico, sua utilização também tem emergido como uma alternativa viável as demais vias de administração, principalmente, pela ausência das limitações inerentes a BHE e possibilidade de entrega direta de fármacos ao SNC (COSTANTINO et al., 2007; GRASSIN-DELYLE et al., 2012; MUJAWAR et al., 2014; NAKAZAWA; OHSAWA, 1998; PAUN; BAGADA; RAVAL, 2010). As vantagens dessa via residem na ausência de interferência do metabolismo de primeira passagem e de não requerer esterilização, além de ser uma via indolor e não-invasiva e, portanto, mais confortável para o paciente. Por outro lado, vários aspectos referentes à fisiologia e anatomia nasal podem influenciar na administração de fármacos/moléculas por essa via (COSTANTINO et al., 2007; GRASSIN-DELYLE et al., 2012; MUJAWAR et al., 2014; NAKAZAWA; OHSAWA, 1998; PAUN; BAGADA; RAVAL, 2010).

Basicamente, a cavidade nasal é dividida verticalmente em duas metades pelo septo nasal, denominadas fossas nasais. Cada fossa nasal é subdividida em três segmentos: o vestíbulo nasal, o átrio e os cornetos (subdividido em inferior, médio e superior). Na região respiratória (compreendida pelo corneto inferior) é onde na maioria das vezes ocorre a entrada de fármacos pela via nasal, devido extensa superfície de absorção (120 – 150 cm²) e presença de microvilosidades, alto grau de vascularização e alta permeabilidade (CSABA; GARCIA-FUENTES; ALONSO, 2009; GRASSIN-DELYLE et al., 2012; UGWOKÉ et al., 2005). Já a região olfatória (Figura 1) é uma pequena região localizada na parte superior da cavidade nasal composta basicamente por células epiteliais. Recobrimo estas células existe o muco nasal, uma camada com espessura aproximada de 5 µm, a qual fornece uma barreira física protetora a essas células e ao mesmo tempo à absorção de fármacos por esta via. O muco é uma mistura viscosa composta, principalmente, por água, seguida de outros componentes como glicoproteínas (mucina), proteínas (enzimas, imunoglobulinas entre outros), sais e componentes lipídicos, sendo sua propriedade de alta viscosidade atribuída à presença da mucina. Aproximadamente, 1,5 – 2 litros de muco são produzidos diariamente (CSABA; GARCIA-FUENTES; ALONSO, 2009; GRASSIN-DELYLE et al., 2012; UGWOKÉ et al., 2005). Apesar da sua pequena área superficial (1 - 5 cm²), o epitélio olfatório representa uma via única para a

administração direta ao SNC, sem ter a limitação da BHE, através do bulbo olfatório. A BHE está localizada ao nível da microvasculatura cerebral e é crítica para a manutenção da homeostase no SNC. Embora restrinja a entrada de substâncias potencialmente neurotóxicas ao cérebro, a mesma também representa um importante obstáculo para a entrega de agentes terapêuticos diretamente ao SNC, imprescindível para terapias neuroprotetoras (LOCHHEAD; THORNE, 2012; MISTRY; STOLNIK; ILLUM, 2009).

Outra limitação à absorção de fármacos por esta via é a depuração mucociliar. A presença de cílios, os quais compreendem de pequenas projeções nas superfícies das células epiteliais, promovem o movimento do muco até a nasofaringe, acontecendo uma rápida remoção e reposição de muco (GRASSIN-DELYLE et al., 2012; UGWOKÉ et al., 2005).

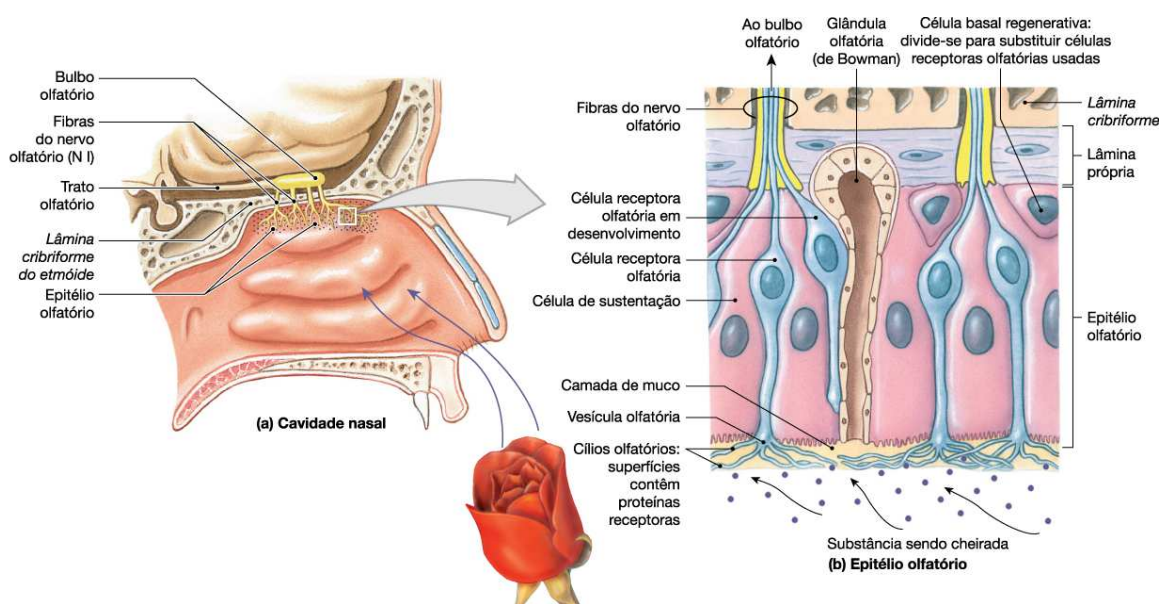


Figura 1. Figura ilustrativa da cavidade nasal e região olfatória (Fonte: TIMMONS, M. J.; TALLITSCH, R. B. Anatomia humana. 6.ed. Porto Alegre: Artmed, 2009).

Tendo em vista as barreiras e limitações da via nasal, algumas estratégias vêm sendo estudadas para melhorar a absorção de fármacos administrados por essa via, como o emprego de lipossomas, géis, micropartículas, entre outros; destacando-se nesse trabalho, o emprego de sistemas nanoestruturados associados a polímeros mucoadesivos (CASETTARI; ILLUM, 2014; CSABA;

GARCIA-FUENTES; ALONSO, 2009; ESKANDARI et al., 2011; KUMAR et al., 2008; ONG; SHALINI; COSTANTINO, 2014; SHINDE; JINDAL; DEVARAJAN, 2011; UGWOKÉ et al., 2005). Os sistemas nanoestruturados lipídicos, especialmente as nanoemulsões, têm sido empregados pelo nosso grupo de pesquisa e descritos para incorporação de substâncias ativas e extratos vegetais pouco solúveis em água, de forma a aumentar sua solubilidade e permeabilidade através das membranas biológicas. As nanoemulsões são dispersões de nanogotículas oleosas em uma fase aquosa externa estabilizadas por um sistema tensoativo, as quais possuem aparência leitosa, reduzido diâmetro de gotícula e baixa viscosidade (ANTON; VANDAMME, 2009; ARGENTA et al., 2014; BALESTRIN et al., 2016; BIDONE et al., 2014; BRUXEL et al., 2012; DOH et al., 2013; KELMANN et al., 2008; MARTINI et al., 2007; ZORZI et al., 2015).

Os polímeros mucoadesivos, sintéticos ou naturais, representam uma classe de biomateriais com potencial carreador transmucosal de sistemas nanoestruturados. Dentre os polímeros, a quitosana, um polissacarídeo catiônico derivado da quitina, vem sendo bastante explorada devido a sua propriedade mucoadesiva relacionada com a interação eletrostática do polímero com os grupos siálicos da mucina. O potencial desses sistemas mucoadesivos consiste em prolongar o tempo de residência da preparação no local de ação ou absorção, intensificando o contato do fármaco com a barreira epitelial das mucosas (CASETTARI; ILLUM, 2014; PREGO et al., 2005, 2006).

Neste contexto, na presente tese objetivamos desenvolver nanoemulsões revestidas por polímero mucoadesivo contendo ácido rosmarínico para administração nasal visando uma terapia neuroprotetora

Para tanto, desenvolvemos um método por cromatografia líquida de ultra-eficiência (CLUE) para determinação do AR em diferentes matrizes, incluindo nanoemulsões, pele, mucosa nasal suína, sangue e plasma de ratos. O objetivo foi dispor de um método rápido, simples e indicativo de estabilidade para a avaliação do AR em formulações, bem como para avaliar o AR em estudos de retenção, permeação e biodistribuição em matrizes biológicas. Apesar da existência de estudos envolvendo cromatografia líquida de alta eficiência e ultra eficiência para determinação do AR em

extratos e matrizes (JIROVSKÝ et al., 2007; LI et al., 2004; STELMAKIENĖ; RAMANAUSKIENĖ; BRIEDIS, 2015; ZHENG et al., 2015), este foi o primeiro estudo envolvendo a determinação do AR em distintas amostras biológicas. A CLUE foi selecionada com base em sua capacidade em reduzir o tempo de análise e aumentar a precisão e sensibilidade do método, bem como diminuir o impacto ambiental ao reduzir o consumo de solventes (TRONCOSO et al., 2005). Uma coluna C18 com tamanho de partícula de 2,6 µm foi empregada, e acetonitrila e ácido trifluoroacético a 0,1% (v / v) foram escolhidos devido ao seu desempenho cromatográfico e capacidade de garantir a supressão da ionização da AR durante a análise. A otimização das condições cromatográficas foi realizada testando-se diferentes sistemas de eluição isocrático. Alta temperatura (55 °C) e fluxo (0.55 mL) foram necessários de forma a garantir uma pressão adequada e para obter um tempo mais rápido de análise.

Os resultados advindos desta primeira etapa demonstraram que um método rápido comparado aos demais descritos na literatura (ACHAMLALÉ; REZZONICO; GRIGNON-DUBOIS, 2009; ADHAM, 2015; AGÊNCIA NACIONAL DE VIGILÂNCIA SANITÁRIA, 2010; CANELAS; DA COSTA, 2007; CAROCHO et al., 2015; COUTO et al., 2011; DE OLIVEIRA; DE OLIVEIRA, 2013; GUDZENKO, 2013; JIROVSKÝ et al., 2007; LIU et al., 2013; MODARRES et al., 2014; ÖZTÜRK et al., 2011; WANG; PROVAN; HELLIWELL, 2004; ZHU et al., 2014), com tempo total de análise de 3,5 minutos, foi desenvolvido, atendendo aos critérios de adequabilidade do sistema (SHABIR, 2003).

O referido método foi também validado seguindo as diretrizes internacionais para validação analítica e bioanalítica (EUROPEAN MEDICINE AGENCY (EMA), 2012; FOOD AND DRUG ADMINISTRATION (FDA), 2013; INTERNATIONAL CONFERENCE ON HARMONIZATION (ICH), 2005). E, quanto aos resultados obtidos, o método demonstrou-se específico para determinação do AR, mantendo sua pureza mesmo na presença dos produtos de degradação e das matrizes. Além, de linear, na faixa de 0,1-10 µg/mL para matrizes não-biológicas e de 0,5-10 µg/mL para matrizes biológicas, preciso e exato, sem apresentar efeito de matriz. A estabilidade nas matrizes em 24 h também foi avaliada, sendo demonstrada instabilidade apenas na matriz de mucosa nasal suína. A robustez do método foi

avaliada por um desenho experimental do tipo *Plackett-Burman* (HEYDEN et al., 2001), o qual demonstrou que o método é robusto a pequenas variações na proporção de fase móvel, na concentração de ácido trifluoracético na fase móvel, e na temperatura da coluna. Quanto a recuperação da extração nas matrizes biológicas, pele e mucosa nasal suína, resultados satisfatórios foram obtidos após diferentes protocolos serem testados. Por último, a aplicabilidade do método através de estudos de retenção cutânea e permeação em mucosa nasal das nanoemulsões contendo AR foi avaliada. Os resultados obtidos demonstraram adequada precisão do método nesses estudos, e boa repetibilidade para determinação do AR nas nanoemulsões, sendo o primeiro relato de um método para essas aplicações.

Dando continuidade à nossa proposta, desenvolvemos e otimizamos, através de um desenho experimental, nanoemulsões revestidas por quitosana contendo AR para administração pela via nasal. O principal objetivo foi a obtenção de um sistema lipídico nanoestruturado revestido por um polímero mucoadesivo com características físico-químicas adequadas para administração pela via nasal utilizando o método de emulsificação espontânea.

Estudos preliminares realizados com nanoemulsões revestidas por quitosana, tendo como base as nanoemulsões empregadas na primeira etapa da tese contendo núcleo oleoso 10% (p/v), correspondendo 8% (p/v) a triglicerídeos de cadeia média e 2% (p/v) a lecitina de gema de ovo, demonstraram que a concentração de núcleo oleoso, a proporção de lecitina no núcleo oleoso, e a concentração de quitosana, eram fatores importantes a serem considerados na otimização de uma nova formulação contendo AR. A partir desses estudos, um modelo experimental do tipo Box-Behken foi selecionado para realizarmos a otimização de nanoemulsões contendo AR revestidas por quitosana (FERREIRA et al., 2007). Tendo em vista, que tínhamos três fatores e elencamos três níveis para estudarmos, totalizando 15 corridas randomizadas e quatro respostas para cada corrida (tamanho de gotícula, índice de polidispersão, potencial zeta e teor de AR).

Dentre os principais resultados dessa otimização, observamos a influência direta da proporção da lecitina na fase oleosa nos resultados obtidos de tamanho de gotícula e índice de polidispersão. Além da influência da concentração de quitosana

e de fase oleosa no potencial zeta e teor de AR, respectivamente. O modelo experimental selecionado mostrou-se adequado, e a condição ótima foi estabelecida minimizando as respostas de tamanho de gotícula e índice de polidispersão, e maximizando os resultados de potencial zeta e teor de AR. Um núcleo oleoso de 8,5% (p/v), contendo 3:10 ou 2,6% (p/v) de lecitina de gema de ovo e 6,4% de triglicerídeos de cadeia média no núcleo oleoso, e revestidas por quitosana 0,1% (p/v), foram obtidos na otimização. Os resultados da quintuplicata aplicada nesse modelo, demonstraram resultados de tamanho de gotícula de $259,07 \pm 5,93$ nm, índice de polidispersão de $0,274 \pm 0,01$, potencial zeta de $45,73 \pm 1,76$ mV e de teor de AR de $92,66 \pm 1,43\%$, dentro da faixa estabelecida na otimização.

Após a otimização das nanoemulsões, as formulações com e sem revestimento com quitosana foram caracterizadas. Os resultados da caracterização físico-química ficaram de acordo com estudos anteriores de nanoemulsões obtidas pela técnica de emulsificação espontânea (ARGENTA et al., 2016; BALESTRIN et al., 2016; FASOLO; BASSANI; TEIXEIRA, 2009), observando gotículas com tamanho de cerca de 250 nm, monodispersas e com as mesmas características observadas e confirmadas por microscopia eletrônica de transmissão. Embora as nanoemulsões revestidas por quitosana tenham apresentado tamanho de gotícula e IP significativamente superior aos obtidos pelas nanoemulsões sem revestimento, o que pode ser associado a presença de quitosana na interface da nanoemulsão, a qual também teve influência na viscosidade. Quanto aos resultados de teor de AR e eficiência de associação, ambas nanoemulsões apresentaram resultados semelhantes e superiores a 92% e 89%, respectivamente. Em relação ao potencial zeta, os resultados em módulo demonstraram valores superiores a 20 mV, em pH próximo a 4,0, sugestivo de uma boa estabilidade física das formulações. As NE revestidas com quitosana apresentaram onde uma maior força mucoadesiva, estando essa propriedade associada à interação das cargas positivas (quitosana) com os grupos siálicos presentes na mucina da mucosa nasal (BARBI et al., 2014; PREGO et al., 2005).

Quanto aos perfis de liberação em membrana sintética e permeação/retenção em mucosa nasal suína, também avaliados nesta etapa, os resultados demonstraram uma liberação mais lenta do AR nas nanoemulsões em comparação

ao controle (tampão fosfato de potássio pH 5.8) e uma cinética de permeação prolongada da nanoemulsão revestida por quitosana contendo AR em relação à sem revestimento. Adicionalmente, uma quantidade significativamente superior de AR, provenientes desta última formulação, ficou retida na mucosa nasal suína, também demonstrada pela retenção de maiores quantidades de sonda fluorescente (NBD-PE) nas imagens histológicas, em consonância com os resultados anteriores a qual demonstraram um maior potencial mucoadesivo da nanoemulsão revestida por quitosana contendo AR.

Em uma última etapa, estudos *in vitro* de viabilidade celular e marcação de necrose celular em fibroblastos foram realizados para investigar o potencial citotóxico do AR e das formulações desenvolvidas. Os resultados desta etapa demonstraram a ausência de citotoxicidade em concentrações inferiores a 50 μM em 24 h e 25 μM em 48 h para as formulações, sendo a toxicidade atribuída as nanoemulsões propriamente ditas em concentrações igual ou abaixo de 50 μM e ao AR em concentrações acima de 50 μM (YOSHIDA et al., 2005).

Em um terceiro momento desta tese, propomos a avaliação do potencial de proteção e reversão *in vitro* das nanoemulsões contendo AR revestidas por quitosana, assim como, das nanoemulsões contendo AR e do AR livre, em um modelo de inflamação e estresse oxidativo induzido por lipopolissacarídeo (LPS) em cultura primária de astrócitos obtidas a partir do córtex cerebral de ratos Wistar neonatos. Para tanto, o perfil de segurança das nanoemulsões contendo AR e do AR livre foi avaliado através dos ensaios de viabilidade, proliferação e marcação de necrose celular em astrócitos nas concentrações de 6.25-50 μM e em um período de no máximo de 72 horas. Os resultados obtidos demonstraram ausência de citotoxicidade das nanoemulsões contendo AR e do AR livre em células saudáveis do SNC, nas concentrações e tempos testados. Posteriormente, nossos achados demonstraram a capacidade glioprotetora das nanoemulsões contendo AR revestidas por quitosana em astrócitos contra a inflamação e o estresse oxidativo induzido por LPS. Os resultados obtidos nesta etapa demonstraram, que os pré-tratamentos com as nanoemulsões contendo AR, bem como o AR livre, antes da exposição ao LPS (protocolo de proteção) minimizaram as alterações induzidas por LPS na viabilidade, proliferação e marcação de necrose celular em quase todas as

concentrações de AR (6,25 - 25,0 μ M) associado a redução da disfunção mitocondrial induzida por LPS (PACHECO et al., 2018).

Por outro lado, as nanoemulsões contendo AR, bem como o AR livre, não demonstraram potencial de reversão do dano induzido por LPS na viabilidade, proliferação e marcação de necrose celular em astrócitos. Estes resultados estão de acordo com os estudos *in vitro* envolvendo diferentes modelos de indução de dano em neurônios e células gliais encontrados na literatura que demonstraram apenas o potencial protetor do AR (ANDRADE et al., 2016; BRAIDY et al., 2014; DU et al., 2010; FALLARINI et al., 2009; GHAFARI et al., 2014; LEE et al., 2008; REN et al., 2009). No entanto, este é o primeiro estudo a contemplar uma avaliação de glioproteção e o uso de novas abordagens tecnológicas para o AR. Sendo de extrema importância este último tópico, pois inúmeros autores relatam como limitação a baixa biodisponibilidade, principalmente, pela via oral e no SNC do AR, já apresentados nesta discussão.

Tendo em vista os resultados promissores de glioproteção das nanoemulsões contendo AR, bem como do AR livre, parâmetros oxidativos, de migração celular e de marcação de astrócitos reativos também foram avaliados no protocolo de proteção. Os resultados desta etapa demonstraram que o pré-tratamento com as nanoemulsões contendo AR, bem como o AR livre, aumenta o status antioxidante na inflamação e no estresse oxidativo induzido por LPS em astrócitos, através da regulação do potencial redox celular (diminuição na produção de espécies reativas de oxigênio e óxido nítrico, e preservação da glutathiona redutase), a qual já havia sido reportado na literatura para o AR em outros modelos de neurotoxicidade *in vitro* (COSTA et al., 2013; DU et al., 2010; GHAFARI et al., 2014). Além disso, nossos resultados mostraram, pela primeira vez, a capacidade das nanoemulsões contendo AR, bem como do AR livre, em prevenir a ativação migratória dos astrócitos e o acúmulo de astrócitos reativos hipertróficos induzido pelo LPS.

Na última etapa da presente tese, demonstramos que a administração nasal das nanoemulsões contendo AR revestidas por quitosana (2 mg/mL) facilita o alcance cerebral da AR, confirmada pela quantificação no cérebro do AR ($0,173 \pm 0,038 \mu$ g) após 6 dias de administração nasal (100 μ L/ narina, 2 vezes ao dia),

embora no plasma não tenha sido detectado. Esses resultados promissores nos conduziram a avaliar *in vivo* (em modelo de perda de memória induzido por LPS em ratos Wistar adultos) o impacto do uso das formulações desenvolvidas, considerando que apenas um estudo envolvendo o uso de nanopartículas lipídicas sólidas contendo AR, via nasal e doença de Huntington foi encontrado (BHATT et al., 2014) na literatura. Os testes comportamentais de reconhecimento de objetos demonstraram que o LPS administrado intraperitonealmente induziu um comprometimento da memória, devido à redução ($p < 0,001$) do índice de reconhecimento em comparação ao grupo controle (salina). Observou-se também que a administração pela via nasal da nanoemulsão contendo AR revestida por quitosana, assim como do AR livre, antes da indução do dano por LPS, foi capaz de proteger contra déficits de memória, devido ao aumento ($p < 0,001$) do índice de reconhecimento em comparação ao grupo LPS. Assim, este foi o primeiro relato de emprego de nanoemulsões mucoadesivas contendo AR para aumento de sua residência na cavidade nasal e aumento de sua biodisponibilidade no SNC, demonstrando sua atividade neutroprotetora.

Como perspectivas deste trabalho, novos estudos serão realizados para a avaliação e elucidação das atividades anti-inflamatória e antioxidante da nanoemulsão contendo AR revestida por quitosana e do AR livre nos tecidos cerebrais, empregando-se o mesmo protocolo de administração nasal em modelo de indução de dano por LPS. Estes estudos serão de extrema importância para avaliar o impacto do sistema proposto em outros parâmetros envolvidos nas DN, de forma a compreendermos de que maneira a maior detecção de AR no SNC, evidenciada nesta última etapa, influencia nessas doenças.

Referências

ACHAMLALÉ, S.; REZZONICO, B.; GRIGNON-DUBOIS, M. Rosmarinic acid from beach waste: Isolation and HPLC quantification in *Zostera detritus* from Arcachon lagoon. **Food Chemistry**, v. 113, n. 4, p. 878–883, 2009.

ADHAM, A. N. Comparative extraction methods , phytochemical constituents , fluorescence analysis and HPLC validation of rosmarinic acid content in *Mentha piperita*, *Mentha longifolia* and *Osimum basilicum*. **Journal of Pharmacognosy and Phytochemistry**, v. 3, n. 6, p. 130–139, 2015.

AGÊNCIA NACIONAL DE VIGILÂNCIA SANITÁRIA. **Farmacopeia Brasileira**. . v. 1. 2010.

ALBARRACIN, S. L. et al. Effects of natural antioxidants in neurodegenerative disease. **Nutritional Neuroscience**, v. 15, n. 1, p. 1–9, 2012.

ANDERSEN, J. K. Oxidative stress in neurodegeneration : cause or consequence ? **Nature Reviews**, n. July, p. 18–25, 2004.

ANDRADE, J. M. DE et al. Combining *in vitro* and *in silico* approaches to evaluate the multifunctional profile of rosmarinic acid from *Blechnum brasiliense* on targets related to neurodegeneration. **Chemico-Biological Interactions**, v. 254, p. 135–145, 2016.

ANTON, N.; VANDAMME, T. F. The universality of low-energy nano-emulsification. **International Journal of Pharmaceutics**, v. 377, n. 1–2, p. 142–147, 2009.

ARGENTA, D. F. et al. Factorial design applied to the optimization of lipid composition of topical antiherpetic nanoemulsions containing isoflavone genistein. **International Journal of Nanomedicine**, v. 9, p. 4737–4747, 2014.

ARGENTA, D. F. et al. *In vitro* evaluation of mucosa permeation/retention and antiherpes activity of genistein from cationic nanoemulsions. **Journal of Nanoscience and Nanotechnology**, v. 16, n. 2, p. 1282–90, 2016.

BALESTRIN, L. A. et al. Protective effect of a hydrogel containing *Achyrocline satureioides* extract-loaded nanoemulsion against UV-induced skin damage. **Journal of Photochemistry and Photobiology B: Biology**, v. 163, p. 269–276, 2016.

BARBI, M. D. S. et al. Preparation and characterization of chitosan nanoparticles for AZT nasal delivery. **Journal of Nanoscience and Nanotechnology**, v. 14, p. 1–10, 2014.

BARNHAM, K. J.; MASTERS, C. L.; BUSH, A. I. Neurodegenerative diseases and oxidative stress. **Nature Reviews**, v. 3, p. 205–214, 2004.

BHAT, A. H. et al. Oxidative stress, mitochondrial dysfunction and neurodegenerative diseases; a mechanistic insight. **Biomedicine & pharmacotherapy**, v. 74, p. 101–110, 2015.

BHATT, R. et al. Development, characterization and nasal delivery of rosmarinic acid-loaded solid lipid nanoparticles for the effective management of Huntington's disease. **Drug delivery**, p. 1–9, 2014.

- BHULLAR, K. S.; RUPASINGHE, H. P. V. Polyphenols: Multipotent therapeutic agents in neurodegenerative diseases. **Oxidative Medicine and Cellular Longevity**, v. 2013, p. 1–18, 2013.
- BIDONE, J. et al. Incorporation of *Achyrocline satureioides* (Lam .) DC extracts into topical nanoemulsions obtained by means of spontaneous emulsification procedure. **Industrial Crops and Products**, v. 62, p. 421–429, 2014.
- BRAIDY, N. et al. Neuroprotective effects of rosmarinic acid on ciguatoxin in primary human neurons. **Neurotoxicity Research**, p. 226–234, 2014.
- BRUXEL, F. et al. Nanoemulsões como sistemas de liberação parenteral de fármacos. **Química Nova**, v. 35, n. 9, p. 1827–1840, 2012.
- CAMPOS, D. A. . et al. Optimization of the production of solid Witepsol nanoparticles loaded with rosmarinic acid. **Colloids and Surfaces B: Biointerfaces**, v. 115, p. 109–117, 2014.
- CANELAS, V.; DA COSTA, C. T. Quantitative HPLC analysis of rosmarinic acid in extracts of *Melissa officinalis* and spectrophotometric measurement of their antioxidant activities. **Journal of Chemical Education**, v. 84, n. 9, p. 1502–1504, 2007.
- CAROCHO, M. et al. *Melissa officinalis* L. decoctions as functional beverages: a bioactive approach and chemical characterization. **Food Funct.**, 2015.
- CASSETTA, I.; GOVONI, V.; GRANIERI, E. Oxidative stress, antioxidants and neurodegenerative diseases. **Current Pharmaceutical Design**, v. 11, n. 16, p. 2033–52, 2005.
- CASSETTARI, L.; ILLUM, L. Chitosan in nasal delivery systems for therapeutic drugs. **Journal of Controlled Release**, v. 190, p. 189–200, 2014.
- COSTA, P. et al. Protective effects of *Lavandula viridis* L'Hér extracts and rosmarinic acid against H₂O₂-induced oxidative damage in A172 human astrocyte cell line. **Industrial Crops and Products**, v. 50, p. 361–365, 2013.
- COSTANTINO, H. R. et al. Intranasal delivery: Physicochemical and therapeutic aspects. **International Journal of Pharmaceutics**, v. 337, n. 1–2, p. 1–24, 2007.
- COUTO, R. O. et al. Validated HPLC-PDA method for rosmarinic acid quantification in rosemary. **Latin American Journal of Pharmacy**, v. 30, p. 1951–1956, 2011.
- CSABA, N.; GARCIA-FUENTES, M.; ALONSO, M. J. Nanoparticles for nasal vaccination. **Advanced Drug Delivery Reviews**, v. 61, n. 2, p. 140–157, 2009.
- CUNNINGHAM, C. et al. Systemic inflammation induces acute behavioral and neurodegenerative disease. **Biological Psychiatry**, v. 65, n. 4, p. 304–312, 2009.
- DA SILVA, S. B. et al. Natural extracts into chitosan nanocarriers for rosmarinic acid drug delivery. **Pharmaceutical Biology**, v. 53, n. 5, p. 642–652, 2014.
- DE OLIVEIRA, K. B.; DE OLIVEIRA, B. H. A HPLC/DAD Determination of rosmarinic acid in *Salvia officinalis*: sample preparation optimization by factorial design. **Article J. Braz. Chem. Soc**, v. 24, n. 1, p. 85–91, 2013.

DOH, H. J. et al. A novel lipid nanoemulsion system for improved permeation of granisetron. **Colloids and Surfaces B: Biointerfaces**, v. 101, p. 475–480, 2013.

DU, T. et al. Rosmarinic acid antagonized 1-methyl-4-phenylpyridinium (MPP⁺)-induced neurotoxicity in MES23.5 dopaminergic cells. **International Journal of Toxicology**, v. 29, n. 6, p. 625–633, 2010.

ESKANDARI, S. et al. Brain delivery of valproic acid via intranasal administration of nanostructured lipid carriers: *in vivo* pharmacodynamic studies using rat electroshock model. **International Journal of Nanomedicine**, v. 6, p. 363–371, 2011.

EUROPEAN MEDICINE AGENCY (EMA). **Guideline on bioanalytical method validation**, 2012.

FALLARINI, S. et al. Clovamide and rosmarinic acid induce neuroprotective effects in *in vitro* models of neuronal death. **British Journal of Pharmacology**, v. 157, n. 6, p. 1072–1084, 2009.

FASOLO, D.; BASSANI, V. L.; TEIXEIRA, H. F. Development of topical nanoemulsions containing quercetin and 3- O -methylquercetin. **Pharmazie**, v. 64, p. 726–730, 2009.

FERREIRA, S. L. C. et al. Box-Behnken design: An alternative for the optimization of analytical methods. **Analytica Chimica Acta**, v. 597, n. 2, p. 179–186, 2007.

FISCHER, R.; MAIER, O. Interrelation of oxidative stress and inflammation in neurodegenerative disease: Role of TNF. **Oxidative Medicine and Cellular Longevity**, v. 2015, p. 1–18, 2015.

FOOD AND DRUG ADMINISTRATION (FDA). **Guidance for industry: Bioanalytical method validation center for drug evaluation and research**, 2013.

GHAFFARI, H. et al. Rosmarinic acid mediated neuroprotective effects against H₂O₂-induced neuronal cell damage in N2A Cells. **Life sciences**, v. 113, n. 1–2, p. 7–13, 2014.

GRASSIN-DELYLE, S. et al. Intranasal drug delivery: An efficient and non-invasive route for systemic administration - Focus on opioids. **Pharmacology and Therapeutics**, v. 134, n. 3, p. 366–379, 2012.

GUDZENKO, A. Development and validation of a method for the determination of rosmarinic acid in *Mentha piperita* L. using solid-phase extraction and RP-HPLC with photodiode array detection. **Journal of Chemical and Pharmaceutical Research**, v. 5, n. 9, p. 40–45, 2013.

HEYDEN, Y. V. et al. Guidance for robustness/ruggedness tests in method validation. **Journal of Pharmaceutical and Biomedical Analysis**, v. 24, n. 5–6, p. 723–753, 2001.

INTERNATIONAL CONFERENCE ON HARMONIZATION (ICH). **Validation of analytical procedures : Text and methodology Q2 (R1)**, 2005.

JIROVSKÝ, D. et al. HPLC analysis of rosmarinic acid in feed enriched with aerial parts of *Prunella vulgaris* and its metabolites in pig plasma using dual-channel coulometric detection. **Journal of Agricultural and Food Chemistry**, v. 55, n. 19, p. 7631–7637, 2007.

- KELMANN, R. G. et al. Preliminary study on the development of nanoemulsions for carbamazepine intravenous delivery: an investigation of drug polymorphic transition. **Drug Development and Industrial Pharmacy**, v. 34, n. 1, p. 53–58, 2008.
- KELSEY, N. A.; WILKINS, H. M.; LINSEMAN, D. A. Nutraceutical antioxidants as novel neuroprotective agents. **Molecules**, v. 15, n. 11, p. 7792–7814, 2010.
- KIM, G.-D. et al. Production and applications of rosmarinic acid and structurally related compounds. **Applied Microbiology and Biotechnology**, v. 99, p. 2083–2092, 2015.
- KOPPULA, S. et al. Recent advances on the neuroprotective potential of antioxidants in experimental models of Parkinson's disease. **International Journal of Molecular Sciences**, v. 13, n. 8, p. 10608–10629, 2012.
- KUMAR, M. et al. Intranasal nanoemulsion based brain targeting drug delivery system of risperidone. **International Journal of Pharmaceutics**, v. 358, n. 1–2, p. 285–291, 2008.
- LEE, H. J. et al. Rosmarinic acid protects human dopaminergic neuronal cells against hydrogen peroxide-induced apoptosis. **Toxicology**, v. 250, n. 2–3, p. 109–115, 2008.
- LI, X. et al. Simultaneous determination of magnesium lithospermate B, rosmarinic acid, and lithospermic acid in beagle dog serum by liquid chromatography/tandem mass spectrometry. **Rapid Communications in Mass Spectrometry**, v. 18, n. 23, p. 2878–2882, 2004.
- LIU, J. et al. Determination of the content of rosmarinic acid by HPLC and analytical comparison of volatile constituents by GC-MS in different parts of *Perilla frutescens* (L.) Britt. **Chemistry Central journal**, v. 7, n. 1, p. 61, 2013.
- LIU, Z. et al. Oxidative stress in neurodegenerative diseases: from molecular mechanisms to clinical applications. **Oxidative Medicine and Cellular Longevity**, v. 2017, n. Figure 1, p. 1–11, 2017.
- LOCHHEAD, J. J.; THORNE, R. G. Intranasal delivery of biologics to the central nervous system. **Advanced Drug Delivery Reviews**, v. 64, n. 7, p. 614–628, 2012.
- LOSADA-BARREIRO, S.; BRAVO-DÍAZ, C. Free radicals and polyphenols: The redox chemistry of neurodegenerative diseases. **European Journal of Medicinal Chemistry**, v. 133, p. 379–402, 2017.
- LULL, M. E.; BLOCK, M. L. Microglial activation and chronic neurodegeneration. **Neurotherapeutics**, v. 7, n. 4, p. 354–365, 2010.
- MARTINI, É. et al. Adsorção de oligonucleotídeos em nanoemulsões obtidas por emulsificação espontânea. **Química Nova**, v. 30, n. 4, p. 930–934, 2007.
- MEDRONHO, B.; VALENTE, A. J. M.; COSTA, P. Inclusion complexes of rosmarinic acid and cyclodextrins: stoichiometry, association constants, and antioxidant potential. **Colloid and Polymer Science**, v. 292, p. 885–894, 2014.
- MISTRY, A.; STOLNIK, S.; ILLUM, L. Nanoparticles for direct nose-to-brain delivery of drugs. **International Journal of Pharmaceutics**, v. 379, n. 1–2, p. 146–157, 2009.
- MODARRES, M. et al. Simultaneous determination of rosmarinic acid, salvianolic acid

b and caffeic acid in *Salvia leriifolia* Benth. root, leaf and callus extracts using a high-performance liquid chromatography with diode-array detection technique. **Journal of Liquid Chromatography & Related Technologies**, v. 37, n. 12, p. 1721–1730, 2014.

MUJAWAR, N. et al. Nasal drug delivery: Problem solution and its application. **Journal of Current Pharma Research**, v. 4, n. 3, p. 1231–1245, 2014.

NAKAZAWA, T.; OHSAWA, K. Metabolism of rosmarinic acid in rats. **Journal of Natural Products**, 1998.

ONG, W.; SHALINI, S.; COSTANTINO, L. Nose-to-brain drug delivery by nanoparticles in the treatment of neurological disorders. **Current Medicinal Chemistry**, v. 21, p. 4247–4256, 2014.

ÖZTÜRK, N. et al. Determination of rosmarinic acid by high-performance liquid chromatography and its application to certain *Salvia* species and rosemary. **Food Analytical Methods**, v. 4, n. 3, p. 300–306, 2011.

PACHECO, S. M. et al. Glioprotective effects of lingonberry extract against altered cellular viability, acetylcholinesterase activity, and oxidative stress in lipopolysaccharide-treated astrocytes. **Cellular and Molecular Neurobiology**, v. 38, n. 5, p. 1107–1121, 2018.

PAUN, J. S.; BAGADA, A A; RAVAL, M. K. Nasal drug delivery – As an effective tool for brain targeting - A Review. **International Journal of Pharmaceutical and Applied Sciences**, v. 1, n. 2, p. 43–55, 2010.

PÉREZ-HERNÁNDEZ, J. et al. A potential alternative against neurodegenerative diseases. **Oxidative Medicine And Cellular Longevity**, p. 1–19, 2016.

PETERSEN, M. et al. Evolution of rosmarinic acid biosynthesis. **Phytochemistry**, 2009.

PETERSEN, M. Rosmarinic acid : new aspects. **Phytochemistry Reviews**, v. 12, p. 207–227, 2013.

PREGO, C. et al. Transmucosal macromolecular drug delivery. **Journal of Controlled Release**, v. 101, n. 1–3 SPEC. ISS., p. 151–162, 2005.

PREGO, C. et al. Efficacy and mechanism of action of chitosan nanocapsules for oral peptide delivery. **Pharmaceutical Research**, v. 23, n. 3, p. 549–556, 2006.

RAMASSAMY, C. Emerging role of polyphenolic compounds in the treatment of neurodegenerative diseases: A review of their intracellular targets. **European Journal of Pharmacology**, v. 545, n. 1, p. 51–64, 2006.

REN, P. et al. Rosmarinic acid inhibits 6-OHDA-induced neurotoxicity by anti-oxidation in MES23.5 cells. **Journal of Molecular Neuroscience**, v. 39, n. 1–2, p. 220–225, 2009.

SHABIR, G. A. Validation of high-performance liquid chromatographic methods for the pharmaceutical analysis: Understanding the differences and similarities between the requirements of the US Food and Drug Administration, and the US Pharmacopeia and the International Con. **Journal of Chromatography A**, v. 987, n. 1–2, p. 57–66, 2003.

- SHINDE, R. L.; JINDAL, A. B.; DEVARAJAN, P. V. Microemulsions and nanoemulsions for targeted drug delivery to the brain. **Current Nanoscience**, v. 7, n. 1, p. 119–133, 2011.
- SILVA, A. P. C. et al. Development of topical nanoemulsions containing the isoflavone genistein. **Pharmazie**, v. 64, p. 1–4, 2009.
- SOLANKI, I.; PARIHAR, P.; PARIHAR, M. S. Neurodegenerative diseases: From available treatments to prospective herbal therapy. **Neurochemistry International**, v. 95, p. 100–108, 2016.
- SOOD, S.; JAIN, K.; GOWTHAMARAJAN, K. Intranasal therapeutic strategies for management of Alzheimer's disease. **Journal of drug targeting**, v. 22, n. 4, p. 279–94, 2014.
- STELMAKIENĖ, A.; RAMANAUSKIENĖ, K.; BRIEDIS, V. Release of rosmarinic acid from semisolid formulations and its penetration through human skin *ex vivo*. **Acta Pharmaceutica**, v. 65, 2015.
- TRONCOSO, N. et al. Fast high performance liquid chromatography and ultraviolet – visible quantification of principal phenolic antioxidants in fresh rosemary. **Journal of Chromatography A**, v. 1100, p. 20–25, 2005.
- UGWOKE, M. I. et al. Nasal mucoadhesive drug delivery: Background, applications, trends and future perspectives. **Advanced Drug Delivery Reviews**, v. 57, n. 11, p. 1640–1665, 2005.
- UTTARA, B. et al. Oxidative stress and neurodegenerative diseases: a review of upstream and downstream antioxidant therapeutic options. **Current Neuropharmacology**, v. 7, n. 1, p. 65–74, 2009.
- WANG, H.; PROVAN, G. J.; HELLIWELL, K. Determination of rosmarinic acid and caffeic acid in aromatic herbs by HPLC. **Food Chemistry**, v. 87, n. 2, p. 307–311, 2004.
- WANG, J. et al. Dual effects of antioxidants in neurodegeneration: Direct neuroprotection against oxidative stress and indirect protection via suppression of gliamediated inflammation. **Current Pharmaceutical Design**, v. 12, p. 3521–3533, 2006.
- WYSS-CORAY, T.; MUCKE, L. Inflammation in neurodegenerative disease — A double-edged sword. **Neuron**, v. 35, p. 419–432, 2002.
- YANG, J. et al. Enhanced oral bioavailability and prophylactic effects on oxidative stress and hepatic damage of an oil solution containing a rosmarinic acid – phospholipid complex. **Journal of Functional Foods**, v. 19, p. 63–73, 2015.
- YOSHIDA, M. et al. Antiproliferative constituents from umbelliferae plants VII . Active triterpenes and rosmarinic acid from *Centella asiatica*. **Biological and Pharmaceutical Bulletin**, v. 28, n. 1, p. 173–175, 2005.
- ZHENG, L. et al. A UPLC-MS/MS method for simultaneous determination of danshensu, protocatechuic aldehyde, rosmarinic acid, and ligustrazine in rat plasma, and its application to pharmacokinetic studies of *Shenxiang glucose* injection in rats. **Journal of Chromatography B**, v. 997, p. 210–217, 2015.

ZHU, F. et al. Rosmarinic acid extract for antioxidant, antiallergic, and α -glucosidase inhibitory activities, isolated by supramolecular technique and solvent extraction from *Perilla* leaves. **Journal of Agricultural and Food Chemistry**, v. 62, 2014.

ZORZI, G. K. et al. On the use of nanotechnology-based strategies for association of complex matrices from plant extracts. **Brazilian Journal of Pharmacognosy**, v. 25, n. 4, p. 426–436, 2015.

CONCLUSÕES

O conjunto dos resultados obtidos ao longo dessa tese demonstra as potencialidades do uso de nanoemulsões (NE) revestidas por polímero mucoadesivo para administração por via nasal do ácido rosmarínico (AR) com vistas a uma terapia neuroprotetora, com base nas seguintes conclusões:

- Foi desenvolvido e validado um método analítico e bioanalítico específico, linear, exato, preciso, e robusto para a determinação do AR em diferentes matrizes por cromatografia líquida de ultra-eficiência;
- NE contendo AR revestidas por quitosana foram desenvolvidas e otimizadas através de um modelo experimental do tipo Box-Behnken;
- A caracterização físico-química e a força mucoadesiva das NE otimizadas foram avaliadas, demonstrando características adequadas para formulações para aplicação nasal;
- Os perfis de liberação e de permeação/retenção do AR a partir das formulações otimizadas foram avaliados, observando-se uma liberação e permeação do AR em mucosa nasal suína prolongada, bem como uma maior retenção do mesmo em mucosa nasal suína;
- A citotoxicidade *in vitro* das NE otimizadas foi avaliada em fibroblastos (MRC-5) e os resultados obtidos não demonstraram citotoxicidade em 24 e 48 horas na faixa de concentração de AR entre 3,125 – 50 μ M e 3,125 – 25 μ M, respectivamente;
- A citotoxicidade *in vitro* das formulações otimizadas foi avaliada em cultura primária de astrócitos, demonstrando ausência de citotoxicidade na faixa de concentração de AR entre 6,25 - 50,0 μ M e em um período de no máximo de 72 horas em células gliais do sistema nervoso central;
- A atividade glioprotetora *in vitro* (cultura primária de astrócitos) das nanoemulsões otimizadas em modelo de inflamação/estresse oxidativo induzido por lipopolissacarídeo (LPS) foi avaliada e comprovada;
- A atividade neuroprotetora *in vivo* (ratos Wistar) das NE otimizadas foi avaliada e demonstrada através de estudos comportamentais de reconhecimento de objetos em modelo de déficit de memória induzido por LPS.